1996

Physical and Chemical Stability of Spray Dried Sugars and Protein-Sugar Molecular Mixtures for Inhalation

Venkatesh Naini

Virginia Commonwealth University
School of Pharmacy

This is to certify that the dissertation prepared by Venkatesh Naini entitled "Physical and Chemical Stability of Spray Dried Sugars and Protein-Sugar Molecular Mixtures for Inhalation" has been approved by his committee as satisfactory completion of the dissertation requirement for the degree of Doctor of Philosophy.

[redacted]

Peter R. Byron, Ph.D., Director of Dissertation

[redacted]

H. Thomas Karnes, Ph.D., School of Pharmacy

[redacted]

Jurgen Venitz, M.D., Ph.D., School of Pharmacy

[redacted]

Jan F. Chlebowski, Ph.D., School of Medicine

[redacted]

William H. Soine, Ph.D., School of Pharmacy

[redacted]

William H. Barr, Ph.D., Chair, Department of Pharmacy & Pharmaceutics

[redacted]

John S. Ruggiero, Ph.D., Dean, School of Pharmacy

[redacted]

Jack Haar, Ph.D., Dean, School of Graduate Studies

June 27, 1996

Date

Physical and Chemical Stability of Spray Dried Sugars and Protein-Sugar Molecular Mixtures for Inhalation

A dissertation submitted in partial fulfillment of the requirements for the degree of Doctor of Philosophy at Virginia Commonwealth University

By

Venkatesh Naini
B.Pharm., BITS, Pilani, India, 1987
M.Pharm., Jadavpur University, Calcutta, India, 1989

Director: Peter R. Byron, Ph.D.
Professor
Department of Pharmacy and Pharmaceutics
School of Pharmacy

Virginia Commonwealth University
Richmond, Virginia
August, 1996

Acknowledgements

I am deeply indebted to my mentor and advisor Dr. Peter Byron for patiently guiding me through this research project. He is an excellent scientist and teacher and always inculcated, in me, the ideas of independent thinking and problem solving. I would also like to thank Dr. Richard Dalby, who initiated me into research during the initial stages of my graduate career.

I sincerely thank my graduate research committee members: Drs. H. Thomas Karnes, Jürgen Venitz, Jan Chlebowski and William Soine for their help and guidance during various stages of this project.

I would also like to thank past and present graduate students and postdoctoral fellows at Virginia Commonwealth University, especially, Dilraj, Elaine, Frank, John, Jennifer, Mike, Raj, Rose and Roshni for their friendship and support. In addition, I would like to express my gratitude to the administrative staff of the department: Adrienne, Judy, Loretta, Mia and Sue.

My friends and family, here and in India, have been extremely supportive of my endeavors during the past few years. I would especially like to thank my cousin Kiron and her family, my sisters Arpita, Kavita and Rajita and their families, my mom and my wife Sandhya. This dissertation is dedicated to the memory of my late father, who always encouraged me to strive for and achieve the best in life.

TABLE OF CONTENTS

Page

LIST OF TABLES ix

LIST OF FIGURES. xi

LIST OF ABBREVIATIONS. xvi

ABSTRACT. xx

CHAPTER

I. BACKGROUND AND INTRODUCTION. 1

II. HYPOTHESES AND SPECIFIC AIMS 18

III. PHYSICOCHEMICAL STABILITY OF CRYSTALLINE SUGARS AND THEIR SPRAY DRIED FORMS: DEPENDENCE ON RELATIVE HUMIDITY AND SUITABILITY IN POWDER INHALERS. 21

III.a INTRODUCTION. 21

III.b MATERIALS AND METHODS. 24

III.b.1 Materials. 24
III.b.2 Methods. 24
III.b.2.1 Sieve fractionation of sugars. . . . 24
III.b.2.2 Spray drying of sugars. 26
III.b.2.3 Moisture sorption studies. 26
III.b.2.4 Differential scanning calorimetry. . 27
III.b.2.5 Thermogravimetric analysis. . . . 27
III.b.2.6 Particle size determination. . . . 28
III.b.2.7 Hot stage microscopy. 28
III.b.2.8 X-ray powder diffraction. 29
III.b.2.9 Karl Fischer moisture determination. 29

III.c RESULTS AND DISCUSSION. 30

III.c.1 Chemistry and kinetics of mutarotation. . . 33
III.c.2 Crystalline sieve fractions, A and B. . . . 36
III.c.2.1 Lactose. 36
III.c.2.2 Trehalose.. 42
III.c.2.3 Sucrose. 49
III.c.2.4 Mannitol. 53
III.c.3 Spray dried sugars, C. 55

III.d SUMMARY AND CONCLUSIONS. 62

IV. CHARACTERIZATION AND OPTIMIZATION OF SPRAY DRYING AND ELECTROSTATIC PRECIPITATION APPARATUS FOR COLLECTION OF INHALABLE MICROPARTICLES. 65

IV.a INTRODUCTION.. 65

IV.b MATERIALS AND METHODS. 66
IV.b.1 Materials.. 66
IV.b.2 Methods. 67
IV.b.2.1 Particle collection apparatus. . . 67
IV.b.2.2 Effect of electrostatic precipitator (EP) voltage, nebulized solution concentration and hot air gun voltage on collection efficiency 72
IV.b.2.3 Effect of air flow and temperature on particle collection efficiency.. . . 73
IV.b.2.4 Photomicrography and scanning electron microscopy of electrostatically precipitated particles.. 74
IV.b.2.5 Theoretical particle collection efficiencies during electrostatic precipitation. 75

IV.c RESULTS AND DISCUSSION. 76
IV.c.1 Spray drying and electrostatic precipitation. . 76
IV.c.1.1 Effect of electrostatic precipitator (EP) voltage, nebulized solution concentration and hot air gun voltage on collection efficiency. 78
IV.c.1.2 Effect of drying air flow and temperature on particle collection efficiency. 88
IV.c.1.3 Theoretical particle collection efficiencies during electrostatic

precipitation. 100

IV.d SUMMARY AND CONCLUSIONS. 102

V. STABILITY OF SPRAY DRIED ALKALINE PHOSPHATASE DURING DRYING AND STORAGE: PROTECTION AFFORDED BY MOLECULAR DISPERSION IN LACTOSE, TREHALOSE, SUCROSE AND MANNITOL. 105

V.a INTRODUCTION.. 105

V.b MATERIALS AND METHODS. 108

V.b.1 Nebulization, drying and electrostatic precipitation. 109
V.b.1.1 Bacterial alkaline phosphatase. . . 113
V.b.1.2 Bovine intestinal alkaline phosphatase. 116
V.b.2 Solid state stability of dried protein and protein-sugar mixtures. 118
V.b.3 Solution degradation kinetics of bovine intestinal alkaline phosphatase (BIAP).. 118
V.b.4 Effect of droplet drying on protein concentration determination by the method of Bradford. . . 119
V.b.5 Scanning electron microscopy of dried BAP and BAP-sugar mixtures. 120
V.b.6 Statistical analyses. 121

V.c RESULTS AND DISCUSSION. 123

V.c.1 Solution degradation kinetics of bovine intestinal alkaline phosphatase. 123
V.c.2 Effect of droplet drying on protein content determination. 129
V.c.3 Spray drying and electrostatic collection of bacterial alkaline phosphatase(BAP). . . . 131
V.c.4 Spray drying and electrostatic collection of bovine intestinal alkaline phosphatase (BIAP). . . 148
V.c.5 Stability of dried protein and protein-sugar mixtures. 159

V.d SUMMARY AND CONCLUSIONS. 163

VI. DETERMINATION OF MOISTURE IN CRYSTALLINE AND SPRAY DRIED SUGARS USING ISOTHERMAL

THERMOGRAVIMETRIC ANALYSIS (TGA) AND KARL FISCHER (KF) COULOMETRIC TITRATION. 166

VI.a INTRODUCTION.. 166

VI.b PRINCIPLE OF COULOMETRIC KARL FISCHER TITRATION. 167

VI.c MATERIALS AND METHODS. 168

VI.c.1 Materials.. 168
VI.c.2 Methods. 169
VI.c.2.1 Spray drying of sugars. 169
VI.c.2.2 Sieve fractionation of sugars. . . 169
VI.c.2.3 Thermogravimetric analysis (TGA). 169
VI.c.2.4 Karl Fischer (KF) moisture determination. 170

VI.d RESULTS AND DISCUSSION. 172

VI.e SUMMARY AND CONCLUSIONS. 182

VII. DETERMINATION OF TOTAL PROTEIN CONTENT AND ALKALINE PHOSPHATASE ENZYME ACTIVITY IN SOLUTION.. 184

VII.a INTRODUCTION. 184

VII.b MATERIALS AND METHODS. 184

VII.b.1 Protein content determination. 185
VII.b.2 Determination of alkaline phosphatase activity. 187
VII.b.2.1 *Calibration plot of paranitrophenol* in 1.0 N NaOH solution. 187
VII.b.2.2 Limits of linearity for product (p-nitrophenol) accumulation vs incubation time. 187
VII.b.2.3 Limits of linearity for enzyme activity vs apparent protein concentration in enzyme solutions. 189

VII.c RESULTS AND DISCUSSION. 190

VII.c.1 Protein content determination. 190

VII.c.2 Determination of enzyme activity. 196
VII.c.2.1 Calibration plot of product. . . . 196
VII.c.2.2 Linearity of product released vs incubation time. 196
VII.c.2.3 Linearity of enzyme activity vs apparent protein concentration in the enzyme solution assayed. . . . 199
VII.c.2.4 Estimation of enzyme specific activity in unknown solutions. 199

VIII. OVERALL SUMMARY AND CONCLUSIONS. 203

LIST OF REFERENCES. 213

APPENDICES

AI. CALCULATION OF THEORETICAL PARTICLE COLLECTION EFFICIENCIES INSIDE THE ELECTROSTATIC PRECIPITATOR USING PARTICLE CHARGING THEORY. 226

AI.a INTRODUCTION. 226

AI.b THEORETICAL CALCULATION OF AEROSOL COLLECTION EFFICIENCY IN A WIRE-IN-TUBE ELECTROSTATIC PRECIPITATOR. 227

AI.c CALCULATION OF A TYPICAL THEORETICAL COLLECTION EFFICIENCY. 230

AII. DETERMINATION OF TOTAL VOLUMETRIC AIR FLOW THROUGH THE PARTICLE COLLECTION APPARATUS. . . 234

AII.a INTRODUCTION. 234

AII.b CALIBRATION OF THE PNEUMOTACHOGRAPH. . . 234

AII.c MEASUREMENT OF VOLUMETRIC AIR FLOWS IN THE PARTICLE COLLECTION APPARATUS USING THE CALIBRATED PNEUMOTACHOGRAPH AND MICROMANOMETER. 238

AIII. SUMMARY OF RAW DATA FOR ALKALINE PHOSPHATASE ENZYME ACTIVITIES AND PROTEIN CONCENTRATIONS (IN BSAE) USED IN CALCULATION OF ENZYME SPECIFIC

ACTIVITIES. 241

AIV. THERMAL ANALYSIS OF CRYSTALLINE SUGARS AND THEIR SPRAY DRIED FORMS. 246

AV. PARTICLE SIZE DETERMINATION OF SPRAY DRIED SUGARS USING THE AEROSIZER® WITH THE AERODISPERSER®. 263

AVI. PARTICLE SIZE MEASUREMENT OF CRYSTALLINE SIEVE FRACTIONS OF SUGARS USING SCANNING ELECTRON MICROSCOPY AND OPTICAL MICROSCOPY. . 268

AVII. X-RAY POWDER DIFFRACTION (XRPD) OF CRYSTALLINE SUGARS AND THEIR SPRAY DRIED FORMS. 281

AVIII. HOT STAGE MICROSCOPY OF SPRAY DRIED SUGARS OBSERVED UNDER CROSSED POLARS. 286

AIX. INSTRUCTIONS MANUAL FOR THE SMALL PARTICLE AEROSOL GENERATOR (SPAG). 291

VITA. 301

LIST OF TABLES

Table		Page
III.1	Experimental conditions for spray drying sugars.	25
III.2	Moisture contents of sugars determined by TGA.	37
III.3	Median aerodynamic diameters for spray dried sugars.	38
III.4	Summary of DSC results for lactose.	39
III.5.	Summary of DSC results for trehalose.	44
III.6	Summary of DSC results for sucrose.	50
III.7	Summary of DSC results for mannitol.	54
IV.1	Percentage collection efficiencies in the particle collection apparatus as function of electrostatic precipitator voltage.	79
IV.2	Percentage collection efficiencies in the particle collection apparatus as a function of nebulized solution concentration.	82
IV.3	Percentage collection efficiencies in the particle collection apparatus as a function of hot air gun voltage.	85
IV.4	Collection efficiencies at a drying temperature of 28.4 °C and volumetric air flow of 29.1 liters/min.	89
IV.5	Collection efficiencies at a drying temperature of 41.0 °C and volumetric air flow of 29.1 liters/min.	91
IV.6	Collection efficiencies at a drying temperature of 26.8 °C and volumetric air flow of 50.6 liters/min.	93
IV.7	Collection efficiencies at a drying temperature of 39.5 °C and volumetric air flow of 50.6 liters/min.	95
V.1	Summary of enzyme solutions spray dried.	110
V.2	Solution degradation kinetics of bovine intestinal alkaline	

phosphatase at 63 °C. 124

V.3 Effect of droplet drying on protein content determination by method of Bradford. 130

V.4 Specific activity of bacterial alkaline phosphatase (BAP) following nebulization, drying and/or storage. 133

V.5 Summary of ANOVA results for BAP enzyme activities. . . . 134

V.6 Specific activity of bovine intestinal alkaline phosphatase (BIAP) following nebulization, drying and/or storage. 150

V.7 Summary of ANOVA results for BIAP enzyme activities. . . 151

V.8 Summary of significance levels for ANOVA of BIAP activities. . 152

VI.1 Isothermal TGA of sugars. 174

VI.2 Moisture contents of sugars using KF analysis.. 181

VII.1 Summary of validation parameters for protein determination by the method of Bradford. 191

AI.1 Theoretical collection efficiencies inside the precipitator. . . . 233

AII.1 Volumetric flow rates at different settings of the hot air gun. . 240

AIII.1Summary of raw data for BAP activity and protein contents. . 242

AIII.2Summary of raw data for BIAP activity and protein contents. . 244

LIST OF FIGURES

Figure		Page
III.1	Molecular structures of sugars.	31
III.2	X-ray diffractograms for lactose.	40
III.3	X-ray diffractograms for trehalose, sucrose and mannitol. .	45
III.4	Typical TGA and DSC thermograms for lactose before and after storage at different RHs.	47
III.5	Typical TGA and DSC thermograms for trehalose, sucrose and mannitol before and after storage at different RHs. . .	51
IV.1	Schematic diagram of the particle collection apparatus. . .	68
IV.2	Exploded view of the secondary drying chamber with dimensions..	69
IV.3	Exploded view of the electrostatic precipitator column with dimensions..	70
IV.4	Effect of EP voltage on deposition in the apparatus.. . . .	80
IV.5	Effect of nebulized solution concentration on deposition in the apparatus.	83
IV.6	Effect of hot air gun voltage on deposition in the apparatus. .	86
IV.7	Photomicrographs of lactose particles collected inside the precipitator..	87
IV.8	Deposition in the apparatus following spray drying at 28 °C and volumetric flow rate of 29.1 liters/min.	90
IV.9	Deposition in the apparatus following spray drying at 41 °C and volumetric flow rate of 29.1 liters/min.	92
IV.10	Deposition in the apparatus following spray drying at 27 °C and volumetric flow rate of 50.6 liters/min.	94

IV.11 Deposition in the apparatus following spray drying at 40 °C and volumetric flow rate of 50.6 liters/min. 96

IV.12 SEM of lactose and fluorescein particles dried at 29 °C and collected inside the precipitator. 97

IV.13 SEM of lactose and fluorescein particles dried at 41 °C and collected inside the precipitator. 98

IV.14 SEM of lactose and fluorescein particles dried at 63 °C and collected inside the precipitator. 99

IV.15 Comparison of theoretical and experimental collection efficiencies in the electrostatic precipitator. 101

V.1 Schematic diagram of the particle collection apparatus. . . 111

V.2 Log-linear plot of loss of detectable protein vs time for BIAP.. 125

V.3 Solution degradation kinetics of BIAP at 63 °C. 126

V.4 Log-linear profiles of BIAP plotted as percentage activity remaining using Units/ml and specific activity(Units/μgBSAE)127

V.5 Specific activities of BAP in initial solution and following spray drying and/or storage. 136

V.6 A cartoon representation of the monomer of bacterial alkaline phosphatase. 137

V.7 SEM of BAP spray dried from sugar-free solutions. . . . 138

V.8 SEM of BAP spray dried with lactose.. 139

V.9 SEM of BAP spray dried with trehalose. 140

V.10 SEM of BAP spray dried with sucrose. 141

V.11 SEM of BAP spray dried with mannitol. 142

V.12 Specific activities of BIAP in initial solution and following spray drying and/or storage. 154

V.13 Molecular structures of sugars. 157

VI.1 Schematic diagram of Mitsubishi moisture meter.. . . . 173

VI.2 Isothermal TGA of sodium tartrate dihydrate. 176

VI.3 Isothermal TGA of crystalline and spray dried forms of trehalose. 177

VI.4 Isothermal TGA of crystalline and spray dried forms of lactose 178

VI.5 Isothermal TGA of crystalline and spray dried forms of sucrose. 179

VII.1 Calibration curve for protein estimation by method of Bradford (Assay Lot # 51143A). 193

VII.2 Calibration curve for protein estimation by method of Bradford (Assay Lot # 51558A). 194

VII.3 Calibration curve for p-nitrophenol in 1.0 N NaOH. . . . 195

VII.4 Plot of p-nitrophenol concentration vs incubation time for BAP. 197

VII.5 Plot of p-nitrophenol concentration vs incubation time for BIAP 198

VII.6 Plot of enzyme activity vs apparent protein concentration for BAP. 200

VII.7 Plot of enzyme activity vs apparent protein concentration for BIAP. 201

AI.1 Exploded view of the precipitator column. 228

AII.1 Calibration of the pneumotachograph. 235

AII.2 Experimental set up for flow measurement in the apparatus. 236

AII.3 *Calibration plot of apparent cumulative air volume entering* the pneumotachograph vs air flow in liters/min. 237

AIV.1 TGA and DSC for A_0, B_0 and $A_{30a,b,c,d,e}$ and $B_{30a,b,c,d,e}$ for lactose. 247

AIV.2 TGA and DSC for C_0 and C_{30a} for lactose. 248

AIV.3 TGA and DSC for C_{30b} for lactose. 249

AIV.4 TGA and DSC for $C_{30c,d,e}$ of lactose. 250

AIV.5 TGA and DSC for A_0, B_0 and $A_{30a,b,c,d,e}$ and $B_{30a,b,c,d,e}$ for trehalose. 251

AIV.6 TGA and DSC for C_0 and C_{30a} for trehalose. 252

AIV.7 TGA and DSC for C_{30b} for trehalose. 253

AIV.8 TGA and DSC for $C_{30c,d,e}$ of trehalose.. 254

AIV.9 TGA and DSC for A_0, B_0 and $A_{30a,b,c,d}$ and $B_{30a,b,c,d}$ for sucrose. 255

AIV.10 TGA and DSC for C_0 and C_{30a} for sucrose. 256

AIV.11 TGA and DSC for C_{30b} for sucrose.. 257

AIV.12 TGA and DSC for $C_{30c,d}$ of sucrose. 258

AIV.13 TGA and DSC for A_0, B_0 and $A_{30a,b,c,d,e}$ and $B_{30a,b,c,d,e}$ for mannitol. 259

AIV.14 TGA and DSC for C_0 and C_{30a} for mannitol. 260

AIV.15 TGA and DSC for C_{30b} for mannitol. 261

AIV.16 TGA and DSC for $C_{30c,d,e}$ of mannitol.. 262

AV.1 Particle size distribution of spray dried lactose as measured by Aerosizer. 264

AV.2 Particle size distribution of spray dried trehalose as measured by Aerosizer. 265

AV.3 Particle size distribution of spray dried sucrose as measured by Aerosizer. 266

AV.4 Particle size distribution of spray dried mannitol as measured by Aerosizer. 267

AVI.1 SEMs of "coarse" and "fine" fractions of lactose.. 269

AVI.2 SEMs of "coarse" and "fine" fractions of trehalose. 270

AVI.3 SEMs of "coarse" and "fine" fractions of sucrose. 271

AVI.4 SEMs of "coarse" and "fine" fractions of mannitol. 272

AVI.5 Particle size distribution of "coarse " lactose as measured by optical microscopy. 273

AVI.6 Particle size distribution of "fine " lactose as measured by optical microscopy. 274

AVI.7 Particle size distribution of "coarse " trehalose as measured by optical microscopy. 275

AVI.8 Particle size distribution of "fine " trehalose as measured by optical microscopy. 276

AVI.9 Particle size distribution of "coarse " sucrose as measured by optical microscopy. 277

AVI.10 Particle size distribution of "fine " sucrose as measured by optical microscopy. 278

AVI.11 Particle size distribution of "coarse " mannitol as measured by optical microscopy. 279

AVI.12 Particle size distribution of "fine " mannitol as measured by optical microscopy. 280

AVII.1 XRPD patterns for lactose. 282

AVII.2 XRPD patterns for trehalose. 283

AVII.3 XRPD patterns for sucrose. 284

AVII.4 XRPD patterns for mannitol. 285

AVIII.1 Photomicrography of spray dried lactose under crossed polars at (a) 30 °C and (b) 140 °C. 287

AVIII.2 Photomicrography of spray dried lactose under crossed polars at (a) 170 °C and (b) 190 °C. 288

AVIII.3 Photomicrography of spray dried sucrose under crossed polars at (a) 30 °C and (b) 106 °C. 289

AVIII.4 Photomicrography of spray dried sucrose under crossed polars at (a) 151 °C and (b) 192 °C. 290

LIST OF ABBREVIATIONS

A	Collection surface area in the electrostatic precipitator
A_{404}	Absorbance at 404 nm
A_{595}	Absorbance at 595 nm
ANOVA	Analysis of variance
BAP	Bacterial alkaline phosphatase
BIAP	Bovine intestinal alkaline phosphatase
BSA	Bovine serum albumin
BSAE	Protein content expressed in terms of BSA equivalents
C	Temperature in degree centigrade
cal	Calories
CFC	Chlorofluorocarbon
cm	Centimeter
CV	Coefficient of variation
d	Diameter of an aerosol particle
DPI	Dry powder inhaler
DSC	Differential scanning calorimetry
e	Charge on an electron
E	Electric field strength
E'	Collection efficiency in electrostatic precipitation

EP	Electrostatic precipitator
FT-IR	Fourier transformed infra red spectroscopy
g	gram
J	Joules
JCPDS	Joint Committee for Powder Diffraction Standards
KDa	Kilodaltons
kg	Kilogram
KF	Karl Fischer moisture analysis
kgf/cm^2	Pressure expressed as kilogram force per square cm.
kV	Kilovolts
L	Lactose
LOD	Loss on drying
LOQ	Limit of quantitation
M	Mannitol
mM	Millimolar
min	minute
mg	milligram
MW	Molecular weight
N_i	Ion number concentration
n	Number of charges acquired by a particle
nm	Nanometer
p	Level of significance (in statistical analysis)
pMDI	Pressurized metered dose inhaler

psig	Pounds per square inch, gauge
Q	Volumetric flow rate
rDNA	Recombinant deoxyribonucleic acid
rhDNase	Recombinant human deoxyribonuclease
rhG-CSF	Recombinant human granulocyte colony stimulating factor
rConIFN	Recombinant consensus interferon
RH	Relative humidity
rpm	Revolutions per minute
r_t	Radius of tube of a wire-in-tube type precipitator
r_w	Radius of wire of a wire-in-tube type precipitator
S	Sucrose
s	second
SD	Standard deviation
SDS	Sodium dodecyl sulfate
SEM	Scanning electron microscopy
SPAG	Small Particle Aerosol Generator
T	Trehalose
T_g	Glass transition temperature
TGA	Thermogravimetric analysis
Tris	Tris(hyroxymethyl)-aminomethane
UK	United Kingdom
USA	United States of America
USP/NF	United States Pharmacopeia/National Formulary

V	Volts
V_{TE}	Terminal electrostatic velocity
W/g	Heat flow in watts/gram
XRPD	X-ray powder diffraction
Z_i	Mobility of ions in electrostatic precipitation
α	α anomer of lactose
β	β anomer of lactose
% w/v	Percentage weight in volume
ΔH	Enthalpy
Θ	X-ray diffraction angle
μl	Microliter
μ m	Micrometer
μ	Viscosity of air
ΔW	Difference in voltage between wire and tube in an electrostatic precipitator
min^{-1}	Units for a first order rate constant
r^2	Coefficient of determination
ε	Dielectric constant

ABSTRACT

PHYSICAL AND CHEMICAL STABILITY OF SPRAY DRIED SUGARS AND PROTEIN-SUGAR MOLECULAR MIXTURES FOR INHALATION

BY Venkatesh Naini, M.Pharm.

A dissertation submitted in partial fulfillment of the requirements for the degree of Doctor of Philosophy at Virginia Commonwealth University.

Virginia Commonwealth University, 1996.

Director: Peter R. Byron, Ph.D.
Professor
Department of Pharmacy and Pharmaceutics

The feasibility of producing inhalable microparticles of sugars and protein-sugar molecular mixtures using spray drying was investigated as an alternative to conventional micronization techniques. Four sugars; lactose (L), trehalose (T), sucrose (S) and mannitol (M) were spray dried using a commercial bench-top spray dryer and their physicochemical stability, with respect to particle size, moisture uptake and crystallinity changes, investigated after storage at 23%, 52%, 75% and 93% relative humidity (RH) and 25 °C for 30 days. Two crystalline size fractions ("coarse" = 125-212 μm and "fine" = 44-74 μm) of each sugar, were also characterized, as possible replacements for lactose as carriers for admixture with drugs in dry powder inhalers (DPIs). Sieve fractions of lactose, trehalose and mannitol failed to show significant moisture uptake at RHs ≤ 93% and 25 °C

indicating their thermodynamic stability under most realistic storage conditions. While sucrose failed to show moisture uptake at ≤ 75% RH, it dissolved in sorbed moisture at 93% RH. Spray dried sugars were collected successfully in particle sizes suitable for inhalation. Spray dried lactose, trehalose and sucrose were amorphous and remained in this state after storage at 23% RH. At higher RHs, however, they recrystallized completely in ≤ 30 days. Spray dried mannitol was completely crystalline after collection from the spray dryer. It did not show moisture uptake or physical state changes at all RHs.

A fine particle collection apparatus incorporating a nebulizer and a wire-in-tube type electrostatic precipitator (EP), built and characterized for particle collection efficiency, was used to review protein activity following spray drying with or without the four sugars as stabilizers. Bacterial (BAP) and bovine intestinal alkaline phosphatase (BIAP) were used as model proteins. Sugar free BAP solutions (apparent protein concentration ~120 μg/ml) lost 23% of initial enzyme specific activity after spray drying at ~63 °C and collection in the EP. Protection offered by the sugars to BAP during drying, was however statistically indistinguishable from the sugar-free protein solution (dried from the same protein concentration solution). When BIAP was dried from sugar free solutions (apparent protein concentration ~1 mg/ml), it lost 31% of its initial specific activity; activity which could be completely recovered when BIAP was co-dried with L, T or S (ANOVA, $p < 0.05$). However, M which crystallized during spray drying

failed to protect the enzyme from this loss of activity. These results implied that the physical state of sugar (amorphous or crystalline) in the final dried product may be an important determinant for offering protection to proteins during spray drying and storage. Even so, multiple factors could potentially influence the selection of a sugar to form inhalable microparticles with a protein. These factors are described and discussed in this thesis, whether or not they appeared to be important with respect to the drying and stability of particular proteins selected for experimental investigation.

I. BACKGROUND AND INTRODUCTION

Although inhalation of vapors and gases has been used since ancient times for the treatment of a variety of respiratory disorders (Yernault, 1994), drug delivery by this route only became significant in the last 50 years. The first breakthrough to enable easy drug aerosol inhalation came with the introduction of the pressurized metered dose inhaler (pMDI) in 1956 (Medihaler®, Riker). Since then, there has been an increasing number of drugs and devices that have been used for delivery to the lung. Three main types of inhalation devices are presently used in therapy; the pressurized metered dose inhaler (pMDI), nebulizer (air-blast and ultrasonic) and the dry powder inhaler (DPI). pMDIs usually consist of drug suspended in liquefied propellant along with a surfactant (Byron, 1990a) although solution systems are also possible. Although pMDIs currently garner the bulk of the inhalation market worldwide, their future *seems* uncertain as a result of the impending ban on chlorofluorocarbon (CFC) propellants which have been implicated in the depletion of the ozone layer (Molina and Rowland, 1974; Dalby et al., 1990; Daly, 1993). As a result there has been increased focus on formulation and development of propellant free devices: nebulizers and dry powder inhalers (Martin et al., 1994). Nebulizers atomize aqueous solutions into fine droplets which are

then inhaled by the patient (Byron, 1990b). DPIs either consist of the pure drug or drug mixed with an inert carrier like lactose (Ganderton and Kassem, 1992). In DPIs, the patient's respiratory effort usually provides the energy to dislodge the drug from the carrier during inhalation (Byron, 1990a).

The majority of inhalation drug delivery systems in the market today, administer ß-adrenergic bronchodilator or steroid drugs to the lungs for treating bronchoconstriction or inflammation responses, associated with airway diseases like asthma and bronchitis (Byron, 1990a and 1990b). These compounds elicit their pharmacologic action in the lungs, and thus, inhalation delivery offers an excellent way of targeting these drugs to the site of action (Gonda, 1992). However, there has also been a recent increase in attempts to deliver drugs to the systemic circulation after aerosol delivery via the lung (Byron and Patton, 1994; Adjei and Gupta, 1994; Niven, 1993; Patton et al., 1994). This increased interest has been in part due to the biotechnology revolution (Wallace and Lasker, 1993; Eddington, 1991). Recombinant DNA (rDNA) technology has made available a wide variety of newer, high molecular weight biotherapeutics which can be potentially administered to the lung for absorption into the systemic circulation (Byron and Patton, 1994; Patton and Platz, 1992). If this strategy is successful, frequent injections of these drugs may be avoidable, since many of them need to be administered in a pulsatile fashion more than once per day. Drug delivery via the lungs also offers distinct advantages over other

alternative (to injections) routes of delivery, such as oral, nasal and transdermal routes, for protein and peptide drugs (Patton et al., 1994). These include, a relatively large absorptive area, avoidance of hepatic first pass metabolism and possibly lowered enzymatic drug degradation (Patton and Platz, 1992).

Many proteins and peptides have been investigated in animals and humans for their potential absorption into the blood stream following lung administration (Byron and Patton, 1994; Patton et al., 1994; Niven, 1993; Adjei and Gupta, 1994). Two peptides, insulin (for diabetes) and leuprolide acetate (for endometriosis and prostatic carcinoma) have been extensively studied for administration through the lung. Recently, Laube et al. (1993), investigated the feasibility of aerosol insulin in humans and found that after administering a 0.2 Units/kg dose of regular insulin, by nebulizer, resulted in an average maximum decrease of plasma glucose from baseline by 55% compared to 13% for the placebo (Laube et al., 1993). Aerosol leuprolide acetate, being developed by Abbott laboratories, is presently in Phase III clinical trials (Niven, 1993). Adjei and Garren, looked at bioavailability of leuprolide acetate in human volunteers after administration of the drug to the lungs as solution and suspension pMDI formulations (Adjei and Garren, 1990). They reported 3-4 fold higher plasma levels of leuprolide for a pressurized suspension aerosol formulation compared to the solution, with 14-18% absolute bioavailabilities for the suspension formulation. If the < 20% lung deposition values (Gonda,

1992) reported for most pMDIs are taken into account, this corresponds to almost quantitative (stoichiometric) absorption of drug actually deposited in the lung. Besides these two peptides many other protein and peptide drugs like human growth hormone, α-interferon, calcitonin, colony stimulating factors (CSF) and parathyroid hormone are being investigated for administration through the lung (Byron and Patton, 1994, Patton et al., 1994, Adjei and Gupta, 1994).

In addition to the above mentioned examples for systemic delivery, aerosol technology offers an excellent method for administering protein and peptide drugs to the lungs for local action. Some of these drugs include recombinant human DNase (rhDNase) for cystic fibrosis, γ-interferon for *Pneumocystis carinii* in AIDS patients, cyclosporine for lung transplant rejection and α-1-antitrypsin and α-1-protease inhibitors in emphysema. DNase now forms a classic example of research and development of an aerosol delivery system for a therapeutic protein for local activity in the lung (Gonda et al., 1994; Cipolla et al., 1994a and 1994b). An aqueous solution formulation (Pulmozyme® Nebulizer Solution) of DNase is currently approved by the FDA for administration to the lungs using a nebulizer.

Although protein and peptide drugs have been formulated as solutions for nebulization (DNase) and as pMDIs (leuprolide acetate), DPIs are also highly favored as delivery systems for such drugs. This

formulation strategy avoids dispersion of protein or peptide drugs in hydrophobic propellants and avoids stability problems associated with aqueous nebulizer solutions and processes (shear forces and exposure to a large air-water interface in jet nebulizers and high temperatures in ultrasonic nebulizers) provided the protein in question can be dried successfully. In addition nebulizers are varied; their drug output and operation are usually uncontrolled (Dalby and Tiano, 1994). Moreover, many nebulizers and their accessories are cumbersome to use which may result in reduced patient compliance. In view of these problems with pMDIs and nebulizers, it seems attractive to formulate proteins and peptides as DPIs.

Successful respiratory drug delivery requires the production of fine particles with aerodynamic diameters in the range of 1 to 10 μm. However, particles with aerodynamic diameters less than 5 μm are considered optimal for lung delivery of bronchodilators and steroids (Byron, 1990b). To reach the peripheral lung and to be most efficiently absorbed systemically, particles of the order of 2 to 3 μm are required (Clark, 1995). Comminution to produce such particles is usually accomplished by jet (gas impact) milling or in some cases by ball milling in a low volatility propellant such as CFC-11; and also by controlled microcrystallization (Byron, 1990a). Milling in a liquid medium and controlled microcrystallization suffer from several disadvantages such as contamination from the milling medium, difficulty in controlling the nucleation rate and recovery of particles from

the medium. Hence, jet milling is usually the method of choice for production of fine particles suitable for inhalation (Byron, 1990a; Parrott, 1974). In jet milling, the particulate material is suspended and conveyed at high velocities by compressed gas and impacted against itself, causing the break up as a result of attrition (Parrott, 1974). This method works well for brittle crystalline materials with high melting points (Byron, 1990). However, the recovery of small particles from the air stream, is difficult and usually requires filtration through a fabric screen. Jet milling may not be a suitable method for production of fine particles of protein and peptide drugs for inhalation, because of their plastic (non brittle) nature. This may not be a problem if only large quantities of crystalline macromolecular drugs could be produced reproducibly. Unfortunately, this problem is not easily solved. In addition, administration of more potent protein and peptide drugs via the lung may require tighter controls on the final particle size (narrow particle size distribution) compared to traditional bronchodilator drugs. This is fairly difficult to achieve by jet milling or other existing techniques.

Alternative particulate processing technologies are being investigated for the production of fine particles for inhalation. Methods cited in the literature which are generally suitable for pharmaceutical materials are processing from supercritical fluids and spray drying. Supercritical fluids have now been used to produce fine particles of small molecules like lovastatin, ß-estradiol and phenacetin and peptides like

insulin (Tom and Debendetti, 1991; Phillips and Stella, 1993; Yeo et al., 1993). However, the application of this technique to pharmaceutical materials is not well developed and involves expensive instrumentation.

On the other hand spray drying is a well established process in the pharmaceutical industry for drying of tablet granulations and production of particulate materials (Broadhead et al., 1992; Masters, 1991a; Fell and Newton, 1971). Spray drying consists of four stages: 1) atomization of liquid feed into a spray of fine droplets 2) spray-air contact resulting in the mixing of droplets and air 3) drying of the droplets (solvent evaporation) and 4) separation of the dried product from the air stream (Masters, 1991a). Dry powders of drugs for inhalation produced by spray drying may be mixed with larger crystalline carriers like lactose or alternatively produced as molecular mixtures with the carrier. In the latter case the carrier is inhaled with the drug. Spray drying has also been used to produce fine particles for inhalation of the antiallergenic compound, disodium cromoglycate (Vidgren et al., 1987; Vidgren et al., 1989) and the bronchodilator, albuterol (Chawla et al., 1994). Vidgren and colleagues compared the physical and inhalation properties of disodium cromoglycate powders produced by spray drying and jet milling (Vidgren et al., 1987; Vidgren et al., 1989). They used 1:1 drug/carrier (lactose) powder blends consisting of either the spray dried or jet milled drug to study their inhalation behavior using a cascade impactor as the size segregation technique. Both formulations were similar when particles < 7 μm were

considered, with spray dried and milled formulations producing 33% and 31% of particles < 7 μm by mass respectively. However, when particles < 3 μm were considered they behaved quite differently. The spray dried formulation produced 17% of particles < 3 μm by mass, compared to 8% for the milled formulation (Vidgren et al., 1989). Results like these may not be therapeutically significant for drugs like albuterol or disodium cromoglycate, but they become quite profound if the inhalation route is to be used successfully for systemic delivery of proteins and peptides.

There have been several reports in the literature on spray drying of proteins, although only a few studies have used the technique for production of inhalable microparticles (Masters, 1991b; Labrude et al., 1989; Mumenthaler et al., 1994; Broadhead et al., 1994; Foster and Leatherman, 1995). Traditionally, enzymes have been spray dried as bulk powders for use as detergents (lipase), in wound debridement (trypsin), in cheese making (rennin) and ice-cream making (lactase) [Masters, 1991b]. Reports on spray drying of pharmaceutically relevant proteins like oxyhemoglobin (Labrude et al., 1989), recombinant human growth hormone, tissue plasminogen activator (Mumenthaler et al., 1994) and bovine somatotropin (Foster and Leatherman, 1995) have also appeared only recently, but even these reports do not deal with the unique problem of producing powders for inhalation.

Only two reports appeared in the literature dealing with spray drying of proteins for inhalation purposes (Broadhead et al., 1994; French et al., 1995). The first study (Broadhead et al., 1994) used a model protein, ß-

galactosidase and the second report (French et al., 1995) utilized therapeutic proteins; recombinant human granulocyte colony stimulating factor (rhG-CSF) and recombinant consensus interferon (rConIFN). However, proteins may be reversibly or irreversibly denatured and chemically degraded due to high temperatures and desiccation during the spray drying process (Masters, 1991b). Spray drying process may induce increased aggregation of therapeutic proteins, which may have antigenicity and toxicity potential. Spray drying of oxyhemoglobin at an inlet temperature of 60 °C resulted in the retention of only 49% of the originally active protein, the remaining 51% being the degradation product methemoglobin (Labrude et al., 1989). Broadhead et al., report a residual enzyme activity of 42% for ß-galactosidase spray dried to a residual moisture content of 4.5% at an inlet temperature of 105 °C (Broadhead et al., 1994).

Spray drying proteins with stabilizers has been suggested but not thoroughly documented, as a method for preventing protein denaturation during the drying process (Masters, 1991b; Broadhead et al., 1994; Labrude et al., 1989). Of several stabilizers investigated, some disaccharide sugars seem to be very effective in imparting stability to proteins during drying and storage of the dried powders (Labrude et al., 1989; Broadhead et al., 1994; Carpenter, 1987). Sugars have been traditionally used as protein stabilizers in aqueous solutions and are known to increase resistance of proteins to denaturation by heat (Arakawa and Timasheff, 1982; Back et al., 1979) and

also during freeze drying (Pikal, 1990; Franks and Berg, 1992; Izutsu et al., 1993). Protein stabilization by disaccharides in solution has been explained on the basis of "preferential hydration" mechanism proposed by Timasheff (Timasheff and Arakawa, 1989). According to this hypothesis, stabilization is attributed to preferential exclusion of sugar molecules (relative to the bulk solution) in the immediate vicinity of the protein and thus, the protein is preferentially hydrated. Thus, addition of sugar to a protein solution is believed to increase the chemical potential of the protein in aqueous solution and thus the free energy of the system (water + protein). This is thermodynamically unfavorable for the unfolded state of the protein (since unfolding increases the area of contact between protein and solvent). Therefore, in the presence of sugar, the equilibrium is shifted towards the folded or native conformation, resulting in stabilization (Arakawa et al., 1991). Although this mechanism may explain the stabilization of macromolecules in solution prior to spray drying, air drying or freeze drying, it does not explain the stability afforded during the end stages of drying and during storage as dried powders, since under these processing conditions, there is almost complete water removal from the system (Carpenter et al., 1987).

Two additional hypotheses have been suggested to explain protein stabilization by sugars during drying and storage of protein as dry powder. According to the "water replacement" hypothesis suggested by Carpenter and colleagues, during the end stages of drying, sugar molecules hydrogen

bond to polar residues on the protein, stabilizing the protein's conformation and thus imparting stability (Carpenter et al., 1989; Carpenter et al., 1987; Prestrelski et al., 1993). In an elegant piece of work, Prestrelski and co-workers used Fourier-transform infrared spectroscopy (FT-IR) to study conformational changes on several proteins on dehydration and their inhibition by sugars (Prestrelski et al., 1993). They showed that sugars which stabilize lactate dehydrogenase (LDH) during freeze drying (sucrose and lactose) give an identical FT-IR spectra for the dried powder compared to the spectrum for the pre-dried protein solution (native conformation) in the amide I region (1720 - 1610 cm^{-1}; corresponding to the peptide backbone); this spectral match correlated well with enzyme activity retention. This indicated that the sugars stabilized the native conformation in the dried state.

However, the kind of structural explanation detailed in the last paragraph is not fully consistent with the relative efficiency of different sugars to stabilize proteins to varying degrees (Green and Angell, 1989). Hence, an alternative hypothesis based on the material science approach of *glass* transition theory has been proposed (Green and Angell, 1989; Franks et al., 1991; Levine and Slade, 1992). According to this hypothesis, during drying of protein-sugar mixtures, the protein is entrapped in a glassy amorphous matrix which immobilizes the protein, reducing long range molecular motion and thus imparting stability (Green and Angell; 1989; Levine and Slade, 1992). Glassy amorphous materials are usually obtained

by processes like spray drying and freeze drying which require high energy input and completely destroy the crystalline structure (Matsuda et al, 1992; Saleki-Gerhardt et al., 1994). Such materials exhibit a characteristic temperature called the glass transition temperature (T_g). This temperature identifies the temperature of a critical event which determines physical stability, chemical stability and viscoelastic properties, especially when this temperature is approached or exceeded during processing , i.e. drying and storage (Hancock and Zografi, 1994). At temperatures below the T_g, an amorphous material, exists in the glassy state where molecular motion is arrested. However, if processing or storage temperature exceeds T_g, the material becomes rubbery and has increased molecular mobility. This increased mobility increases the chance of degradative chemical reactions (between sugar and protein) and physical instability like recrystallization (Ahlneck and Zografi, 1990). The T_g of a glassy material can be depressed by many plasticizers, most important of which is water (Hancock and Zografi, 1994). Hence, a metastable amorphous glass can remain stable for pharmaceutically relevant time periods if the processing temperature (drying and storage) is kept below the T_g of the material. There is some consensus in the literature that the two hypotheses detailed above may not be mutually exclusive, in that, although a glassy matrix is required for stabilization, some non-specific bonding between the sugar and protein may also be required.

Long term storage of dried protein-sugar mixtures can have unique

chemical stability problems (Hageman, 1988; Ford and Dawson, 1993; Tarelli and Wood, 1981). In a series of papers, Tarelli and colleagues have shown that proteins react with reducing sugars like glucose and lactose via Maillard reactions whereby the aldehyde form of the sugar reacts with free amino groups on the protein to form Schiff bases. These bases, in turn undergo Amadori rearrangement, leading to irreversible loss of protein activity (freeze dried protein-sugar mixtures; Tarelli and Wood, 1981; Tarelli and White, 1982; Tarelli et al., 1987; Bristow et al., 1988; Calam and Tarelli, 1988). They reported that a number of factors like temperature, moisture content and pH influenced the reaction rate between protein and a reducing sugar. They measured free lysine present in freeze dried bovine serum albumin (BSA)-sugar mixtures after storage at 37 °C and 65% RH for 26 weeks. In the presence of the non-reducing sugars like sucrose and trehalose, lysine residues (with a free amino group) remained unaffected, and these results were in parallel with retention of BSA antigenic activity (bioassay), as measured by a radial diffusion assay. However, BSA dried and stored with glucose and lactose (reducing sugars) showed that 85% and 70%, respectively, of the original lysine residues on the protein had undergone modification, after identical storage conditions, and this was also reflected by the loss of BSA antigenic activity (Tarelli and Wood, 1981).

The amount of solids in an atomized droplet during spray drying is dependent upon the concentration of solution sprayed. This, in turn, determines the final particle size of the spray dried powder, with finer

particles being produced from lower concentration solutions. However, the majority of commercially available bench top spray dryers have atomizer technology which creates overly large droplets. These instruments also have poor collection efficiencies for fine particles when spray drying low concentration solutions (Broadhead, 1994).

The poor particle collection problem is addressed in this dissertation by the use of a purpose designed electrostatic precipitator (Dalby et al., 1992). Electrostatic precipitation is a particle charging technique employed in pollution control, to limit particulate emissions in industrial exhausts (White, 1963; Oglesby and Nichols, 1978). It has been shown, at least in theory to collect fine particles ($\leq$ 1 μm) with a high degree of efficiency (Hinds, 1982). Collection efficiencies depend on the precipitator geometry, electric field strength generated, volumetric air flow through the system and particle size of material being charged and collected (Hinds, 1982). Atomization of low concentration (1% w/v) aqueous solutions followed by droplet drying and electrostatic precipitation (laboratory scale model) was shown to be capable of collecting fine particles suitable for inhalation (Dalby et al., 1992; Naini et al., 1993). Such a collection apparatus could then be used to spray dry and collect small amounts of protein for evaluating protein activity following spray drying in the presence and absence of stabilizers. In the long term, it is certainly possible to scale the collection device to deal with larger masses of materials (White, 1963).

This dissertation is arranged to answer some of the questions

addressed in the paragraphs above. Chapter II cites the individual hypotheses and specific aims to be addressed in the following chapters. Each of the main chapters consists of an introduction, materials and methods section, followed by a presentation and discussion of the experimental results and an overall summary. Chapter III discusses production and characterization of four spray dried sugars; lactose, trehalose, sucrose and mannitol. These four sugars were chosen for their different properties. Lactose, trehalose and sucrose are disaccharides, while mannitol is a sugar alcohol. Lactose is a reducing sugar, while trehalose, sucrose and mannitol are non-reducing. Trehalose, has received a lot of attention lately for its excellent protein stabilizing properties (Colaco at al., 1993; Levine and Slade; 1993). Although there are reports in the literature detailing these features of trehalose, reports on physicochemical characterization of spray dried amorphous trehalose are few. Comparison of the physicochemical properties of spray dried sugars were made with two crystalline sieve fractions of each sugar characterized in a similar fashion; this because powder inhalers can be formulated with drug in molecular or particle size associations with sugar diluents. Characterization of the sugars included particle size determinations, measurement of crystallinity changes using differential scanning calorimetry (DSC) and X-ray powder diffraction (XRPD) after storage under different relative humidity environments for 30 days at 25 °C (these conditions are typical of those which formulations may experience in

different places in the USA). Moisture uptake at different storage conditions was determined using thermogravimetric analysis (TGA) validated by Karl Fischer analysis.

Chapter IV deals with the design and characterization of a particle collection apparatus for fine particle collection. This chapter describes the experiments performed to determine particle collection efficiencies inside the electrostatic precipitator as a function of applied precipitator voltage, volumetric air flow, temperature of drying and sprayed solution concentration. Those experiments were performed primarily with lactose using disodium fluorescein as a water soluble marker.

Chapter V describes the use of the particle collection apparatus (Chapter IV) for the review of protein activity, following spray drying and electrostatic precipitation. Spray drying and collection conditions validated in Chapter IV were employed throughout. Two model proteins, bacterial alkaline phosphatase (BAP) and bovine intestinal alkaline phosphatase (BIAP) were selected for study. These protein solutions in 10 mM Tris buffer pH 8.0 were sprayed, dried and electrostatically collected with or without the addition of one of the four sugars (lactose, trehalose, sucrose and mannitol), to the original solution. Collected and apparently dried aerosols were either washed and reconstituted with 10 mM Tris buffer pH 8.0 or stored in the dry state at 23% RH and 25 °C (conditions under which amorphous sugars obtained by spray drying remained physically stable without recrystallization; Chapter III), before washing and reconstitution

with buffer. The reconstituted solutions were then assayed for residual enzyme activity and apparent protein content (in BSA equivalents - BSAE). Stabilizing properties of the four sugars during drying and storage of alkaline phosphatase enzymes was rationalized based on their physicochemical properties described in Chapter III.

Outside of the theme of the majority of this thesis (Chapters I to V), Chapter VI describes the Karl Fischer moisture analysis of spray dried and crystalline sugars using the coulometric method and compares these results to those obtained by isothermal TGA. Chapter VII describes the method development for assay of alkaline phosphatase enzyme activity in solution and determination of protein contents (in terms of BSAE) using a dye binding assay. These two chapters were included to attest to the validity of those procedures which are used and quoted extensively in Chapters IV and V. Chapter VIII provides an overall summary of the thesis, especially as they relate to the original hypotheses.

II. HYPOTHESES AND SPECIFIC AIMS

II.a HYPOTHESES

1. A commercial bench top spray dryer may be used to produce dry respirably sized powders of four sugars; lactose, trehalose, sucrose and mannitol, suitable for inhalation purposes. These spray dried sugars may have different physicochemical stabilities at different relative humidities (with respect to particle size and crystallinity) compared to characterized sieve fractions of each sugar.

2. A novel particle collection apparatus may be designed, incorporating a custom built wire-in-tube type electrostatic precipitator. Such an apparatus, when coupled to a nebulizer, can be characterized with respect to its operating variables, for particle collection efficiency, using inert materials.

3. Once characterized the particle generation and collection apparatus assembly may be used to review the enzyme activities of two model enzymes following spray drying and electrostatic collection; this to assess the feasibility of stabilizing the model enzymes during drying and in the dried state, following co-drying with each of the four sugars:

lactose, trehalose, sucrose and mannitol.

4. The ability of each of the four sugars: lactose, trehalose, sucrose and mannitol to stabilize the model enzymes may be related to its capacity to form an amorphous glass during spray drying.

II.b SPECIFIC AIMS

1. To prepare spray dried forms of lactose, trehalose, sucrose and mannitol using a bench top laboratory spray dryer.
2. To prepare two size fractions (coarse and fine fractions) of the crystalline form of each sugar using sieve fractionation.
3. To characterize the particle size distribution of the spray dried sugars using the Aerosizer® with Aerodisperser®.
4. To characterize the sieve fractions and spray dried form of each sugar for moisture uptake and crystallinity changes using thermal analysis (TGA, DSC and Hot Stage Microscopy) and X-ray powder diffraction (XRPD).
5. To validate moisture content analysis by thermogravimetric analysis (TGA) using Karl Fischer analysis.
6. To characterize particle deposition in a spray drying and electrostatic precipitation apparatus, with respect to applied precipitator potential, temperature of droplet drying, volumetric air flow rate and concentration of the sprayed solution.

7. To spray dry and electrostatically collect bacterial alkaline phosphatase (BAP) and bovine intestinal alkaline phosphatase (BIAP) with or without the addition of four sugars; lactose, trehalose, sucrose and mannitol and to evaluate resultant enzyme specific activities.
8. To evaluate the storage stability of similarly spray dried enzyme-sugar molecular mixtures at 23% RH and 25 °C for 14 days.
9. To assess the ability of the four sugars to protect the enzymes during drying and storage and correlate this with their physicochemical properties in the spray dried form.
10. To evaluate the statistical significance of enzyme protection afforded by the four sugars during drying and storage of each alkaline phosphatase using analysis of variance.

III. PHYSICOCHEMICAL STABILITY OF CRYSTALLINE SUGARS AND THEIR SPRAY DRIED FORMS: DEPENDENCE ON RELATIVE HUMIDITY AND SUITABILITY IN POWDER INHALERS

III.a INTRODUCTION

Propellant-free, powder inhalers are being developed to avoid the problems associated with the replacement of CFCs in pressurized metered dose aerosols (Byron et al., 1994). They also show promise for the delivery of aerosolized peptides and proteins to the lung, prior to those compounds' systemic absorption (Byron and Patton, 1994; Patton and Platz, 1992). For both conventional drugs and macromolecules, the active ingredient is usually diluted with lactose (Ganderton and Kassem, 1992). From a toxicologic point of view however, most sugars are likely to be acceptable for this purpose. Powder formulations for conventional small molecular weight drugs, usually involve the preparation of an ordered mixture of a micronized (jet milled to < 5 μm, and respirable) crystalline drug, with a relatively free-flowing (larger particle sizes; > 40 μm) crystalline sugar, like alpha lactose monohydrate. The flow characteristics of the sugar aid in packaging, and emptying of the dosage form during use (Ganderton and Kassem, 1992). Ideally, drug particles should be attached to the surface of the larger carrier particles with forces of sufficient magnitude to prevent

de-segregation (during dosage form manufacture and storage); conversely, these interparticulate adhesion forces must be small enough to enable drug detachment from the carrier, in the turbulent airstream created by the patient's inhalation (Staniforth, 1994). Because different drugs have different adhesion properties, and these also depend on the excipient chosen as carrier, a larger excipient menu would be clearly useful.

Powder formulations for proteins may require excipient dilution for different reasons. Biological macromolecules can rarely be milled in conventional ways (Niven, 1993) and, although spray drying may be used to create respirable particulates (majority < 5 μm; Chawla et al., 1994; Naini et al., 1992), proteins may denature during the process. Thus, sugar-diluents have been used to stabilize proteins, both during drying and storage in the solid state (Carpenter et al., 1987; Franks et al., 1991; Broadhead et al., 1993; Labrude et al., 1989; Mumenthaler et al., 1994). However, sugar selection and the concentration dependence of stabilization, remain subjects for empirical review (Levine and Slade, 1992; Prestrelski et al.,1993). Similarly, because spray drying often leads to the formation of metastable, high energy amorphous forms (Matsuda et al., 1992; Vidgrén et al., 1987), which may recrystallize over time and render a formulation "non-respirable" (Byström and Briggner, 1994), some sugars may be more suitable than others as protein and peptide diluents in powder inhalers. Ideally, formulations should be unaffected by storage or use in different environmental conditions (Jashnani et al., 1995).

This chapter reviews the suitability of four different sugars for use as excipients in dry powder inhalers. Suitability of these sugars as carriers in DPIs for the purposes of this study was defined in terms of thermodynamic stability; recrystallization from the amorphous state during storage has an adverse effect on aerosolization behavior of DPI formulations. In addition, RH of the air throughput through a DPI may affect the respirable fraction of the dose emitted from the inhaler (Jashnani et al, 1995). Although this factor was not investigated in this study, its effect on selection of a particular sugar carrier is likely to be low. Each of the sugars: lactose, sucrose and mannitol are widely available in USP-NF pharmaceutical grades. Trehalose is currently being considered as a new excipient, because of its reported protein stabilization properties (Colaco et al., 1992). All four were assumed to be toxicologically acceptable for inhalation. Each sugar was characterized as spray dried respirable particulates, and two typical crystalline sieve fractions before and after 30 days storage at different relative humidities. Their physicochemical behavior is discussed as it relates to each sugar form's suitability as a powder inhaler excipient, along with the need to protect formulations from humidity induced changes in powder characteristics.

III.b MATERIALS AND METHODS

III.b.1 MATERIALS

D-Mannitol, Sucrose and α,α-Trehalose dihydrate were obtained from Sigma Chemical Company (St. Louis, MO). α-Lactose monohydrate was obtained from Foremost Ingredient Group (Baraboo, WI). Karl Fischer reagents Aquamicron-AS® and Aquamicron-CS® were obtained from Cosa Instrument Corp. (Norwood, NJ). All other chemicals used were obtained from Fisher Scientific Company (Raleigh, NC) and were of reagent grade quality.

III.b.2 METHODS

III.b.2.1 Sieve fractionation of sugars

All sugars were sieved in a Cenco-Meinzer sieve shaker (Central Scientific Co., Chicago, IL). Sucrose crystals were lightly crushed in a mortar, to comminute and remove agglomerates, prior to sieving; other sugars were sieved exactly as received. Sieve fractions, were retained which were thought representative of those used in inhalation products. These are designated "coarse fraction", A; 125-212 μm and "fine fraction", B; 44-74 μm, throughout this paper. After fractionation, A and B were retained in tightly closed amber bottles and stored in desiccators over

Table III.1 Experimental conditions for spray drying (Yamato ADL-31) of sugars from 10% w/v aqueous solutions

Condition	Lactose	Trehalose	Sucrose	Mannitol
Inlet Temperature (°C)[a]	150 (147-154)	125[b] (122-132)	125[b] (118-125)	150 (142-154)
Outlet Temperature (°C)[a]	70 (73-76)	70 (59-64)	70 (60-63)	70 (73-77)
Atomizing pressure (kgf/cm^2)[a]	3.0 (2.8-3.0)	3.0 (2.8-3.0)	2.8 (2.8-3.0)	3.0 (2.8-3.0)
Feed flow rate (ml/min)	10	10	10	10
Aspirator setting	4	2[c]	4	4

[a] Values are instrument settings (recorded ranges)

[b] 125 °C was used, since a crusty product was obtained when 150 °C was employed

[c] Aspirator setting was held at 2 to prevent powder loss from collection vessel into the air suction hose

phosphorous pentoxide prior to further study.

III.b.2.2 Spray drying of sugars

A 10% w/v aqueous solution of each sugar was spray dried using the Yamato ADL-31 Mini-Spray Dryer (Yamato Scientific America Inc., Orangeburg, NY). Inlet temperatures, atomizing pressure and other spray drying conditions are summarized in Table III.1. Spray dried sugars are designated C, throughout this chapter. Immediately after their collection, sugars were packed into tightly closed amber bottles and stored in desiccators, over phosphorous pentoxide, prior to further study.

III.b.2.3 Moisture sorption studies

Approximately, 2 g samples of each sugar in forms A, B and C were spread uniformly in open petri dishes (Cat. # 09-753-52A, Fisher Scientific Co., Raleigh, NC). Each of these was immediately transferred to a designated "desiccator vessel" (Cat # 08-595-2E, Fisher Scientific Co., Raleigh, NC), with a saturated salt solution in its base, for timed exposure to a fixed relative humidity (RH) environment (Callahan et al., 1982). Salts used, in excess at 25 °C, were potassium acetate (23% RH), magnesium chloride (52% RH), sodium chloride (75% RH) and potassium nitrate (93% RH). The desiccator vessels were housed inside an environmental cabinet (Model 435314, Hotpack, Philadelphia, PA), maintained at 25 °C. Samples were reanalyzed after 30 days storage.

III.b.2.4 Differential scanning calorimetry (DSC)

Samples of the crystalline coarse and fine sieve fractions (A and B), and the spray dried sugars (C; before and after 30 days storage at 25 °C and different relative humidities), were studied using a DSC 7 (Perkin Elmer, Norwalk, CT). Between 2 and 10 mg, accurately weighed in a crimp-sealed (non-hermetic) aluminum sample pan, was scanned at a heating rate of 10 °C/min under a nitrogen gas purge. An empty crimped pan served as the reference and all scans were performed in triplicate. The instrument was calibrated prior to sample analysis, using an indium standard (Perkin Elmer; melting point = 156.6 °C, ΔH_m = 28.45 J/g).

III.b.2.5 Thermogravimetric analysis (TGA)

Thermogravimetric analysis was performed on sugar forms A, B and C as defined above. Samples were weighed into open pans and studied in a Perkin Elmer TGS2 with a System 4 microprocessor controller (Perkin Elmer, Norwalk, CT). A heating rate of 10 °C/min was used at all times with a nitrogen gas purge. All scans were performed in triplicate. The instrument calibration check was performed using alumel (Perkin Elmer; magnetic transition temperature = 163 °C). After confirmation by Karl Fischer titration (below) the percentage of the initial weight which was lost during the (non-isothermal) heating process from 31 °C (weights equivalent to those determined under ambient conditions) to 160, 180, 200 and 200 °C (temperatures chosen as the midpoints of plateau regions) was ascribed to

the water content of sucrose, trehalose, mannitol and lactose respectively.

III.b.2.6 Particle size determination

Particle size distributions of spray dried sugars were determined using an Aerosizer®, equipped with AeroDisperser™ (Amherst Process Instruments, Inc., Hadley, MA) as described previously by Hindle and Byron (1995). Instrument settings were held constant with "shear force" = 0.5 psi, "size limit" = 220 μm, "feed rate" = 1000 particle counts/s with "pin vibration" activated and "deagglomeration" set to high. Size distributions were displayed and calculated using API Aerosizer MACH2 software V6.02.32 in terms of aerodynamic diameter. The values for true density (employed in the calculation of aerodynamic size distributions) were determined by helium pycnometry on the spray dried materials (Micromeritics Corporation, Norcross, Georgia) using an outgassing temperature of 27.7 °C.

III.b.2.7 Hot stage microscopy

Hot stage microscopy was performed as a diagnostic test on selected samples, to better interpret DSC thermal events. A Mettler FP 82 Hot Stage attached to a Mettler FP 80 Central Processor (Mettler Instrument Corp., Hightstown, NJ) was employed with a scanning rate of 10 °C/min and a nitrogen purge. The hot stage furnace was cross calibrated with the DSC 7 under these conditions using stearic acid and indium melting transitions

(69.1 and 156.6 °C, respectively). Sample behavior was observed under crossed polars using incident and transmitted light (Nikon Optiphot, Nikon, Tokyo, Japan).

III.b.2.8 X-ray powder diffraction

This was performed on both sieved sugars, A and B, prior to humidity testing. Spray dried sugars, C, were tested before and after 30 days exposure to different RH environments. Each powder sample was loaded into the sample holder of a Rigaku Geigerflex, Model 2028 X-ray diffractometer (Rigaku Denki Corp., Tokyo, Japan) and depressed with a glass slide, to produce a sample bed flush with the surface of the holder. Sugars which had recrystallized to form a fused mass at higher humidities were crushed to powder in a glass mortar prior to sample preparation. All samples were scanned between 2Θ = 5 to 45° under the following measurement conditions: target = Cu, filter = Ni, voltage = 35 kV and current = 22.5 mA. In preliminary experiments, angular positions of the most intense peaks for several of the sugars were compared to JCPDS (Joint Commission for Powder Diffraction Standards, 1974) data files to ensure accurate angular calibration of the instrument.

III.b.2.9 Karl Fischer moisture determination

Karl Fischer analysis was performed on the fine sieve fractions of all sugars prior to humidity testing, to confirm that the initial weight loss

recorded by TGA was due to dehydration. Analysis employed a Mitsubishi Moisture Meter, Model CA-05 (Mitsubishi Kasei Corp., Tokyo, Japan). Between 100 and 300 mg of each sugar was weighed accurately and dissolved in 10 ml of formamide; 400 µl of this solution was injected and titrated for water, coulometrically. A blank formamide injection was titrated prior to each sample injection. The water concentration of the blank was subtracted from the water content of the sample. Reported values are the mean of five such (sample - blank) determinations.

III.c RESULTS AND DISCUSSION

Much of the discussion to be centered around the physicochemical stability of the various forms of these sugars will rest upon the structures shown in Figure III.1 and the data shown graphically in Figures III.2 through III.5. Importantly, the X-ray powder diffraction patterns (Figures III.2 and III.3) and thermograms (Figures III.4 and III.5) are broad summaries which enable a discussion of the major physical transformations seen in these investigations. Tables III.2 through III.7, on the other hand, are condensed forms of the data collected during the many experiments performed in the study. They summarize, for lactose, trehalose, sucrose and mannitol, the precision of the calorimetric and thermogravimetric determinations and define, for future reference, ranges of values for water content, dehydration, recrystallization and melting temperatures and enthalpies, as functions of sample pretreatment and

Figure III.1 Molecular structures of sugars used in this investigation. Ring structures are numbered with and without primes ('), only for convenient textual reference. The structure of β-lactose is shown because a mixture of the α and β isomers forms quite rapidly in solution, following dissolution of α-lactose monohydrate in water.

4-*O*-β-D-Galactopyranosyl-D-glucopyranose

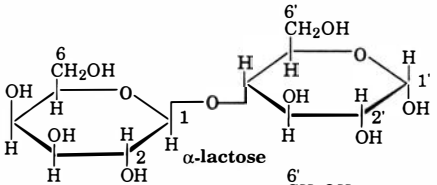

α-lactose

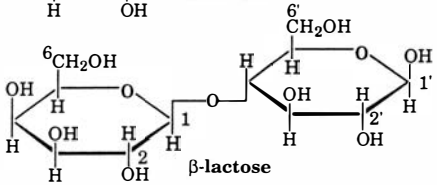

β-lactose

α-D-Glucopyranosyl α-D-Glucopyranoside

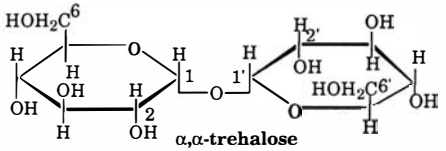

α,α-trehalose

β-D-Fructofuranosyl α-D-Glucopyranoside

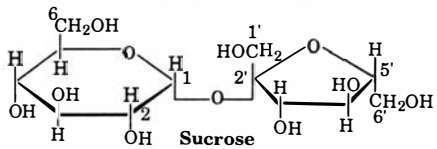

Sucrose

1,2,3,4,5,6-Hexanehexol

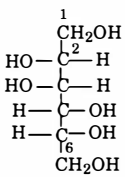

D-Mannitol

process variables. The data for water content for the various forms of each sugar, before and after storage at different relative humidities (Table III.2), is reported following thermogravimetric analysis for percent weight loss to the midpoint of each sugar's TGA plateau region (upper curve of the left frame for trehalose, Figure III.5, for example). These values were more precise than, and correlated well with, Karl Fischer titrations for water, as shown in footnote c of Table III.2.

III.c.1 Chemistry and kinetics of mutarotation

The chemistry involved in the transformation of alpha to beta lactose (Figure III.1; mutarotation requires ring opening at the ether linkage to the 1' anomeric carbon, rotation of the 1' - 2' bond and subsequent ring closure) is a prerequisite to the discussion of the chemical and physical instability of this "reducing sugar" (Pine, 1987a). Importantly, α and β lactose are chemically distinct isomers; they are not polymorphs or different crystal forms. Understanding the essentials of this subject further enables the selection of non-reducing sugars (eg. trehalose, sucrose and mannitol) which do not mutarotate significantly. Reducing sugars have ketone or aldehyde groups in their straight chain forms and have been shown to degrade freeze dried proteins in the solid state (Tarelli and Wood, 1981).

Sugars exist in both cyclic and straight chain forms in equilibrium, although one of these forms invariably predominates. Mutarotation of

hexoses, at rates likely to cause problems to the formulation chemist, only occurs when the straight chain form has an aldehyde or ketone at the C-1, anomeric carbon and an aliphatic alcohol at C-5. Under these circumstances, intramolecular alcohol addition occurs at the C-1 carbonyl group (Pine, 1987b) to form the hemiacetal or hemiketal respectively (lactose is a hemiacetal). For lactose, this process is shown diagrammatically in Scheme 1:

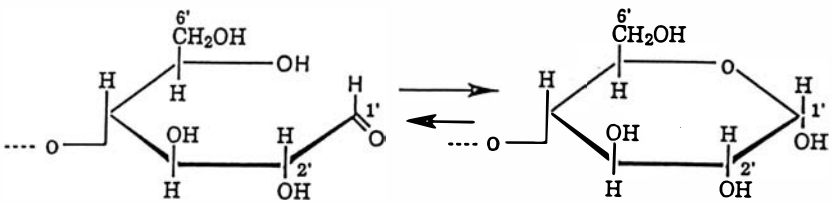

α-lactose (hemiacetal)

Scheme 1

In all cases, and thus, as a rule, the oxygen atom of the alcohol (on the 5' carbon of lactose) forms a bond with the carbonyl carbon atom (on the 1' anomeric carbon of lactose) of the aldehyde or ketone (lactose has an aldehyde in its straight chain form), and the hydroxy hydrogen atom (of the

alcohol) bonds to the carbonyl oxygen atom of the aldehyde or ketone (to form the hemiacetal or hemiketal, respectively). In the case of lactose, the ring opened, straight chain structure, has a 1' - 2' bond which can rotate freely. Ring closure, which is thermodynamically favored, thus forms a mixture of α and β lactose which differ with respect to the positioning of the 1'-hydroxy group (Figure III.1). Completing the story with respect to lactose, at 20 °C in aqueous solution, the equilibrium favors β–lactose for stereo-chemical reasons (62.8% β; Pigman and Anet, 1972). Thus during production, the alpha monohydrate is isolated preferentially from aqueous solutions by crystallization at cold temperatures, where its solubility is less than that of the β form (Handbook, 1986). However, when α–lactose is dissolved in water at 20 °C, mutarotation commences immediately with a half-life to equilibrium of 147.5 minutes (Pigman and Anet, 1972). Conversion of alpha lactose to the beta form has also been noted in the solid state in the present study and elsewhere (Otsuka et al., 1992).

In order to generalize, and determine whether mutarotation is likely to be a problem with other sugars, it is necessary to visualize the reaction, shown in Scheme 1, and follow the rules for it, in both directions. When sugars are shown in cyclic form (eg. sucrose and trehalose, Figure III.1), the oxygen in the ring(s) must be linked to a carbon atom with a directly attached hydroxyl group for ring opening (to produce a reactive aldehyde or ketone) to be favored. This is not the case for any of the ring oxygens of

trehalose or sucrose (which are therefore non reducing sugars); nor is it the case for lactose's second ring oxygen. Conversely, when sugars are shown in straight chain form (eg. mannitol, Figure III.1), they should not cyclize, and thus mutarotate, unless they contain a carbonyl group which can undergo alcohol addition. Thus mannitol is not a reducing sugar, nor does it have mutarotation problems.

III.c.2 Crystalline sieve fractions, A and B

III.c.2.1 Lactose

Usually isolated from cow's milk as a byproduct during cheese manufacture, alpha lactose monohydrate is readily obtainable in crystalline form and was recently the subject of the first harmonized pharmacopeial excipient monograph (USP23/NF18, 1994a). The crystal structure of alpha lactose monohydrate has been reported (Fries et al., 1971; Beevers and Hansen, 1971). From suppliers such as DMV (Veghel, The Netherlands) it is available in different particle size distributions (Hindle and Byron, 1995), some of which are preferred for use as drug diluents and carriers in powder inhalers. Both the coarse and fine sieve fractions prepared from Foremost brand alpha lactose monohydrate in this study behaved similarly. They were highly crystalline following sieve fractionation (Figure III.2, X-ray powder diffraction) and complied with compendial specifications for water content (4.5 to 5.5% by weight;

Table III.2 Moisture contents of sugars before and after 30 days storage at 25 °C and different relative humidities as determined by thermogravimetric analysis (TGA)

Sample	Temp. Range Used for Weight Loss	% Moisture Content[a]				
		Initial[b]	23% RH	52% RH	75% RH	93% RH
Lactose	31 - 200 °C					
Coarse fraction, A		4.83(0.14)	4.91(0.05)	4.95(0.05)	4.84(0.03)	4.65(0.03)
Fine fraction, B		5.34(0.12)	5.29(0.19)	5.21(0.12)	5.35(0.05)	5.33(0.20)
Spray dried, C		2.58(0.15)	5.08(0.34)	4.29(0.37)	4.94(0.30)	5.02(0.43)
Trehalose	31 - 180 °C					
Coarse fraction, A		9.12(0.16)	9.12(0.14)	9.21(0.07)	9.33(0.09)	9.30(0.04)
Fine fraction, B		8.87(0.06)[c]	8.95(0.04)	9.44(0.19)	9.53(0.05)	9.54(0.16)
Spray dried, C		4.09(0.27)	5.62(0.68)	9.50(0.08)	9.42(0.17)	9.46(0.13)
Sucrose	31 - 160 °C					
Coarse fraction, A		ND[d]	ND[d]	ND[d]	ND[d]	43.35[e]
Fine fraction, B		ND[c d]	ND[d]	ND[d]	ND[d]	41.24[e]
Spray dried, C		2.36(0.19)	4.57(0.33)	1.82(1.35)	ND[d]	40.04[e]
Mannitol	31 - 200 °C					
Coarse fraction, A		ND[d]	ND[d]	ND[d]	ND[d]	ND[d]
Fine fraction, B		ND[c d]	ND[d]	ND[d]	ND[d]	ND[d]
Spray dried, C		ND[d]	ND[d]	ND[d]	ND[d]	ND[d]

[a] Values are mean ± (experimental range), n=3; %Moisture = (weight loss/initial weight) x 100

[b] Stored in sealed bottles over P_2O_5 and tested on day zero and day 30

[c] Mean (sample SD, n=5) moisture contents of fine fractions as determined by Karl Fischer analysis were 5.1(0.8), 8.4(0.1), 0.03(0.06) and 0.02(0.06) for lactose, trehalose, sucrose and mannitol respectively.

[d] No detectable weight loss

[e] Sucrose dissolved in sorbed moisture at this RH. % Moisture contents determined from gross weight changes from initial sample weights (n=1).

Table III.3 Median aerodynamic diameters[a] for spray dried sugars based on volume distributions, as determined by Aerosizer® with Aerodisperser™

Sample	Median aerodynamic diameter (μm)	Geometric standard deviation
Lactose	5.56 (0.25)	1.64 (0.26)
Trehalose	5.23 (0.47)	1.64 (0.39)
Sucrose	12.53 (2.72)	2.18 (0.34)
Mannitol	4.79 (0.09)	1.46 (0.02)

a Values are averages (experimental ranges) of two determinations of the median aerodynamic diameter, where aerodynamic diameter= [equivalent spherical diameter x (density)$^{1/2}$]. Density was determined by helium pycnometry for spray dried lactose, trehalose, sucrose and mannitol as: 1.54,1.52, 1.53 and 1.43 g cm^{-3} respectively.

Table III.4 Summary of differential scanning calorimetry (DSC) results for lactose

Sample[a]	Glass Transition[b]		Dehydration[b]			Recrystallization[b]			Melting[b]		
	Onset (°C)	Midpoint (°C)	Onset (°C)	Peak (°C)	ΔH (J/g)	Onset (°C)	Peak (°C)	ΔH[c] (J/g)	Onset (°C)	Peak (°C)	ΔH (J/g)
A_0	ND[d]	ND[d]	144.8 (0.3)	149.5 (0.3)	125.1 (6.5)	ND[d]	ND[d]	ND[d]	211.8 (1.5)	219.2 (0.2)	135.0 (6.5)
B_0	ND[d]	ND[d]	143.6 (0.3)	148.9 (0.1)	133.2 (8.0)	ND[d]	ND[d]	ND[d]	207.7 (3.9)	217.1 (0.7)	127.4 (3.2)
C_0, $C_{30\,a}$	115.7 (1.3)	116.9 (0.9)	ND[d]	ND[d]	ND[d]	166.8 (0.5)	172.3 (1.0)	-111.4 (6.9)	211.5 (0.2)	215.8 (0.8)	132.8 (6.5)
$C_{30\,b}$	115.1 (0.9)	117.1 (0.1)	ND[d]	ND[d]	ND[d]	165.9 (0.1)	171.4 (0.0)	-106.4 (7.7)	211.4 (0.1)	215.5 (0.3)	127.4 (5.4)
$C_{30\,c}$	ND[d]	ND[d]	125.6 (2.4)	136.3 (2.3)	97.3 (6.3)	ND[d]	ND[d]	ND[d]	213.7 (0.7)	218.8 (0.8)	95.0 (12.7)
$C_{30\,d}$	ND[d]	ND[d]	134.5 (1.8)	142.0 (3.2)	125.2 (11.9)	ND[d]	ND[d]	ND[d]	214.0 (6.8)	219.2 (4.5)	99.2 (6.8)
$C_{30\,e}$	ND[d]	ND[d]	139.2 (1.1)	145.0 (2.1)	121.4 (18.4)	ND[d]	ND[d]	ND[d]	212.3 (1.7)	217.7 (0.9)	119.5 (6.7)

[a] A = Coarse fraction, B = Fine fraction and C = Spray dried. Subscripts 0 and 30 refer to before and after 30 days storage at 25 °C, in sealed bottles over P_2O_5 (a), 23% RH (b), 52% RH (c), 75% RH (d) and 93% RH (e).

[b] Values are mean ± (experimental ranges), n=3

[c] Negative values are exothermic enthalpies

[d] No detectable thermal event

Figure III.2 Typical X-ray diffractograms of lactose before (subscript 0) and after (subscript 30) storage for 30 days at 25 °C and different relative humidities. Key: A = coarse sieve fraction, B = fine sieve fraction, C = spray dried. Subscripts: a = stored in sealed bottles over P_2O_5; b - e were stored open at b = 23%, c = 52%, d = 75% and e = 93% RH. XRPD was not performed on coarse or fine sieve fractions after storage at different relative humidities.

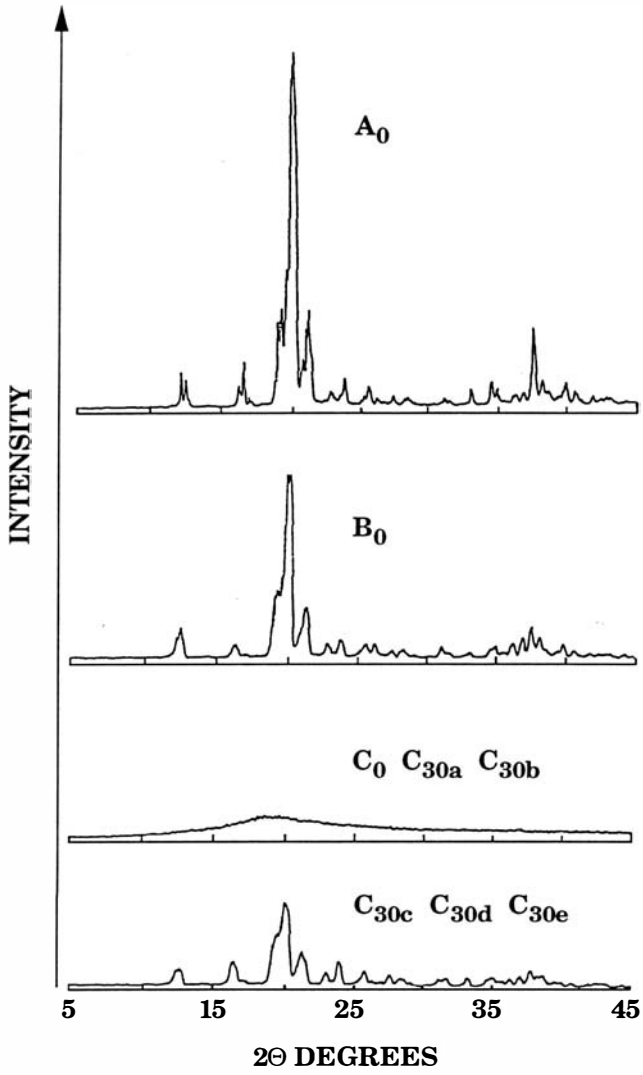
INTENSITY
A0
B0
C0 C30a C30b
C30c C30d C30e
5
15
25
35
45
2Θ DEGREES

USP23/NF18, 1994a) and theoretical calculation based on the 1:1 stoichiometry of alpha lactose monohydrate (5.0%; Table III.2, by thermogravimetric analysis). There was no significant tendency to sorb or lose water at any of the storage conditions tested over a 30 day period, for either the coarse (A = 125 - 212 μm) or the fine (B = 44 - 74 μm) sieve fractions (Table III.2), although the fine sieve fraction, B, had a higher overall water content (surface moisture, over its larger specific surface; Zografi, 1988). Scanning calorimetry showed that there were no significant differences between sieve fractions A and B, with respect to onset and peak dehydration or melting temperatures, or dehydration and melting enthalpies (Table III.4). Thermograms showed a dehydration endotherm (120 - 160 °C), a small recrystallization exotherm at 172 °C and a melting endotherm (in agreement with literature reports; Berlin et al., 1971; Raemy and Schweizer, 1983) between 190 and 225 °C. The microscopic size and appearance of the crystals, was unaffected by 30 days storage at different humidities, indicating that alpha lactose monohydrate was thermodynamically stable at 25 °C.

III.c.2.2 Trehalose

Extracted from both insect and vegetable sources, this disaccharide is a non-reducing sugar which is being explored for use as an excipient and cryoprotectant in lyophilized products (Carpenter et al., 1986). Clearly therefore, it is also a candidate for use as a diluent, stabilizer and/or carrier

with proteins and peptides in powder products for inhalation. The crystal structure of trehalose dihydrate has been reported (Taga et al., 1972; Brown et al., 1972). It was easily obtained as a stoichiometric dihydrate (theoretical water content = 9.5%) in crystal sizes ranging from approximately 20 through 250 μm; sieve fractionation of 1 kilogram provided 120 and 33 g of the coarse and fine sieve fractions respectively. Both sieve fractions behaved similarly with respect to their XRPD (Figure III.3) and water contents, although the fine sieve fraction, B, showed a tendency to sorb more water at increased relative humidities (Table III.2). This was unlike the behavior of lactose fraction B and appeared to be surface moisture associated with an increased weight fraction of smaller crystals (fines) in the trehalose as originally supplied (Zografi, 1988). Scanning calorimetry showed that there were no significant differences between the coarse and fine fractions with respect to their onset and peak melting temperatures and melting enthalpies (Table III.5). Thermograms showed dehydration and melting endotherms at 97 °C and 207 °C respectively (Table III.2 and Figure III.5). Its reported melting by Slade and Levine (203 °C, 1991) was consistent with our data, although the value reported in Merck Index (96 - 97 °C; Budavari, 1989) was clearly incorrect. When observed on the hot stage microscope under crossed polars, birefringence was lost beginning at approximately 92 °C (as confirmed recently by Taylor et al., 1994). However, those authors reported melting at 130 °C (followed by recrystallization from the melt, and a final melt at 215 °C) while we saw only a single melt at 207 °C on hot stage

Table III.5 Summary of differential scanning calorimetry (DSC) results for trehalose

Sample[a]	Glass Transition[b]		Dehydration[b]			Recrystallization[b]			Melting[b]		
	Onset (°C)	Midpoint (°C)	Onset (°C)	Peak (°C)	ΔH (J/g)	Onset (°C)	Peak (°C)	ΔH[c] (J/g)	Onset (°C)	Peak (°C)	ΔH (J/g)
A_0	ND[d]	ND[d]	91.2 (0.3)	97.7 (0.1)	206.4 (12.0)	ND[d]	ND[d]	ND[d]	201.5 (4.4)	207.4 (1.4)	130.5 (5.0)
B_0	ND[d]	ND[d]	89.8 (0.1)	96.1 (0.4)	220.2 (3.9)	ND[d]	ND[d]	ND[d]	204.9 (0.4)	207.9 (0.3)	141.2 (4.6)
C_0, $C_{30\,a}$	119.2 (0.5)	120.3 (0.2)	ND[d]	ND[d]	ND[d]	ND[d]	ND[d]	ND[d]	ND[d]	ND[d]	ND[d]
$C_{30\,b}$	118.7 (0.8)	120.1 (0.4)	ND[d]	ND[d]	ND[d]	ND[d]	ND[d]	ND[d]	ND[d]	ND[d]	ND[d]
$C_{30\,c}$	ND[d]	ND[d]	97.7 (0.3)	101.4 (2.4)	165.6 (9.0)	ND[d]	ND[d]	ND[d]	208.8 (6.8)	212.7 (2.5)	52.2[e] (66.4)
$C_{30\,d}$	ND[d]	ND[d]	96.8 (0.4)	100.8 (0.7)	170.3 (27.9)	ND[d]	ND[d]	ND[d]	208.1 (4.0)	211.9 (0.7)	53.5[e] (73.1)
$C_{30\,e}$	ND[d]	ND[d]	97.2 (0.4)	100.6 (1.3)	195.4 (24.7)	ND[d]	ND[d]	ND[d]	ND[d]	ND[d]	ND[d]

[a] A = Coarse fraction, B = Fine fraction and C = Spray dried. Subscripts 0 and 30 refer to before and after 30 days storage at 25 °C, in sealed bottles over P_2O_5 (a), 23% RH (b), 52% RH (c), 75% RH (d) and 93% RH (e).

[b] Values are mean ± (experimental ranges), n=3

[c] Negative values are exothermic enthalpies

[d] No detectable thermal event

[e] Melting behavior of recrystallized trehalose was not reproducible

Figure III.3 Typical X-ray diffractograms of trehalose, sucrose and mannitol before (subscript 0) and after (subscript 30) storage for 30 days at different relative humidities. Key: A = coarse sieve fraction, B = fine sieve fraction, C = spray dried. Subscripts: a = stored in sealed bottles over P_2O_5; b - e were stored open at b = 23%, c = 52%, d = 75% and e = 93% RH. XRPD was not performed on coarse or fine sieve fractions after storage at different relative humidities. No diffraction pattern is shown for spray dried sucrose, C_{30e}, which dissolved in its own sorbed moisture at 93% RH.

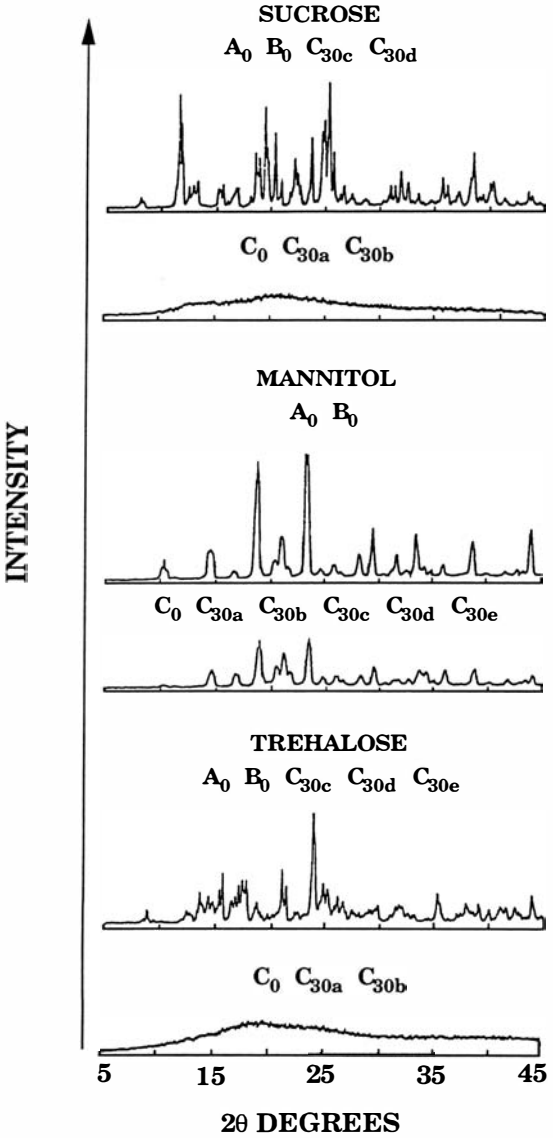
SUCROSE
A_0 B_0 C_{30c} C_{30d}
C_0 C_{30a} C_{30b}
MANNITOL
A_0 B_0
C_0 C_{30a} C_{30b} C_{30c} C_{30d} C_{30e}
TREHALOSE
A_0 B_0 C_{30c} C_{30d} C_{30e}
C_0 C_{30a} C_{30b}
INTENSITY
5
15
25
35
45
2θ DEGREES

Figure III.4 Typical TGA and DSC thermograms of lactose before (subscript 0) and after (subscript 30) storage for 30 days at different relative humidities. Key: A = coarse sieve fraction, B = fine sieve fraction, C = spray dried. Subscripts: a = stored in sealed bottles over P_2O_5; b - e were stored open at b = 23%, c = 52%, d = 75% and e = 93% RH. Only TGA was performed on A and B before and after exposure at different RH.

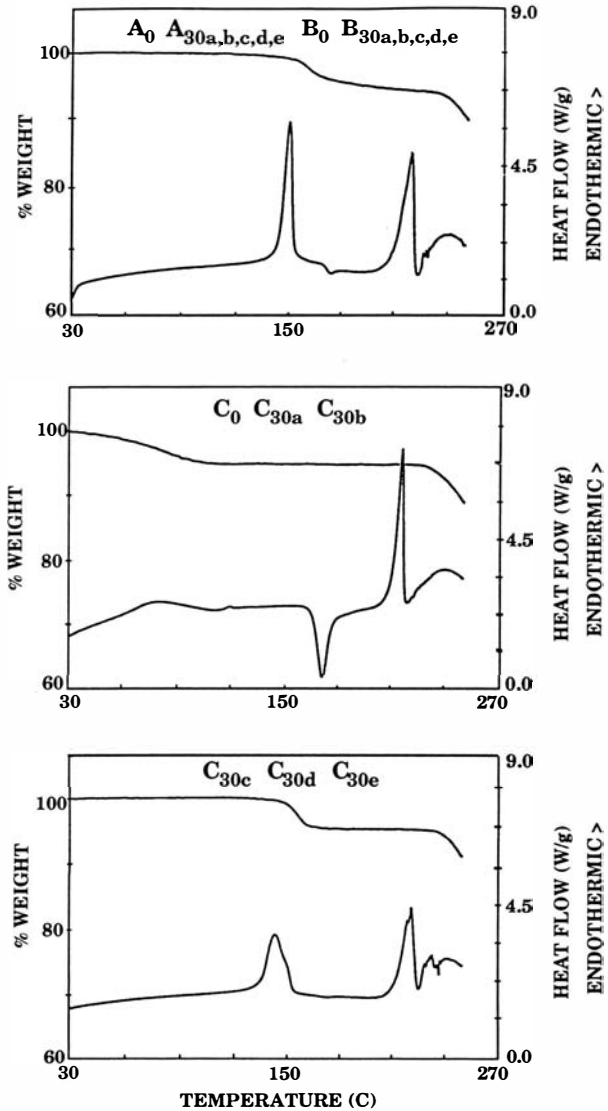
A0 A30a,b,c,d,e B0 B30a,b,c,d,e
C0 C30a C30b
C30c C30d C30e
% WEIGHT
HEAT FLOW (W/g)
ENDOTHERMIC >
100
80
60
9.0
4.5
0.0
30
150
270
TEMPERATURE (C)

and DSC, with no exotherms (for recrystallization) in the thermograms. The microscopic size and appearance of the crystals, was unaffected by 30 days storage at up to and including 93% RH, showing the thermodynamic stability of trehalose dihydrate at 25 °C.

III.c.2.3 Sucrose

Derived from a number of vegetable sources, sucrose can be obtained easily as anhydrous crystals (without water of crystallization). The crystal structure of sucrose has been reported (Brown and Levy, 1963). Crystal size of the material obtained from Sigma Chemical Co. (St. Louis, MO) was large (> 212 μm). Thus, it required comminution before use; sucrose from several other suppliers we reviewed was similar in this respect, meaning that there was substantial waste following sieve fractionation unless considerable size reduction was employed. This was avoided in this study, because of the possibility of creating a large amorphous content. Thus, 1 kilogram of the lightly crushed material provided only 30 and 18 g of the coarse and fine sieve fractions respectively. Both sieve fractions A and B behaved similarly; they were anhydrous and highly crystalline (Figure III.3). Scanning calorimetry showed that there were no significant differences between the coarse and fine fractions with respect to onset and peak melting temperatures and enthalpies (Table III.6). Thermograms (Figure III.5) showed a melting endotherm only, between 175 and 200 °C (in agreement with literature reports; Raemy and Schweizer, 1983; Roos, 1993)

Table III.6 Summary of differential scanning calorimetry (DSC) results for sucrose

Sample[a]	Glass Transition[b]		Dehydration[b]			Recrystallization[b]			Melting[b]		
	Onset (°C)	Midpoint (°C)	Onset (°C)	Peak (°C)	ΔH (J/g)	Onset (°C)	Peak (°C)	ΔH[c] (J/g)	Onset (°C)	Peak (°C)	ΔH (J/g)
A_0	ND[d]	ND[d]	ND[d]	ND[d]	ND[d]	ND[d]	ND[d]	ND[d]	186.8 (0.2)	189.5 (0.2)	123.4 (2.6)
B_0	ND[d]	ND[d]	ND[d]	ND[d]	ND[d]	ND[d]	ND[d]	ND[d]	188.1 (0.0)	189.8 (0.2)	130.2 (1.9)
C_0, $C_{30\,a}$	60.2 (2.8)	62.7 (1.0)	ND[d]	ND[d]	ND[d]	111.7 (13.7))	126.1 (5.2)	-82.9 (11.3)	186.5 (1.6)	188.8 (0.2)	120.8 (7.1)
$C_{30\,b}$	ND[d]	ND[d]	ND[d]	ND[d]	ND[d]	116.4[e] (4.4)	123.3[e] (1.0)	-18.6[e] (27.8)	187.1 (1.5)	188.7 (1.0)	109.6 (26.9)
$C_{30\,c}$	ND[d]	ND[d]	ND[d]	ND[d]	ND[d]	ND[d]	ND[d]	ND[d]	183.1 (1.4)	185.8 (0.5)	107.2 (3.0)
$C_{30\,d}$	ND[d]	ND[d]	ND[d]	ND[d]	ND[d]	ND[d]	ND[d]	ND[d]	182.4 (0.7)	185.2 (1.2)	102.4 (6.8)

[a] A = Coarse fraction, B = Fine fraction and C = Spray dried. Subscripts 0 and 30 refer to before and after 30 days storage at 25 °C, in sealed bottles over P_2O_5 (a), 23% RH (b), 52% RH (c) and 75% RH (d).
[b] Values are mean ± (experimental range), n=3
[c] Negative values are exothermic enthalpies
[d] No detectable thermal event
[e] Values are mean ± (experimental range), n=2

Figure III.5 Typical TGA and DSC thermograms of trehalose, sucrose and mannitol before (subscript 0) and after (subscript 30) storage for 30 days at different relative humidities. Key: A = coarse sieve fraction, B = fine sieve fraction, C = spray dried. Subscripts: a = stored in sealed bottles over P_2O_5; b - e were stored open at b = 23%, c = 52%, d = 75% and e = 93% RH. The second (melting) endotherm shown for trehalose, shown in the top left frame, was poorly reproducible for spray - dried material which had recrystallized on storage ($C_{30c,d,e}$). Sucrose, A_{30e}, B_{30e}, and C_{30e}, dissolved in sorbed moisture at 93% RH. Only TGA was performed on A and B before and after exposure at different RH.

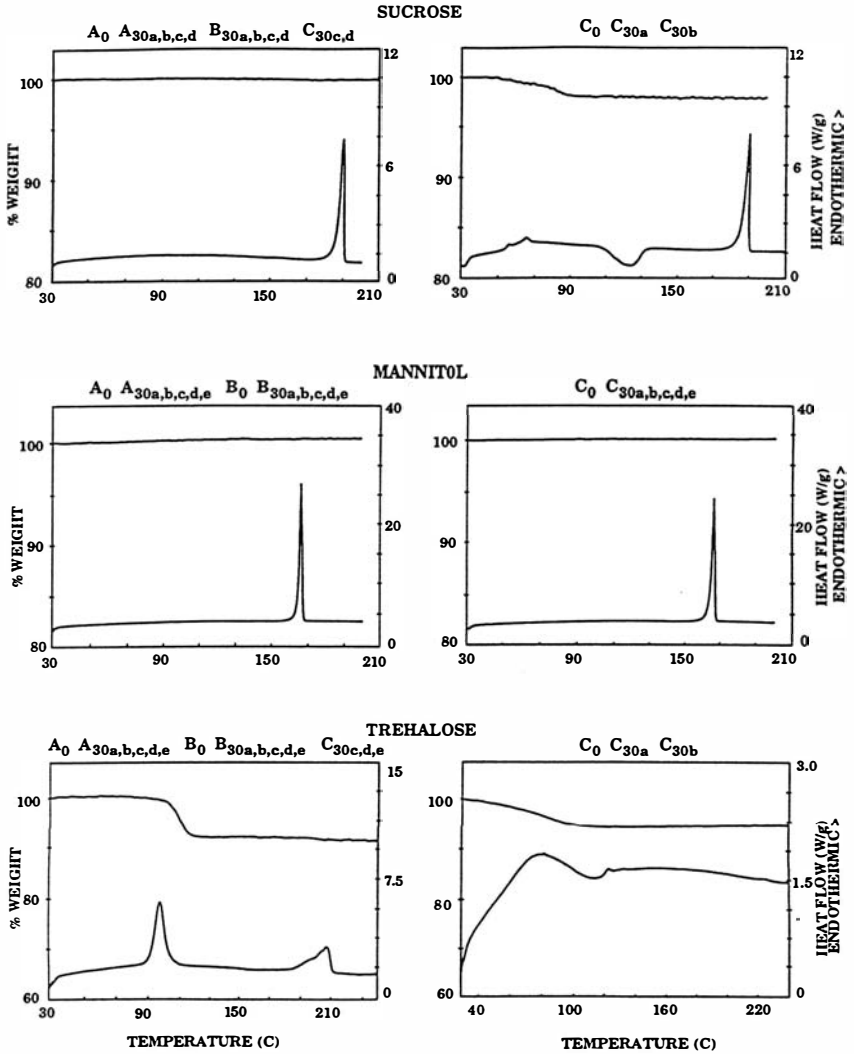
SUCROSE
A0 A30a,b,c,d B30a,b,c,d C30c,d
C0 C30a C30b
% WEIGHT
HEAT FLOW (W/g)
ENDOTHERMIC >
MANNITOL
A0 A30a,b,c,d,e B0 B30a,b,c,d,e
C0 C30a,b,c,d,e
TREHALOSE
A0 A30a,b,c,d,e B0 B30a,b,c,d,e C30c,d,e
C0 C30a C30b
TEMPERATURE (C)
TEMPERATURE (C)

with no dehydration event or detectable weight loss at up to 160 °C (Table III.2; sucrose melts at 188 °C). These characteristics, and the microscopic size or appearance of the crystals, were unaffected by 30 days storage at up to and including 75% RH, indicating the stability of anhydrous crystalline sucrose under most conditions at 25 °C. At 93% RH for 30 days however, crystalline sucrose dissolved in its own sorbed moisture (Table III.2) to form syrup (due to its known hygroscopicity and critical relative humidity = 84%; Makower and Dye, 1956; Van Campen et al., 1983).

III.c.2.4 Mannitol

Derived from seaweeds and by synthesis from other sugars, mannitol was obtained as anhydrous crystals (without water of crystallization). Crystal structures of several polymorphic forms of mannitol have been reported (Rye and Sorum, 1952; Berman et al., 1968). Crystal sizes ranged from approximately 10 through 260 μm; sieve fractionation of 1 kilogram provided 16 and 300 g of the coarse and fine sieve fractions respectively. Both sieve fractions A and B behaved similarly; they were anhydrous and highly *cry*stalline (Figure III.3). Scanning calorimetry showed that there were no significant differences between the coarse and fine fractions with respect to onset and peak melting temperatures and enthalpies (Table III.7). Thermograms (Figure III.5) showed a sharp melting endotherm only, between 150 and 175 °C (in agreement with literature reports; Raemy and Schweizer, 1983) and no dehydration event or detectable weight loss at up to

Table III.7 Summary of differential scanning calorimetry (DSC) results for mannitol

Sample[a]	Glass Transition[b]		Dehydration[b]			Recrystallization[b]			Melting[b]		
	Onset (°C)	Midpoint (°C)	Onset (°C)	Peak (°C)	ΔH (J/g)	Onset (°C)	Peak (°C)	ΔH[c] (J/g)	Onset (°C)	Peak (°C)	ΔH (J/g)
A_0	ND[d]	ND[d]	ND[d]	ND[d]	ND[d]	ND[d]	ND[d]	ND[d]	164.8 (0.1)	166.9 (0.4)	268.5 (22.4)
B_0	ND[d]	ND[d]	ND[d]	ND[d]	ND[d]	ND[d]	ND[d]	ND[d]	165.1 (0.4)	167.4 (1.1)	282.6 (11.5)
C_0, $C_{30\,a}$	ND[d]	ND[d]	ND[d]	ND[d]	ND[d]	ND[d]	ND[d]	ND[d]	163.9 (0.5)	166.3 (0.4)	297.8 (53.1)
$C_{30\,b}$	ND[d]	ND[d]	ND[d]	ND[d]	ND[d]	ND[d]	ND[d]	ND[d]	164.1 (0.1)	166.3 (0.2)	279.3 (52.9)
$C_{30\,c}$	ND[d]	ND[d]	ND[d]	ND[d]	ND[d]	ND[d]	ND[d]	ND[d]	164.2 (0.5)	166.3 (0.2)	276.5 (25.1)
$C_{30\,d}$	ND[d]	ND[d]	ND[d]	ND[d]	ND[d]	ND[d]	ND[d]	ND[d]	164.0 (0.2)	166.6 (0.5)	283.0 (28.3)
$C_{30\,e}$	ND[d]	ND[d]	ND[d]	ND[d]	ND[d]	ND[d]	ND[d]	ND[d]	164.4 (0.2)	166.3 (0.3)	275.4 (43.9)

[a] A = Coarse fraction, B = Fine fraction and C = Spray dried. Subscripts 0 and 30 refer to before and after 30 days storage at 25 °C, in sealed bottles over P_2O_5 (a), 23% RH (b), 52% RH (c), 75% RH (d) and 93% RH (e).

[b] Values are mean ± (experimental ranges), n=3

[c] Negative values are exothermic enthalpies

[d] No detectable thermal event

200 °C (Table III.2). These characteristics, and the microscopic size or appearance of the crystals, were unaffected by 30 days storage at and up to including 93% RH, indicating the stability of anhydrous mannitol at 25 °C. Closer examination of X-ray diffraction patterns of the crystalline fractions revealed that mannitol was in the β polymorphic form.

III.c.3 Spray dried sugars, C

The spray drying conditions for each sugar are listed in Table III.1. Spray drying particulates small enough for inhalation purposes required a high collection efficiency, small droplet spray dryer. Many commercial devices are inappropriate because their droplet dispersions are too large, thus demanding small nonvolatile concentrations (the alternative means of producing small particulates); this in turn, reduces efficiency by demanding long spray drying times. The Yamato ADL-31 and the nominal spray drying conditions for use with these sugars were chosen based on a systematic experimental review reported previously (Carvajal et al., 1994). Nominal spray drying conditions were held constant and close to optimal (Carvajal et al., 1994) for all four sugars. Reductions in the nominal inlet temperature of 150 °C (to 125 °C) were required in the case of sucrose and trehalose, which formed a crusty mass at 150 °C, instead of the free flowing material collected with the reduced inlet temperature; the aspirator setting was also reduced for trehalose, as described in Table III.1. All spray dried sugars were collected as apparently dry, free flowing powders, at rates ≥ 1

g/min, by cyclone separation. Table III.3 shows the apparent particle size distributions of each of the four products in terms of median aerodynamic diameters and geometric standard deviations, following replicate determinations using the Aerosizer® with Aerodisperser™. Results are expressed as aerodynamic diameters because of the common association of this term with the prediction of aerosol deposition in the lung (Byron, 1990b). With the exception of sucrose, which formed cohesive agglomerates [apparent median aerodynamic diameter = 12.5 μm; agglomerates failed to deaggregate even under high shear conditions (Hindle and Byron, 1995)], product median aerodynamic diameters were approximately 5 μm. Theoretically, spheres with identical diameters should vary in terms of their aerodynamic diameter if their densities are different (aerodynamic diameter = equivalent spherical diameter x density$^{1/2}$). Table III.3 shows that the median aerodynamic diameters of lactose, trehalose and mannitol ranked in order of product density, as predicted.

Lactose, sucrose and trehalose were all obtained in the amorphous form following spray drying, as expected (Matsuda et al., 1992; Elamin et al., 1995). None of these products showed birefringence under crossed polars and all three displayed a typical amorphous "halo" after X-ray powder diffraction (Figures III.2 and III.3). Conversely, and contrary to the conventional wisdom, which presumes that materials which are spray dried are amorphous, spray dried mannitol was birefringent under crossed polars and highly crystalline according to XRPD (Figure III.3). Spray

drying is usually believed to offer insufficient opportunity for nucleation and crystal growth because average droplet drying times are short (approximately 11 seconds in the Yamato ADL-31 under the operating conditions shown in Table III.1).

Attempts were made to quantify the amorphous content of the spray dried mannitol, C, before and after storage at different relative humidities. Assuming that the original material purchased from Sigma was effectively 100% crystalline, the decreases seen in peak height following XRPD could be crystal size and orientation effects (Cullity, 1978); there was no evidence, on the diffractograms for the spray dried mannitol, of an amorphous interference pattern (compare A and B to C, for mannitol in Figure III.3). Moreover, the spray dried material showed a statistically identical, storage and humidity independent, melting endotherm (Figure III.5, Table III.7). No significant difference (by single factor ANOVA) between melting endotherms of the crystalline starting materials and mannitol type C, stored under any study conditions were observed. There were no shifts from baseline in the calorimetric thermograms for type C, other than the melting endotherm (Figure III.5), and TGA profiles were also unchanged by spray drying or storage conditions (Table III.2). Exposure of the spray dried mannitol to high humidity in a microcalorimeter (VTI, Hialeah, FL) also failed to induce any observable recrystallization event. Thus, mannitol type C in these studies was, to all intents and purposes, 100% crystalline.

The amorphous form collected following spray drying of lactose,

trehalose and sucrose was unstable in the solid state at 25 °C, reverting to the crystalline form (forming sintered and cemented masses) in all cases at relative humidities $\geq$ 52%. Type C materials showing an amorphous halo after XRPD before storage (Figures III.2 and III.3) produced diffraction patterns which were indistinguishable from the original starting materials, indicating the return of identical crystal structures, after storage at RHs $\geq$ 52%. In the case of lactose, because the α and β isomers are known to have different crystal structures and diffraction patterns (Otsuka et al., 1991; the beta form has a major peak at $2\theta = 10°$, for example), there was no evidence of crystalline beta lactose in the XRPD data for the recrystallized, spray dried product. We estimated, based upon known mutarotation kinetics for lactose (Pigman and Anet, 1972), and a solution to dry product time difference of approximately 45 min, that 5 - 7% of the β-isomer was present in this spray dried lactose. In samples stored at 52 and 75% RH however, there was evidence of further alpha to beta mutarotation in the solid state (Figures III.4 and below), even though XRPD data failed to show its existence. We must conclude therefore, that the XRPD similarity between type A or B (pure α–lactose) and the recrystallized type C (α and β; Figure III.1) indicates that there was either insufficient of the recrystallized β–form for detection by XRPD, or that the β–form had not recrystallized (in the presence of α-lactose), or both.

None of the sugars, other than lactose, in this study, show mutarotation in solution and thus, the spray dried forms, C, of trehalose, sucrose and mannitol, do not contain mixtures of isomers. As a direct result of this observation, interpretation of the thermograms for these spray dried sugars was straightforward and is summarized in Tables III.5, III.6 and III.7. The amorphous trehalose and sucrose (C_0,$C_{30a,b}$) showed weight loss beginning at approximately 31 °C. Thus, moisture which was sorbed into the amorphous powders (Table III.2), following spray drying, was loosely bound (Zografi, 1988). During calorimetry, amorphous trehalose showed increasing energy requirements (climbing baseline) until the sorbed water was driven off, followed by a glass-to-rubber transition at about 120 °C (Table III.5) with no melting endotherm (Figure III.5; typical of an amorphous solid, behaving as a supercooled liquid). There was no recrystallization when calorimetry was performed in regular DSC pans, unlike the recent report (French et al., 1995), that spray dried trehalose recrystallized at 134 °C during scanning calorimetry in hermetically sealed pans. Water, which is retained during heating in the hermetically sealed pans, can enhance molecular mobility (Zografi, 1988) and this probably enabled recrystallization under those circumstances. Amorphous sucrose (Table III.6), on the other hand, showed a "glass transition" during the evolution of sorbed water (approximately 60 °C), a recrystallization exotherm (confirmed by hot-stage microscopy), at about 125 °C and a resultant melting endotherm between 180 and 190 °C. Following moisture induced

recrystallization for 30 days at RH $\geq$ 52%, the thermal behavior of sucrose and trehalose became typical of the original crystalline materials.

Spray dried lactose thermograms, before and after the solid state recrystallization events described above (RH $\geq$ 52%), are complicated by the presence of an admixture of the α and β isomers in the product; the ratio of the two is frequently variable in spray dried lactose (Lerk, 1993). Thus, the results shown in Figure III.4 and Table III.4 for lactose type C, may well be different if the ratio of the isomers in the sample is different. While the onset of weight loss for amorphous, spray dried lactose (Figure III.2, $C_0, C_{30a,b}$ - check) was also 31 °C, the results of calorimetry showed an initial broad endotherm corresponding to loss of sorbed moisture, a glass transition (T_g) at 117 °C, an exothermic recrystallization event at 172 °C and a melting endotherm at 216 °C. The value for T_g was as expected, and was typical of those for dry sugars, after the loss of sorbed water (Roos and Karel, 1991; Hancock and Zografi, 1994, Saleki-Gerhardt and Zografi, 1994). Following moisture induced recrystallization, enthalpies of dehydration and melting (Table III.4), were lower than the expected values for crystalline α-lactose monohydrate. This was indicative of variations in the content of β-lactose; the progressive decrease in the enthalpy of melting (Table III.4, type C, with increasing RH to 75%) showing the continuing mutarotation of lactose in the solid state at moderately high relative humidities (Otsuka et al., 1990). The sample stored at 93% RH however,

showed the increased stability of α-lactose monohydrate, once in the crystalline form. In this case of very high humidity, recrystallization occurred very rapidly and before substantive further mutarotation could occur in the amorphous glass. Thus, in this sample, stored at 93% RH, the content of β-lactose was similar to that of the original spray dried product. Also, in the samples stored at 52% RH and 75% RH (Figure III.4) there was a small endotherm at around 230 °C, the melting point of anhydrous β-lactose (Berlin, 1971).

Spray dried lactose, trehalose and sucrose showed moisture uptake at all relative humidites with or without changes in their physical form. At 23% RH all three sugars showed increased moisture contents relative to their initial values (Table III.2). However no crystallization was detected in these samples by DSC (Figures III.4 and III.5) and XRPD (Figures III.2 and III.3) in the time frame of exposure, i.e. after 30 days. Although the XRPD pattern for spray dried sucrose stored at 23% RH showed an amorphous halo (Figure III.3), similar to the one obtained prior to exposure, it did not show a clear T_g or a recrystallization exotherm on DSC (Figure III.5). This may be because, the increased moisture content accelerated the crystallization process during heating in the DSC. Moreover, amorphous spray dried sucrose has been shown to remain in the amorphous form at this RH, within the time frame employed in this study (Makower and Dye, 1956).

III.d SUMMARY AND CONCLUSIONS

This work was initiated to dovetail with other investigations of crystalline drug carriers (with different interparticulate bonding strengths and/or electrostatic behavior; Hindle et al., 1994) and aerosolizable spray drying excipients with the capacity to protect some proteins against denaturation (Naini et al., 1993). At present, lactose is the only acceptable carrier for dry powder inhalation systems in the United States. However, all sugars obtained as crystalline sieve fractions in this investigation appeared to be suitable for admixture with micronized drugs and presentation in powder inhalers, at least at an investigational level. Only crystalline sucrose, which dissolved in its own sorbed moisture at 93% RH, appeared to require extraordinary packaging precautions, in order to protect against moisture induced formulation changes in high humidity environments. There was no evidence of mutarotation of alpha lactose monohydrate, at any of the storage humidities (water contents and calorimetry were unchanged), showing the rigidity and stability of its crystal structure at 25 °C (mutarotation in the solid state requires molecular mobility). It remains to be seen whether all of these sugars will also afford the apparent short-term moisture protection (Hindle et al., 1994), seen with aerosolization of albuterol sulfate in the presence of lactose at high humidites. That drug formed cohesive agglomerates over a < 3 minute time frame, when aerosolized in the absence of a lactose diluent (Jashnani et al., 1995). These examples are cited to illustrate the importance of an

improved menu of substances for use in powder inhalers. It is likely that alternate crystalline sugars can be used to advantage in powder inhalers, when a given drug blend with lactose has been shown to perform poorly (Phillips et al., 1994).

Spray dried sugars stored at high humidities showed predictable recrystallization changes over time with the exception of mannitol. Mannitol defied conventional wisdom and crystallized during the brief (11 sec) spray drying period, prior to collection and storage. While its behavior with co-spray dried solutes was not studied here, its capacity to form stable, humidity independent crystallites, during spray drying, was surprising and unique among this array of sugars. Mannitol is a non-reducing sugar and, as we have discussed above, our efforts to show the presence of even small amounts of amorphous content in the spray dried bulk were unsuccessful. Mannitol should certainly be studied further for its capacity to afford molecular protection to proteins during drying and storage; development of crystalline formulations for powder inhalers may be easier than their amorphous counterparts, both from a packaging and aerosolization point of view.

Spray dried formulations, which are respirable (Table III.3) are likely to have to deal with at least some amorphous content which will require protection against humidity induced changes. Spray dried sucrose was intensely hygroscopic and difficult to deaggregate even under dry conditions. Trehalose and lactose, formed sintered masses over 30 days at

humidities > 23%. Although the kinetics of solid state recrystallization were not studied here, these changes can be rapid and must not be allowed to occur in powder inhaler formulations. Thus, both powder packaging and the water content of the inlet air to the inhaler should be controlled for such products. Provided this can be achieved, and thus powder deaggregation made to occur reproducibly, the choice of a particular sugar as an excipient may well depend upon its stabilizing capacity (against protein denaturation and chemical degradation). Lactose, as described above, is a potentially reactive reducing sugar, which may preclude its use with certain proteins. It has the further disadvantage that spray dried products are bound to be mixtures of both the α and β isomers. The ratio can only be considered constant if the solution from which spray drying has occurred has either stood for 6 - 7 mutarotation half lives (about 17 hours at 20 °C) or, if the spray drying conditions are very carefully controlled and the product is kept dry (to prevent further mutarotation). If sucrose and lactose are rejected for the above reasons, mannitol may be unsuitable (for protection against protein denaturation) because a sugar's protein stabilizing capacity is believed to require its presence as an amorphous glass (with its glass transition temperature, in the presence of any sorbed moisture, above that of the storage temperature). Trehalose, with a high glass transition temperature in its dry state, and a tendency to retain relatively large amounts of moisture without recrystallizing, may have excellent stabilizing properties in this regard (Green and Angell, 1989).

IV. CHARACTERIZATION AND OPTIMIZATION OF SPRAY DRYING AND ELECTROSTATIC PRECIPITATION APPARATUS FOR COLLECTION OF INHALABLE MICROPARTICLES

IV.a INTRODUCTION

Spraying of aqueous solutions of drug followed by droplet drying has been used as an alternative to jet milling to produce particles for inhalation in the laboratory (Chawla et al., 1994; Vidgren et al., 1987). Such a technique can also be used for producing fine particles of proteins and peptides for potential administration through the lung (Broadhead et al., 1994). However, in the developmental stage, large amounts of expensive protein are required for solution formulation and drying optimization (Foster and Leatherman, 1995). In addition, until recently, most commercially available laboratory spray dryers had low spraying and collection efficiencies for small particles (< 5 μm). Thus, in order to review protein activity following spray drying and to study the affect of various sugars on protein stability during drying (Chapter V), an apparatus capable of collecting fine particles, following spraying of low concentration aqueous solutions was necessary.

Commercially available nebulizers like the small particle aerosol generator (SPAG, ICN Pharmaceuticals) are capable of atomizing low

solids concentration aqueous solutions into fine droplets (Byron et al.,1988; May, 1973). Such droplets could be dried by supplying further warm air to the droplets prior to particle collection. Fine particles suspended in the air stream could then be charged and separated inside an electrostatic precipitator, which, at least in theory is capable of collecting fine particles to a high degree of efficiency (Hinds, 1982; Oglesby and Nichols, 1978).

A particle collection apparatus, assembled using the principles outlined above was initially characterized with respect to electrostatic precipitator voltage and starting solute concentration. In addition the collection efficiency was evaluated as a function of volumetric air flow and temperature of drying air. This chapter describes these experiments as a precursor to the work described in Chapter V and also attempts comparisons between experimental and theoretical collection efficiencies calculated using known precipitator geometry and particle charging theory.

IV.b MATERIALS AND METHODS

IV.b.1 MATERIALS

Lactose NF (Paddock Laboratories, Minneapolis, MN) and disodium fluorescein (Fisher Scientific Company, Raleigh, NC) were used as received. All other chemicals used were of reagent grade quality and were purchased from Fisher Scientific Company (Raleigh, NC). Water used was

deionized by reverse osmosis.

IV.b.2 METHODS

IV.b.2.1 Particle collection apparatus

The particle collection apparatus, incorporating a small particle aerosol generator (SPAG, ICN Pharmaceuticals, Costa Mesa, CA) and an in-house built wire-in-tube electrostatic precipitator, is shown in Figure IV.1. The exploded views of different parts of the apparatus with exact dimensions are shown in Figures IV.2 and IV.3. Aqueous solutions were placed inside the reservoir of the nebulizer (A, Figure IV.1) and atomized by supplying compressed air. The inlet pressure on the nebulizer was kept constant at 26 psig (SPAG Instructions Manual, ICN Pharmaceuticals, Costa Mesa, CA, 1989). Nebulizer air flow (NA, Figure IV.1) was adjusted to 7 liters/min and the drying air flow (DA, Figure IV.1) was held at 10 liters/min. Aerosols exiting the primary drying chamber (B, Figure IV.1) were introduced into a secondary drying chamber (C, Figures IV.1 and IV.2). Additional drying air was supplied to a cylindrical chamber C, by means of a hot air gun (D, Figure IV.1). In some experiments the air flow and temperature of the hot air gun, D, were independently controlled by means of two variable autotransformers (E & F, Figure IV.1) and temperature of drying air inside the chamber C was measured by a thermometer (H, Figure IV.1). Air flows through the complete apparatus

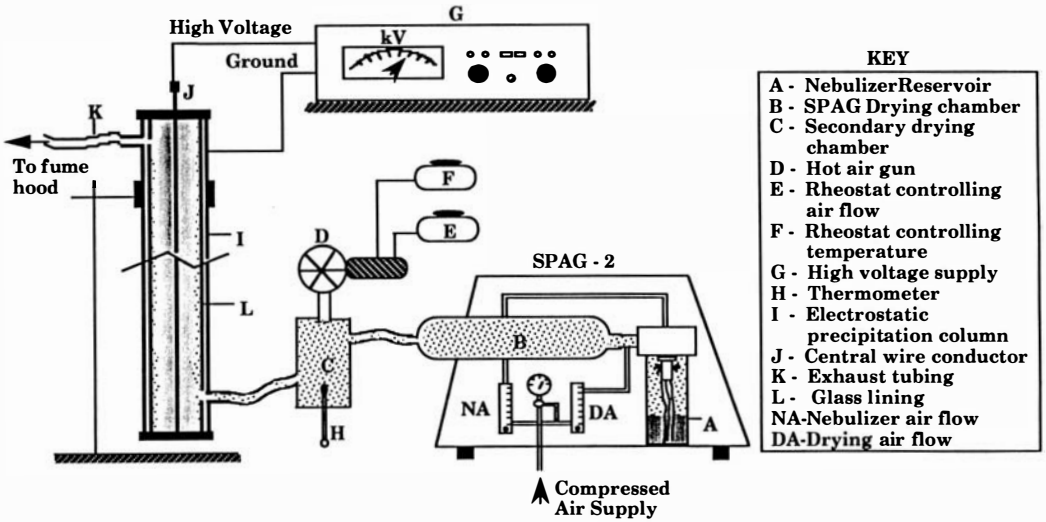

Figure IV.1 Schematic diagram of the particle collection apparatus.

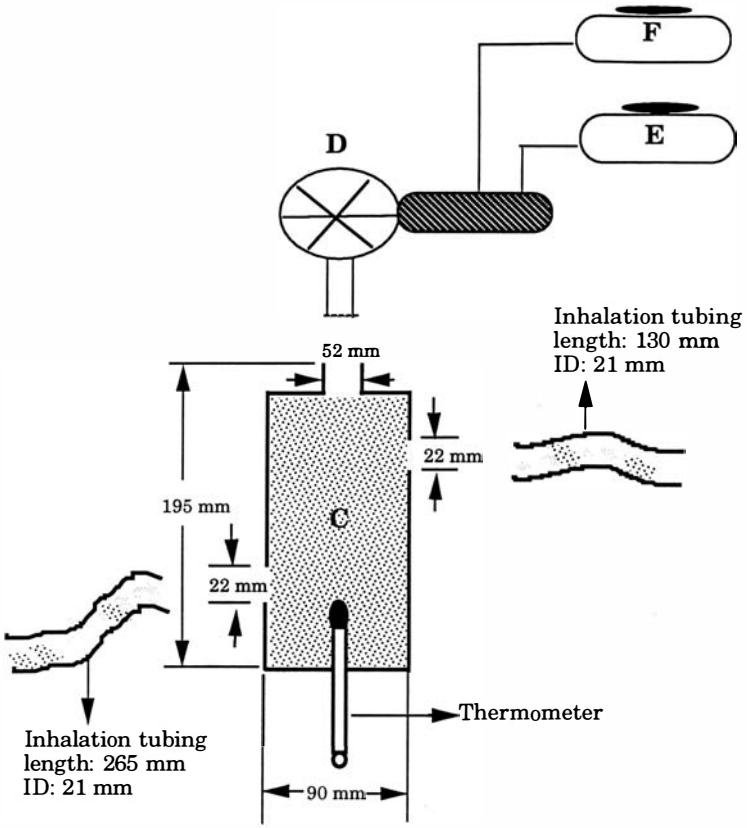

Figure IV.2 Exploded view of the secondary drying chamber C, with dimensions. The inhalation tubes shown in this figure were considered as part of the drying chamber for particle recovery purposes.

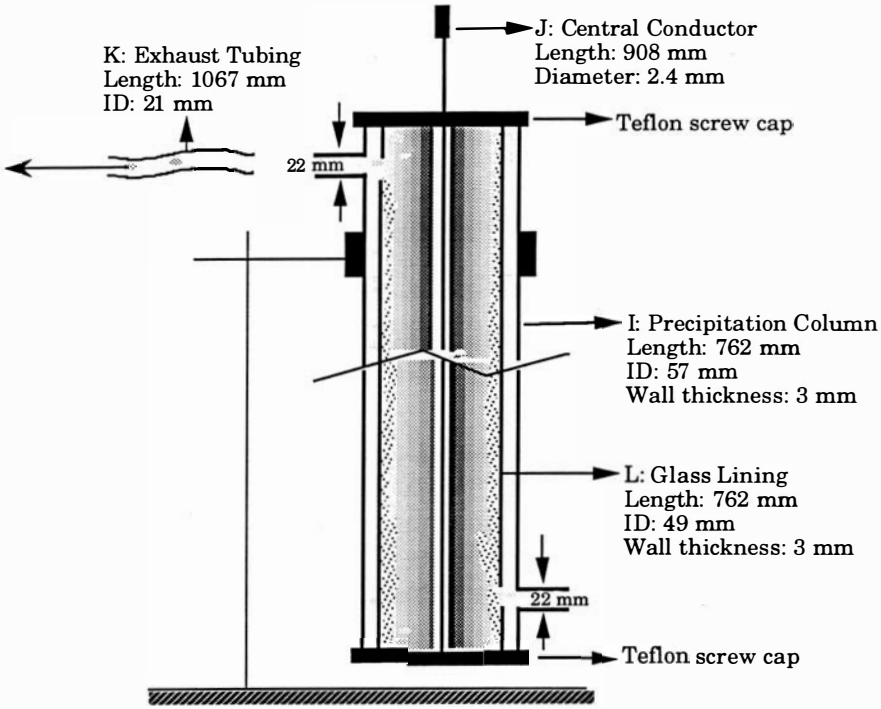

Figure IV.3 Exploded view of the electrostatic precipitation column shown with the central wire conductor, glass lining and exhaust tube with dimensions.

were measured using a micromanometer connected to a pneumotachograph head placed at the end of the exhaust tubing (K, Figure IV.1), in sham experiments (in the absence of nebulized solutions) at different settings of the autotransformer controlling air flow of the heat gun (A detailed description of calibration of the pneumotachograph with air flow measurement can be found in Appendix AII). Particles were then collected in a wire-in-tube type electrostatic precipitator column (I, Figures IV.1 and IV.3). High voltages in the range of 0 - 20 kV (negative polarity) were applied to the central wire conductor (J, Figures IV.1 and IV.3) by means of a high voltage generator (G, Figure IV.1; Model #2807R, Brandenburg/Astec, Alpha II Series, Stourbridge, UK). Aerosols were generated and collected inside the column (I, Figures IV.1 and IV.3) for lengths of time in the range of 10 min to 30 min, dictated by experimental requirements. At the end of each experiment the apparatus was dismantled and the column (I, Figure IV.1), exhaust tubing (K, Figures IV.1 and IV.3), secondary drying chamber (C, Figures IV.1 and IV.2) and the primary drying chamber (B, Figure IV.1) washed with sufficient volume of 0.1 N NaOH solution, and fluorescein was spectrophotometrically detected at 490 nm (Varian DMS 100S UV-VIS Spectrophotometer, Varian Associates, Walnut Creek, CA). Total solids deposition per minute at each of these sites was estimated following fluorescein determination from the mass ratio of fluorescein to lactose in the initial solution (1:19).

At the beginning of each run total output from the nebulizer

(operating at NA and DA of 7 liters/min and 10 liters/min respectively) was isokinetically collected (vacuum flow rate = aerosol supply rate) on an absolute glass fiber filter (Gelman Sciences, Ann Arbor, MI) through which air was drawn, in order to determine the mass output of fluorescein and lactose per minute of nebulization. Deposition at each of the above described sites was calculated as a percentage of the total solids output from the nebulizer. Particles failing to deposit at any of the four sites were estimated as "Losses".

IV.b.2.2 Effect of electrostatic precipitator (EP) voltage, nebulized solution concentration and hot air gun voltage on collection efficiency

In these experiments, particles were collected inside the column (I, Figure IV.1) without the glass collection surface. Also, in preliminary characterization experiments, temperature and volumetric air flow of drying air being supplied to drying chamber C (Figure IV.1) were not independently varied. Only a single autotransformer was used to control the hot air gun (D, Figure IV.1) and voltages supplied to the fan and heating coils were identical. Collection characteristics of the apparatus were quantified using aqueous solutions of lactose and fluorescein (19:1 weight ratio). A range of solution concentrations between 10 - 75 mg/ml of total solids (1 - 7.5% w/v) and hot air gun voltages settings between 0 - 60 V (by adjusting the autotransformer) were tested. Solutions (100 ml volume at time zero in reservoir A, Figure IV.1) were nebulized for different lengths

of time, collected in different regions of the apparatus and quantified as described above.

IV.b.2.3 Effect of drying air flow and temperature on particle collection efficiency

In these experiments a glass collection surface (L, Figure IV.1) was introduced inside the precipitator column (I, Figure IV.1) identical to that which was to be employed in protein drying experiments (Chapter V). This facilitated washing and recovery of particles with low volumes of solvent, prior to analysis. This was important when the apparatus was used for protein particle collection following nebulization of low concentration solutions (Chapter V). Also, drying air supplied to chamber C (Figure IV.1) was independently controlled for temperature and volumetric air flow, in order to assess the effect both of these variables on particle collection efficiency.

Aqueous solutions of disodium fluorescein and lactose were used with a total concentration of 10 mg/ml (1% w/v) in a weight ratio of 1:19. Fifty milliliters (50 ml) solutions were nebulized, dried and electrostatically collected for 15 min. At the end of 15 min the apparatus was dismantled and different parts of the apparatus, including the glass collection surface (L, Figure IV.1) were washed with 0.1 N NaOH, prior to spectrophotometric detection of fluorescein at 490 nm. Total solids were calculated from the weight ratio of fluorescein and lactose in the initial solution (1:19) as before.

Two targeted air temperatures of 30 °C and 40 °C as measured by a thermometer (H, Figure IV.1) in chamber C (Figure IV.1) were used. Volumetric air flows of 29.1 liters/min and 50.6 liters/min, calculated as described above and in Appendix AII were studied. At the beginning of each experimental run, total solids output per minute from the nebulizer was calculated by isokinetically collecting the output on an absolute glass fiber filter for 10 min. Particle recovery in each of the components of the apparatus per unit time was expressed as a percentage of the total rate of solids output.

IV.b.2.4 Photomicrography and scanning electron microscopy of electrostatically precipitated particles

Aqueous lactose solutions in concentrations of 10 mg/ml, 50 mg/ml and 75 mg/ml were nebulized, dried (hot air gun voltage of 60 V) and electrostatically collected at 20 kV onto glass slides placed inside the precipitator column (I, Figure IV.1) for 15 min. These slides were then photographed (Nikon N2000 camera, Tokyo, Japan) under a microscope (Nikon Optiphot, Tokyo, Japan) using a x40 magnification objective in order to assess their appearance.

In separate experiments a 1% w/v solution of fluorescein and lactose (mass ratio of 1:19) was nebulized and dried at different temperatures (as recorded in chamber C, Figure IV.1). Three different temperatures were studied: 29 °C, 41 °C and 63 °C. Scanning electron microscope (SEM) stubs

were introduced inside the precipitator column (I, Figure IV.1) and particles were electrostatically collected at each of the drying temperatures and an air flow of 29 liters/min and an applied EP voltage of 20 kV. At the end of 15 min collection the stubs were removed, sputter coated with gold-palladium followed by scanning electron microscopy.

IV.b.2.5 Theoretical particle collection efficiencies during electrostatic precipitation

Theoretical collection efficiencies inside the precipitator column were calculated using particle charging theory and known precipitator geometry. Efficiencies were calculated using the Deustch-Anderson equation (Hinds, 1982; Oglesby and Nichols, 1978):

$E' = 1 - e^{(-V_{TE} * A/Q)}$ ..... Equation IV.1

where E' = Collection efficiency

V_{TE} = Terminal electrostatic velocity

A = Collection surface area

and Q = Volumetric air flow rate

The terminal electrostatic velocity, V_{TE} is given by (Hinds, 1982):

$V_{TE} = neE/(3\pi\mu d)$ ..... Equation IV.2

where E = Electric field strength

n = Number of charges on a particle

μ = Viscosity of air

e = Charge on an electron

and d = Diameter of the particle

Electric field strength for a wire-in-tube type electrostatic precipitator can be calculated from (Hinds, 1982):

$E = \Delta W/[r_t \ln (r_t / r_w)]$ ..... Equation IV.3

where ΔW = Difference in voltage between wire and tube

r_t = Radius of tube

r_w = Radius of wire

Collection efficiencies were calculated assuming particle Reynold's numbers > 1, indicating turbulent air flow (Hinds, 1982), and an assumed uniform particle size distribution of 1 μm for the SPAG generator (Byron et al., 1988) and also when dried at 40 °C as seen from the SEM. A description of field charging theory used to calculate number of charges (n) on the particles with a sample efficiency calculation is given in Appendix AI.

IV.c RESULTS AND DISCUSSION

IV.c.1 Spray drying and electrostatic precipitation

The "Small Particle Aerosol Generator" or SPAG is a modified three jet Collison nebulizer (SPAG Instructions Manual, ICN Pharmaceuticals, Costa Mesa, CA, 1989; Appendix AIX).The SPAG was driven by compressed gas, which passed through an external pressure compensated

flowmeter (NA, Figure IV.1) before entering the nebulizer. This facilitated a reliable reading when the NA flowmeter was operated at 7 liters/min, but has been reported to be less accurate when operated at lower air flows (Byron et al., 1988). The DA (Figure IV.1) flow meter on the other hand has been shown to give reliable readings at all flow rates (Byron et al., 1988). Due to expansion of the high pressure air jets inside the nozzle, there is a reduction of static pressure which causes the solution to be drawn up the three nebulizer tubes (Venturi effect). This is then broken up by the air jet into a dispersion of droplets (May, 1973). In SPAG a majority of these droplets impact on the walls of the nebulizer reservoir which are then recirculated. This enables only fine droplets to escape the reservoir.

To facilitate drying of droplets in the primary drying chamber (B, Figure IV.1) a maximum drying air flow (DA, Figure IV.1) of 10 liters/min was used. The incoming compressed air was kept at 26 psig by means of the SPAG pressure regulator as recommended by the manufacturer. An external compressed gas source of 50 psig was used throughout.

Electrostatic precipitation has been traditionally used in industrial air pollution control of particulate emissions (White, 1963 and Robinson, 1973). The process is based on the principle of charging particles in a corona discharge generated under high electric field strengths. In a wire-in-tube type electrostatic precipitator (used in this study), when high voltages are applied to the central wire conductor, a highly non-uniform electric field develops close to the wire (Oglesby and Nichols, 1978). This

field accelerates the electrons in the surrounding gas to high velocities, causing ionization of the gas in the region around the wire. This phenomenon is called a corona discharge. The ions thus generated migrate towards the outer passive electrode (column inner surface maintained at ground potential in this case). If a gas laden with particles is introduced inside the precipitator column, the ions get attached to the particles, imparting an electric charge. This charge acquisition by the particles allows them to migrate towards the column inner surface where they are deposited. Deposition efficiency depends on several factors like number of charges acquired by the particles, electric field strength, volumetric air flow through the system, particle size distribution, electrical conductivity or resistivity of the particles and particle re-entrainment in the air stream (Oglesby and Nichols, 1978; and Hinds 1982). The deposited particles are held on to the surface by a combination of electrical and molecular forces (Oglesby and Nichols, 1978).

IV.c.1.1 Effect of electrostatic precipitator (EP) voltage, nebulized solution concentration and hot air gun voltage on collection efficiency

These preliminary experiments were performed to characterize particle deposition with respect to EP voltage, nebulized solution concentration and hot air gun voltage (fan supply voltage = heating coil

Table IV.1 Percentage collection efficiencies[a] in the particle collection apparatus as a function of electrostatic precipitator (EP) voltage[b,c,d]

EP Voltage (kV)	Exit Tube-K[e]	Dryer-C[e]	Dryer-B[e]	Column-I[e]	Losses
0.0	1.9 (0.9)	1.1 (0.3)	1.8 (0.6)	0.8 (0.1)	94.4 (0.9)
7.7	3.0 (1.7)	1.8 (0.8)	2.3 (0.3)	28.7 (6.9)	64.3 (5.2)
10.0	2.9 (1.6)	2.4 (1.5)	2.4 (0.7)	24.5 (6.9)	67.8 (10.3)
17.8	3.0 (1.4)	2.4 (1.5)	2.5 (0.7)	39.9 (14.6)	52.2 (13.1)
20.0	0.8 (0.3)[f]	1.5 (0.4)[f]	2.7 (1.0)[f]	63.5 (14.8)[f]	31.5 (14.0)[f]

a Collection efficiencies are expressed as percentages of total solids output rate from the nebulizer, estimated by isokinetic collection on an absolute glass fiber filter.
b In these experiments air flow and temperature of the hot air gun (D, Figure IV.1) were not controlled independently. Also no glass collection lining (L, Figure IV.1) was used inside the column (I, Figure IV.1).
c Hot air gun voltage (as in text) and nebulized solution concentration were kept constant at 60 V and 10 mg/ml respectively.
d Values are mean (sample SD), n=3.
e The letters K, C, B and I correspond to different components in Figure IV.1.
f Values are mean (sample SD), n=6.

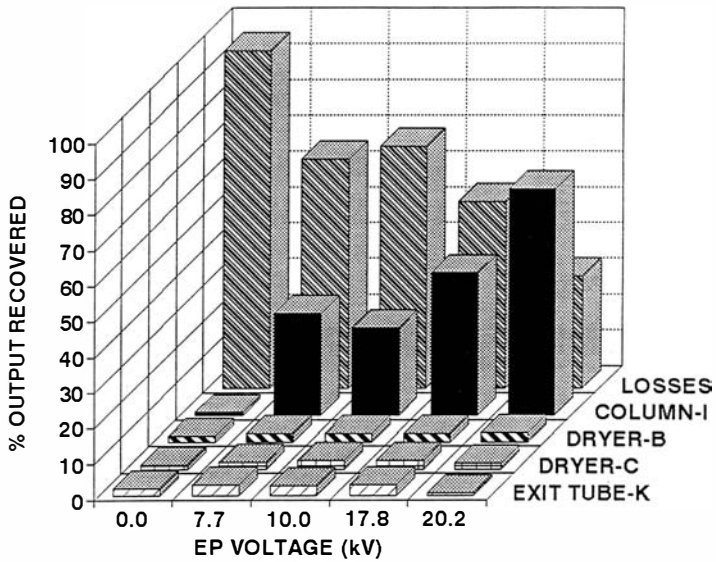

Figure IV.4 Effect of electrostatic precipitator (EP) voltage on deposition in the apparatus. In these experiments hot air gun voltage and nebulized solution concentration were kept constant at 60 V (both heating coil supply and fan motor supply were 60 V) and 10 mg/ml respectively. Particles inside the column were collected on the metal inner column surface without the glass lining (Figure IV.3).

voltage = hot air gun voltage). Particle collection efficiencies [calculated as percentage of the total solids output from the nebulizer (A, Figure IV.1)] as a function of EP voltage are given in Table IV.1. The mean percentage collection efficiencies are also plotted in Figure IV.4. These experiments were performed with a fixed solution concentration of 10 mg/ml and a hot air gun voltage setting of 60 V. As can be seen from Figure IV.4, particle collection in the exit tube-K, dryer-C and dryer-B was minimal. Particles were either collected inside the precipitator column (I, Figure IV.1) or lost to the exhaust ("Losses"). Percentage of the total output recovered inside the column-I increased with increasing EP voltage, although only a 64% maximum recovery was possible at 20 kV (Table IV.1), the maximum voltage which could be maintained with this voltage generator.

Percentage collection efficiencies as a function of nebulized solution concentration are given in Table IV.2 and the mean values are plotted in Figure IV.5. These experiments were performed at a constant EP voltage of 20 kV and hot air gun voltage setting of 60 V. Once again percentage of output recovered in the exit tube-K, dryer-C and dryer-B was minimal. Although the total mass of particles depositing in the column increased with increasing solution concentration, the percentage of each solution's total solids output which was collected in the column, decreased with increasing solution concentration. This may be due to increased particle build up on walls of the column, at higher solids concentration, which causes less efficient charging and deposition of subsequent particles

Table IV.2 Percentage collection efficiencies[a] in the particle collection apparatus as a function of nebulized solution concentration[b,c,d]

Concentration (mg/ml)	Exit Tube-K[e]	Dryer-C[e]	Dryer-B[e]	Column-I[e]	Losses
10.0	0.8 (0.3)[f]	1.5 (0.4)[f]	2.7 (1.0)[f]	63.5 (14.8)[f]	31.5 (14.0)[e]
25.0	1.1 (0.1)	1.3 (0.1)	4.6 (0.7)	37.7 (2.4)	55.3 (2.6)
50.0	2.2 (0.5)	2.7 (0.1)	4.9 (1.2)	32.2 (6.7)	57.9 (7.6)
75.0	2.9 (0.4)	3.8 (0.9)	3.9 (0.9)	25.8 (11.4)	63.6 (9.3)

a Collection efficiencies are expressed as percentages of total solids output rate from the nebulizer, estimated by isokinetic collection on an absolute glass fiber filter.
b In these experiments air flow and temperature of the hot air gun (D, Figure IV.1) were not controlled independently. Also glass collection lining (L, Figure IV.1) was not used inside the column (I, Figure IV.1).
c Hot air gun voltage and EP voltage were kept constant at 60 V and 20 kV respectively.
d Values are mean (sample SD), n=3.
e The letters K, C, B and I correspond to different components in Figure IV.1.
f Values are mean (sample SD), n=6.

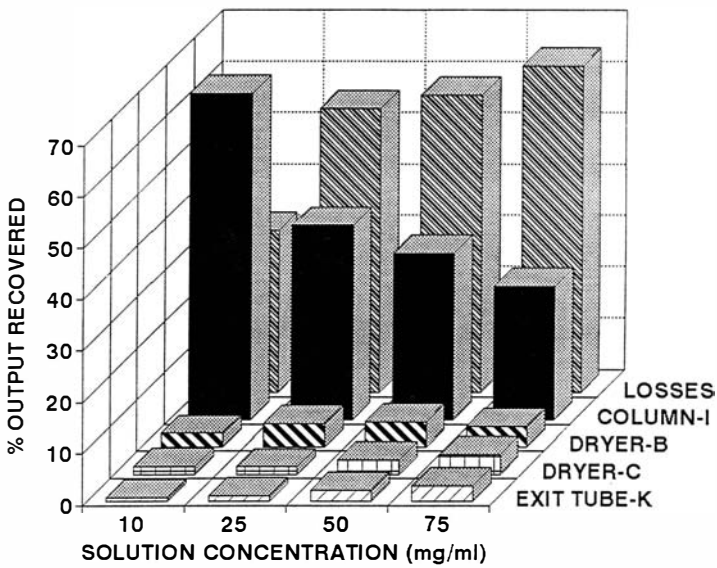

Figure IV.5 Effect of nebulized solution concentration on deposition in the apparatus. In these experiments hot air gun voltage and EP voltage were kept constant at 60 V (both heating coil supply and fan motor supply were 60 V) and 20 kV respectively. Particles inside the column were collected on the metal inner column surface surface without the glass lining (Figure IV.3).

(White, 1951). Reduced collection efficiency could also be due to increased particle re-entrainment in the air stream with the larger overall amounts being deposited per minute with higher solution concentrations in the nebulizer (White, 1963).

Table IV.3 and Figure IV.6 show deposition patterns in the apparatus for different voltage settings on the autotransformer controlling the hot air gun. These experiments were performed at an EP voltage of 20 kV and a solution concentration of 10 mg/ml (1% w/v). Voltage settings of 0 - 60 V did not affect the fractional deposition in the column (ranged between 59 - 64%). However when the hot air gun voltage setting was increased to 90 V almost 88% of the output was recovered in the column. This may be a result of faster water evaporation from the nebulized droplets producing particles which because of their smaller size exhibit higher capture efficiencies and larger electrophoretic mobility. However in these experiments the combined effects of air flow and drying air temperature could not be distinguished.

Photomicrographs of particles recovered inside the column following nebulization and drying are shown in Figure IV.7. Particles appeared dry, discrete and relatively monodisperse with respect to size in all cases. Although drying of higher solids concentrations produced larger particles, the majority of the particles observed under the microscope were $< 5\ \mu m$ for all three solutions (10 mg/ml, 50 mg/ml and 75 mg/ml).

Table IV.3 Percentage collection efficiencies[a] in the particle collection apparatus as a function of heat gun voltage[b,c,d]

Hot Air Gun Voltage (V)	Exit Tube-K[e]	Dryer-C[e]	Dryer-B[e]	Column-I[e]	Losses
0	0.8 (0.2)	1.6 (0.5)	3.3 (0.5)	62.8 (15.8)	31.5 (15.3)
30	0.5 (0.1)	1.0 (0.2)	3.3 (0.2)	58.8 (1.3)	36.4 (1.2)
60	0.8 (0.3)[f]	1.5 (0.4)[f]	2.7 (1.0)[f]	63.5 (14.8)[f]	31.5 (14.0)[f]
90	0.2 (0.0)	1.5 (0.2)	3.7 (0.8)	87.8 (5.3)	6.9 (4.8)

a Collection efficiencies are expressed as percentages of total solids output rate from the nebulizer, estimated by isokinetic collection on an absolute glass fiber filter.
b In these experiments air flow and temperature of the heat gun (D, Figure IV.1) were not controlled independently. Also glass collection lining (L, Figure IV.1) was not used inside the column (I, Figure IV.1).
c Nebulized solution concentration and EP voltage were kept constant at 10 mg/ml and 20 kV respectively.
d Values are mean (sample SD), n=3.
e The letters K, C, B and I correspond to different components in Figure IV.1.
f Values are mean (sample SD), n=6.

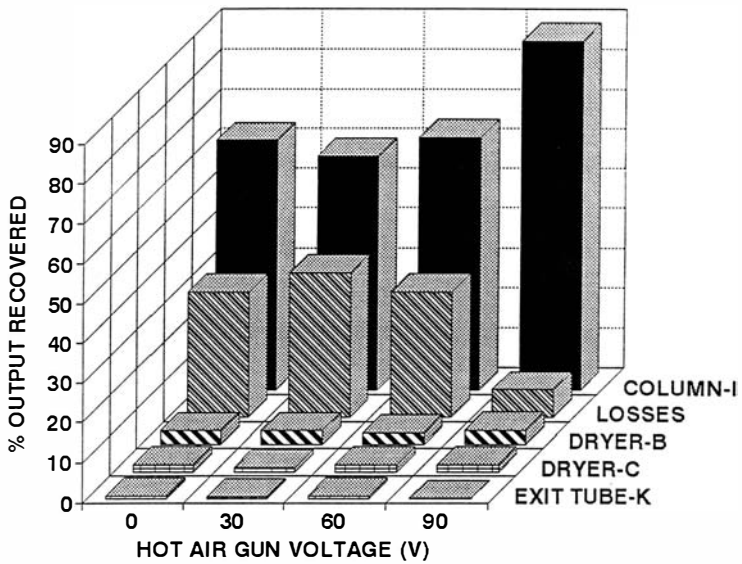

Figure IV.6 Effect of hot air gun voltage (heating coil supply and fan motor supply) on deposition in the apparatus. In these experiments nebulized solution concentration and EP voltage were kept constant at 10 mg/ml and 20 kV respectively. Particles inside the column were collected on the metal inner column surface without the glass lining (Figure IV.3).

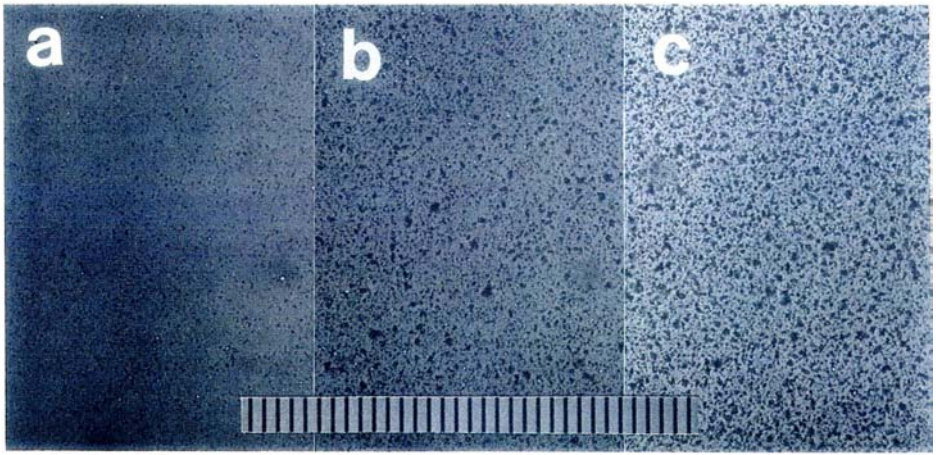

Figure IV.7 Photomicrographs of lactose particles collected from the electrostatic precipitator. The nebulized solution concentration was (a) 10 mg/ml (b) 50 mg/ml and (c) 75 mg/ml without the glass lining and collected at an EP voltage of 20 kV and hot air gun voltage of 60 V. All photomicrographs were taken at the same magnification (x40). The distance between the scale marks is 10 μm.

IV.c.1.2 Effect of drying air flow and temperature on particle collection efficiency

In order to better characterize the electrostatic collection process, drying air temperature and flow rate were independently varied. This was achieved by modifying the circuitry of the hot air gun and by attaching it to two autotransformers (D and E, Figure IV.1). Particle deposition was studied at two air flow rates of 29.1 $\pm$ 0.8 liters/min and 50.6 $\pm$ 1.5 liters/min and two mean temperatures for the mixed air and aerosol leaving dryer-C (Figure IV.1). Air flow measurements were made by operating the apparatus under solution free conditions and are described in Appendix W. Summary of the percentage collection efficiencies obtained under different air flow and temperature conditions are given in Tables IV.4 - IV.7 and Figure IV.8 - IV.11. Percentage of the output deposited in the column increased with increasing precipitator potential (EP voltage) at all flow rates and temperatures employed. However particle deposition in the column was dependent on the total air flow rate. Increased deposition was observed at the lower air flow rate of 29.1 liters/min compared to 50.6 liters/min at both the drying temperatures (Figures IV.8 - IV.11). This implied that the collection efficiency was a simple function of the particle residence time inside the column. Although temperature is known to affect the collection efficiency by altering the corona generating voltage and particle size of the collected particles, no differences were noted in the deposition in the column for different drying temperatures under

Table IV.4 Summary of particle collection efficiencies[a] at a drying temperature of 28.4 °C (1.8)[b] and volumetric air flow of 29.1 liters/min (0.8)[c] as a function of electrostatic precipitator voltage

EP Voltage (kV)	Exit Tube-K[d]	Dryer-C[d]	Dryer-B[d]	Column-I[d]	Losses
5	1.6 (0.7)	2.4 (0.3)	3.7 (1.6)	20.3 (1.3)	72.1 (0.6)
10	0.9 (0.2)	2.3 (0.3)	4.9 (1.8)	29.9 (1.7)	61.9 (3.1)
15	1.0 (0.2)	2.9 (0.5)	5.4 (2.1)	41.6 (2.5)	49.1 (1.4)
20	0.6 (0.0)	2.7 (0.2)	7.4 (1.6)	45.3 (3.1)	44.0 (3.7)

[a] Collection efficiencies are expressed as percentages of total solids output rate from the nebulizer, estimated by isokinetic collection on an absolute glass fiber filter.Values are mean (sample SD), n=3.

[b] Rheostat F (Figure IV.1) controlling temperature of hot air gun was set between 30 - 32 V and temperatures recorded in dryer C (Figure IV.1). Value is mean (sample SD), n=12.

[c] Rheostat E (Figure IV.1) controlling air flow to hot air gun was set at 8 V (Appendix AII). Value is mean (sample SD), n=3

[d] The letters K, C, B and I correspond to different components in Figure IV.1.

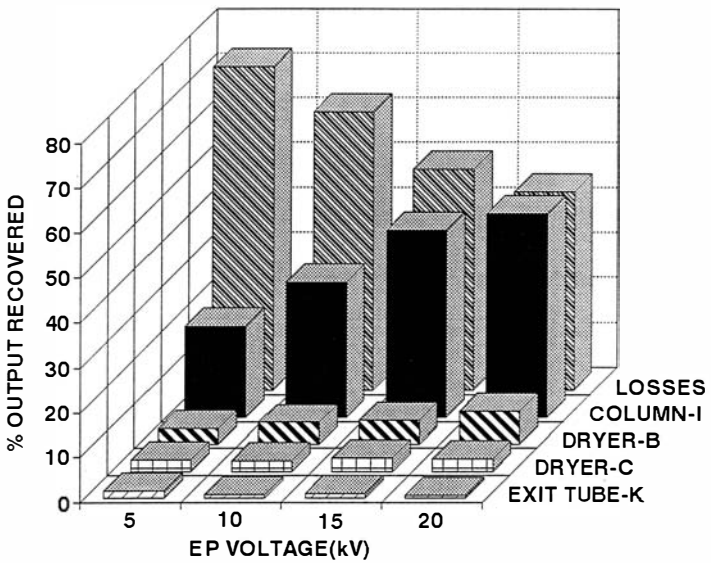

Figure IV.8 Deposition in the apparatus following spray drying and electrostatic collection of 10 mg/ml solution at 28 ± 2 °C (rheostat F, kept between 30 - 32 V and temperatures were measured in dryer C, Figure IV.1) and a volumetric air flow of 29.1 ± 0.8 liters/min (rheostat E, Figure IV.1, kept at 8 V, Appendix AII). In these experiments the particles were collected on glass lining (L, Figure IV.3).

Table IV.5 Summary of particle collection efficiencies[a] at a drying temperature of 41.0 °C (0.7)[b] and volumetric air flow of 29.1 liters/min (0.8)[c] as a function of electrostatic precipitator (EP) voltage

EP Voltage (kV)	Exit Tube-K[d]	Dryer-C[d]	Dryer-B[d]	Column-I[d]	Losses
5	0.7 (0.4)	1.8 (0.8)	4.0 (3.0)	18.9 (0.5)	74.6 (3.3)
10	1.0 (0.2)	2.2 (0.5)	8.4 (1.6)	30.6 (1.0)	57.8 (1.6)
15	1.2 (0.3)	2.3 (0.9)	4.7 (2.3)	41.8 (1.8)	50.0 (1.5)
20	0.8 (0.1)	3.0 (0.6)	6.2 (1.5)	45.2 (3.8)	44.8 (3.0)

[a] Collection efficiencies are expressed as percentages of total solids output rate from the nebulizer, estimated by isokinetic collection on an absolute glass fiber filter.Values are mean (sample SD), n=3.

[b] Rheostat F (Figure IV.1) controlling temperature of hot air gun was set between 50 - 58 V and temperatures recorded in dryer C (Figure IV.1). Value is mean (sample SD), n=12.

[c] Rheostat E (Figure IV.1) controlling air flow to hot air gun was set at 8 V (Appendix AII). Value is mean (sample SD), n=3

[d] The letters K, C, B and I correspond to different components in Figure IV.1.

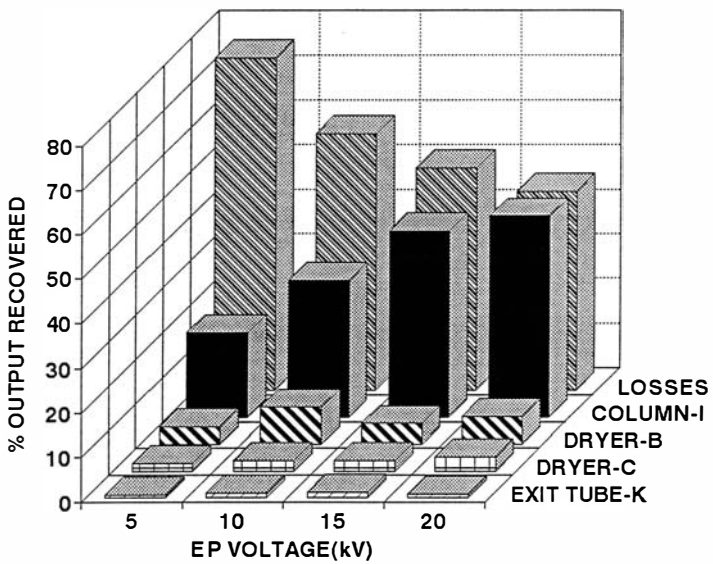

Figure IV.9 Deposition in the apparatus following spray drying and electrostatic collection of 10 mg/ml solution at 41 $\pm$ 1 °C (rheostat F, kept between 50 - 58 V and temperatures were measured in dryer C, Figure IV.1) and a volumetric air flow of 29.1 $\pm$ 0.8 liters/min (rheostat E, Figure IV.1, kept at 8 V, Appendix AII). In these experiments the particles were collected on glass lining (L, Figure IV.3).

Table IV.6 Summary of particle collection efficiencies[a] at a drying temperature of 26.8 °C (0.7)[b] and volumetric air flow of 50.6 liters/min (1.5)[c] as a function of electrostatic precipitator (EP) voltage

EP Voltage (kV)	Exit Tube-K[d]	Dryer-C[d]	Dryer-B[d]	Column-I[d]	Losses
5	0.9 (0.7)	2.7 (1.1)	5.3 (2.3)	15.1 (2.2)	76.1 (2.4)
10	1.0 (0.3)	2.9 (0.8)	5.1 (0.3)	26.2 (0.9)	64.8 (1.8)
15	1.1 (0.3)	2.3 (0.7)	2.8 (0.6)	36.9 (1.4)	57.0 (0.9)
20	0.8 (0.1)	3.1 (0.9)	4.2 (3.1)	36.6 (1.5)	55.3 (2.7)

a Collection efficiencies are expressed as percentages of total solids output rate from the nebulizer, estimated by isokinetic collection on an absolute glass fiber filter.Values are mean (sample SD), n=3.

b Rheostat F (Figure IV.1) controlling temperature of hot air gun was set between 30 - 32 V and temperatures recorded in dryer C (Figure IV.1). Value is mean (sample SD), n=12.

c Rheostat E (Figure IV.1) controlling air flow to hot air gun was set at 12 V (Appendix AII). Value is mean (sample SD), n=3

d The letters K, C, B and I correspond to different components in Figure IV.1.

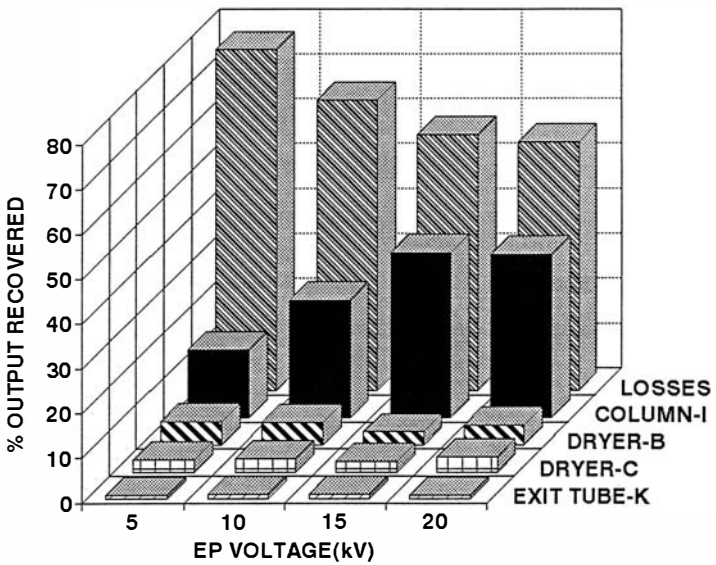

Figure IV.10 Deposition in the apparatus following spray drying and electrostatic collection of 10 mg/ml solution at 27 ± 1 °C (Rheostat F, kept between 30 - 32 V and temperatures were measured in dryer C, Figure IV.1) and a volumetric air flow of 50.6 ± 1.5 liters/min (Rheostat E, Figure IV.1 kept at 12 V, Appendix AII). In these experiments the particles were collected on glass lining (L, Figure IV.3)

Table IV.7 Summary of particle collection efficiencies[a] at a drying temperature of 39.5 °C (0.5)[b] and volumetric air flow of 50.6 liters/min (1.5)[c] as a function of electrostatic precipitator (EP) voltage

EP Voltage (kV)	Exit Tube-K[d]	Dryer-C[d]	Dryer-B[d]	Column-I[d]	Losses
5	1.0 (0.9)	1.8 (0.1)	4.0 (2.7)	14.2 (1.6)	79.0 (4.1)
10	1.3 (0.5)	2.2 (0.8)	5.1 (2.3)	24.9 (0.6)	66.5 (2.2)
15	1.0 (0.2)	2.2 (0.5)	3.5 (1.8)	31.7 (0.8)	61.6 (3.2)
20	1.0 (0.1)	2.3 (0.0)	6.5 (3.4)	33.5 (0.4)	56.8 (3.6)

[a] Collection efficiencies are expressed as percentages of total solids output rate from the nebulizer, estimated by isokinetic collection on an absolute glass fiber filter.Values are mean (sample SD), n=3.

[b] Rheostat F (Figure IV.1) controlling temperature of hot air gun was set between 50 - 58 V and temperatures recorded in dryer C (Figure IV.1). Value is mean (sample SD), n=12.

[c] Rheostat E (Figure IV.1) controlling air flow to hot air gun was set at 12 V (Appendix AII). Value is mean (sample SD), n=3

[d] The letters K, C, B and I correspond to different components in Figure IV.1.

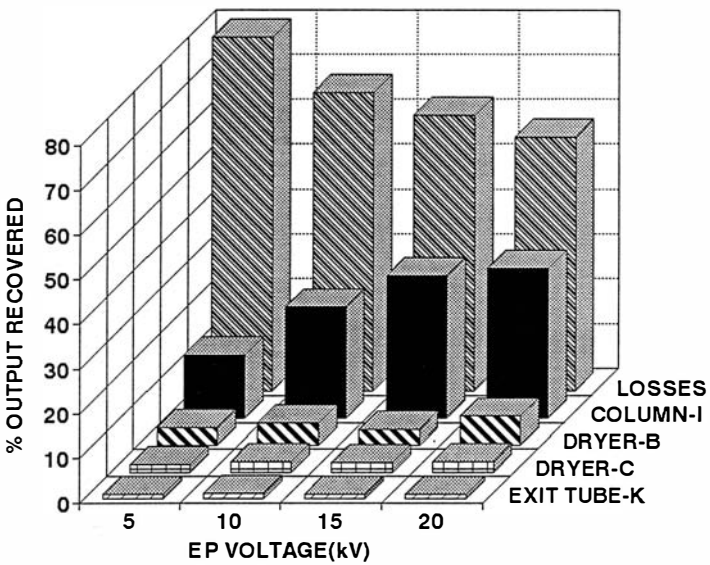

Figure IV.11 Deposition in the apparatus following spray drying and electrostatic collection of 10 mg/ml solution at 40 ± 1 °C (rheostat F, kept between 50 - 58 V and temperatures were measured in dryer C, Figure IV.1) and a volumetric air flow of 50.6 ± 1.5 liters/min (rheostat E, Figure IV.1 kept at 8 V, Appendix AII). In these experiments particles were collected on the glass lining (L, Figure IV.3).

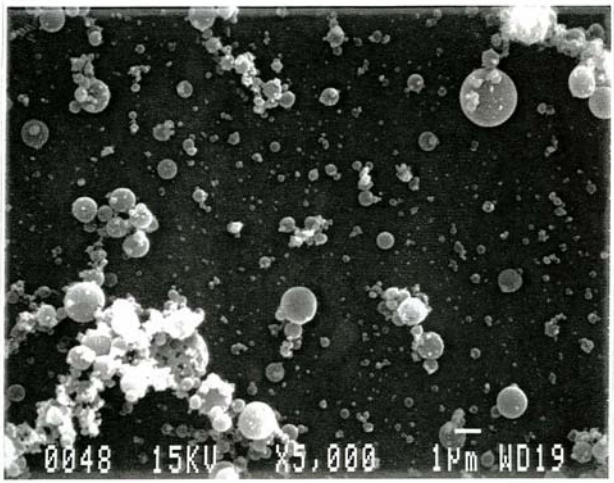

Figure IV.12 Scanning electron micrograph (SEM) of lactose and fluorescein particles sprayed from a 10 mg/ml solution, dried at 29 °C (rheostat F, Figure IV.1 set at 30 V) and volumetric flow rate of 29.1 ± 0.8 liters/min (rheostat E, Figure IV.1 set 8 V, Appendix AII) and electrostatically collected inside the glass lined column at an EP voltage of 20 kV for 15 min.

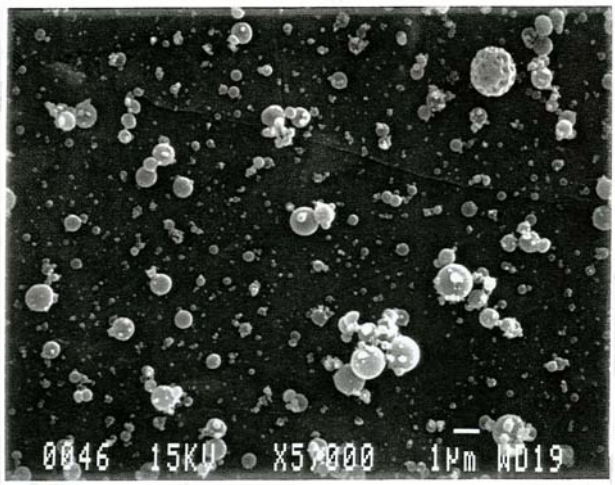

Figure IV.13 Scanning electron micrograph (SEM) of lactose and fluorescein particles sprayed from a 10 mg/ml solution, dried at 41 °C (rheostat F, Figure IV.1 set at 50 V) and volumetric flow rate of 29.1 ± 0.8 liters/min (rheostat E, Figure IV.1 set at 8 V, Appendix AII) and electrostatically collected inside the glass lined column at an EP voltage of 20 kV for 15 min.

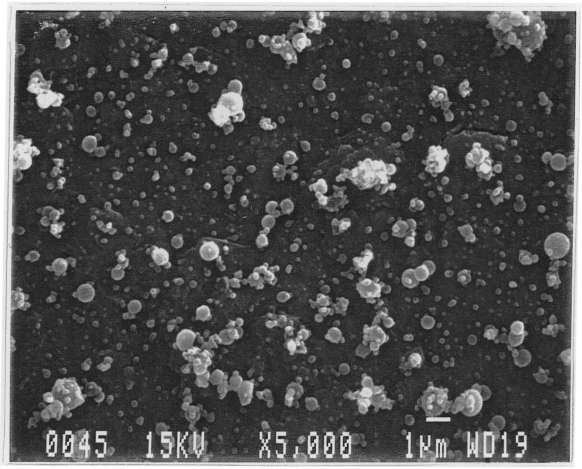

Figure IV.14 Scanning electron micrograph (SEM) of lactose and fluorescein particles sprayed from a 10 mg/ml solution, dried at 63 °C (rheostat F, Figure IV.1 set at 70 V) and volumetric flow rate of 29.1 ± 0.8 liters/min (rheostat E, Figure IV.1 set at 8 V, Appendix AII) and electrostatically collected inside the glass lined column at an EP voltage of 20 kV for 15 min.

conditions of the same air flow.

Figures IV.12 - IV.14 show the scanning electron micrographs (SEM) of electrostatically collected particles at 20 kV and drying temperatures of 29 °C (Figure IV.12), 41°C (Figure IV.13 and 63 °C (Figure IV.14). As expected, smaller and better dried particles were obtained when higher temperatures were used.

IV.c.1.3 Theoretical particle collection efficiencies during electrostatic precipitation

Experimental particle collection efficiencies obtained at a drying temperature of 41 °C and the two air flows of 29.1 liters/min and 50.6 liters/min were compared to theoretical collection efficiencies calculated for the two flow regimes assuming a particle size of 1 μm when drying was performed at 41 °C. Theoretical collection efficiencies were calculated employing the Deutsch-Anderson equation (Equation IV.1) and using field charging theory and known geometry of the collection surface (Hinds, 1982). The results are shown in Figure IV.15. Calculated collection efficiencies consistently overestimated the experimental collection efficiencies. This may be due to several factors like particle re-entrainment in the air stream, decreased field strength due to the presence of a glass collection surface between the conducting electrode (wire J, Figure IV.1) and the passive electrode (column surface in this case). Also, the assumption that particles have a uniform particle size (1 μm) may affect

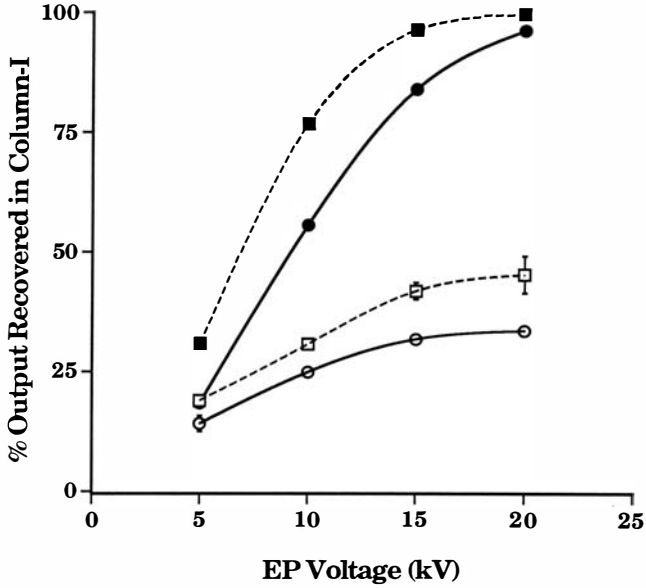

Figure IV.15 Comparison of theoretical and experimental collection efficiencies during electrostatic collection. Closed symbols represent theoretical collection efficiciencies, calculated using Equation IV.1 as described in the methods section (IV.b.2.5), at two air flow rates of 29.1 liters/min (■) and 50.6 liters/min (●) and assuming a particle size of 1 μm at the drying temperature of 41 °C. Open symbols represent experimental collection efficiencies expressed in terms of the percentage output recovered in column I with glass lining (L, Figure IV.1) at air flow rates of 29.1 liters/min (□) and 50.6 liters/min (○) and a drying temperature of 41 °C.

the theoretical calculations since, in practice, spray drying results in a particle size distribution and not particles of uniform size. Calculations of particle charges assuming a particle size distribution is complicated and is beyond the scope of this thesis. While it is attractive to imagine that precipitators can be designed for collection of micronized powders , purely on the basis of theory, this does seem to be possible. These results show the importance of empirical determinations of collection efficiency at a variety of operating conditions in order to optimize the drying and collection process.

IV.d SUMMARY AND CONCLUSIONS

A particle collection apparatus incorporating a commercial nebulizer and a wire-in-tube type electrostatic precipitator was built and characterized with respect to particle drying and collection efficiency. Empirical determinations of collection efficiency were made under a variety of operating conditions using aqueous solutions of lactose and disodium fluorescein.

Only particles collected inside the precipitator column (I, Figure IV.1) are potentially recoverable for further study. Under all operating conditions, percentage of particles depositing in parts of the apparatus other than the column were minimal. Particles were either recovered in the column or lost in the air stream ("Losses").

At all conditions, percentage deposition in the column increased with

increasing precipitator potential, indicating that higher electric field strengths are required for better collection efficiencies. Increasing the concentration of nebulized solution, decreased the percentage of total output being recovered in the column (64 % and 26% of outputs recovered inside the column after nebulization of 10 mg/ml and 75 mg/ml solutions respectively, Table IV.2).

In separate experiments, the hot air gun (D, Figure IV.1) was modified to enable independent control of drying air temperature and volumetric air flow rate. A 10 mg/ml solution was nebulized and electrostatically collected at two drying temperatures of 28 °C and 41 °C and two air flow rate of 29.1 liters /min and 50.6 liters/min. The temperature of the drying air did not affect the fractional deposition in the column, although better dried particles were apparently obtained when drying was performed at higher temperatures, as shown by SEM. Deposition in the column however, was dependent on volumetric air flow rate, with lower air flow showing higher fractional deposition in the column. This showed that deposition was a function of particle residence time (and electrophoretic mobility) inside the column.

Experimentally obtained column recoveries were compared to theoretical collection efficiencies calculated using particle charging theory and geometry of the wire-in-tube precipitator. Theoretical efficiencies overestimated the experimental observations at the conditions used in this study and showed the importance of empirically determining of collection

efficiencies under a variety of operating conditions, when designing precipitators for fine particle collection.

The particle collection apparatus developed and described in this chapter could be used for the collection of low amounts of fine particles suitable for inhalations. This apparatus was used for evaluating protein activity following spray drying and electrostatic precipitation of two model proteins, bacterial alkaline phosphatase (BAP) and bovine intestinal alkaline phosphatase (BIAP) and is described in Chapter V.

V. STABILITY OF SPRAY DRIED ALKALINE PHOSPHATASE DURING DRYING AND STORAGE: PROTECTION AFFORDED BY MOLECULAR DISPERSION IN LACTOSE, TREHALOSE, SUCROSE AND MANNITOL.

V.a INTRODUCTION

Delivery via the pulmonary route is coming under increased scrutiny for the systemic administration of drugs (Byron and Patton, 1994). With the discovery of newer protein and peptide drugs, inhalation offers some distinct advantages over other routes (Adjei and Gupta, 1994; Patton et al., 1994). One protein drug (recombinant human DNase, Pulmozyme®) has been approved for administration to the lung by nebulization of aqueous solutions, for alleviating symptoms of cystic fibrosis. DNase is a mucolytic enzyme whose topical action in the lung helps reduce sputum viscosity (Cipolla et al., 1994a). However, in future the lung may also serve as a conduit for protein therapeutics which have access to the systemic circulation (Niven, 1993).

Practical realization of the potential of this route of administration, requires the production of aerosolizable, respirable particles with aerodynamic diameters < 5 μm (Byron, 1990b). Such particles may be formulated and delivered using dry powder inhalers (DPIs) which seem to be the delivery systems of choice for proteins, since powder inhalation

avoids dispersion in hydrophobic propellants (in pressurized metered dose inhalers; MDIs) and chemical and conformational instability in aqueous solution associated with nebulizer liquids and the process(es) of nebulization (Martin et al., 1994). Traditionally, such small particles of bronchodilator and steroid drugs for lung administration were produced by air-jet milling of crystalline drug substances (Moren, 1987). Difficulties in production of crystallized proteins and the high temperatures produced during such processing make this technique an unattractive method for thermolabile and plastic materials like proteins. Furthermore, plastic materials are difficult to micronize to respirable particle sizes of the order of micrometers. Thus, alternative particulate technologies like processing from supercritical fluids (Yeo et al., 1993; Phillips and Stella, 1993) and spray drying (Broadhead et al., 1994) are being explored for the production of protein microparticles for inhalation.

Spraying, using a commercially available nebulizer followed by droplet drying and electrostatic precipitation has been shown to produce apparently dry particles < 5 μm (Naini, et al., 1993 and Chapter IV). Furthermore, sugars have been traditionally used in stabilizing proteins in solution (Arakawa and Timasheff, 1982) and as cryoprotectants during freeze drying (Carpenter et al., 1986). Recently there has been increased interest in the study of stabilizing proteins during air drying (Carpenter et al., 1987), spray drying (Broadhead et al., 1994) and long term storage of the dried mixtures, partly because of the interest in production of respirable dry

protein particulates. The mechanism by which sugars offer protection during drying and storage is not well understood. Even so, the molecular structure of sugars are believed to offer multiple hydrogen bonding sites which can potentially bind to polar residues on the protein molecule acting as a "water substitute" and thus stabilize its conformational structure (Prestrelski et al., 1993). Alternatively, a hypothesis based on the material science approach of glass to rubber transitions in amorphous materials has been proposed, to explain stabilization of proteins by excipients during drying and storage in the solid state (Franks et al., 1991). According to this hypothesis, when a protein-sugar solution is dried, the protein is entrapped in an amorphous glassy matrix of the sugar which reduces molecular motion and thus the frequency of destabilizing reactions. The amorphous glassy matrix should be below its glass transition temperature (T_g) to theoretically remain stable for pharmaceutically relevant time periods. Only when storage temperatures exceed the glass transition temperature does the amorphous bulk become rubbery, molecular mobility increases, and materials then become prone to recrystallization and increased chances of degradative chemical reactions in the solid state (Ahlneck and Zografi, 1990).

Designing a protein powder formulation for inhalation, requires that it should be physically and chemically stable in the dry state over its shelf life. It should also be readily reconstitutable in lung fluids for the protein to elicit its local or systemic pharmacological effect. This chapter deals with

the feasibility of using spray drying and electrostatic collection for producing enzymically active reconstitutable protein-sugar microparticles. Since the protein forms a molecular mixture embedded in a sugar matrix inside the microparticles, the sugar must be inhaled along with the drug. This is in contrast to traditional carriers in dry powder inhalers, where the carrier is detached from micronized drug particles, before the patient inhales the drug. Alkaline phosphatase (bacterial and bovine intestinal) was chosen as the model protein for studying spray drying and electrostatic collection in the apparatus described in Chapter IV, with and without the addition of lactose, trehalose, sucrose or mannitol to the initial solution. Stability of the dried solids was also investigated after storage at 23% RH and 25 °C for 14 days, conditions under which each of these sugars in the solid state, was proven to retain their its original physicochemical characteristics for 30 days after collection as a spray dried respirable solid in the absence of added protein (Chapter III).

V.b MATERIALS AND METHODS

Bacterial (*E.coli*) alkaline phosphatase (Product #P4252, Lot #101H40191), as a suspension in 2.5 M ammonium sulfate solution and bovine intestinal alkaline phosphatase (Product #P7640, Lot #043H7185), as a freeze-dried powder, substrate disodium p-nitrophenol phosphate (Product #104-0, Lot #123H50083), p-nitrophenol standard solution (Product #104-1, Lot #014H6137) bovine serum albumin protein standard (Product

#P0914, Lot #14H8530), sucrose, D-mannitol and α,α-trehalose dihydrate were all obtained from Sigma Chemical Company (St. Louis, MO). α-Lactose monohydrate was obtained from Foremost Ingredient Group (Baraboo, WI). Tris [Tris(hydroxymethyl)-aminomethane] and sodium dodecyl sulphate (SDS) were obtained from Pharmacia LKB (Piscataway, NJ). Protein assay kits (Product #500-006, Lot#'s 51143A and 51558A) were from Bio-Rad Laboratories (Hercules, CA). All other chemicals used, were of reagent grade quality and obtained from Fisher Scientific Company (Raleigh, NC).

A series of solutions were spray dried, collected and characterized in the apparatus developed and described in Chapter IV. Each of these solutions was coded and summarized in Table V.1. The remainder of this section details procedures employed in each case.

V.b.1 Nebulization, drying and electrostatic precipitation

The apparatus used for spray-drying and electrostatic precipitation of protein and protein-sugar mixtures is shown in Figure V.1. The apparatus was completely characterized with respect to particle collection efficiency, using lactose and disodium fluorescein as described in Chapter IV. Briefly, the apparatus consisted of a Small Particle Aerosol Generator (SPAG-2, ICN Pharmaceuticals, Costa Mesa, CA), which included the nebulizer reservoir (A), drying chamber (B), nebulizer airflow controller (NA), drying

Table V.1 Summary of enzyme solutions spray dried and electrostatically collected.

Solution Code	Target Protein Conc.[a] (μg/ml)	Target Protein Amt.[a] (mg)	Buffer & other solids[b] (mg)	Sugar Added Sugar	Sugar Added Amt. (mg)	Volume (ml)	Concentration[c] (mg/ml)
Bacterial Alkaline Phosphatase (BAP)							
BAP	120	3	30	No sugar	0	25	1.3
BAPL	120	3	30	Lactose	217	25	10.0
BAPT	120	3	30	Trehalose	217	25	10.0
BAPS	120	3	30	Sucrose	217	25	10.0
BAPM	120	3	30	Mannitol	217	25	10.0
Bovine Intestinal Alkaline Phosphatase (BIAP)							
BIAP	1000	25	55	No sugar	0	25	3.2
BIAPL	1000	25	55	Lactose	170	25	10.0
BIAPT	1000	25	55	Trehalose	170	25	10.0
BIAPS	1000	25	55	Sucrose	170	25	10.0
BIAPM	1000	25	55	Mannitol	170	25	10.0

[a] Protein was determined in the actual experiments by the Bradford assay in terms of BSA equivalents (BSAE); thus actual protein concentrations may be greater or smaller than those quoted.

[b] Altered buffer salt (Tris) content in the final dried product could affect maximal enzyme activity of alkaline phosphatase.

[c] Total concentration of non volatile ingredients.

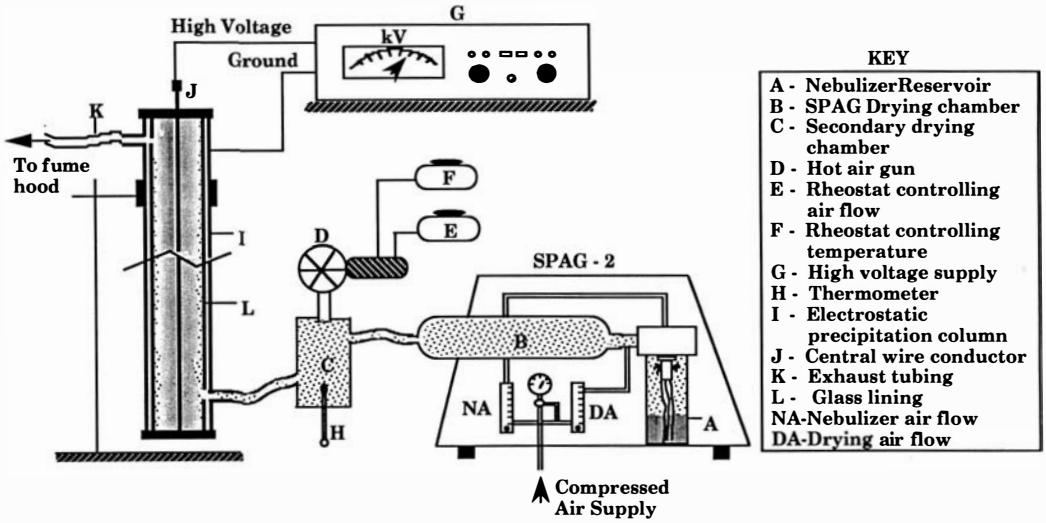

Figure V.1 Schematic diagram of the particle collection apparatus.

air flow controller (DA) and an inlet for compressed air supply (Figure V.1). A controlled inlet air pressure of 26 psig enabled a nebulizer air flow (NA) of 7 liters/min and a drying air flow (DA) of 10 liters/min to be used throughout. Aerosol generated from the SPAG was introduced via inhalation tubing into a secondary drying chamber (C). Additional drying air (12 liters/min) was introduced into the chamber by means of a hot air gun (D) whose air flow and temperature were controlled by means of two variable transformers (E & F respectively). Dimensions of all components in Figure V.1 were as described in Chapter IV, and shown in Figures IV.2 and IV.3.

The steady state air temperature (approximated by the dry-bulb temperature) inside the drying chamber (C) was monitored during the experiment by means of a thermometer (H), introduced into the chamber. In all experiments a total air flow of 29.1 liters/min was measured at the outlet of the precipitator column (I), and a targeted temperature of 63 °C in the secondary drying chamber (C), corresponding to a voltage range between 70 and 80 V on the transformer controlling temperature (F), were used. Dried particles exiting the chamber (C) were then introduced into a wire-in-column type electrostatic precipitator, which consisted of a charging and collection column (I) and a central wire conductor (J). To facilitate easy recovery of collected material, sections of large bore glass tubing were introduced inside the precipitator column (I) whose dimensions are given in Chapter IV, Figure IV.3. The column was

exhausted into a fume hood through inhalation tubing (K). A voltage of -20 kV (negative polarity) was applied to the central conductor (J) of the precipitator by means of a high voltage generator (G, Model #2807R, Brandenburg/Astec, Alpha II Series, Stourbridge, UK). Aerosols were generated from solutions placed in the nebulizer reservoir (A, Figure V.1) and collected on the glass collection surfaces (I) inside the column for 90 minutes in each case.

V.b.1.1 Bacterial Alkaline Phosphatase

Bacterial alkaline phosphatase (BAP) was obtained as a suspension in 2.5 M ammonium sulfate solution and contained 4.1 mg/ml of protein (as determined by the Warburg-Christian method; Sigma certificate of analysis). This suspension was desalted by ultrafiltration prior to use, hence the final nebulized solutions contained the pure enzyme and Tris buffer salt.

Briefly, three 250 µl aliquots of the enzyme suspension were pipetted *into* three Microcon-10 (MW cut off = 10 kDa, Product #42406, Amicon, Beverly, MA) microconcentrator sample reservoirs attached to filtrate vials. 250 µl of 10 mM Tris buffer pH 8.0 was added to each reservoir. These solutions were spun in a bench top centrifuge (Eppendorf, Centrifuge 5415, Brinkmann Instruments, Westbury, NY) at 7000 rpm for 10 min. At the end of the 10 min run, two additional 10 min spins were performed, with 250 µl of fresh buffer added to the sample reservoir at the end of each spin.

After three spins, 100 µl of fresh buffer was added to each sample reservoir, inverted into fresh retentate vials and briefly spun for 2 min at 4000 rpm, to collect the desalted enzyme fraction. The three desalted enzyme fractions were mixed and reconstituted to 25 ml with 10 mM Tris buffer pH 8.0 (Solution BAP, Table V.1). Solution BAP had a targeted protein concentration of 120 µg BSAE/ml. Protein concentrations quoted throughout this chapter and Chapter VI, are apparent protein concentrations expressed in terms of bovine serum albumin (BSA) equivalents (BSAE). Thus for solution BAP (Table V.1) the total concentration of nonvolatile ingredients was 1.3 mg/ml (0.1% w/v; protein:buffer components = 1:10).

For spray drying protein-sugar mixtures, 217 mg of one of the sugars (lactose, trehalose, sucrose or mannitol) was added to the desalted enzyme fractions prior to reconstitution with Tris buffer pH 8.0 to 25 ml. These solutions are coded as: BAPL, BAPT, BAPS and BAPM for enzyme solutions containing lactose, trehalose, sucrose and mannitol respectively (Table V.1). Final protein concentration of these solutions was targeted to 120 µg BSAE/ml. The total concentration of non-volatile ingredients of BAPL, BAPT, BAPS and BAPM in the final solution was 10 mg/ml (1% w/v; protein:buffer components:sugar = 3:30:217, Table V.1). A 1 ml aliquot of this solution was retained at ambient conditions (temperature 20 - 23 °C) for further analysis. The remaining 24 ml was placed in the nebulizer reservoir (A, Figure V.1). Hot air gun (D, Figure V.1) was turned on and

the transformer controlling air flow (E) was kept at 8 V (corresponding to an total air flow of 29.1 liters/min, Appendix AII). Transformer controlling temperature of the drying air (F) was adjusted between 70 and 80 V and a steady state air temperature of 63 °C was achieved inside the secondary drying chamber (C), as measured by the thermometer (H). The high voltage generator (G) was then switched on and applied voltage on the electrostatic precipitator (J) was adjusted to -20 kV (negative polarity). Controlled inlet air pressure of 26 psig was supplied to the SPAG by an air compressor (Figure V.1). Nebulizer and drying air flow of the SPAG were adjusted to 7 liters/min and 10 liters/min by turning the knobs on NA and DA gauges respectively (Figure V.1). The resulting aerosol generated from the SPAG was dried and electrostatically collected as described in Section V.b.1 for 90 min. Temperatures in the secondary drying chamber (C, Figure V.1) were recorded at the beginning, middle and end of each 90 min experiment. At the end of 90 min, the nebulizer, high voltage generator (G) and the hot air gun (D) were turned off in that order. The apparatus was dismantled, glass columns (I) from inside the precipitator column (J) were washed and reconstituted to 10 ml using 10 mM Tris buffer pH 8.0. The initial solution, column wash and residual solution in the nebulizer reservoir were analyzed in duplicate for protein content (in BSAE) and enzyme activity after appropriate dilutions with 10 mM Tris buffer pH 8.0. Protein content was determined by the method of Bradford (Bradford, 1976) using the Bio-Rad protein assay kit (Bio-Rad, Hercules, CA) and protein contents were

expressed in terms of BSA equivalents (BSAE). Enzyme activity was determined by following the initial reaction rate of the hydrolysis of p-nitrophenol phosphate to p-nitrophenol at 37 °C (Torriani, 1968). One unit of enzyme activity was defined as the amount of enzyme that releases 1 nmol of p-nitrophenol per minute at 37 °C. Specific activities of the enzyme were expressed as Units/μg BSAE in assayed solutions. Each solution was assayed in duplicate and reported values are the mean of three 90 min experimental runs. Detailed descriptions of the enzyme and protein assays are given in Chapter VI.

V.b.1.2 Bovine Intestinal Alkaline Phosphatase

Bovine intestinal alkaline phosphatase was obtained as a freeze-dried powder. The specific lot (#043H7185) used in this investigation consisted of 59.1% protein (phosphatase plus other proteins) and the remaining was made up of buffer salts (Tris, $MgCl_2$ and $ZnCl_2$; Sigma Technical Information). However, specific information on the nature of proteins, other than phosphatase, was not available from Sigma. This made it difficult to compare the bacterial and bovine alkaline phosphatase enzymes used in this study. This is often the problem with biologics, since their pharmaceutical chemistry is poorly defined when compared to small molecular weight drugs. It has been reported that a highly purified intestinal phosphatase preparation has significantly higher catalytic activity compared to the bacterial enzyme of similar overall purity (Chappelet-

Tordo et al., 1974). However, the pH at which this maximal activity occurs are different for the two enzymes (8.5 and 10.5 for BAP and BIAP respectively). The crude enzyme preparation as obtained from Sigma was used without purification.

Fifty milligrams of the crude enzyme powder was dissolved and reconstituted to 25 ml using 10 mM Tris buffer pH 8.0 (solution BIAP, Table V.1), to give a protein concentration of ~1 mg/ml. The total concentration of non-volatile ingredients in solution BIAP (Table V.1) was 3.2 mg/ml (0.3% w/v; protein:other solids ratio = 5:11, Table V.1).

For spray drying BIAP-sugar mixtures, 170 mg of one of the sugars (lactose, trehalose, sucrose or mannitol) was added to 50 mg enzyme powder before dissolution and reconstituted to 25 ml in 10 mM Tris buffer pH 8.0. These are coded as BIAPL, BIAPT, BIAPS and BIAPM for solutions containing lactose, trehalose, sucrose and mannitol respectively (Table V.1). The total concentration of non-volatile ingredients in solutions BIAPL, BIAPT, BIAPS and BIAPM was 10 mg/ml (1% w/v; protein: other solids:sugar ratio = 5:11:34, Table V.1). One ml of this solution was retained at ambient conditions (temperature 20 - 23 °C) for further analysis. The remaining 24 ml was placed in the nebulizer reservoir. Aerosols were generated and collected for 90 min as described in Sections V.b.1 and V.b.1.1. Protein content in terms of BSA equivalents (BSAE) and enzyme activity of the initial solution, column wash and residual nebulizer solution were analyzed after appropriate dilutions with 10 mM Tris buffer pH 8.0, as

described above and in Chapter VI.

V.b.2 Solid state stability of dried protein and protein-sugar mixtures

Aerosols were generated and collected using bacterial (BAP) and bovine intestinal alkaline phosphatase (BIAP) as described in Sections V.b.1.1 and V.b.1.2 respectively. At the end of 90 min collection, initial and residual nebulizer reservoir solutions were analyzed for protein and enzyme activity as described above. However, the glass collection surfaces (I, Figure V.1) in the precipitator were removed and quickly transferred to desiccator vessels in which a constant relative humidity (RH) of 23% was maintained with a saturated salt solution (potassium acetate; Callahan et al., 1982). Desiccator vessels were maintained at 25 °C in an environmental chamber (Model 435314, Hotpack, Philadelphia, PA) for 14 days. After this period, the glass collection surfaces were removed, washed and reconstituted to 10 ml, using 10 mM Tris buffer pH 8.0. This solution was analyzed for protein content (in BSAE) and enzyme activity as described above and in Chapter VI. Reported values are mean of three such storage experiments.

V.b.3 Solution degradation kinetics of bovine intestinal alkaline phosphatase (BIAP)

A worst case scenario of enzymic degradation at temperatures similar to those seen within the spray drying process was simulated in solution for

BIAP. It was also used to look at the effect of solution temperature on protein concentration determination by the method of Bradford (Bradford, 1976). A 2 mg/ml (corresponding to a protein concentration of ~1 mg BSAE/ml) solution of the crude enzyme powder was prepared in 10 mM Tris buffer pH 8.0. One milliliter of this solution was incubated in a test tube at 63 °C in a constant temperature water bath (Model #9505, Fisher Scientific, Raleigh, NC). Forty microliter (40 µl) aliquots of the enzyme solution were withdrawn at different time points, transferred to a 10 ml volumetric flask and diluted with 10 mM Tris buffer pH 8.0 kept at ambient temperature (22 - 23 °C). A 40 µl sample withdrawn just prior to incubation at 63 °C provided the sample for initial enzyme activity. These solutions were analyzed for protein content (in BSAE) and enzyme activity as described in Chapter VI.

V.b.4 Effect of droplet drying on protein concentration determination by the method of Bradford

Experiments were performed to determine the effect of phase transformation of the enzyme from the droplet state to the dried state on apparent protein content determination by the method of Bradford (Bradford, 1976). This because BSAE/ml was used as the quotient in the determination of specific activity (Chapter VI). A 2 mg/ml (corresponding to a protein concentration of ~1 mg BSAE/ml) of BIAP crude enzyme powder was made up in 10 mM Tris buffer pH 8.0. This solution was

assayed for protein content (in BSAE) using the method of Bradford (Bradford, 1976). Density of the solution was determined at room temperature (20 - 23 °C) using a specific gravity bottle. A known volume of the solution was sprayed using a small spray bottle into large volume test tubes. These tubes were dried at 45 °C for 90 min in an oven. At the end of 90 min, 20 ml of 10 mM Tris buffer pH 8.0 was pipetted into the tubes along with four drops of 0.1% w/v sodium dodecyl sulphate (SDS) solution. SDS was added to prevent protein loss by adsorption to the tube walls (earlier experiments performed by spraying enzyme solution into larger glass chambers without undergoing the drying process, resulted in greater losses of protein, indicating that protein was being lost by adsorption to glass at these low concentrations). Twenty milliliters (20 ml) of the wash solution was then assayed for protein content (in BSAE) and the apparent percentage of protein recovered determined.

V.b.5 Scanning electron microscopy of dried BAP and BAP-sugar aerosols

Scanning electron microscopy (SEM) stubs were attached to the glass collection surface inside the precipitator column (I, Figure V.1), by means of double sided sticky tape (Scotch, 3M, St. Paul, MN). Aerosols of BAP alone and in admixture with one of the four sugars (solutions coded as BAP, BAPL, BAPT, BAPS and BAPM, Table V.1) were generated and collected for 15 min under conditions described in Section V.b.1.1. At the

end of 15 min, the stubs were removed from the column (I, Figure V.1), coated with gold-palladium using an Eiko IB-2 Ion Coater (Eiko Engineering, Ibaraki, Japan) under a vacuum, prior to SEM and photomicrography.

V.b.6 Statistical analyses

Statistical analyses were performed to detect differences in enzyme specific activities before and after spray drying and electrostatic collection of both BAP and BIAP, when dried with or without addition of the four sugars. All statistical analyses were performed at a level of significance of α=0.05, while ensuring normality of the resulting residuals.

The following linear statistical model was used to test the various hypotheses:

$$X_{ij} = \mu + COND_i + SOLN_j + (COND_i \bullet SOLN_j) + \varepsilon_{ij}$$

where:

X_{ij} = Observation at i^{th} level of COND effect and j^{th} level of SOLN effect (X_{ij} refers to specific activity in these experiments).

μ = overall mean effect

$COND_i$ = Experimental condition effect at level i. Four levels of experimental conditions were tested; i.e. 1) Initial solution, 2) nebulizer reservoir solution, 3) spray dried and 4) spray dried and stored at 23% RH and 25 °C for 14 days.

$SOLN_j$ = Solution formulation effect at level j. Five levels of solution effect were tested for each of the enzymes, BAP and BIAP; i.e. 1) sugar free enzyme formulations (BAP and BIAP), 2) enzyme with lactose (BAPL and BIAPL), 3) enzyme with trehalose (BAPT and BIAPT), 4) enzyme with sucrose (BAPS and BIAPS) and 5) enzyme with mannitol (BAPM and BIAPM).

$COND_i \bullet SOLN_j$ = Effect of interaction between the two main factors $COND_i$ and $SOLN_j$.

ε_{ij} = Error component (residuals).

Hypotheses were tested using a two way analysis of variance (ANOVA) with an interaction term as described above. Raw data for specific activities of BAP and BIAP obtained using different formulation and experimental conditions are given in Appendix AIII. For example, consider the situation where the difference in specific activity between spray dried BIAP and BIAPM was being assessed. The procedure was run with X_{ij} = 6.5, 6.0 and 5.9 Units/μg BSAE (for BIAP) and X_{ij} = 5.0, 5.3 and 5.4 Units/μg BSAE (for BIAPM). These values were obtained by dividing enzyme activities (Units/ml) with their respective apparent protein concentrations (μg BSAE/ml) as given in Table AIII.2 (Appendix AIII). Significant differences for individual comparisons due to the main factors were detected using Scheffe's multiple comparison test. If the two way ANOVA showed a significant interaction effect, a follow up one way ANOVA was used to

detect the source of difference; individual comparisons were then performed using the Scheffe's multiple comparison test. All statistical analyses were performed using the program STATGRAPHICS Plus, Version 6 (Manugistics Inc., Rockville, MD, 1992).

V.c RESULTS AND DISCUSSION

In the bulk of the experiments described in this chapter, activities and specific activities of BAP and BIAP are compared after spray drying and collection from a variety of formulations. Because specific activity (Units/μg BSAE) required both a protein assay and enzyme activity assay, to determine their ratio, the effect of solution degradation and drying upon enzyme protein and activity were first studied independently. The results of these experiments are described in Sections V.c.1 and V.c.2.

V.c.1 Solution degradation kinetics of bovine intestinal alkaline phosphatase

Solution degradation kinetics of BIAP were studied in 10 mM Tris at an enzyme concentration of ~1 mg BSAE/ml and 63 °C. The results are summarized in Table V.2. The first column gives the protein concentration in terms of BSA equivalents as determined by the Bradford assay, which shows a small loss of detectable protein when solution was incubated for 90 min at 63 °C. This underestimation must be due to chemical changes in the protein at this temperature. A molecular weight threshold of 3000 Daltons

Table V.2 Solution degradation kinetics of bovine intestinal alkaline phosphatase (BIAP) incubated at 63 °C and its effect on protein concentration determination by the method of Bradford.

Time of incubation (min)	Protein Conc.[a,b,c] (μg/ml)	Enzyme Activity[a,b,d] (Units/ml)	Specific Activity[b] (Units/μg protein)
0	3.4 (0.1)	36.6 (0.2)	10.8 (0.2)
1	3.2 (0.1)	32.9 (0.8)	10.2 (0.2)
2	3.2 (0.1)	29.2 (1.0)	9.2 (0.3)
5	3.0 (0.1)	21.3 (1.2)	7.1 (0.3)
30	2.6 (0.1)	8.7 (0.8)	3.3 (0.2)
90	2.7 (0.1)	2.2 (0.3)	0.8 (0.1)

a Protein concentration and enzyme activity were determined for 40 μl aliquots withdrawn at diferent time intervals and reconstituted to 10 ml with 10 mM Tris buffer pH 8.0.

b Values are mean (sample SD) of three determinations.

c Protein concentrations were determined by the method of Bradford in terms of BSA equivalents.

d One Unit of enzyme activity was defined as the amount of enzyme that releases 1 nmol of p-nitrophenol per minute at 37 °C.

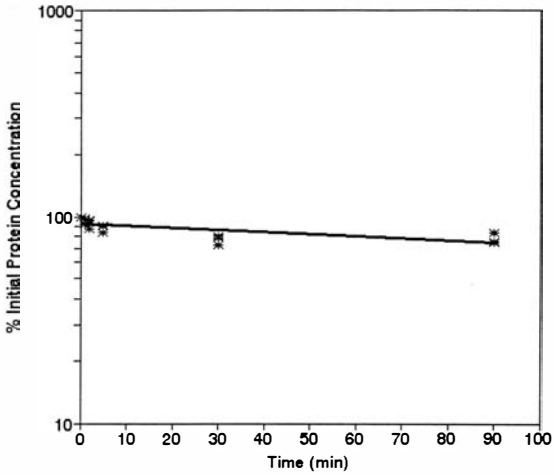

Figure V.2 Log-linear plot of loss of detectable protein vs time for bovine intestinal alkaline phophatase incubated in solution at 63 °C. Plotted values are experimentally obtained data. The solid line shows the best fit by linear regression of the data ($y = -0.001x + 1.97$; $r^2 = 0.52$; standard error of slope = 0.00024; $n = 18$).

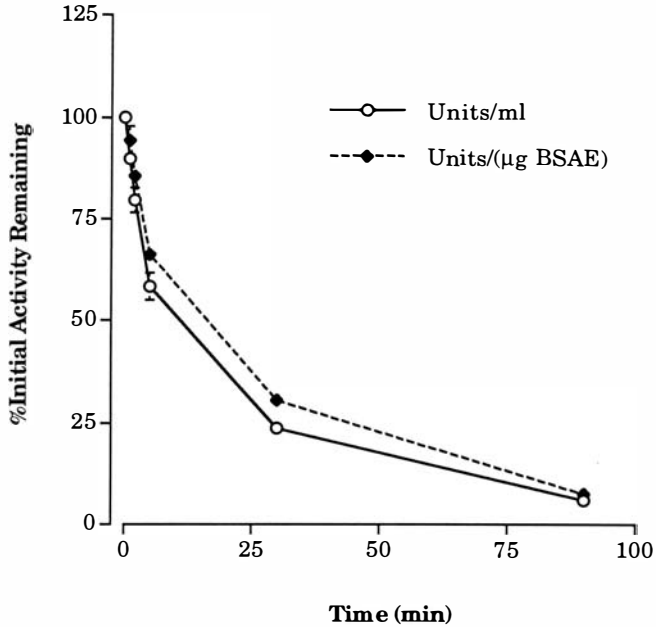

Figure V.3 Solution degradation kinetics of bovine intestinal alkaline phosphatase (BIAP) in 10 mM Tris buffer pH 8.0, incubated at 63 °C shown on linear-linear plot. Activities were either calculated as Units/ml (o) or Units/µg BSAE (specific activity; ♦). Data points are means of three determinations (error bars are sample SD). Error bars are not shown where sample SD was smaller than the size of the symbol used for the data point.

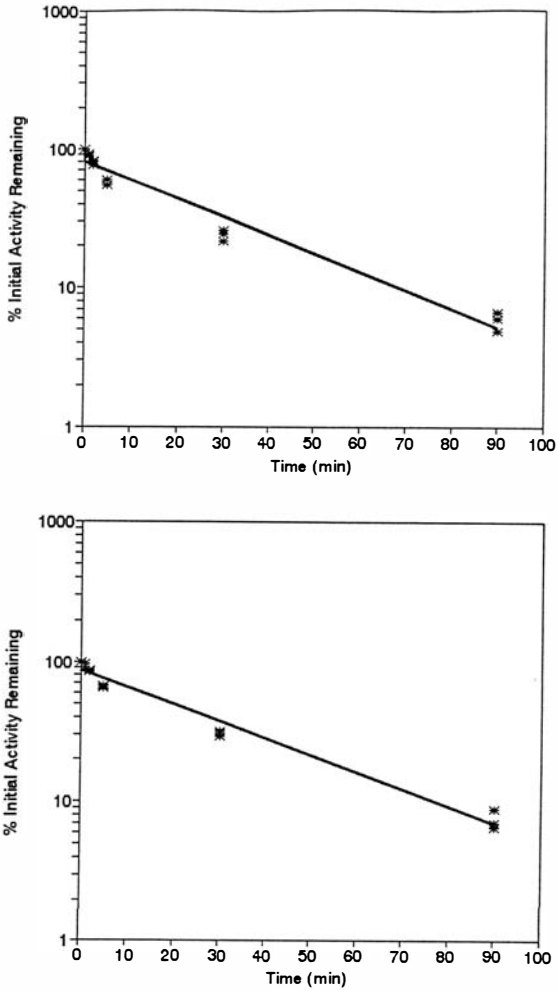

Figure V.4 Solution degradation kinetics of bovine intestinal alkaline phosphatase (BIAP) in 10 mM Tris buffer, pH 8.0, incubated at 63 °C. Plots are log-linear profiles of percentage initial activity (top panel: Units/ml; bottom panel: Units/μg BSAE, specific activity vs time. Plotted values are experimentally obtained data. Solid lines show the best line fits by linear regression (top panel: $y = -0.01326x + 1.90915$; $r^2 = 0.96$; standard error of slope = 0.00066; n=18, bottom panel: $y = -0.01225x + 1.94179$; $r^2 = 0.98$; standard error of slope = 0.00047; n=18).

for binding of Coomassie Blue G-250 to the polypeptide has been reported in the literature (Chapter VI, Sedmak and Grossberg, 1977) and progressive hydrolysis to form smaller fragments is feasible at this temperature. Assuming that the loss of detectable protein followed first-order kinetics, the negative log-linear slope of percentage initial protein concentration vs time was determined by linear regression analysis (Figure V.2). A value for the degradation rate constant of 0.002 min^{-1} was determined from this plot. From the perspective of this study, at a volumetric air flow rate of 29 L/min, droplet residence time inside the apparatus (nebulizer to collection surface should be $\leq$ 3 sec). Thus, even in the extreme and unlikely case of droplets reaching the air temperature of 63 °C, the loss of detectable protein should be minimal during residence time of the droplet drying in these experiments.

The enzyme also lost considerable activity when incubated at 63 °C in solution (Table V.2). Enzyme activity was expressed in this Table and the resultant plots as both Units/ml and Units/μg BSAE in order to show that enzyme activity changes were not paralleled by changes in apparent protein concentration. The loss of detectable protein during the course of 90 min and the enzyme degradation profile were similar, as shown from the percentage initial activity vs time plots (Figure V.3). Assuming that loss of enzyme activity followed first-order kinetics, rate constants of 0.028 min^{-1} (percentage of initial specific activity remaining vs time) and 0.031 min^{-1} (percentage of initial activity remaining vs time), were obtained from the

log-linear plots in Figure V.4.

V.c.2 Effect of droplet drying on protein content determination

These experiments were performed to see if the phase transformation from droplet to dry particle affected the apparent protein content values after their determination by the method of Bradford (Bradford, 1976). The result of three drying experiments as described in Section V.b.3 are shown in Table V.3. Ninety two percent (92%) of the original protein content sprayed into large volume test tubes and dried was recovered. The small loss of protein (8%) was probably due to adsorption and not due to loss of detectable protein, since at these low concentrations, proteins are known to adsorb to surfaces like glass. In addition, when enzyme solution was impacted as a wet aerosol onto the walls of a larger glass chamber (greater surface area for adsorption) and immediately reconstituted (without droplet drying), greater losses of protein were seen indicating, once more that loss was due to adsorption and not droplet drying. To avoid adsorption of protein to glass a few drops of 0.1% w/v SDS solution was included in the wash solution. Larger amounts of SDS could not be used since SDS is known to interfere with the Bradford assay at higher concentrations (Bio-Rad Protein Assays, Bio-Rad Laboratories, Inc., Richmond, CA, 1991). During spray drying experiments performed as described in this Chapter, some loss of protein may also have resulted from adsorption to the glass collection surface (I, Figure V.1).

Table V.3 Effect of droplet drying[a] on protein content[b] determination by the method of Bradford in BIAP solutions.

Experiment #	Amount sprayed[c] (μg)	Amount recovered from wash solution[d] (μg)	% Recovery
1	75.1	67.2	89.5
2	75.0	70.4	93.9
3	74.8	69.6	93.0
		Mean % Recovery	92.1
		SD	2.3

a Solution of BIAP in 10 mM Tris buffer pH 8.0 was sprayed into large volume test tubes and dried at 45 °C for 90 min.

b Protein concentrations are expressed in terms of BSA equivalents.

c Volume of solution sprayed was determined by weight difference of the spray bottle before and after spraying and the density of enzyme solution.

d Tubes were washed with 10 mM Tris buffer pH 8.0 along with four drops of 0.1 %w/v SDS solution following drying of the droplets.

V.c.3. Spray-drying and electrostatic collection of bacterial alkaline phosphatase (BAP)

Early work on which the temperature selection of 63 °C for drying was based, involved the spray drying and electrostatic collection of sugar free aerosols containing BAP and buffer salt under identical conditions. Collected aerosols, which were apparently dry particulates as observed on the glass collection surface and by electron microscopy (Figure V.7) were reconstituted with 10 mM Tris buffer pH 8.0 kept at room temperature (20 - 23 °C). The average specific activity of the enzyme in the reconstituted solutions in the sugar free experiments was 12.2 Units/μg BSAE, which showed a 23% loss in specific activity compared to the initial solution. While a loss of this magnitude was not large, it was significant relative to the initial specific activity (ANOVA, $p < 0.05$, Table V.5) and could be attributed to drying and/or collection of particulates. Importantly, as was discussed in Sections V.c.1 and V.c.2, it was unlikely that the protein assay responsible for this change. That assay should not be affected by the processing conditions employed in these experiments. The initial hypothesis therefore, that these sugars may offer protection against degradation during drying and collection of BAP, was theoretically testable by co-drying and collecting BAP along with the different sugars, then assaying the products for specific activity. Experimental results for enzyme specific activity using bacterial alkaline phosphatase (BAP) as the model protein for spray-drying are summarized in Table V.4 and Figure V.5.

BAP is a dimeric Zn-metalloprotein of molecular weight 94000 Daltons, composed of two identical monomers (Coleman and Gettins, 1983). The complete amino acid sequence (Bradshaw et al., 1981) and the three dimensional structure (Sowadski et al., 1985; Kim and Wyckoff, 1991) of BAP have been reported. A cartoon representation of the three dimensional structure of the BAP monomer is shown in Figure V.6. The isolated enzyme consists of two Zn^{+2} and one Mg^{+2} ion per monomer (Coleman and Gettins, 1983; Coleman and Chlebowski, 1979). The presence of metal ions has been shown to be critical for stabilizing the three dimensional structure and for enzyme activity (Coleman and Gettins, 1983). Using high sensitivity differential scanning calorimetry (DSC), Chlebowski and Mabrey have shown that apoalkaline phosphatase (enzyme whose metal ions have been removed by chelation) undergoes a reversible thermally induced denaturation at 57.5 °C, which dramatically increases to 85 °C, on binding to two Zn^{+2} ions per dimer (Chlebowski and Mabrey, 1977). The native dimeric form of the enzyme (with 4 Zn^{+2} and two Mg^{+2} ions) was shown to be remarkably heat stable with a denaturation temperature of 96 °C (Chlebowski and Mabrey, 1977).

In these experiments, total apparent protein content of the nebulized solution (solutions coded as BAPL, BAPT, BAPS and BAPM; Table V.1) was held at ~1.2% w/v with respect to other non volatile ingredients (3 mg BSAE in 250 mg total solids). Nebulizer solution concentrations were held at ~1% w/v total solids, exactly as used during equipment validation experiments

Table V.4 Specific activity of bacterial alkaline phosphatase (BAP) following nebulization and spray drying with sugars, electrostatic collection and storage.

	Initial Solution[c]		Nebulizer Reservoir[d]		Spray Dried[e]	Storage[f]
	Spec. Act.[b] (Units/μg prot)	Prot. Conc. (μg/ml)	Spec. Act.[b] (Units/μg prot)	Prot. Conc. (μg/ml)	Spec. Act.[b] (Units/μg prot)	Spec. Act.[b] (Units/μg prot)
BAP[a]	15.7 (1.4)	123.8 (8.1)	15.5 (1.8)	281.7 (63.9)	12.1 (1.1)	10.5 (1.2)
BAPL[a]	15.7 (1.2)	127.8 (12.7)	15.6 (1.4)	241.2 (74.8)	12.2 (2.5)	11.3 (3.3)
BAPT[a]	14.9 (1.2)	132.6 (9.6)	14.7 (2.0)	259.0 (67.1)	13.0 (2.7)	10.9 (2.1)
BAPS[a]	15.2 (1.0)	129.2 (10.4)	14.8 (1.2)	264.4 (41.6)	12.6 (1.3)	11.0 (1.9)
BAPM[a]	15.9 (1.7)	117.7 (22.0)	15.4 (1.4)	251.9 (73.3)	9.3 (2.5)	9.0 (4.4)

a Solutions correspond to coded solutions as tabulated in Table V.1.
b One unit is defined as the amount of enzyme that releases 1 nmol of p-nitrophenol per minute at 37 °C. Protein content was expressed in terms of BSA equivalents (BSAE).
c Values are mean (sample standard deviation), n=6.
d Solution assayed from the nebulizer reservoir at the end of 90 min. Values are mean (sample standard deviation), n=6.
e Spray dried and collected for 90 min. Values are mean (experimental range), n=3.
f Spray dried and collected for 90 min prior to storage at 23% RH and 25 °C for 14 days. Values are mean (experimental range), n=3.

Table V.5 Summary of two way analysis of variance (ANOVA)[a] results for enzyme specific activities of bacterial alkaline phosphatase (BAP).

Source of variation	Sum of squares	Degrees of freedom	Mean Square	F-ratio	Significance level
Main Effects					
SOLN[b]	15.27	4	3.82	1.85	NS[d]
COND[c]	358.99	3	119.66	58.05	$p < 0.05$
Interaction					
COND . SOLN	33.02	12	2.75	1.34	NS[d]
Residual	144.31	70	2.06		
Total	544.61	89			

a The statistical model tested was:
$X_{ij} = \mu + COND_i + SOLN_j + (COND_i . SOLN_j) + \varepsilon_{ij}$ and is described in Section V.b.4.

b Five levels of solution effect (SOLN) were tested; BAP, BAPL, BAPT, BAPS and BAPM.

c Four levels of experimental condition effect (COND) were tested; initial solution, nebulizer reservoir solution, spray dried and spray dried and stored at 23 %RH and 25 °C for 14 days.

d No significant difference.

described in Chapter IV. Sugar and buffer components made up the remaining solids (86.8% and 12%, respectively). In sugar free experiments with BAP (solution coded as BAP; Table V.1) the total solids concentration was ~0.1% w/v, of which ~9% (3 mg in 33 mg total solids) was protein and ~91% (30 mg in 33 mg total solids) buffer components. Sugar free solutions (BAP; Table V.1) showed an average specific activity of 15.7 Units/μg BSAE. This activity in solution as shown in the first column of Table V.4, was statistically unchanged by the addition of the four sugars (Table V.5).

The process of atomization during nebulization can potentially denature some proteins. This may be due to combination of factors. Typically, shear forces associated with air-jet nebulization, the recirculation of a large proportion of the solution before exiting as aerosol, the presence of a large air-water interface within the nebulizer and evaporation of droplets leading to a concentration effect within both the droplets and the nebulizer solution have all been shown to play a part in denaturation. Specifically, shear forces encountered during air-jet nebulization may irreversibly destabilize certain proteins (Charm and Wong, 1970) . Niven and coworkers showed that, lactate dehydrogenase and recombinant human granulocyte colony stimulating factor (rhG-CSF) irreversibly lost 20% and 30-40% of their initial activities, respectively, after 10 min air jet nebulization; they also reported that this loss of activity was affected by the applied nebulization air pressure, time of nebulization and initial reservoir volume, with greater losses occurring at lower reservoir

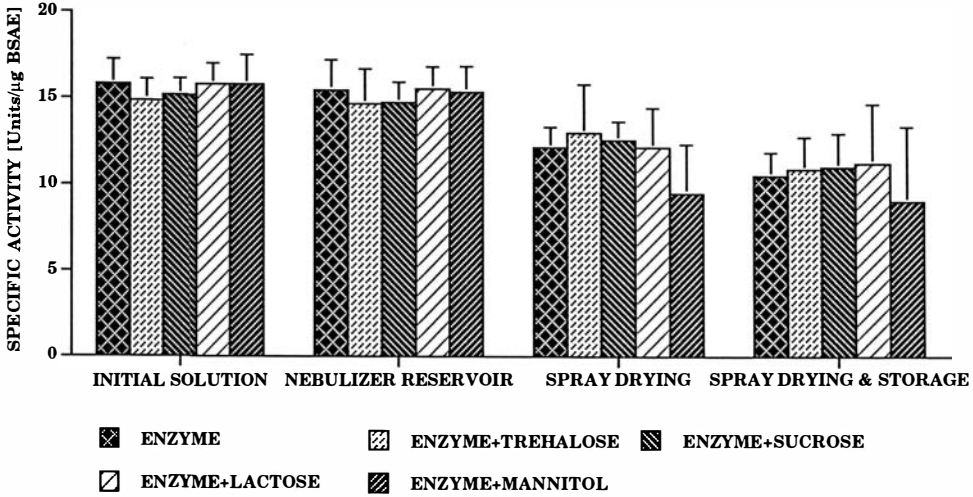

Figure V.5 Specific activities of bacterial alkaline phosphatase (BAP) in initial solution and following nebulization, spray drying with electrostatic collection and storage of dried solids at 23% RH and 25 °C for 14 days. For "INITIAL SOLUTION" and "NEBULIZER RESERVOIR" plotted values are mean, n=6 (error bars are SD). For "SPRAY DRYING" and "SPRAY DRYING AND STORAGE" plotted values are mean, n=3 (error bars are experimental ranges).

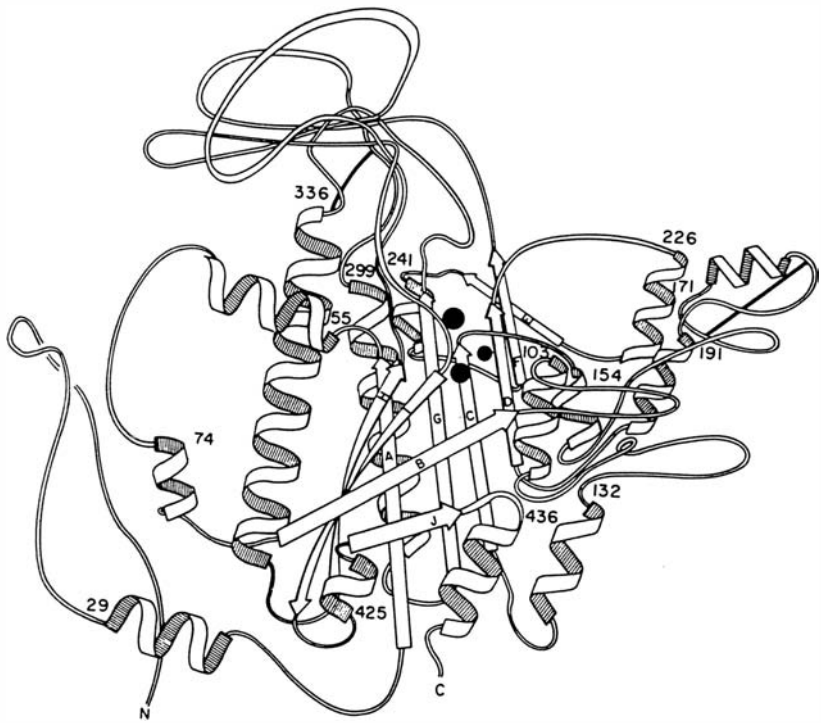

Figure V.6 A cartoon representation of the monomer of bacterial alkaline phosphatase enzyme. The three functional metal sites are shown as black circles; the two larger circles representing Zn^{+2} ions and the smaller circle representing Mg^{+2} ion. The numbers indicate N termini of the corresponding helices (Adapted from Sowadski et al., *J. Mol. Biol.*, 186 (1985) 416-422).

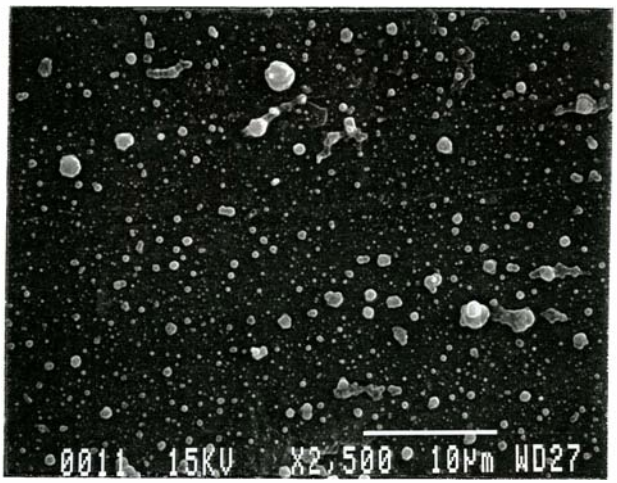

Figure V.7 Scanning electron micrograph (SEM) of bacterial alkaline phosphatase (BAP) spray dried with buffer salts alone and electrostatically collected at 63 °C for 15 min. Concentration of solution nebulized was ~0.1% w/v with respect to total solids.

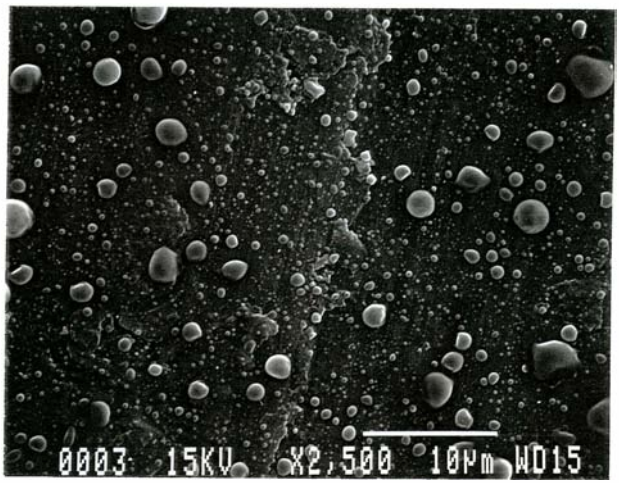

Figure V.8 Scanning electron micrograph (SEM) of bacterial alkaline phosphatase (BAP) spray dried with lactose and electrostatically collected at 63 °C for 15 min. Concentration of solution nebulized was ~1% w/v with respect to total solids.

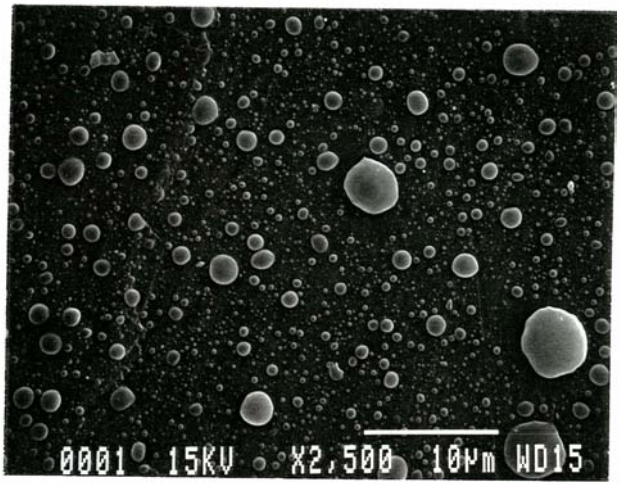

Figure V.9 Scanning electron micrograph (SEM) of bacterial alkaline phosphatase (BAP) spray dried with trehalose and electrostatically collected at 63 °C for 15 min. Concentration of solution nebulized was ~1% w/v with respect to total solids.

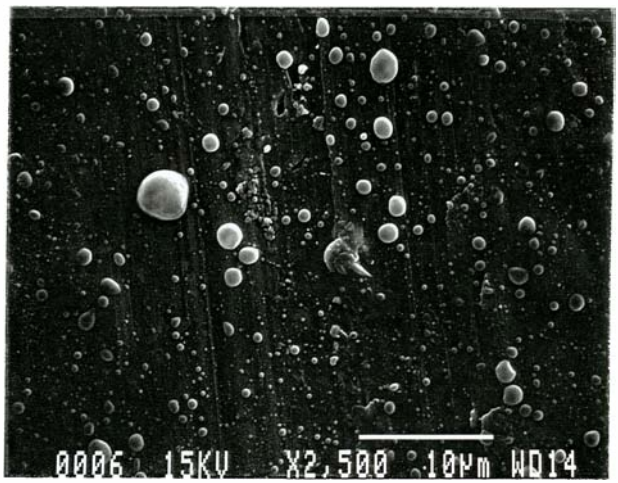

Figure V.10 Scanning electron micrograph (SEM) of bacterial alkaline phosphatase (BAP) spray dried with sucrose and electrostatically collected at 63 °C for 15 min. Concentration of solution nebulized was ~1% w/v with respect to total solids.

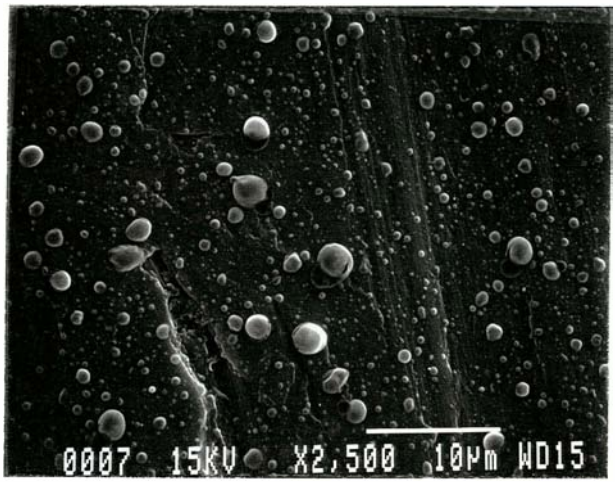

Figure V.11 Scanning electron micrograph (SEM) of bacterial alkaline phosphatase (BAP) spray dried with mannitol and electrostatically collected at 63 °C for 15 min. Concentration of solution nebulized was ~1% w/v with respect to total solids.

starting volumes, higher nebulization pressures and longer nebulization times (Niven et al., 1994). However results are also protein dependent. Cipolla et al., reported that recombinant human deoxyribonuclease (rhDNase), showed no loss of activity after typical air jet nebulization as indicated by its activity assay (Cipolla et al.,1994a).

In the experiments described in this chapter, BAP showed no appreciable loss of activity in the nebulizer solution at the end of 90 min nebulization (26 psig and starting reservoir volume = 24 ml) as indicated by specific activity of solution sampled from the nebulizer reservoir. This result was despite the doubling of concentration of this solution over the 90 min nebulization period (Table V.4). The presence of trehalose, sucrose, lactose and mannitol furthermore, did not affect the residual activity in solution at the end of 90 min nebulization (ANOVA, Table V.5) and nor was there any precipitation in these solutions due to the doubling of concentration in the reservoir solution during the experiment (Table V.4)

Once the atomized droplets come into contact with dilution air, evaporation begins from the droplet surface. This process alone causes a reduced droplet surface temperature, although these temperatures can be approximated by the wet-bulb temperature of the drying air (Masters, 1991). This must be less than the recorded dry-bulb temperature (measured as 63 °C in these experiments, by the thermometer placed inside the drying chamber C; Figure V.1). However the complete process of droplet drying may be thought of as a two phase process (Daemen and van der Stege, 1982).

In the first phase of drying, the wet-bulb temperature at the droplet surface lasts as long as the water activity at the surface of the droplet approaches that of free water. This phase must be followed by an increasing droplet surface temperature, above the wet-bulb temperature on account of decreasing water activity due to dissolved solids at the droplet-air interface. Heat induced enzyme damage is expected mainly during the second phase of the process and is determined by a combination of drying time, temperature, moisture content of the particle and thermolability of the solids content (Daemen and van der Stege, 1982).

Aerosols exiting the primary drying chamber (B, Figure V.1) of the nebulizer were introduced into the secondary drying chamber (C, Figure V.1), to which heated air at a targeted air temperature of 63 °C (dry-bulb temperature) was supplied, in a co-current fashion (See Section V.b.1). In the co-current mode of spray drying, atomized droplets and the drying air pass in the same direction (Masters, 1991a). Under these conditions, the hottest drying air contacts droplets at their maximum moisture content. The rapid evaporation that follows assures low droplet temperatures and is most suitable for drying of thermolabile materials (Masters, 1991). A drying air temperature of 63 °C was selected based on the initial lactose/disodium fluorescein system validation experiments, which resulted in the collection of dried particles in the precipitator column (Chapter IV). Scanning electron microscopy (SEM) of spray dried BAP and BAP-sugar mixtures are shown in Figure V.7 (BAP with buffer salts alone), Figure V.8 (BAP with

lactose), Figure V.9 (BAP with trehalose), Figure V.10 (BAP with sucrose) and Figure V.11 (BAP with mannitol). The drying temperature used in the secondary dryer (C, Figure V.1) was 63 °C and electrostatic collection time was 15 min. When enzyme was spray dried with buffer salts alone (Figure V.7), the particles were apparently dry and the particle size smaller than when compared to products resulting from co-drying with sugars (Figures V.8 - V.11); this due to lower nebulized solids concentration in these solutions (0.1% w/v compared to 1% w/v in solutions with sugars). However, in all cases, the product appeared to be in the form of dry, spherical, discrete particles which were smaller than 5 μm in diameter (Figures V.7 - V.11). Those products containing spray dried sugars often showed smooth spherical particles typical of many spray-dried products (Masters, 1991a).

When trehalose and sucrose were included in the nebulizer solution, the activities retained in the dried, reconstituted solutions were 87% and 83% of their initial solution activities, respectively. Trehalose and sucrose appeared to offer some protection to the drying-induced loss of BAP activity although the small increases in specific activity over the sugar free state were statistically insignificant (ANOVA, Table V.5). Hence the effect of each of the four sugars on spray dried BAP was statistically indistinguishable. Lactose certainly showed no protective effect on BAP during drying and collection, under the conditions studied. It remains possible that some degradation shown in the presence of lactose, was due to reaction with the aldehyde of lactose in the ring opened, reducing form

(Chapter III). When mannitol was included in the solution, a significantly greater loss of activity (42%) was observed compared to the 23% loss when the enzyme was spray-dried alone, but again this effect was not statistically significant for the reasons described above (Table V.5). In independent experiments described earlier (Chapter III) the four sugars were spray dried in a bench top spray dryer and their physical properties characterized with respect to crystallinity changes and moisture uptake. These experiments are described in detail in Chapter III. Only lactose, trehalose and sucrose were obtained in the glassy amorphous state when spray dried in the bench top spray dryer (Yamato ADL-31, Yamato Scientific America, Inc., Orangeburg, NY), whereas mannitol was crystalline after spray drying, as shown by differential scanning calorimetry (DSC) and X-ray powder diffraction (XRPD). Dry product visualization under crossed polars for the mannitol-BAP mixture confirmed the presence of crystallites in the particulates in this case (birefringence was observed). This indicated that this sugar's tendency to crystallize during drying could be positively harmful to the BAP's enzyme activity possibly because of protein shear during crystal nucleation and growth.

Sugars have been used for a long time in the stabilization of biological macromolecules, in solution and dried solid state. It is well established that sugars stabilize proteins in solution by means of preferential hydration mechanism proposed by Timasheff (Arakawa and Timasheff, 1982). However, the ability of sugars to protect against dehydration induced

destabilization, during freeze drying (Pikal, 1990; Prestrelski et al., 1993), air drying (Carpenter et al., 1987) and spray-drying (Labrude et al., 1989; Broadhead et al., 1993), is not very well understood. Two hypotheses have been proposed, to explain the dehydration induced protection of proteins by sugars. In the water replacement hypothesis, it is theorized that the water removed by dehydration is replaced by sugar molecules, which hydrogen bond to the protein during the end stages of drying and stabilize the native conformation (Carpenter and Crowe, 1989). However sugars with similar hydrogen bonding capacities have widely varying protein stabilization effects (Levine and Slade, 1992). An alternate hypothesis based on the materials science approach of glass transition has been proposed (Franks et al., 1991; Green and Angell, 1989). According to this hypothesis, when a solution of protein-sugar is dried, at the end stage of drying, the protein is entrapped in an amorphous glassy matrix of the sugar, thereby reducing molecular motions and hence destabilization effects during dehydration and long term storage (Franks et al., 1991). Such a glass is physically metastable at temperatures below its glass transition temperature (T_g). However, at temperatures greater than T_g, molecular mobility increases, leading to physical instability such as recrystallization and an increased chance of degradative chemical reactions (Ahlneck and Zografi, 1988). It is also well established that T_g of a glass is dependent on its residual moisture content, with increased moisture content leading to a depression of the T_g, since water acts as plasticizer of amorphous materials (Roos and Karel,

1991). If T_g is decreased below the storage temperature, physical and chemical stability can be expected to occur in the solid state. Although, this hypothesis does not fully explain the effect of all excipients on stabilizing proteins, it partially explains the relative capacity of certain sugars to stabilize proteins during dehydration. In these experiments with BAP dried in the presence and absence of sugars, it was not statistically possible to rank the sugars which form amorphous glasses in terms of their protective effects on this enzyme's activity. For this reason, it was not possible to speculate further on the importance of these glass transition temperature values on BAP stability during the drying and collection phase; and further to use the value of T_g as a means of selecting a sugar as a protein stabilizer during spray drying.

V.c.4 Spray drying and electrostatic collection of bovine intestinal alkaline phosphatase (BIAP)

A second alkaline phosphatase, from a different source, structure and purity, was subjected to a similar series of experiments to determine whether BAP results were typical or unique of this class of enzyme. Bovine intestinal alkaline phosphatase (BIAP) is a dimeric metallo-glycoprotein (~12% carbohydrate content by weight) of molecular weight 138000 Daltons, composed of two monomers of 69000 each (Coleman and Gettins, 1983; Fosset et al., 1974). The three dimensional structure of BIAP has not been reported to date. However, a partial amino acid sequence analysis revealed

that it bears close sequence homology to BAP, especially with regards to the three amino acids (Asp-Ser-Ala) that make up the active site on the monomer (Coleman and Gettins, 1983). In spite of such structural similarities, resistance of BIAP to thermal degradation has been reported to be much poorer than that of the bacterial enzyme. Denaturation temperatures for the bovine enzyme have been reported to occur at ~65 °C.

In experiments with BIAP the total protein content was ~10% (25 mg in 250 mg total solids for solutions coded as BIAPL, BIAPT, BIAPS and BIAPM for solutions containing lactose, trehalose, sucrose and mannitol; Table V.1) in a 1% w/v solution with respect to total non-volatile solids; this was because BIAP had a much lower specific activity (and possible purity) than BAP (BAP = 15.7 Units/μg BSAE and BIAP = 8.8 Units/μg BSAE). Buffer components and sugar constituted the remaining 22% and 68% of the solids respectively (Table V.1). In sugar free experiments total solids concentration in the nebulizer solution was ~0.3% w/v (solution coded as BIAP; Table V.1), of which 32% was protein and 68% buffer salts. Nebulization and droplet drying and particulate collection conditions were used, which were identical to those used for BAP. Results for specific activity of BIAP are summarized in Table V.6 and Figure V.12. Protein containing sugar free solutions (BIAP; Table V.1) showed a specific activity of 8.8 Units/μg BSAE. This enzyme activity in solution was not affected by the addition of any of the four sugars, lactose, trehalose, sucrose and mannitol, and/or air-jet nebulization at 26 psig for 90 min, with an initial

Table V.6 Specific activity of bovine intestinal alkaline phosphatase (BIAP) following nebulization and spray drying with sugars, electrostatic collection and storage.

	Initial Solution[c]		Nebulizer Reservoir[d]		Spray Dried[e]	Storage[f]
	Spec. Act.[b] (Units/μg prot)	Prot. Conc. (μg/ml)	Spec. Act.[b] (Units/μg prot)	Prot. Conc. (μg/ml)	Spec. Act.[b] (Units/μg prot)	Spec. Act.[b] (Units/μg prot)
BIAP[a]	8.8 (0.6)	885.2 (88.1)	9.0 (0.5)	1739.9 (329.5)	6.1 (1.1)	4.8 (1.0)
BIAPL[a]	9.5 (1.3)	867.1 (85.2)	9.7 (1.7)	1650.7 (244.7)	10.4 (2.5)	8.8 (1.0)
BIAPT[a]	8.6 (0.8)	932.4 (81.4)	9.0 (1.1)	1796.7 (251.3)	9.7 (0.7)	8.8 (0.9)
BIAPS[a]	8.6 (1.0)	928.5 (100.5)	8.8 (0.8)	1687.5 (266.0)	9.6 (0.9)	9.5 (1.7)
BIAPM[a]	8.9 (0.7)	899.0 (76.5)	9.2 (0.6)	1699.1 (329.5)	5.2 (0.4)	4.4 (1.8)

a Solutions correspond to coded solutions as tabulated in Table V.1.
b One unit is defined as the amount of enzyme that releases 1 nmol of p-nitrophenol per minute at 37 °C. Protein content was determined in terms of BSA equivalents (BSAE).
c Values are mean (sample standard deviation), n=6.
d Solution assayed from the nebulizer reservoir at the end of 90 min. Values are mean (sample standard deviation), n=6.
e Spray dried and collected for 90 min. Values are mean (experimental range), n=3.
f Spray dried and collected for 90 min prior to storage at 23% RH and 25 °C for 14 days.Values are mean (experimental range), n=3.

Table V.7 Summary of two way analysis of variance (ANOVA)[a] results for enzyme specific activities of bovine intestinal alkaline phosphatase (BIAP).

Source of variation	Sum of squares	Degrees of freedom	Mean Square	F-ratio	Significance level
Main Effects					
SOLN[b]	93.69	4	23.42	26.72	$p < 0.05$
COND[c]	39.95	3	13.32	15.19	$p < 0.05$
Interaction					
COND . SOLN	91.78	12	7.65	8.73	$p < 0.05$
Residual	61.36	70	0.88		
Total	243.71	89			

[a] The statistical model tested was:
$X_{ij} = \mu + COND_i + SOLN_j + (COND_i \cdot SOLN_j) + \varepsilon_{ij}$ and is described in Section V.b.4 ($\alpha = 0.05$).

[b] Five levels of solution effect (SOLN) were tested; BIAP, BIAPL, BIAPT, BIAPS and BIAPM.

[c] Four levels of experimental condition effect (COND) were tested; initial solution, nebulizer reservoir solution, spray dried and spray dried and stored at 23 %RH and 25 °C for 14 days.

Table V.8 Summary of significance levels for individual follow up one way analyses of variance (ANOVA)[a] for specific activities of bovine intestinal alkaline phosphatase (BIAP).

Source of variation	COND=Intial solution	COND=Nebulizer Reservoir	COND=Spray Dried	COND=Spray dried & stored
Between ($SOLN_j$)[b]	NS[d]	NS[d]	$p < 0.05$	$p < 0.05$

Source of variation	SOLN=BIAP	SOLN=BIAPL	SOLN=BIAPT	SOLN=BIAPS	SOLN=BIAPM
Between ($COND_i$)[c]	$p < 0.05$	NS[d]	NS[d]	NS[d]	$p < 0.05$

[a] All statistical analysis was performed at $\alpha = 0.05$

[b] $SOLN_j$ = Formulation effect; j = BIAP, BIAPL, BIAPT, BIAPS or BIAPM.

[c] $COND_i$ = Experimental condition effect; i = Intial solution, nebulizer reservoir, spray dried and spray dried and stored.

[d] No significant difference.

reservoir volume of 24 ml (Table V.8). At end of 90 min nebulization however a frothy solution remained in the nebulizer reservoir, probably because of surface activity of the protein after its concentration had doubled during 90 min of nebulization (Table V.6).

Aerosols of BIAP with and without lactose, trehalose, sucrose and mannitol were dried and electrostatically collected using the apparatus shown in Figure V.1. Dried aerosols collected on the glass collection surface inside the precipitation column (I, Figure V.1), were rinsed with 10 mM Tris buffer pH 8.0. Reconstituted solutions were appropriately diluted and analyzed for protein content and enzyme activity.

In case of BIAP spray dried in the absence of added sugar the dried and reconstituted solution showed a similar drop in specific activity to that seen with BAP. Thus an average of 6.1 Units/μg BSAE was recovered, a 31% loss of activity compared to the initial solution (protein content determination was probably unaffected by processing as discussed in Sections V.c.1 and V.c.2). This increased loss of BIAP activity may be due to *its* lower thermal denaturation temperature (~65 °C) compared to BAP (96 °C). Hence, at the drying temperature of 63 °C used in this study, a greater fraction of BIAP may be expected to be in the denatured state compared to BAP. However, in the presence of lactose, trehalose or sucrose, activity was completely retained when BIAP was spray-dried, collected electrostatically and subsequently reconstituted with Tris buffer pH 8.0 (Table V.6). Similar to BAP, and probably for similar reasons, spray drying BIAP with mannitol

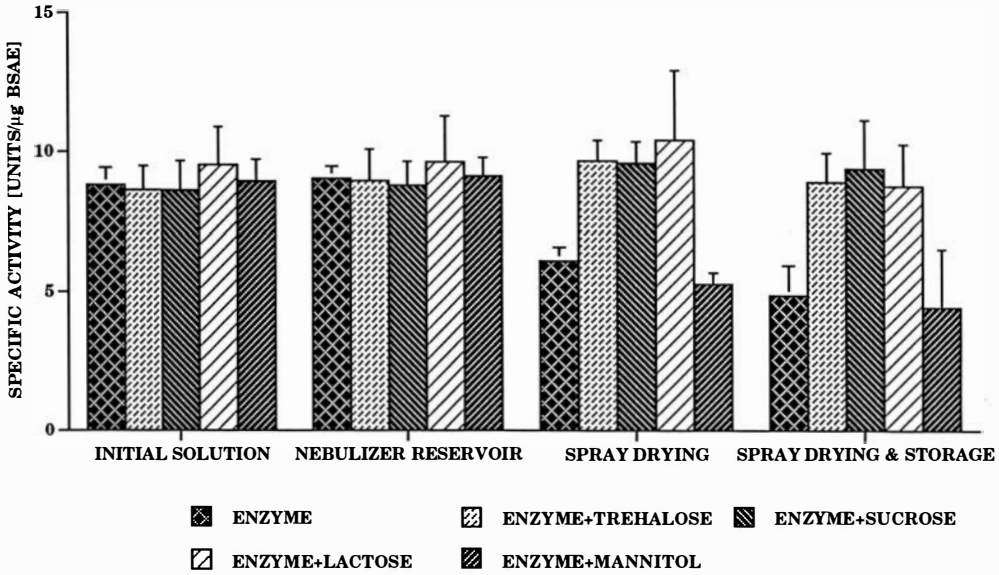

Figure V.12 Specific activities of bovine intestinal alkaline phosphatase (BIAP) in initial solution and following nebulization, spray drying with electrostatic collection and storage of dried solids at 23% RH and 25 °C for 14 days. For "INITIAL SOLUTION" and "NEBULIZER RESERVOIR" plotted values are mean, n=6 (error bars are SD). For "SPRAY DRYING" and "SPRAY DRYING AND STORAGE" plotted values are mean, n=3 (error bars are experimental ranges).

resulted in a 42% loss of initial activity, a result which indicated significantly greater degradation than when BIAP was dried in the absence of sugar (ANOVA, individual comparisons by Scheffe's multiple comparison test, $p < 0.05$). Once more, mannitol co-dried BIAP showed the presence of crystallization when observed under crossed polars (birefringence). It was not possible however, to discriminate statistically between the protective effects of trehalose, sucrose and lactose, even though on average, lactose appeared to enable or even cause some BIAP degradation.

In independent experiments described in Chapter III, spray dried lactose, sucrose and trehalose were amorphous and spray dried mannitol was crystalline (Chapter III). It was impossible in these experiments, where product yields were small to fully characterize the spray dried particulates as well as determining protein contents and activities. It seems reasonable however that during nebulization and electrostatic collection in these experiments, similar physical forms of each sugar was formed, although conditions employed for drying were different from those using the Yamato spray dryer (as described in Chapter III). Admixture of buffer salts and proteins to mannitol probably reduced the degree of that sugar's overall crystallization but did not prevent it entirely (birefringence under cross polars).

Some of the results presented above may be confounded by the presence of altered buffer (Tris) components in the dried and reconstituted

products. This because increasing concentration of Tris has been shown to increase the maximal activity of alkaline phosphatase (Chappelet-Tordo et al., 1974). However, such effects have been reported to become significant only at high concentrations of Tris (molar range) and, thus, may not be a factor in these experiments. These results with BAP and BIAP seem to support the hypothesis, that formation of an amorphous glassy matrix of the sugar was a prerequisite for offering protein protection during spray drying even though, in the case of some fairly stable proteins (BAP in this case) no statistically proven protection was afforded by the addition of a glass-forming sugar (trehalose and sucrose; Table V.4). Some non-specific bonding between protein and sugar in the dried mixture may also have contributed to the stabilization, as previously reported (Carpenter and Crowe, 1989), but this was not tested in this study. Spray dried lactose, sucrose and trehalose showed distinctly different glass transition temperatures (T_g) of 117 °C, 75 °C and 120 °C respectively, in their completely dry state, as determined by crimped pan DSC (Chapter III). It was not possible to differentiate between glass-forming sugars and the protection they offered in terms of their quoted T_g values. This was due to several confounding factors such as residual moisture content of the dried solids, thermolability of the protein used and the sensitivity of the assay to show differences and temperature of drying. The crystallization of mannitol along with the protein during the drying process had a positively harmful effect on protein activity and thus structure in both cases. Such a

Figure V.13 Molecular structures of sugars used in this investigation. Ring structures are numbered with and without primes ('), only for convenient textual reference. The structure of β-lactose is shown because a mixture of the α and β isomers forms quite rapidly in solution, following dissolution of α-lactose monohydrate in water.

4-*O*-β-D-Galactopyranosyl-D-glucopyranose

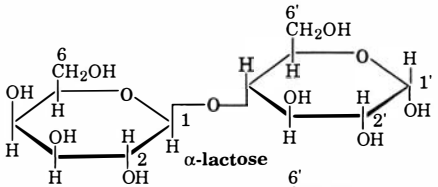

α-lactose

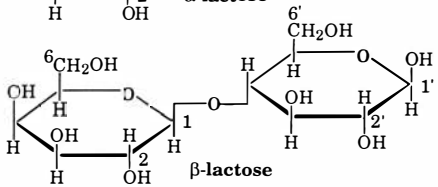

β-lactose

α-D-Glucopyranosyl α-D-Glucopyranoside

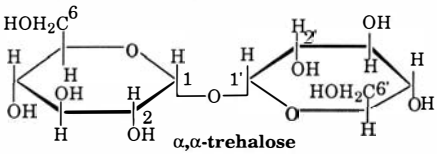

α,α-trehalose

β-D-Fructofuranosyl α-D-Glucopyranoside

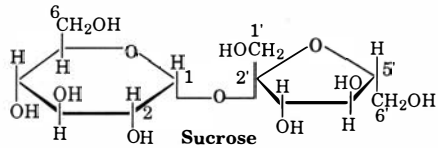

Sucrose

1,2,3,4,5,6-Hexanehexol

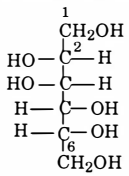

D-Mannitol

decreased protein stabilizing effect has also been reported for cryoprotectants due to their crystallization in freeze dried solids (Izutsu et al., 1993) and thus, it is tempting to speculate that similar protein damage mechanism (Izutsu et al., 1993) was in play in this case also.

V.c.5 Stability of dried protein and protein-sugar mixtures

Excipients like sugars, which stabilize proteins during dehydration, are also believed to offer protection to proteins during long term storage in the solid state (Tarelli and Wood, 1981; Ford and Dawson, 1993; Broadhead et al., 1994). The protective ability of sugars appears to depend on factors such as, the chemical nature of the sugar, the residual moisture content of the sugar-protein molecular mixture and the temperature and relative humidity of storage (Hageman, 1988; Tarelli et al., 1987; Pristoupil et al., 1985; Lea and Hannan, 1949).

Both BAP and BIAP were spray dried in buffered solutions with or without one of the four sugars, as described in Section V.b.1. Protein and sugar concentrations of the nebulizer solutions were kept at the same levels as those described in Section V.c.3. Dried aerosols were collected on glass collection tubes introduced inside the precipitator column (I, Figure V.1). The dry particle coated glass tubes were stored at 25 °C and 23% RH for 14 days, as described in Section V.b.2, prior to reassay. These conditions were chosen expressly because none of these sugars showed any changes in their physical characteristics over 30 days at this temperature and humidity

(Chapter III); trehalose, sucrose and lactose became crystalline when stored at RH > 23% (Figures III.2 and III.3, Chapter III). Results for enzyme activity after 14 days storage are shown for BAP and BIAP, in the right hand columns of Table V.4 and Table V.6 respectively. BAP spray dried in the presence of buffer salts alone and stored at 25 °C and 23% RH for 14 days, retained only 67% of the initial solution activity, which represented a further loss of about 10% activity, compared to the spray dried material without storage. However, this difference was not statistically significant (Table V.5). No clear protection was offered by any of the sugars to this loss of activity on solid-state storage. Further losses in activity after storage of BAP dried with the four sugars, ranged from 1% (mannitol) to 10% (sucrose) compared to the spray dried material without storage (Table V.4). Surprisingly, mannitol showed the least change in terms of absolute degradation [(Units/μg BSAE)/14 days] while trehalose appeared to offer no protection in the solid state even though it protected BAP during drying and collection. However, none of the four sugars could be statistically distinguished with respect to their protective effect on the enzyme during storage.

BIAP spray dried with buffer salts alone and stored at 25 °C and 23% RH for 14 days showed a further loss of about 15% activity compared to the spray dried material tested prior to storage. However, individual comparisons by Scheffe's test showed no significant differences. With BIAP however, the three glass forming sugars, lactose, sucrose and trehalose

offered statistically equivalent protection both during drying and storage (Table V.8). BIAP dried with mannitol showed an activity of 4.4 Units/μg BSAE on storage, but even this was not statistically different from the activity of spray dried BIAP-mannitol without storage.

Overall and statistically, BIAP activity loss during storage in the solid state did not occur provided trehalose, sucrose, lactose or mannitol were used in the spray drying process. BIAP-mannitol lost substantial activity on drying, but this residual activity was largely retained on further storage. It is possible, of course, that these conclusions may have been different if the storage duration and the number of samples had been increased.

Structures of the sugars used in this study are given in Figure V.12. Mannitol is a non-reducing sugar alcohol, lactose, sucrose and trehalose are disaccharides. Sucrose and trehalose are non-reducing sugars while lactose is a reducing sugar (Tarelli and Wood, 1981). It has been widely reported that reducing sugars like lactose may interact with proteins via the Maillard reaction, whereby the open ring aldehyde form of the sugar undergoes condensation with free amino groups on the protein to form Schiff-bases which eventually undergo Amadori rearrangement. This leads to product discoloration and, loss of activity of the protein (Ford and Dawson, 1993; Hageman, 1988; Tarelli and Wood, 1981). There was no evidence of such reactions occurring in these studies. Non-reducing sugars like sucrose and trehalose may be potentially reducing, after breakage of the inter-glycosidic linkage. However, for many disaccharides such

breakage occurs to a significant extent only in solutions of extreme pH or freeze dried solids kept at high temperatures (Tarelli and Wood, 1981). Moreover, relative stability of the inter-glycosidic bond for different disaccharides varies widely. Tarelli and Wood have shown that in 0.05 M sodium phosphate buffer, pH 7, a greater percentage of sucrose was lost compared to trehalose, after heating at 100 °C for 17 hours, indicating the intrinsic stability of trehalose's inter-glycosidic bond compared to that of sucrose (Tarelli and Wood, 1981). Pazur, quotes activation energies for acid hydrolysis of the glycosidic bond of sucrose, lactose and trehalose as 25830 cal/mole, 26900 cal/mole and 40180 cal/mole respectively, indicating the relative stability for the disaccharide sugars, as trehalose>lactose>sucrose (Pazur, 1970). Pharmaceutically, and in the solid state in these investigations, it is unlikely that the above discussion is even relevant. Nevertheless, lactose remains as a reducing sugar in the disaccharide form, a fact which also enables it to mutarotate via the aldehyde intermediate; the spray dried product must therefore contain a mixture of the two anomeric forms, α-lactose and β-lactose as shown in Figure V.11 (Pigman and Anet, 1972).

Similar to the discussion in Chapter III, the likely content of β-lactose in the lactose containing protein mixtures, was 5 - 7%. Clearly it is impossible to say, from these investigations, whether the α/β lactose ratio may affect lactose's ability to protect BAP or BIAP during drying, collection

or storage, except to note that no real studies have been reported to date, which test the importance of sugar stereochemistry on protein protection.

Under storage conditions used in this study (25 °C and 23% RH for 14 days), no substantial degradative reactions between BAP or BIAP and the sugars occurred. Earlier reports of Maillard reactions between reducing sugars like lactose and proteins in the solid state involved experiments which were performed under more stressful conditions of temperature, relative humidity and duration of storage (Ford and Dawson, 1992; Tarelli and Wood, 1989; Lea and Hannan, 1949). Ford and Dawson studied the activity of bovine intestinal alkaline phosphatase-sugar mixtures freeze dried and stored at different temperatures and time periods (Ford and Dawson, 1992). They showed that alkaline phosphatase, formulated with lactose and trehalose, retained maximal activity after storage for 12 weeks at -20 °C, 20 °C, 37 °C and 45 °C. Only at 56 °C, was there a considerable loss of activity, with a more rapid decline in the lactose formulation (7 - 14 days) compared to the trehalose formulation (21 - 42 days). Trehalose formulation was predicted to retain 42% of its initial activity even after storage at 37 °C for a year (Ford and Dawson, 1992).

V.d SUMMARY AND CONCLUSIONS

A particle collection apparatus built and characterized previously (Chapter IV), was used to review protein activity following spray drying

and electrostatic precipitation. Bacterial alkaline phosphatase (BAP) and bovine intestinal alkaline phosphatase (BIAP) were selected as model proteins to study the effect of nebulization and drying on their residual activity. Four sugars, lactose, trehalose, sucrose and mannitol were co-dried with the enzymes, and form molecular mixtures in the dry state, thus to look at their affect on preventing enzyme activity loss on spray drying and storage of sugar-protein mixtures.

BAP lost 23% of its original activity following spray drying and electrostatic collection, when dried from sugar free solutions. Although lactose, sucrose and trehalose all appeared to prevent of this loss, the results were not statistically different from the sugar-free result. Mannitol, which was crystalline on spray drying alone and in admixture with the protein, also failed to protect BAP. This result however, was also not significantly different from other sugars.

The second enzyme, BIAP, lost 31% of its original activity when spray dried from sugar-free solutions. Lactose, trehalose and sucrose offered complete protection on spray drying and collection (no significant difference in activity from original solution). However, these three sugars were indistinguishable with respect to their stabilizing capacity for BIAP drying. BIAP dried with mannitol showed an activity loss similar to the sugar free solution, indicating that mannitol failed to offer protection to the enzyme.

Both enzymes failed to lose any further activity on storage of the dried solids at 23 %RH and 25 °C for 14 days (no significant difference between

material prior to storage and storage at 23% RH and 25 °C). Storage results were not different from their respective initial spray dried counterparts, for both the enzymes in the presence or absence of the four sugars. The reported degradative chemical reactions between reducing sugars like lactose and proteins in the solid state were not evident under these storage conditions and degradation reactions may only become relevant, under more extreme conditions of temperature and relative humidity.

Lactose, trehalose and sucrose were obtained as amorphous solids on spray drying and remained in this physical form when stored at 23% RH and 25 °C for 30 days (Chapter III). In contrast mannitol was crystalline on spray drying. Moreover, enzyme-mannitol solutions spray dried and electrostatically collected, revealed crystallization, when observed with a microscope under cross polars (birefringence). It appeared that formation of the amorphous glassy state may be a prerequisite for stabilization of proteins like BIAP during spray drying.

The results suggested that it was feasible to produce small particles of active protein when spray dried with glass forming sugars like lactose, trehalose and sucrose. However, the final performance of the dry powder as an aerosol must also depend on physical and chemical stability of the dried mixtures and the ease of their dispersion to form respirable clouds.

VI. DETERMINATION OF MOISTURE IN CRYSTALLINE AND SPRAY DRIED SUGARS USING ISOTHERMAL THERMOGRAVIMETRIC ANALYSIS (TGA) AND KARL FISCHER (KF) COULOMETRIC TITRATION

VI.a INTRODUCTION

Determination of moisture is routinely employed in the quality control of pharmaceutical ingredients. Karl Fischer titration (KF) is the most commonly used method for routine determination of water in solid, liquid and gaseous samples (Scholz, 1984). This is believed to be a more definitive method for water determination than loss-on-drying (LOD) because LOD results may be confounded by the presence of volatiles other than water. However, KF requires the extraction of water from the sample prior to or during titration if it is to produce a reliable result. Water can be extracted from samples by different methods, like dissolving in anhydrous solvents such as methanol or formamide and injecting a suitable portion of the solution into the KF titration vessel. Alternatively, water may be evaporated in a heating chamber attached to a KF titration vessel which is sealed to prevent moisture ingress from the atmosphere. Titration may then be effected specific to the evolved moisture. This technique can be rapid and useful for materials when moisture is loosely bound to the sample,

such as in freeze dried or spray dried materials. However such a method may not always work well, when bound water (eg. crystalline hydrates) is being determined, due to the erratic loss of bound water on heating. In this chapter, the moisture content of crystalline sieve fractions of four different sugars, lactose, trehalose, sucrose and mannitol, and their spray dried forms, was determined using KF coulometric titration. Results were compared, following sugar dissolution in formamide and KF titration, to those following heating of each sugar with subsequent titration of the evolved water in the collection gas passing over the sample. The second evaporative method was performed in order to validate a third; isothermal thermogravimetric analysis (TGA). TGA, a micro LOD method which can be performed quite simply on milligram quantities of sample, is much more convenient than either KF technique. It requires however, that weight loss due to heating first be proven to be due to loss of water.

VI.b PRINCIPLE OF COULOMETRIC KARL FISCHER TITRATION

The Karl Fischer reaction can be shown as follows:

$I_2 + SO_2 + 3Pyridine + CH_3OH + H_2O$ -------> $2Pyridine.HI + Pyridine.H_2SO_4$

---------- Equation VI.b.1

In coulometric KF titration, iodine that is used in the above reaction is not added to the reagent (as in volumetric titration mode), but is produced in an iodide containing solution by anodic oxidation as shown in Equation VI.b.2 (Scholz, 1984)

$2I^{-1} - 2e \text{ --------> } I_2$ ---------- Equation VI.b.2

When sample is added to the anodic solution (Figure VI.1) containing iodide ion, sulfur dioxide, base (pyridine) and methanol as principal components, water in the sample reacts with electrolytically generated iodine (Equation VI.b.2) as shown in Equation VI.b.1. One mole of iodine reacts with one mole of water and thus 1 mg of water is equivalent to 10.71 coulombs. Using this relationship, water content is calculated from the electricity (coulombs) required for electrolysis (Aquamicron Instruction Manual, Mitsubishi Kasei Corporation, Tokyo, Japan).

VI.c MATERIALS AND METHODS

VI.c.1 MATERIALS

D-Mannitol, sucrose and α,α-trehalose dihydrate were obtained from Sigma Chemical Co. (St. Louis, MO). α-Lactose monohydrate was obtained from Foremost Ingredient Group (Baraboo, WI). Karl Fischer reagents Aquamicron-AS® and Aquamicron-CS® were obtained from Cosa Instrument Corp. (Norwood, NJ). KF standards (Hydranal®-Water Standard 1.00; 1 g containing 1.00 ± 0.03 mg water and Hydranal®-Standard sodium tartrate dihydrate; water content = 15.66 ± 0.05%) manufactured by Riedel-de Haën (Seelze, Germany) and other chemicals used were obtained from Fisher Scientific Co. (Raleigh, NC).

VI.c.2 METHODS

VI.c.2.1 Spray drying of sugars

A 10% w/v solution of each sugar was spray dried using a Yamato ADL-31 Mini-Spray Dryer (Yamato Scientific America Inc., Orangeburg, NY) as described in Chapter III. Collected spray dried sugars were quickly packed into amber bottles, tightly closed and stored in desiccators, containing phosphorous pentoxide.

VI.c.2.2 Sieve fractionation of sugars

Two particle size fractions; 44-74 μm ["fine fraction"] and 125-212 μm ["coarse fraction"], of each sugar were obtained by sieve fractionation as described in Chapter III and were retained in tightly closed amber bottles stored over phosphorous pentoxide.

VI.c.2.3 Thermogravimetric analysis (TGA)

Thermogravimetric analysis (TGA) was performed using TGS2 along with System 4 microprocessor controller (Perkin Elmer, Norwalk, CT). TGA was performed in triplicate, in the isothermal mode to determine a time period for complete dehydration of the sugars. Temperatures used for the isothermal TGA runs, were previously determined using TGA in the non-isothermal mode (Naini et al., submitted 1996). These were temperatures corresponding to apparent plateaus in weight loss versus

temperature plots. Conditions used for isothermal TGA are shown in Table VI.1.

VI.c.2.4 Karl Fischer (KF) moisture determination

KF analysis was performed by coulometric titration using a Mitsubishi Moisture Meter, Model CA-05 attached to VA-05 vaporizer oven (Mitsubishi Kasei Corp., Tokyo, Japan). The schematic diagram of the moisture meter set up is shown in Figure VI.1. Two different methods based on coulometric KF titration (Method Ic of USP), were employed to determine moisture content of sugars (USP23/NF18, 1994b).

Method A: Sugars were accurately weighed into glass weigh funnels (catalogue #14-353B, Fisher Scientific Co., Raleigh, NC) and introduced into the sample boat positioned below the sample inlet port (Figure VI.1). Sample sizes of 5 - 10 mg were employed throughout. At time zero the sample boat was slid into the preheated oven connected to KF titration vessel shown in Figure VI.1. Nitrogen (Nitrogen, NF, Airco, Richmond, VA) dried by passing it over phosphorous pentoxide, at a flow rate of 250 ml/min (adjusted by means of the flow valve, Figure VI.1) was used as the carrier gas to transfer the evolved moisture, into the titration vessel by means of a connecting tube. To prevent condensation of the evolved moisture while being transported into the titration vessel, the tube was heated to the same temperature as the oven. Oven temperatures for testing were selected following non isothermal TGA as described earlier. Delay

times for titration, determined by isothermal TGA experiments (time to plateau), were also entered into the program of the moisture meter. The delay times and temperatures used for different sugars are shown in Table VI.2. All reported values are the means of five determinations. Sodium tartrate dihydrate (Hydranal®), with a theoretical water content of 15.66% ± 0.05% (Bryan et al., 1976 and Dietrich, 1994) was used as the standard for Method A.

Method B: Approximately 100 - 500 mg (accurately weighed) of the sugar was dissolved in 10 ml formamide and 400 µl of this solution was injected into the anodic solution through a septum (Figure VI.1), using a syringe (#1705, Hamilton Co., Reno, NV) attached to a non sterile, septum piercing stainless steel needle (Popper & Sons, Inc., New Hyde Park, NY). The accurate weight of each sample solution injected (known concentration) was determined by difference in syringe weight before and after sample injection and used for moisture content calculation. A blank formamide injection was performed prior to each sample injection. Blank moisture content of the solvent was subtracted from the titrated water content of each sample solution. All reported values are mean of five such (sample-blank) determinations. A specific gravity of 1.129 g/ml at 25 °C (certificate of actual lot analysis, Fisher Scientific Co., Raleigh NC) for formamide was used in the calculation of moisture contents. Hydranal® Water Standard 1.00 (water content = 1.00 ± 0.03 mg/g) was used as the standard for Method B and also to check the performance of the moisture

meter (Dietrich, 1994) prior to performing all experiments..

VI.d RESULTS AND DISCUSSION

Results from the isothermal TGA experiments are summarized in Figures VI.2 - VI.5 and Table VI.1. Crystalline fractions of sucrose and mannitol and spray dried mannitol did not show detectable weight loss using isothermal TGA. All other sugars reached a plateau for weight loss vs time curves in less than or equal to 10 min. Coarse fractions of trehalose and lactose (Figures VI.3 & VI.4) showed a thermal lag during dehydration, compared to their fine sieve fraction (Naini et al., submitted 1996). Sodium tartrate dihydrate was used as a reference standard for moisture content determination by Method A. Moisture content of this salt at the end of a 3 min dehydration time (time to plateau) was in close agreement with its theoretical water content of 15.66% (Figure VI.2 & Table VI.1). Based on isothermal TGA data (Figures VI.2 - VI.5), time periods required for effecting complete moisture release were determined and listed in Table VI.1 along with moisture contents corresponding to weight losses at these same time points.

Moisture contents determined by the KF technique using Methods A & B are shown in Table VI.2. Delay times (DT) for heating (times in the oven, prior to titration) for Method A were selected based on isothermal TGA data for complete moisture release (Table VI.1). DTs were chosen so that DT > apparent time to reach a plateau following isothermal TGA

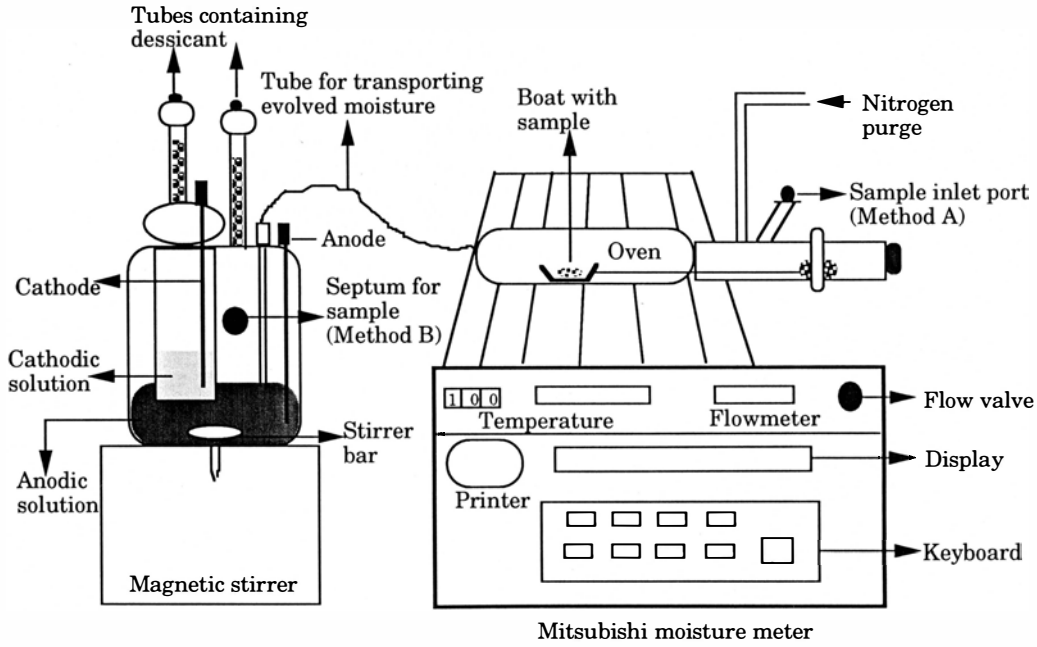

Figure VI.1 Schematic diagram of the Mitsubishi moisture meter with the attached programmable vaporizer oven used for moisture determinations of sugars by coulometric KF titration.

Table VI.1 Isothermal thermogravimetric analysis (TGA) of sugars and sodium tartrate dihydrate.

Sample	Temperature (°C)	% Wt Loss Mean (SD)[a]	Time period for wt loss (min)
Lactose[b]			
Coarse fraction	180	5.15 (0.06)	10
Fine fraction	180	5.22 (0.09)	10
Spray dried	180	2.55 (0.20)	5
Sucrose			
Coarse fraction	100	ND[c]	10
Fine fraction	100	ND[c]	10
Spray dried	100	2.71 (0.38)	5
Trehalose[b]			
Coarse fraction	160	9.12 (0.15)	10
Fine fraction	160	8.93 (0.11)	10
Spray dried	120	4.36 (0.07)	5
Sodium Tartrate Dihydrate[d]	187	15.75 (0.46)	3

[a] Values are mean (sample SD) of three determinations
[b] Theoretical water contents of crystalline sieve fractions of lactose and trehalose are 5.0% and 9.5% respectively.
[c] No detectable weight loss was found after 10 min
[d] Sodium tartrate dihydrate (Hydranal®) with a moisture content of 15.66 ± 0.05%

under identical conditions. All sieve fractions of sugars used in this study were shown to be crystalline using X-ray powder diffraction (Naini et al., submitted 1996). However spray dried lactose, trehalose and sucrose were shown to be completely amorphous by X-ray powder diffraction. As expected, longer delay times were required for complete water release from the crystalline hydrates, whose water was tightly bound compared to the amorphous spray dried forms with loosely bound water (Zografi, 1988). For all materials studied, isothermal TGA results were in close agreement with water contents obtained from the Method B, KF technique. For sodium tartrate dihydrate, moisture estimated using Method A (Table VI.2) was lower than that estimated using isothermal TGA (however the difference was statistically insignificant; t-test, $\alpha = 0.05$) and also its theoretical moisture content of 15.66%. A similar trend was seen with the crystalline hydrates of lactose and trehalose. On the other hand, moisture contents of the spray dried sugars determined using Method A were in close agreement with those from Method B and also the isothermal TGA data (Tables VI.1 and VI.2). This indicated slight underestimations of moisture contents when using Method A for bound crystalline water which may be due to several factors. Obviously, there are differences in the heating environments between the TGA and the KF ovens. More importantly hot N_2, bubbling through the anodic solution in Method A may carry away both the moisture and the volatile components of the anodic solution over time. This appears to be more dramatic with samples containing higher

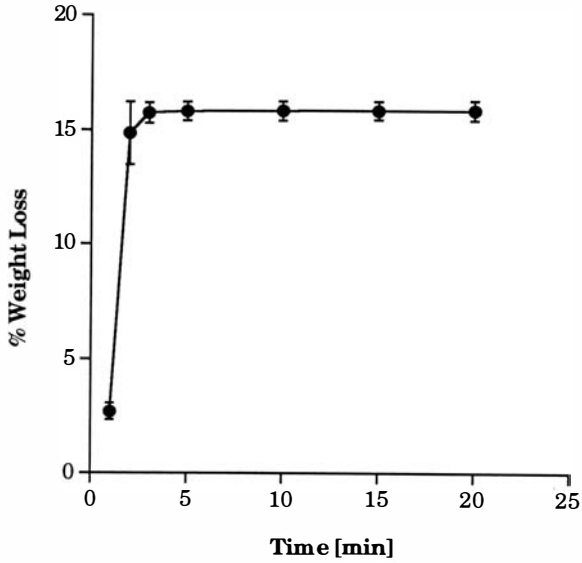

Figure VI.2 Percentage weight loss vs time profile for sodium tartrate dihydrate (theoretical water content=15.66%) determined using isothermal thermogravimetric analysis (TGA). Data points are means of three determinations. Error bars are sample SD, where error bars are not shown, they were smaller than the symbol used for the data point.

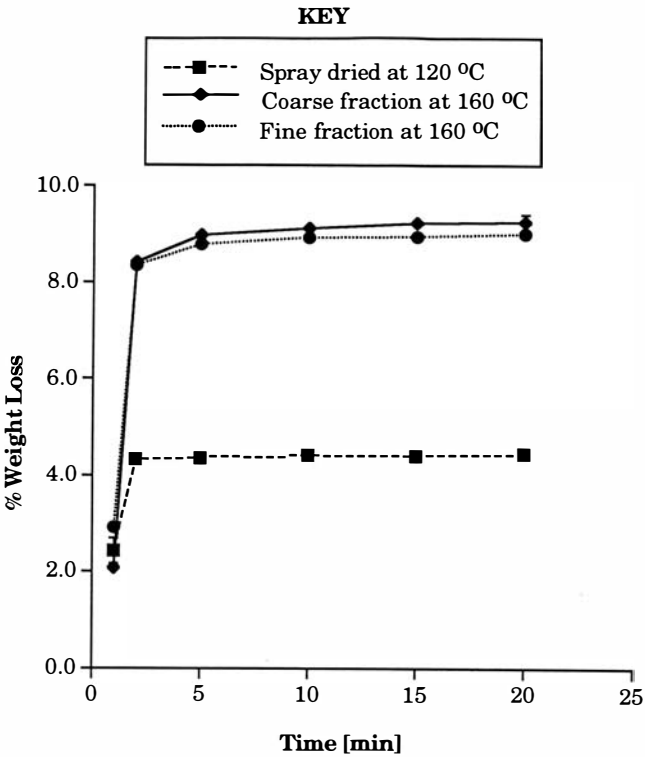

Figure VI.3 Percentage weight loss vs time profiles for crystalline and spray dried trehalose (theoretical water content for crystalline dihydrate=9.5%) determined using isothermal thermogravimetric analysis (TGA) at the temperatures shown in the key. Data points are means of three determinations. Error bars are sample SD; where error bars are not shown, they were smaller than the symbol used for the data point.

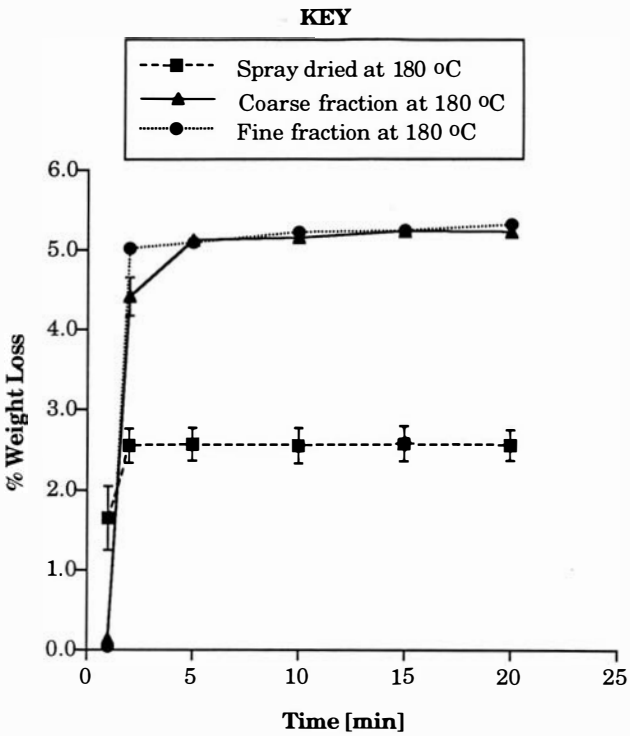

Figure VI.4 Percentage weight loss vs time profiles for crystalline and spray dried lactose (theoretical water content for crystalline α-lactose monohydrate=5.0%) determined using isothermal thermogravimetric analysis (TGA) at the temperatures shown in the key. Data points are means of three determinations. Error bars are sample SD, where error bars are not shown, they were smaller than the symbol used for the data point.

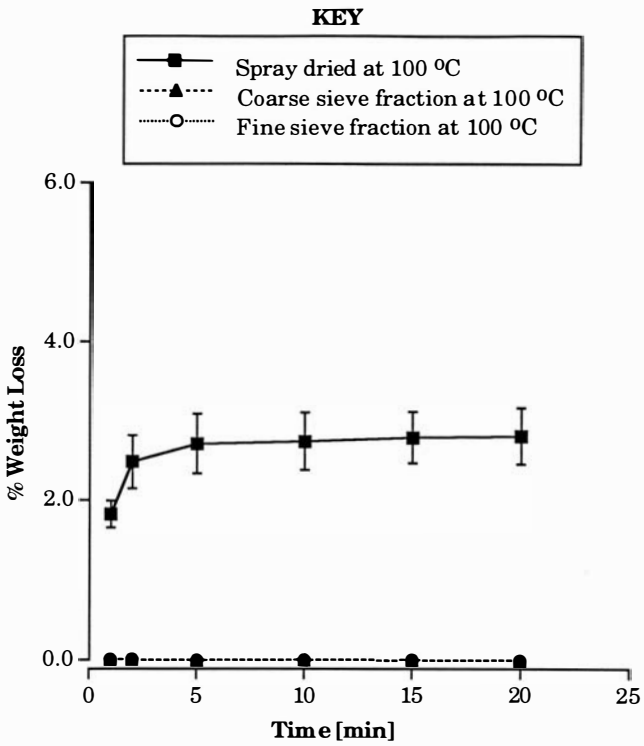

Figure VI.5 Percentage weight loss vs time profiles for crystalline and spray dried sucrose determined using isothermal thermogravimetric analysis (TGA) at the temperatures shown in the key. Data points are means of three determinations. Error bars are sample SD, where error bars are not shown, they were smaller than the symbol used for the data point. The profiles for both the sive fractions of sucrose did not show any weight loss upon TGA.

moisture contents (sodium tartrate and trehalose). There was an apparent trade off between oven temperature and delay time setting when using Method A for determining crystalline water contents in that values went up with increasing temperature and down with increasing delay times. There was no evidence that the different values shown in Table VI.2 was due to any method for these sugars, lacking specificity for water.

Formamide has been reported to be a suitable extraction solvent for determination of hydrate water contents of lactose and maltose, with water contents closely matching those obtained by a vacuum oven method (McComb, 1957). Because of its highly polar nature, formamide was a good solvent for the sugars used in this study. Lactose is capable of existing in the open ring aldehyde form, which can potentially react with methanol in the KF medium to form acetal and water (Scholz, 1984). Water, thus released from this side reaction could produce erroneously high results (Scholz, 1984) when determining water content of lactose using KF titration. The fact that this was not observed in the present study may be due to low amounts of the open ring form present in the sample solutions of lactose in formamide. It is also the proposed solvent for moisture determination in the α-lactose monohydrate monograph in USP23/NF18 (1994b). However the monograph has since been modified to include a 2:1 mixture of methanol and formamide (USP23/NF18 Supplement 1, Jan 1995). This was done to avoid problems with equilibration and stabilization of the KF apparatus when using formamide as the solvent, because of its decreased *conductivity*

Table VI.2 Results for moisture contents of different sugars and sodium tartrate dihydrate following Karl Fischer titration by the two different methods.

Sample	Method A			Method B
	Temp of Oven (C)	Delay Time (min)[f]	% Moisture Mean (SD)[a]	% Moisture Mean (SD)[a]
Lactose[b]				
Coarse fraction	180	10	4.91 (0.45)	5.02 (0.09)
Fine fraction	180	10	4.98 (0.19)	5.07 (0.79)
Spray dried	180	5	2.41 (0.03)	2.37 (0.08)
Sucrose				
Coarse fraction	120	10	ND[c]	0.10 (0.09)
Fine fraction	120	10	ND[c]	0.03 (0.06)
Spray dried	100	5	2.38 (0.32)	2.46 (0.10)
Trehalose[b]				
Coarse fraction	160	10	8.55 (0.31)	8.94 (0.17)
Fine fraction	160	10	8.34 (0.06)	8.35 (0.11)
Spray dried	120	5	3.96 (0.08)	4.24 (0.23)
Mannitol				
Coarse fraction	120	10	ND[c]	0.22 (0.55)
Fine fraction	120	10	ND[c]	0.02 (0.06)
Spray dried	120	10	ND[c]	0.46 (0.34)
Standards	187	3	14.98 (0.56)[d]	0.101 (0.003)[e]

a Values (% w/w) are mean (sample SD) of five determinations

b Theoretical water contents of crystalline sieve fractions of lactose and trehalose are 5.0% and 9.5% respectively

c No detectable moisture was recorded after a 10 minute delay titration.

d Sodium tartrate dihydrate (Hydranal®) with a moisture content of 15.66 ± 0.05%

e Hydranal® Check-Solution 1.00 with stated moisture content of 1.003 µg/mg (SD = 0.002 mg)

f Delay time was the time for which the sample was heated and the vapor collected in the titration vessel, prior to coulometric titration for water.

(Chowhan et al., 1994).

Method B using formamide as the extraction solvent gave reliable estimates for moisture contents with less variability than Method A (Table VI.2). Although, formamide has been implicated in influencing the stoichiometry of the KF reaction (Chowhan et al., 1994), this was not found to be a problem in our experience with moisture determination for any of these sugars.

Although, coulometric titration can detect very small amounts of water (sample moisture contents of 0.1 - 0.0001%), it failed to give reliable estimates for crystalline sucrose and mannitol samples, whose moisture estimates using Method B were statistically indistinguishable from the formamide blank (Table VI.2; t-test, $\alpha = 0.05$).

VI.e SUMMARY AND CONCLUSIONS

Isothermal TGA gave quick and reliable estimates for moisture content in each of the sugars studied. However, it was necessary to establish that the weight loss recorded following TGA was due to moisture using an independent method such as KF titration. Two adaptations of the coulometric KF technique were employed to determine total water contents of four sugars in their crystalline and spray dried forms. Method A, using the evaporative technique gave good estimates for amorphous sugars whose water was loosely bound. However, its suitability for crystalline samples with high moisture contents was questionable. Method B, using formamide

as extraction solvent, although a labor intensive technique was a practical way of determining the absolute moisture contents of all the sugars. Once the water content was established using Method B, isothermal TGA may be used for routine determination of moisture contents using milligram quantities of sugar sample.

VII. DETERMINATION OF TOTAL PROTEIN CONTENT AND ALKALINE PHOSPHATASE ENZYME ACTIVITY IN SOLUTION

VII.a INTRODUCTION

This appendix describes the protein and enzyme assays used to determine specific activities of bacterial (BAP) and bovine intestinal (BIAP) alkaline phosphatase reported in Chapter V. Protein content was assayed using the method of Bradford (Bradford, 1976). It is based on the observation that Coomassie Brilliant Blue G-250 exists in two different color forms, red and blue. The red form is converted to the blue form upon binding to protein, and since the protein-dye complex has a high extinction coefficient, this assay can be used to detect microgram quantities in sample solutions (Bradford, 1976). Also it is not prone to interference from carbohydrates, like the more traditionally used Lowry assay (Bradford, 1976).

Enzyme activity was determined from the initial reaction rates of alkaline phosphatase catalyzed hydrolysis of p-nitrophenol phosphate to yield p-nitrophenol (Torriani, 1968).

VII.b MATERIALS AND METHODS

Bacterial (E.coli) alkaline phosphatase (Product #P4252, Lot #101H40191), as a suspension in 2.5 M ammonium sulfate solution and

bovine intestinal alkaline phosphatase (Product #P7640, Lot #043H7185), as a freeze dried powder, enzyme substrate disodium p-nitrophenol phosphate (Product #104-0, Lot #123H50083), p-nitrophenol standard solution (Product #104-1, Lot #014H6137) and bovine serum albumin (BSA) protein standard (Product #P0914, Lot #14H8530) were obtained from Sigma Chemical Company (St. Louis, MO). Tris [Tris (hydroxymethyl)-aminomethane] was obtained from Pharmacia LKB (Piscataway, NJ). Protein assay dye reagent solutions (Product #500-006, Lots #51143A and #51558A) were obtained from Bio-Rad Laboratories (Hercules, CA). 1 N sodium hydroxide solution of reagent grade quality was obtained from Fisher Scientific Company (Raleigh, NC).

VII.b.1 Protein content determination

The dye reagent concentrate solution contained the dye, phosphoric acid and methanol (Bio-Rad protein assay manual, Bio-Rad Laboratories, Hercules, CA, 1994). Tris buffer at 10 mM concentration was made in deionized distilled water and the pH was adjusted to 8.0 using 1.0 N HCl solution. Four standard solutions of BSA (obtained from Sigma) in the concentration range of 1.25 - 10.00 μg/ml were prepared in the buffer. 600 μl of the dye reagent concentrate was added to 2.4 ml of each protein standard solution and the resulting mixture was vortexed and held at ambient temperature (22 - 23 °C) for a further 5 min, prior to reading the absorbance at 595 nm (Ultrospec II, LKB-Pharmacia, Piscataway, NJ) in glass cuvettes

(Catalogue #14-385-910B, Fisher Scientific Co., Raleigh, NC), since the protein-dye complex binds more strongly to quartz as compared to glass (Bradford, 1976). The cuvettes were cleaned at the end of each experiment by rinsing them with methanol. A protein free buffer solution prepared in a similar fashion served as the blank reference solution. Blank absorbencies were subtracted from the absorbencies of the standard solutions of BSA. A calibration plot of protein (BSA) concentration vs absorbance due to the protein-dye complex was constructed. Plotted values were the mean of three determinations. Since there can be batch to batch variation in dye response, each commercially obtained batch of dye reagent solution used in the assay was used to make a separate calibration plot.

For determining protein content of unknown alkaline phosphatase enzyme solutions, 600 µl of the dye reagent solution was added to 2.4 ml of the enzyme solution in Tris buffer pH 8.0 and the resulting mixture vortexed and held at ambient temperature for 5 min, The absorbance was read at 595 nm in glass cuvettes. An enzyme free buffer solution prepared in a similar fashion served as the blank. Blank subtracted sample absorbance was used to estimate protein concentration by linear interpolation based on the whole of the calibration curve plotted as described above. Hence all protein concentrations of the enzyme solutions are expressed in terms of the relative standard BSA. As a result, in this Chapter, and in Chapter V, protein amounts are expressed in terms of micrograms of BSA equivalents (BSAE) and not as absolute concentrations

of alkaline phosphatase.

VII.b.2 Determination of alkaline phosphatase enzyme activity

VII.b.2.1 Calibration plot of paranitrophenol in 1.0 N NaOH solution

Alkaline phosphatases (BAP and BIAP) catalyze the hydrolysis of p-nitrophenol phosphate (substrate) to p-nitrophenol under alkaline conditions. The product released can be determined quantitatively by spectrophotometry at 404 nm. Six standard solutions of p-nitrophenol (Sigma) in 1.0 N NaOH were prepared in the concentration range 10 - 100 nmol/ml. Absorbencies of the resulting solutions were read at 404 nm. 1.0 N NaOH served as the blank reference solution which was used to adjust A_{404} to zero. Concentrations of p-nitrophenol were plotted vs absorbance. Plotted values are the mean of three determinations.

VII.b.2.2 Limits of linearity for product (p-nitrophenol) accumulation vs incubation time

The maximum product concentration which was able to accumulate before the product concentration vs time curve became non-linear, was established (Segel, 1976) for both the enzymes, BAP and BIAP.

For BAP, the enzyme suspension in ammonium sulfate solution was desalted as described in Section V.b.1.1 (Chapter V). Two enzyme solutions were prepared in 10 mM Tris buffer pH 8.0. Apparent protein

concentrations (in BSAE) of these solutions, as determined by the Bradford assay, were 3.42 μg BSAE/ml and 7.5 μg BSAE/ml. 375 μl of each enzyme solution (for each of the time points tested) was incubated at 37 °C in a water jacketed vessel. Reaction was initiated by the addition of 125 μl of 10 mM p-nitrophenol phosphate (substrate) solution in Tris buffer pH 8.0. At specific time intervals the reaction was stopped by the addition of 3 ml of 1.0 N NaOH solution (Engstrom, 1961) and absorbance read at 404 nm. Enzyme free buffer incubated with 125 μl substrate solution served as the blank or reference solution which was used to adjust A_{404} to zero. Measured absorbencies were used to estimate the product (p-nitrophenol) released by interpolation from the p-nitrophenol calibration curve. A plot of p-nitrophenol concentration vs incubation time was constructed and based on this plot, a constant incubation time in the linear phase of the plot was selected for use in the final assay for enzyme activity.

For BIAP two solutions were prepared in 10 mM Tris buffer by reconstituting the commercially obtained freeze dried powder. Apparent protein concentrations of the solutions as estimated by the Bradford method, were 2.53 μg BSAE/ml and 8.90 μg BSAE/ml. 375 μl of each BIAP solution (for each of the time points tested) was incubated at 37 °C in a water jacketed vessel. Reaction was initiated by the addition of 125 μl of 10 mM p-nitrophenol phosphate (substrate) solution in Tris buffer pH 8.0. At specific time intervals the reaction was stopped by the addition of 3 ml of 1.0 N NaOH and absorbance read at 404 nm. BIAP-free buffer, similarly

incubated with 125 µl substrate solution, served as the blank or the reference solution, which was used to adjust A_{404} to zero. Measured absorbencies were used to estimate p-nitrophenol concentrations by linear interpolation from the p-nitrophenol calibration curve. A plot of p-nitrophenol concentration vs incubation time was made and based on this plot a constant incubation time in the linear phase of the plot was selected for use in the final assay for enzyme activity.

VII.b.2.3 Limits of linearity for enzyme activity vs apparent protein concentration in enzyme solutions

BAP was desalted as described in Chapter V (Section V.b.1.1). BIAP enzyme powder was reconstituted and diluted in 10 mM Tris buffer pH 8.0. Four concentrations of each enzyme solution were made using 10 mM Tris buffer pH 8.0. Apparent protein concentration of the solutions as determined by the Bradford assay were in the concentration range 2.58 - 8.75 µg BSAE/ml (BAP) and 2.19 - 8.43 µg BSAE/ml (BIAP). 375 µl of each enzyme solution was incubated at 37 °C in a water jacketed vessel. The reaction was initiated by the addition of 125 µl of 10 mM p-nitrophenol phosphate (substrate) solution in 10 mM Tris buffer pH 8.0. At the end of 4 min (plots of product release vs incubation time for BAP and BIAP were apparently rectilinear for times ≤ 4 min, see Figures VII.4 and VII.5) incubation time, the reaction was stopped by the addition of 3 ml of 1.0 N NaOH solution and absorbance read at 404 nm. Enzyme-free buffer solution

prepared in a similar fashion served as the blank which was used to zero the spectrophotometer in all cases. Concentrations of p-nitrophenol were estimated by linear interpolation of the absorbance values from the whole calibration curve for p-nitrophenol (see Figure VII.3).

One Unit of enzyme activity was defined as the amount of enzyme that catalyzes the release of 1 nmol of p-nitrophenol per minute at 37 °C and pH 8.0. Activity was calculated as follows:

Enzyme activity of the original enzyme solution assayed =

[p-nitrophenol (nmol/ml) in final solution] X (DF/4)

where DF (dilution factor) = (3.5/0.375); the result was divided by 4 to normalize to a one minute reaction time. The mean BAP (Figure VII.6) and BIAP (Figure VII.7) activities (n = 3) in Units/ml vs apparent protein concentration were constructed.

VII.c RESULTS AND DISCUSSION

VII.c.1 Protein content determination

Protein contents of alkaline phosphatase (BAP and BIAP) solutions *subsequently* assayed for enzymatic activity were determined using the method of Bradford (Bradford, 1976). The assay is based on the observation that there is a shift in the absorbance maximum of Coomassie Brilliant Blue G-250 when it binds to protein. It has been reported that the dye exists as three absorbing species, a red cationic species, a neutral green species

Table VII.1 Summary of assay validation parameters for protein determination by the method of Bradford (Bradford, 1976).

	Linear Range[a] (µg/ml)	r^2	Precision[b] (%CV)	Accuracy[c]	LOQ[d] (µg/ml)
Lot #51143A	1.25 - 10.00	0.99	4.6 - 5.6	7.7 - 1.2	1.25
Lot #51558A	1.25 - 10.00	0.99	7.8 - 2.1	7.8 - 2.4	1.25

a Protein standard used was BSA.

b Precision = (sample standard deviation of absorbance/mean absorbance) x 100, n=3. Values are calculated from the upper and lower limits of the linear concentration range shown.

c Accuracy $=[Abs(A_t - A_i)/A_t] \times 100$, where A_t = True absorbance value and
A_i = Interpolated absorbance from the calibration curve.
Values are calculated from the upper and lower limits of the linear concentration range shown.

d Limit of quantitation was defined as the lower limit of the calibration curve (1.25 µg BSAE/ml in both cases.

and a blue anionic species. Binding of the dye to protein stabilizes the blue anionic form which can be detected at 595 nm (Compton and Jones, 1985). Dye binding essentially requires basic (arginine) or aromatic amino acid residues in the protein (Compton and Jones, 1985). The resulting protein-dye complex has a high extinction coefficient, making microgram quantities of protein detection possible. Also, the dye binds to the protein very rapidly and the dye-protein complex remains in solution for at least 1 hour. This enables rapid detection without critical timing for the assay (Bradford, 1976). The dye assay is also relatively insensitive to the presence of carbohydrates and Tris in the assay solution unlike the more commonly used Lowry assay (Lowry et al., 1951).

Calibration curves constructed by plotting blank subtracted absorbencies vs protein standard (BSA) concentrations are shown in Figures VII.1 and VII.2, for dye reagent batches # 51143A and # 51558A respectively. Both the calibration curves used for protein estimation were evaluated for accuracy, precision, linearity and limit of quantitation (LOQ) using upper and lower limits of concentration ranges shown in Table VII.1. Accuracy of the method was expressed as the percentage difference between calculated and measured values for A_{595} (Karnes et al., 1991). Precision (variability in the measurement of A_{595}) was estimated as percentage coefficient of variation (% CV) in a set of three determinations, although calculations using a set of six determinations are usually recommended (Karnes et al., 1991). Limit of quantitation (LOQ) was defined

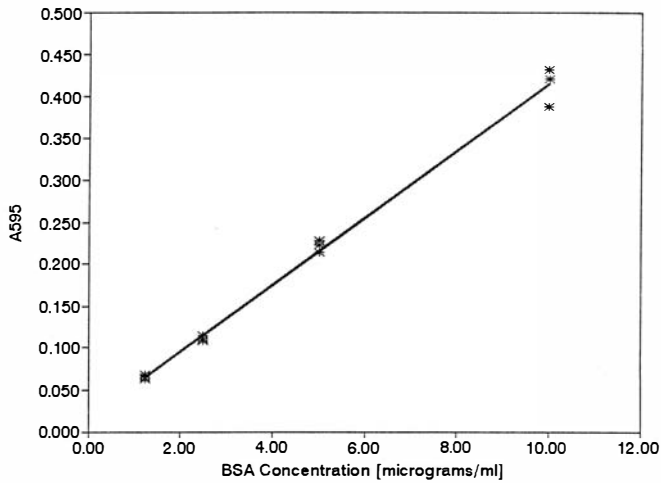

Figure VII.1 Calibration curve for protein estimation by the method of Bradford, using Bio-Rad assay kit (Lot #51143A). Plotted values are experimentally obtained data. The solid line shows the best fit by linear regression of the data ($y = 0.0400x + 0.0149$; $r^2 = 0.99$; standard error of slope = 0.00103; n = 12).

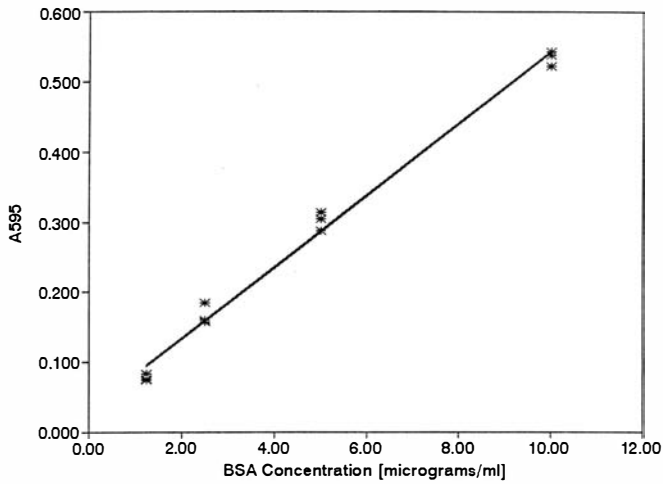

Figure VII.2 Calibration curve for protein estimation by the method of Bradford, using Bio-Rad assay kit (Lot #51558A). Plotted values are experimentally obtained data. The solid line shows the best fit by linear regression of the data ($y = 0.05121x + 0.02977$; $r^2 = 0.99$; standard error of slope = 0.00155; n = 12).

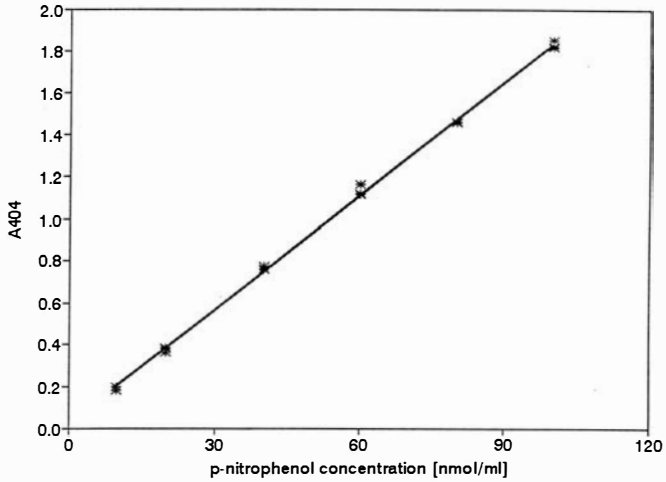

Figure VII.3 Calibration curve for p-nitrophenol in 1.0 N NaOH solution. Plotted values are experimentally obtained data. The solid line shows the best fit by linear regression of the data ($y = 0.01815x + 0.02196$; $r^2 = 0.99$; standard error of slope = 0.00015; n = 18).

as the concentration of the lowest standard i. e. 1.25 μg BSAE/ml (Karnes et al., 1991). The practical limit of quantitation was also established as 1.25 ± 0.20 μg BSAE/ml. Assay validation parameters for both lots of the dye reagent are shown in Table VII.1. Both the calibration curves were apparently rectilinear in the concentration range 1.25 - 10.00 μg/ml (r^2 > 0.99, n = 12) and the values for precision and accuracy were reliable within a 10% margin of error (Table VII.1).

VII.c.2 Determination of enzyme activity

VII.c.2.1 Calibration plot of product (p-nitrophenol)

The calibration plot of p-nitrophenol concentrations (in 1.0 N NaOH) vs A_{404} is shown in Figure VII.3. It was rectilinear in the concentration range 10 - 100 nmol/ml (r^2 > 0.99, n = 18) and thus was used to estimate p-nitrophenol concentrations following enzymatic reactions in unknown solutions.

VII.c.2.2 Linearity of product (p-nitrophenol) released vs incubation time

Plots of incubation time vs p-nitrophenol released for two concentrations of BAP (3.42 μg BSAE/ml and 7.50 μg BSAE/ml) and two concentrations of BIAP (2.53 μg BSAE/ml and 8.90 μg BSAE/ml) are shown in Figures VII.4 and VII.5 respectively. A visual observation of these plots

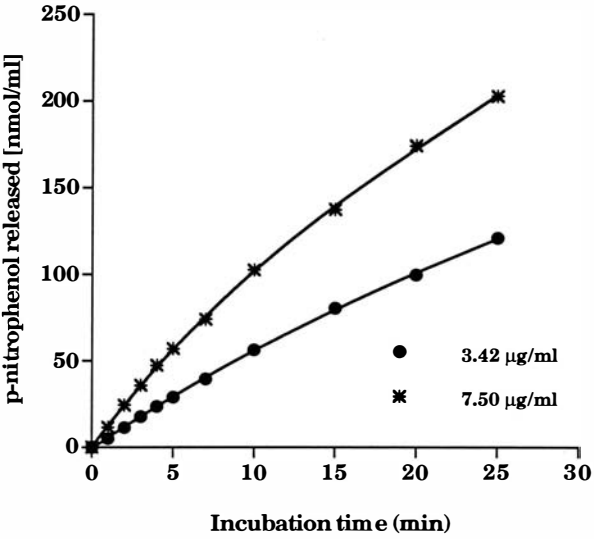

Figure VII.4 Plot of p-nitrophenol concentration vs incubation time for two apparent protein concentrations of bacterial alkaline phosphatase (BAP; • 3.42 µg BSAE/ml; * 7.50 µg BSAE/ml, as determined by the method of Bradford). Each data point is based on a single determination and the solid lines are shown for visual clarity and does not necessarily indicate data continuity.

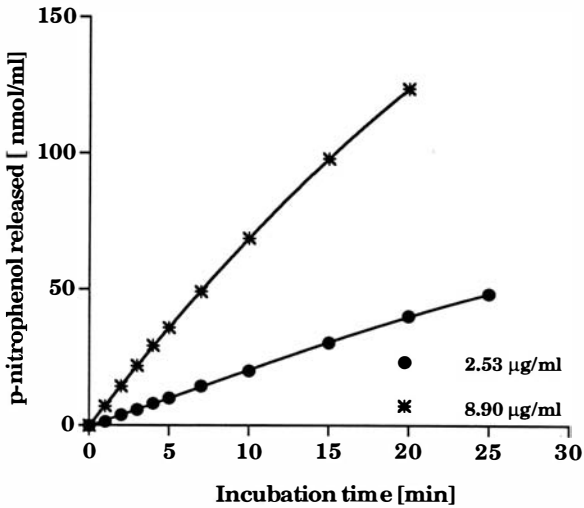

Figure VII.5 Plot of p-nitrophenol concentration vs incubation time for two apparent protein concentrations of bovine intestinal alkaline phosphatase (BIAP; • 2.53 µg BSAE/ml; * 8.90 µg BSAE/ml, as determined by the method of Bradford). Each data point is based on a single determination and the solid lines are shown for visual clarity and does not necessarily indicate data continuity.

revealed that the plots were apparently rectilinear in the initial phase (< 5 min). The product released (phosphate) during the enzyme reaction acts as an inhibitor and this is probably the reason for the non linear product formation curves shown in Figures VII.4 and VII.5. An incubation time of 4 min was chosen for use in the final assay as the incubation time for the final assay of both the enzymes. For both BAP and BIAP, values of $r^2 > 0.99$ were determined at $0 \leq t \leq 4$ min ($n = 4$, in both cases).

VII.c.2.3 Linearity of enzyme activity vs apparent protein concentration in the enzyme solution assayed

Plots of protein concentration vs enzyme activity expressed in Units/ml are shown in Figures VII.6 and VII.7 for BAP and BIAP respectively. The plot for BAP was rectilinear in the apparent protein concentration range 2.58 - 8.75 μg BSAE/ml ($r^2 > 0.99$; $n = 15$). The plot for BIAP was rectilinear in the apparent protein concentration range 2.19 - 8.43 μg BSAE/ml ($r^2 > 0.99$; $n = 15$).

VII.c.2.4 Estimation of enzyme specific activity in unknown solutions

For BAP and BIAP unknown solutions both protein and enzyme activity assays were performed in order to determine specific activities. Apparent protein content was determined by the method of Bradford (Section VII.b.1). If the apparent protein concentrations of BAP solutions were less than the upper limit of the linear range for BAP i.e. 8.75 μg

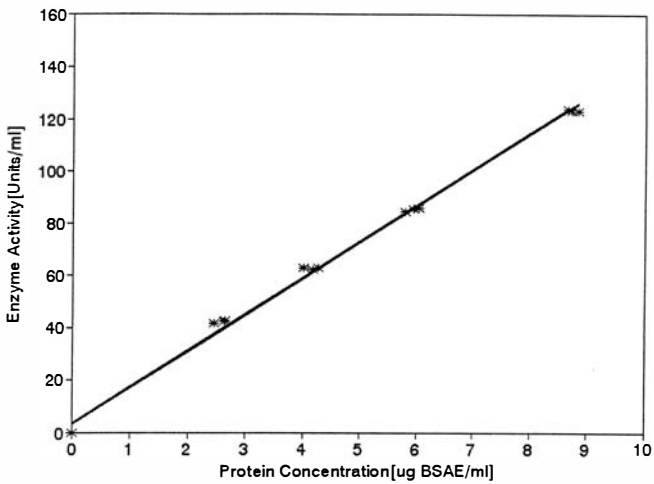

Figure VII.6 Plot of enzyme activity vs protein concentration (determined by the method of Bradford) for bacterial alkaline phosphatase (BAP). Plotted values are experimentally obtained data. The solid line shows the best fit by linear regression of the data ($y = 13.8749x + 3.1195$; $r^2 = 0.99$; standard error of slope = 0.2313; $n = 15$).

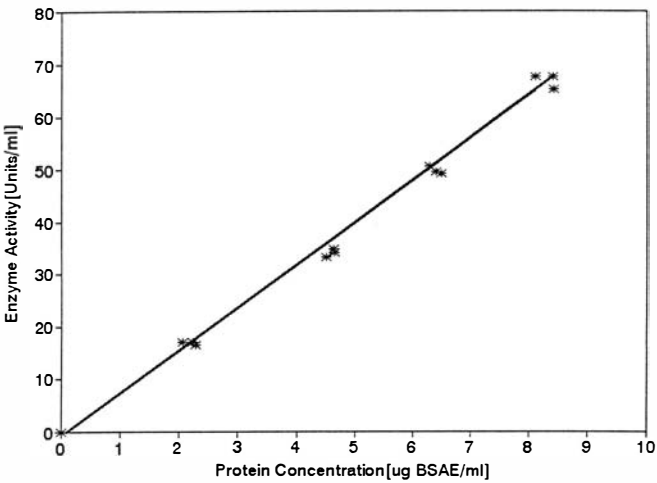

Figure VII.7 Plot of enzyme activity vs protein concentration (determined by the method of Bradford) for bovine intestinal alkaline phosphatase (BIAP). Plotted values are experimentally obtained data. The solid line shows the best fit by linear regression of the data ($y = 8.1278x - 0.8535$; $r^2 = 0.99$; standard error of slope = 0.2349; n= 15).

BSAE/ml (Figure VII.6),the enzyme activity was determined without further dilution. If the apparent protein concentration was > 8.75 μg BSAE/ml sufficient dilution was made with 10 mM Tris buffer pH 8.0 before re-assaying for protein content and then for enzyme activity. Similarly, for BIAP if the protein concentrations were less than the upper limit of its linear range i.e. 8.43 μg BSAE/ml (Figure VII.7), the enzyme activity was determined. If the protein concentrations of the assayed BIAP solutions was > 8.43 μg BSAE/ml, the assays were repeated after dilutions in buffer.

Enzyme specific activity was assayed as follows: 375 μl of the BAP or BIAP solution was incubated at 37 °C. The reaction was started by adding 125 μl of 10 mM of p-nitrophenol phosphate solution (substrate) in 10 mM Tris buffer pH 8.0. At the end of 4 min incubation the reaction was stopped by the addition of 3 ml 1.0 N NaOH solution and absorbance read at 404 nm. Concentration of p-nitrophenol was estimated by interpolation from the p-nitrophenol calibration curve (Figure VII.3). Enzyme activity in Units/ml was calculated as described in Section VII.b.2.3. Specific activity of the enzyme in unknown solutions was then determined from:

$$\text{Specific activity [Units/μg BSAE]} = \frac{\text{Enzyme activity [Units/ml]}}{\text{Protein Concentration [μg BSAE/ml]}} \quad \text{.....Equation VII.1}$$

VIII. OVERALL SUMMARY AND CONCLUSIONS

The feasibility of producing inhalable microparticles of sugars and sugar-protein molecular mixtures was investigated. Four sugars: lactose, trehalose, sucrose and mannitol were selected for review based on their different physicochemical properties. Lactose, trehalose and sucrose were disaccharides, while mannitol was a straight chain sugar alcohol. Chemically, lactose was a reducing sugar, since in the presence of moisture it could exist in equilibrium with its open chain reactive aldehyde form. This property of lactose also caused it to mutarotate and exist in two anomeric forms: (α and β) . α-Lactose could be readily purchased as the stoichiometric crystalline monohydrate (water content = 5% w/w). β-lactose (anhydrous) could not easily be obtained in pure form. Trehalose, sucrose and mannitol were all non-reducing sugars. Sucrose and mannitol are currently used as accepted excipients in other pharmaceutical dosage forms and trehalose is under review as an excipient in lyophilized preparations.

Crystalline α-lactose monohydrate is presently the only approved carrier in dry powder inhalers (DPIs) in the United States. Characterization of additional crystalline sugars with respect to their

behavior under different storage conditions was used to assess their suitability for use as carriers in dry powder inhalers (DPIs). Studies were also performed because sugars have been suggested as stabilizers to protect proteins during spray drying and storage of dried powders. Since spray drying offers an alternative to other particle size reduction techniques, it was developed and tested for the production of microparticles of sugar containing the drug (protein) in intimate molecular mixtures. In these cases, the sugar carrier would be inhaled along with the drug. This contrasts with the use of conventional sugar carriers in DPIs, which consist of a physical admixture of the micronized drug with a larger particle size carrier. In these cases, during inhalation, the drug is intended to separate from the carrier, and be inhaled alone.

Two size fractions: "coarse" (125 - 212 μm) and "fine" (44 - 74 μm) of each of the four sugars: lactose, trehalose, sucrose and mannitol were prepared by sieve fractionation. They were examined for moisture uptake and physicochemical stability after storage at four different relative humidities (RHs): 23%, 52%, 75% and 93% RH and 25 °C for 30 days to assess their suitability for use in physical admixtures with drugs in powder inhalers. All sieve fractions, except sucrose did not show any moisture uptake (as determined by weight loss on thermogravimetric analysis) when stored at the different RHs. Sucrose was stable when stored at ≤ 75% RH, however it dissolved in the sorbed moisture (turning into syrup) when stored at 93% RH, indicating that its critical relative humidity had been

exceeded at this RH. These results indicated that the crystalline sieve fractions were thermodynamically stable at 25 °C (with the exception of sucrose) at all the storage conditions studied and thus, in this respect were suitable for use as carriers in DPIs, and could be used whenever formulations with lactose performed poorly. Sucrose would not necessarily have to be excluded from this generalization, except to say that any sucrose-drug blends to be used in powder inhalers must be stored in sealed moisture-proof packages, to avoid predictable moisture-induced changes in DPI performance.

The four sugars were also spray dried using a Yamato bench top spray dryer from 10% w/v aqueous solutions. Lactose, trehalose and mannitol were obtained with median aerodynamic diameters between 4 - 6 μm as determined by the Aerosizer® equipped with an Aerodisperser®. This showed the feasibility of spray drying these sugars to produce inhalable particulates. Spray dried sucrose on the other hand, was very cohesive and difficult to deaggregate; resulting in apparent median aerodynamic diameters of 12 μm as measured by the Aerosizer®. Spray dried lactose, trehalose and sucrose were obtained as amorphous glasses as indicated by differential scanning calorimetry (DSC) and X-ray powder diffraction (XRPD). However, contrary to the popular belief that spray drying destroys crystalline structure, spray dried mannitol was highly crystalline as assessed by DSC and XRPD. Amorphous spray dried lactose, trehalose and sucrose, showed apparent glass transition temperatures (T_g)

of 117, 120 and 62 °C respectively, in the completely dry state (the presence of moisture in the amorphous glass at 25 °C could feasibly lower these T_g values, since water is a plasticizer for amorphous materials). When stored at 23% RH and 25 °C for 30 days, spray dried lactose, trehalose and sucrose showed increased equilibrium moisture contents compared to the starting material (ranging from 4.6% for spray dried sucrose to 5.6% for spray dried trehalose), but remained in the amorphous form over that time period. This was assessed by DSC and XRPD of the stored materials. However, the amorphous sugars (spray dried lactose, trehalose and sucrose) completely recrystallized after storage at the higher humidities of 52%, 75% and 93% RH. This moisture-induced recrystallization resulted in the formation of stoichiometric hydrates for lactose and trehalose and the anhydrate form of sucrose. A small amount of β-lactose anhydrous was detectable by DSC in recrystallized lactose samples stored at 52% and 75% RH, indicating that some mutarotation of lactose had occurred in the solid state at these RHs. Spray dried mannitol, which was obtained in the crystalline state after spray drying, did not show any further moisture uptake after storage, at any RH employed in this study. Even small amounts of amorphous content were undetectable in spray dried mannitol samples collected here, showing that it was in the same crystal form, although its appearance was physically different to the original starting material.

Because, few commercially available spray dryers are capable of drying and collecting small particles (≤ 5 μm) to a high degree of efficiency,

a small particle collection apparatus was designed. This incorporated a commercially available nebulizer and a purpose-built wire-in-tube type electrostatic precipitator. The apparatus was characterized for particle collection efficiency using aqueous solutions of lactose and disodium fluorescein, as a function of several operating variables; applied precipitator voltage, concentration of nebulized solution, temperature and volumetric flow rate of the drying air through the apparatus. Only particles collected inside the column (I, Figure IV.1) were potentially recoverable for further study. Under all operating conditions, particle deposition in parts of the apparatus other than the electrostatic column was minimal. The total solids output exiting the nebulizer, was either collected inside the column or lost to the air stream. At all conditions, the percentage of the output recovered in the column increased with increasing applied voltage on the precipitator, with 64% recovery at an applied potential of 20 kV. A larger percentage of the output was recovered when using low concentration nebulizer solutions (64% and 26% recoveries in column after nebulizing 10 mg/ml and 75 mg/ml solutions respectively). Using a 10 mg/ml solution, *deposition* in the column was investigated as a function of drying temperature and volumetric air flow rate (in these experiments a glass liner was introduced inside the column to facilitate collection and subsequent detection of particles). Two volumetric air flow rates of 29.1 liters/min and 50.6 liters/min and two drying temperatures of 28 °C and 41 °C were used. Drying air temperature appeared to have no effect on particle

deposition inside the column, even though better dried particles were obtained at higher drying temperatures, as observed by scanning electron micrography (SEM). As expected, deposition was directly dependent on volumetric air flow through the system, with higher efficiencies at lower air flow rate, showing that deposition was a function of particle residence time inside the column.

Once characterized, the particle collection apparatus was used to review protein activity following spray drying and electrostatic collection of protein-sugar mixtures. Two enzymes, bacterial alkaline phosphatase (BAP) and bovine intestinal alkaline phosphatase (BIAP) were selected as model proteins. To investigate the effect of sugars as stabilizers, enzyme solutions were sprayed in the presence and absence of four sugars (lactose, trehalose, sucrose and mannitol), dried at ~63 °C (as measured in dryer C, Figure V.1) and electrostatically collected inside the glass-lined precipitator column for 90 min. Enzyme activity was determined from the initial reaction rates of alkaline phosphatase-catalyzed hydrolysis of p-nitrophenol phosphate (substrate). Enzyme specific activities were expressed as Units/μg BSAE, where one Unit of enzyme activity was defined as the amount of enzyme that catalyzes the release of one nmol of p-nitrophenol per minute at 37 °C and pH 8.0. Each of the enzyme solutions were made in 10 mM Tris buffer pH 8.0 with or without the addition of each of the four sugars: lactose, trehalose, sucrose and mannitol.

Sugar-free solutions of BAP, the purer enzyme of the two model

proteins, had a total non volatile solids content of ~0.1% w/v and showed an average specific activity of 15.7 Units/μg BSAE. This specific activity remained unchanged after the addition of each of the four sugars [total non volatile solids concentration = 10 mg/ml (1% w/v)] and at the end of the 90 min experiment, in the residual nebulizer solution. However, the enzyme spray dried at 63 °C (as measured in dryer-C, Figure V.1) and electrostatically collected in the column (I, Figure V.1), showed a specific activity of 12.1 Units/μg BSAE after reconstitution. This loss of activity was significant compared to the initial solution (ANOVA, $p < 0.05$). Trehalose and sucrose seemed to offer some protection to this drying and/or collection-induced loss, when included with the enzyme in the prenebulized solution, although specific activity values were statistically indistinguishable from those determined following drying from sugar-free solution. Thus, some activity loss appeared to be inevitable in this case. Lactose and mannitol seemed to offer no protection at all to the enzyme during spray drying and electrostatic collection, but once again specific activity values were not significantly different from those following drying from sugar-free solution. *In* separate experiments, BAP was spray dried with or without addition of the four sugars, as described above. These dried powders were stored at 23% RH and 25 °C for 14 days, prior to reconstitution and analysis. The storage conditions were chosen based on the observation that independently spray dried sugars remained as stable amorphous materials, after storage for 30 days at this temperature and RH (Chapter III) and thus,

recrystallization should not occur during storage. Sugar-free BAP and BAP-sugar mixtures did not show a significant change in specific activities compared to their respective prestored materials, indicating that no further loss of activity occurred during storage for 14 days under these conditions.

The second enzyme, bovine intestinal alkaline phosphatase (BIAP) was examined in a similar fashion. BIAP was present in increased total protein concentration in the nebulized solution (~1 mg BSAE/ml compared to ~120 μg BSAE/ml for BAP). Even so, the total non-volatile solids concentration in the BIAP-sugar solutions was held constant at 10 mg/ml (1% w/v). Sugar-free BIAP solutions had a specific activity of 8.8 Units/μg BSAE. This value was unaffected by the addition of sugars or by nebulization for 90 min. However, sugar-free BIAP solution dried at 63 °C and collected inside the column, showed a lowered specific activity of 6.1 Units/μg BSAE, indicating a significant loss of activity compared to the initial solution. In the case of this enzyme, this loss of activity was completely prevented, when either lactose, trehalose and sucrose were used in the initial solution as stabilizers (activities were indistinguishable from the respective initial solution activities). However, co-drying BIAP with mannitol, resulted in a 40% loss of activity. This value was significantly different from the initial solution activity of 8.8 Units/μg BSAE, but was statistically indistinguishable from the activity of the dried sugar-free solution. Storage experiments were performed with BIAP, similar to those conducted with BAP. BIAP and BIAP-sugar mixtures showed a similar

trend to BAP, that it did not lose additional activity during storage at 23% RH and 25 °C for 14 days, when compared to their prestored counterparts. Experimental results with BIAP showed that only those sugars which existed in the glassy state offered protection to this enzyme during spray drying. Mannitol which was crystalline in the spray dried molecular mixture, failed to offer any protection to BIAP. This was consistent with the earlier hypothesis that the ability of some sugars to protect proteins during drying and storage as dry powders, may depend on the physical state (amorphous or crystalline) of the sugar in the final powdered molecular mixture. According to the "glass transition" theory, the amorphous glass immobilizes the protein in the dried mixture, reducing molecular motion, and thus decreasing destabilization reactions. This amorphous glass can then remain "stable" for pharmaceutically relevant time periods. Only when the processing or storage temperature exceeds the glass transition temperature (T_g) of the amorphous glass, should one expect physical instability (recrystallization) and/or increased chances of chemical reactivity between the sugar and protein, due to increased molecular mobility.

If spray dried protein-sugar molecular mixtures are to be successfully used in DPIs, the selection of sugar may depend on several factors. Among these factors are the cohesiveness of the spray dried powder (aerosolizability), its susceptibility to moisture uptake, potential for chemical reactivity and its ability to protect the proteins during drying and

storage. Using these factors as selection criteria, sucrose appeared to be unsuitable at the outset, because of the difficulty in deaggregating this powder into primary particles suitable for inhalation. Lactose, because of its reducing property may also have drawbacks for co-drying and storage with some proteins in the dry state. Surprisingly, mannitol was spray dried and collected in the crystalline form. While this enabled some resistance to moisture-induced changes, mannitol may not be a suitable stabilizer for protein in cases where an amorphous glass is required for stabilization. Trehalose therefore, seemed to survive the screening for protein-protection most successfully. As a carrier for use in amorphous spray dried sugar-protein molecular mixtures it still required packaging to prevent moisture-induced recrystallization. Nevertheless, it is potentially less reactive than lactose. It also spray dries as an amorphous glass and is much less cohesive and hygroscopic than sucrose. Even so, formulations of all spray dried amorphous powders for inhalation require extraordinary precautions with respect to packaging and storage, since such powders are prone to moisture sorption, which can result in a series of physical and chemical changes, all of which have pharmaceutical stability implications.

LIST OF REFERENCES

LIST OF REFERENCES

Adjei, A. and Garren, J., Pulmonary delivery of peptide drugs: effect of particle size on bioavailability of leuprolide acetate in healthy human volunteers. *Pharm. Res.*, 7 (1990) 565-569.

Adjei, A. and Gupta, P., Pulmonary delivery of therapeutic peptides and proteins. *J. Controlled Release*, 29 (1994) 361-373.

Ahlneck, C. and Zografi, G., The molecular basis of moisture effects on the physical and chemical stability of drugs in the solid state. *Int. J. Pharm.*, 62 (1990) 87-95.

Arakawa, T. and Timasheff, S. N., Stabilization of protein structure by sugars. *Biochemistry*, 21 (1982) 6536-6544.

Arakawa, T., Kita, Y. and Carpenter, J. F., Protein-solvent interactions in pharmaceutical formulations. *Pharm. Res.*, 8:3 (1991) 285-291.

Back, J. F., Oakenfull, D. and Smith, M. B., Increased thermal stability of proteins in the presence of sugars and polyols. *Biochemistry*, 18:23 (1979) 5191-5196.

Beevers, C. A. and Hansen, H. N., The structure of α-Lactose Monohydrate. *Acta Cryst.* B27 (1971) 1323-1325.

Berlin, E., Kliman, P.G., Anderson, B.A. and Pallansch, M.J., Calorimetric measurement of the heat of desorption of water vapor from amorphous and crystalline lactose. *Thermochim. Acta*, 2 (1971) 143-152.

Berman, H. M., Jeffrey, G. A. and Rosenstein, R. D., The crystal structures of α' and ß forms of D-Mannitol. *Acta Cryst.* B24 (1968) 442-449.

Bio-Rad Protein Assays, Bulletin #1069, Bio-Rad Laboratories, Inc., Richmond, CA, 1992.

Bowers, G. N. and McComb, R. B., A continuous spectrophotometric method for measuring the activity of serum alkaline phosphatase. *Clin. Chem.*, 12 (1966) 70-89.

Bradford, M. M., A rapid and sensitive method for the quantitation of microgram quantities of protein utilizing the principle of protein-dye binding. *Anal. Biochem.*, 72 (1976) 248-254.

Bradshaw, R. A., Cancedda, F., Ericsson, L. H. Newmann, P. A., Piccoli, S. P., Schlesinger, M. J., Shriefer, K. and Walsh, K. A., Amino acid sequence of *Escherichia coli* alkaline phosphatase. *Proc. Natl. Acad. Sci.,* 78 (1981) 3473-3477.

Bristow, A. F., Dunn, D. and Tarelli, E., Additives to biological substances. IV. Lyophilization conditions in the preparation of international standards: An analysis by high-performance liquid chromatography of the effects of secondary desiccation. *J. Biol. Stand.*, 16 (1988) 55-61.

Broadhead, J., Edmond Rouan, S. K., Hau, I. and Rhodes, C. T., The effect of process and formulation variables on the properties of spray dried β-galactosidase. *J. Pharm. Pharmacol.*, 46 (1994) 458-467.

Brown, G. M. and Levy, H. A., Sucrose: Precise determination of crystal and molecular structure by neutron diffraction. *Science,* 141 (1963) 921-923.

Brown, G. M., Rohrer, D. C., Berking, B., Beevers, C. A., Gould, R. O. and Simpson, R., The crystal structure of α, α-Trehalose dihydrate from three independent X-ray determinations. *Acta Cryst.* B28 (1972) 3145-3158.

Bryan, W. P. and Rao, P. B., Comparison of standards in the Karl Fischer method for water determination. *Anal. Chim. Acta* , 84 (1976) 149-155.

Budavari, S. (Ed.), *The Merck Index, 11th Edition*, Merck & Co., Rahway, NJ, 1989, pp. 1508.

Byron, P. R., Phillips, E. M. and Kuhn, R., Ribavirin administration by inhalation: aerosol-generation factors controlling drug delivery to the lung. *Resp. Care*, 33:11 (1988) 1011-1019.

Byron, P. R.., Aerosol formulation, generation and delivery using metered systems. In Byron, P. R. (Ed.) *Respiratory Drug Delivery*, CRC Press, Boca Raton, Florida, 1990a, 167-205.

Byron, P. R., Aerosol formulation, generation and delivery using nonmetered systems. In Byron, P. R. (Ed.) *Respiratory Drug Delivery*, CRC Press, Boca Raton, Florida, 1990b, 143-165.

Byron, P. R. and Patton, J. S., Drug delivery via the respiratory tract. *J. Aerosol Med.*, 7 (1994) 49-75.

Byron, P. R., Miller, N. C., Blondino, F E., Visich, J. E. and Ward, G. H., Some aspects of alternative propellant solvency. In Byron, P. R., Dalby, R. N. and Farr, S. J. (Eds.), *Respiratory Drug Delivery IV*, Interpharm Press, Buffalo Grove, IL, 1994, 231-241.

Bystrom, K and Briggner, L-E., Microcalorimetry - a novel technique for characterization of powders. In Byron, P. R., Dalby, R. N. and Farr, S. J. (Eds.), *Respiratory Drug Delivery IV*, Interpharm Press, Buffalo Grove, IL, 1994, 297-302.

Calam, D. H. and Tarelli, E., Additives to biological substances. V. The stability of lactose as a carrier for biological standards. *J. Biol. Stand.*, 16 (1988) 63-66.

Callahan, J., Cleary, G.W., Elefant, M., Kaplan, G., Kensler, T. and Nash, R.A., Equilibrium moisture contents of pharmaceutical excipients. *Drug Dev. Ind. Pharm.*, 8 (1982) 335-369.

Carpenter, J. F., Hand, S. C., Crowe, L. M. and Crowe, J. H., Cryoprotection of phosphofructokinase with organic solutes: characterization of enhanced protection in the presence of divalent cations. *Arch. Biochem. Biophys.*, 250 (1986) 505-512.

Carpenter, J. F., Martin, B., Crowe, L. M. and Crowe, J. H., Stabilization of phosphofructokinase during air-drying with sugars and sugar/transition metal mixtures. *Cryobiology*, 24 (1987) 455-464.

Carpenter, J. F. and Crowe, J. H., An infrared spectroscopic study of the interaction of carbohydrates with dried proteins. *Biochemistry*, 28 (1989) 3916-3922.

Carvajal, M. T., Gasior, P., Phillips, E. M., Weinrib, A., Tarantino, R. and Malick, A. W., Spray drying optimization to produce powder for inhalation. *Pharm. Res.*., 11:Suppl. (1994) S-140.

Chappelet-Tordo, D., Fosset, M., Iwatsubo, M., Cache, C. and Lazdunski, M., Intestinal alkaline phosphatase. Catalytic properties and half of the sites reactivity. *Biochemistry,* 13 (1974) 1788-1795.

Charm, S. E. and Wong, B. L., Enzyme inactivation with shearing. *Biotechnol. Bioeng.*, 12 (1970) 1103-1109.

Chawla, A., Taylor, K. M. G., Newton, J. M. and Johnson, M. C. R., Production of spray dried salbutamol sulphate for use in dry powder aerosol formulation. *Int. J. Pharm.*, 108 (1994) 233-240.

Chlebowski, J. F. and Mabrey, S., Differential scanning calorimetry of apo-, apophosphoryl, and metalloalkaline phosphatases. *J. Biol. Chem.,* 252 (1977) 7042-7052.

Chowhan, Z. T, Paul, W. L and Grady, L. T., Harmonization of excipient standards and test methods: challenges and progress. *Pharm. Tech.*, 18:6 (1994):78-96.

Cipolla, D. C., Gonda, I. and Shire, S. J., Characterization of aerosols of human recombinant deoxyribonuclease I (rhDNase) generated by jet nebulizers. *Pharm. Res.*, 11(1994a) 491-498.

Cipolla, D. C., Clark, A. R., Chan, H-K., Gonda, I. and Shire, S. J., Assessment of aerosol delivery systems for recombinant human deoxyribonuclease. *S. T. P. Pharma. Sciences*, 4:1(1994b) 50-62.

Clark, A. R., Medical aerosol inhalers: past, present and future. *Aerosol Sci. Tech.*, 22 (1995) 374-391.

Colaco, C., Sen, S., Thangavelu, M., Pinder, S. and Roser, B., Extraordinary stability of enzymes dried in trehalose: simplified molecular biology. *Bio/Technology,* 10 (1992) 1007-1011.

Coleman, J. E. and Chlebowski, J. F., Molecular properties and mechanism of alkaline phosphatase. In Eichhorn, G. L. and Marzilli, L. G. (Eds.) *Advances in Inorganic Biochemistry - Volume 1*, Elsevier/North Holland, New York, 1979, 1-66.

Coleman, J. E. and Gettins, P., Molecular properties and mechanism of alkaline phosphatase. In Spiro, T. G. (Ed.) *Zinc Enzymes*, Wiley-Interscience, New York, 1983, 153-217.

Compton, S. J. and Jones, C. G., Mechanism of dye response and interference in the Bradford protein assay. *Anal. Biochem.*, 151 (1985) 369-374.

Cullity, B. D. *Elements of X - ray diffraction, 2nd Edition,* Addison-Wesley , Reading, MA, 1978, 284-285.

Dalby, R. N., Byron, P. R., Shepherd, H. R. and Papadopoulos, E., CFC propellant substitution: P-134a as a potential replacement for P-12 in MDIs. *Pharm. Tech.*, 14:3 (1990) 26-33.

Dalby, R. N., Naini, V. and Byron, P. R., Droplet drying and electrostatic collection: a novel alternative to conventional comminution techniques. *J. Biopharm. Sci.*, 3:1/2 (1992) 91-99.

Dalby, R. N. and Tiano, S. L., Rational testing methods for nebulizers and respiratory solutions. In Byron, P. R., Dalby, R. N. and Farr, S. J. (Eds.), *Respiratory Drug Delivery IV*, Interpharm Press, Buffalo Grove, IL, 1994, 249-257.

Daly Jr., J. J. and SanGiovanni, M. L., Replacements for CFC propellants: a technical/environmental overview. *Spray Tech. & Marketing*, 3 (1993) 34-38.

Daemen, A. L. H. and van der Stege, H. J., The destruction of enzymes and bacteria during the spray-drying of milk and whey. 2. The effect of the drying conditions. *Neth. Milk Dairy J.*, 36 (1982) 211-229.

Dietrich, A., Karl Fischer titration, Part 2. Standardization, equipment validation, and control techniques. *Am. Lab.*, March (1994) 33-39.

Eddington, S. M., The anatomy of access: peptide drug delivery. *Bio/Technology*, 9 (1991) 1329-1331.

Elamin, A.A., Sebhatu, T. and Ahlneck, C., The use of amorphous model substances to study mechanically activated materials in the solid state. *Int. J. Pharm.*, 119 (1995) 25-36.

Engström, L., Studies on calf-intestinal alkaline phosphatase. *Biochem. Biophys. Acta*, 52 (1961) 36-48.

Fell, J. T. and Newton, J. M., The production and properties of spray dried lactose: the physical properties of samples of spray dried lactose produced on an experimental drier. *Pharm. Acta Helv.*, 46 (1971) 425-430.

Franks, F., Hatley, R. H. M. and Mathias, S. F., Material science and the production of shelf stable biologicals. *Biopharm*, 3:10 (1991) 38-55.

Franks, F., and Berg, C. V. D., A rational approach to the drying of labile biologicals: the role of salts and stabilizers. In Crommelin, D. J. A. and Midha, K. K. (Eds.), *Topics in Pharmaceutical Sciences - 1991*, Medpharm Scientific, Stuttgart, Germany, 1992, 233-240.

French, D. L., McAuley, A. J., Chang, B. and Niven, R. W., Moisture induced state changes in spray dried trehalose/protein formulations. *Pharm. Res.*, 12:Suppl. (1995) S-83.

Ford, A. W. and Dawson, P. J., The effect of carbohydrate additives in the freeze drying of alkaline phosphatase. *J. Pharm. Pharmacol.*, 45 (1993) 86-93.

Fosset, M., Chappelet-Tordo, D. and Lazdunski, M., Intestinal alkaline phosphatase. Physical properties and quaternary structure. *Biochemistry*, 13 (1974) 1783-1788.

Foster, T. P. and Leatherman, M. W., Powder characteristics of proteins spray dried from different spray dryers. *Drug Dev. Ind. Pharm.*, 21:15 (1995) 1705-1723.

Fries, D. C., Rao, S. T. and Sundaralingam, M., Structural chemistry of carbohydrates. III. Crystal and molecular structure of 4-*O*-ß-D-galactopyranosyl-α -D-glucopyranise Monohydrate (α-Lactose Monohydrate). *Acta Cryst.* B27 (1971) 994-1005.

Ganderton, D. and Kassem, N. M., Dry powder inhalers. *Adv. Pharm. Sci.*, 6 (1992) 165-191.

Gonda, I., Targeting by deposition. In Hickey, A. J. (Ed.) *Pharmaceutical Inhalation Aerosol Technology*, Marcel Dekker, New York, 1992, 61-82.

Gonda, I., Cipolla, D. C., Shire, S. J., Meserve, K., Weck, S., Clark, A. R. and Chan, H-K., A case study in aerosol protein drug development: aqueous solution aerosols of rhDNase. In Byron, P. R., Dalby R. N. and Farr, S. J. (Eds.) *Respiratory Drug Delivery IV*, Interpharm Press, Buffalo Grove, IL, 1994, 47-54.

Green, J.L. and Angell, C.A., Phase relations and vitrification in saccharide-water solutions and the trehalose anomaly. *J. Phys. Chem.*, 93 (1989) 2880-2882.

Hageman, M. J., The role of moisture in protein stability. *Drug Dev. Ind. Pharm.*, 14 (1988) 2047-2070.

Hancock, B.C. and Zografi, G., The relationship between the glass transition temperature and the water content of amorphous pharmaceutical solids. *Pharm. Res.*, 11 (1994) 471-477.

Handbook of Pharmaceutical Excipients, Academic Press, New York, NY, 1986, 155.

Hindle, M. and Byron, P.R., Size distribution control of raw materials for dry powder inhalers using the Aerosizer with the Aero-disperser. *Pharm. Tech.,* 19 (1995) 64-78.

Hindle, M., Jashnani, R.J. and Byron, P. R., Dose emissions from marketed inhalers: influence of flow, volume and environment. In Byron,

P. R., Dalby, R. N. and Farr, S. J. (eds.), *Respiratory Drug Delivery IV*, Interpharm Press, Buffalo Grove, IL, 1994,137-142.

Hinds, W. C., *Aerosol Technology - Properties, Behavior, and Measurement of Airborne Particles*, Wiley-Interscience, New York, 1982, 284-314.

Izutsu, K., Yoshioka, S. and Terao, T., Decreased protein-stabilizing effects of cryoprotectants due to crystallization. *Pharm. Res.*, 10 (1993) 1232-1237.

Jashnani, R.J., Byron, P.R. and Dalby, R.N., Testing of dry powder aerosol formulations in different environmental conditions. *Int. J. Pharm.,* 113 (1995) 123-130.

Karnes, H. T., Shiu, G. and Shah, V. P., Validation of bioanalytical methods. *Pharm. Res.*, 8:4 (1991) 421-426.

Kim, E. E. and Wyckoff, H. W., Reaction mechanism of alkaline phosphatase based on crystal structures. Two metal ion catalysis. *J. Mol. Biol.,* 218 (1991) 449-464.

Labrude, P., Rosolomanana, C., Vigneron, C., Thirion, C. and Chaillot, B., Protective effect of sucrose on spray drying of oxyhemoglobin. *J. Pharm. Sci.*, 78 (1989) 223-229.

Laube, B. L., Georgopoulos, A. and Adams, G. K., Preliminary study of the efficacy of insulin aerosol delivered by oral inhalation in diabetic patients. *J. Am. Med. Assoc.*, 269 (1993) 2106-2109.

Lea, C. H. and Hannan, R. S., Studies of the reaction between proteins and reducing sugars in the "dry state". I. Effect of activity of water, of pH and of temperature on the primary reaction between casein and glucose. *Biochem. Biophys. Acta*, 3 (1949) 313-325.

Lerk, C. F., Consolidation and compaction of lactose. *Drug Dev. Ind. Pharm.,* 19 (1993) 2359-2398.

Levine, H. and Slade, L., Another view of trehalose drying and stabilizing biological materials. *Biopharm*, 5:5 (1992) 36-40.

Lowry, O. H., Roseborough, N. J., Farr, A. L. and Randall, R. J., Protein measurement with Folin phenol reagent. *J. Biol. Chem.*, 193 (1951) 265-275.

Makower, B. and Dye, W.B., Equilibrium moisture content and crystallization of amorphous sucrose and glucose. *J. Agr. Food Chem.*, 4 (1956) 72-77.

Martin, G. P., Onyechi, J. O. and Mariott, C., Future prospects for the pulmonary delivery of drugs. *S. T. P. Pharma. Sciences*, 4 (1994) 5-10.

Masters, K., *Spray Drying Handbook, 5th Edition,* Longman Scientific and Technical, New York, 1991a, 23-66.

Masters, K., *Spray Drying Handbook, 5th Edition,* Longman Scientific and Technical, New York, 1991b, 643-662.

Matsuda, Y., Otsuka, M., Onoe, M and Tatsumi, E., Amorphism and physical stability of spray dried frusemide. *J. Pharm. Pharmacol.*, 44 (1992) 627-633.

May, K. R., The Collison nebulizer: description, performance and application. *Aerosol Sci.*, 4 (1973) 235-243.

McComb, E. A., Formamide as an extraction solvent in Karl Fischer method for determining moisture in lactose and maltose. *Anal. Chem.*, 29 (1957) 1375.

Molina, M. J. and Rowland, F. S., Stratospheric sink for chlorofluoromethanes: chlorine atom-catalyzed destruction of ozone. *Nature*, 249 (1974) 810-812.

Morén, F., Dosage forms and formulations for drug administration to the respiratory tract. *Drug Dev. Ind. Pharm.*, 13 (1987) 695-728.

Mumenthaler, M., Hsu, C.C. and Pearlman, R., Feasibility study on spray drying protein pharmaceuticals: recombinant human growth hormone and tissue plasminogen activator. *Pharm. Res.*, 11 (1994) 12-20.

Naini, V., Byron, P. R. and Dalby, R. N., Collection of spray dried respirable particulates using electrostatic precipitation - Effects of air flow and temperature. *Pharm. Res.*, 10:Suppl. (1993) S-134.

Naini, V., Byron, P. R. and Phillips, E. M., Physicochemical stability of crystalline sugars and their spray dried forms: dependence upon relative humidity and suitability for use in powder inhalers. *Pharm. Dev. Tech.*, submitted, March, 1996.

Niven, R. W., Delivery of biotherapeutics by inhalation aerosols. *Pharm. Tech.*, 17 (1993) 72-82.

Niven, R. W., Ip, A. Y., Mittelman, S. D., Farrar, C., Arakawa, T. and Prestrelski, S. J., Protein nebulization: I. Stability of lactate dehydrogenase and recombinant granulocyte-colony stimulating factor to air-jet

nebulization. *Int. J. Pharm.*, 109 (1994) 17-26.

Oglesby Jr., S. and Nichols., G. B., *Electrostatic Precipitation*. Marcel Dekker, New York, 1978, 1-13.

Otsuka, M., Ohtani, H., Otsuka, K. and Kaneniwa, N., Effect of humidity on solid-state isomerization of various kinds of lactose during grinding. *J. Pharm. Pharmacol.*, 45 (1992) 2-5.

Parrott, E. L., Milling of pharmaceutical solids. *J. Pharm. Sci.*, 63:6 (1974) 813-829.

Patton, J. S., Trinchero, P. and Platz, R. M., Bioavailability of pulmonary delivered peptides and proteins: α-interferons, calcitonins and parathyroid hormones. *J. Controlled Release*, 28 (1994) 79-85.

Patton, J.S. and Platz, R.M., (D) Routes of delivery: case studies, pulmonary delivery of peptides and proteins for systemic action. *Adv. Drug Del. Rev.*, 8 (1992) 179-196.

Pazur, J. H., Oligosaccharides. In Pigman, W. and Horton, D. (Eds.), *The Carbohydrates: Chemistry and Biochemistry, (Volume IIA), 2nd Edition.* Academic Press, New York, 1970, 69-129.

Phillips, E. M. and Stella, V. J., Rapid expansion from supercritical solutions: application to pharmaceutical processes. *Int. J. Pharm.*, 94 (1993) 1-10.

Phillips, E.M., Ahmed, H., Carvajal, M.T., Fanale, K., Sethatekukul, K., Rana, J., Tarantino, R. and Malick, A.W., Formulation development of spray dried powders for inhalation. *Pharm. Res.,* 11:Suppl. (1994) S-158.

Pigman, W. and Anet, E. F. L. J., Mutarotations and actions of acids and bases. In Pigman, W. and Horton, D. (Eds.), *The Carbohydrates - Chemistry and Biochemistry, (Volume 1A), 2nd Edition.*, Academic Press, New York, NY, 1972, 165-194.

Pikal, M. J., Freeze-drying of proteins - Part II: formulation selection. *Biopharm*, 3 (1990) 26-30.

Pine, S. H., *Organic Chemistry, 5th Edition*, McGraw Hill, New York, 1987a, 768-772.

Pine, S. H., *Organic Chemistry, 5th Edition*, McGraw Hill, New York, 1987b, 224-227.

Prestrelski, S. J., Arakawa, T. and Carpenter, J. F., Separation of freezing- and drying-induced denaturation of lyophilized proteins using stress specific stabilization: II. Structural studies using infrared spectroscopy. *Arch. Biochem. Biophys.*, 303 (1993) 465-473.

Prestrelski, S.J., Tedeschi, N., Arakawa, T. and Carpenter, J.F., Dehydration-induced conformational transitions in proteins and their inhibition by stabilizers, *Biophys. J.*, 65 (1993) 661-671.

Pristoupil, T. I., Kramlova, M., Fortova, H. and Ulrych, S., Haemoglobin lyophilized with sucrose: the effect of residual moisture on storage. *Haematologia*, 18 (1985) 45-52.

Raemy, A. and Schweizer, T.F., Thermal behavior of carbohydrates studied by heat flow calorimetry. *J. Therm. Anal.*, 28 (1983) 95-108.

Robinson, M., Electrostatic Precipitation. In Moore, A. D. (Ed.) *Electrostatics and its Applications*,, Wiley, New York, 1973, 180-220.

Roos, Y., Melting and glass transitions of low molecular weight carbohydrates. *Carbohydr. Res.*, 238 (1993) 39-48.

Roos, Y. and Karel, M., Plasticizing effect of water on thermal behavior and crystallization of amorphous food models. *J. Food Sci.*, 56 (1991) 38-43.

Rye, A. and Sorum, H., Crystalline modifications of D-Mannitol. *Acta Chem. Scand.*, 6 (1952) 1128-1129.

Sakharov, I. Y., Makarova, I. E. and Ermolin, G. A., Purification and characterization of intestinal alkaline phosphatase from harp seal. *Comp. Biochem. Physiol.*, 90B (1988) 709-714.

Saleki-Gerhardt, A. and Zografi, G., Non-isothermal and isothermal crystallization of sucrose from the amorphous state. *Pharm. Res.*, 11 (1994) 1166-1173.

Scholz, E. *Karl Fischer Titration, Determination of Water, Chemical Laboratory Practice.* Springer-Verlag, Berlin, 1984.

Sedmak, J. J. and Grossberg, S. E., A rapid, sensitive, and versatile assay for protein using Coomassie blue G250. *Anal. Biochem.*, 79 (1977) 544-552.

Segel, I. H., *Biochemical Calculations, 2nd Edition*. Wiley, New York, 1976, 281-293.

Slade, L. and Levine, H., Beyond water activity: recent advances based on

an alternative approach to the assessment of food quality and safety. *Crit. Rev. Food Sci. Nutr.*, 30 (1991) 115-360.

Small Particle Aerosol Generator - SPAG2, Instructions for Use, ICN Pharmaceuticals, Inc., Costa Mesa, CA, 1989.

Sowadski, J. M., Handshumacher, M. D., Krishna Murthy, H. M., Foster, B. A. and Wyckoff, H. W., Refined structure of alkaline phosphatase from *Escherichia coli* at 2.8 Å resolution. *J. Mol. Biol.* 186 (1985) 416-422.

Staniforth, J. N., The importance of electrostatic measurement in aerosol formulation and preformulation. In Byron, P. R., Dalby, R. N. and Farr, S. J. (eds.), *Respiratory Drug Delivery IV*, Interpharm Press, Buffalo Grove, IL, 1994, 303-311.

STATGRAPHICS Plus, Version 6.0, Manugistics, Inc., Rockville, MD, 1992.

Taga, T., Senma, M. and Osaki, K., The crystal and molecular structure of trehalose dihydrate. *Acta Cryst.* B28 (1972) 3258-3263.

Tarelli, E. and Wood, J. M., Additives to biological substances. I. Effect of added carbohydrates on bovine serum albumin. *J. Biol. Stand.*, 9 (1981) 121-129.

Tarelli, E. and White, C. A., Additives to biological substances. II. Relative stabilities of some carbohydrate additives at and around neutral pH values in the phosphate buffers and water. *J. Biol. Stand.*, 10 (1982) 95-103.

Tarelli, E., Elphick, A. D., Gostick, J. D. and Stammers, R. P., Additives to biological substances. III. The moisture content and moisture uptake of commonly used carrier agents undergoing processing conditions similar to those used in the preparation of international biological standards. *J. Biol. Stand.*, 15 (1987) 331-340.

Taylor, L.S., York, P. and Mehta, V., Phase characterization of trehalose dihydrate. *Pharm. Res.*, 11:Suppl. (1994) S-151.

Timasheff, S. N. and Arakawa, T., Stabilization of protein structure by solvents. In Creighton, T. E. (Ed.), *Protein Structure: A Practical Approach*, IRL Press, Oxford, 1989, 331-345.

Tom, J. W. and Debenedetti, P. G., Particle formation with supercritical fluids - A review. *J. Aerosol Sci.*, 22:5 (1991) 555-584.

Torriani, A., Alkaline phosphatase of *Escherichia coli*. *Methods Enzymol.*,

12B (1968) 212-218.

United States Pharmacopeia, USP23/NF18., United States Pharmacopeial Convention, Rockville, MD, 1994a, 2258-2259.

United States Pharmacopeia, USP23/NF18., United States Pharmacopeial Convention, Rockville, MD, 1994b, 1840-1843.

United States Pharmacopeia, USP23/NF18., First Supplement, United States Pharmacopeial Convention, Rockville, MD, 1995, 2584.

Van Campen, L., Amidon, G.L. and Zografi, G., Moisture sorption kinetics for water soluble substances II: experimental verification of heat transport control. *J. Pharm. Sci.*, 72 (1983) 1388-1393.

Vidgrén, M.T., Vidgrén, P.A. and Paronen, T.P., Comparison of physical and inhalation properties of spray-dried and mechanically micronized disodium cromoglycate. *Int. J. Pharm.*, 35 (1987) 139-144.

Vidgrén, P. A., Vidgrén, M. T. and Paronen, T. P., Physical stability and inhalation behavior of mechanically micronized and spray dried disodium cromoglycate in different humidities. *Acta Pharm. Fenn.*, 98 (1989) 71-78.

Wallace, B. M. and Lasker, J. S., Stand and deliver: getting peptide drugs into the body. *Science*, 260 (1993) 912-913.

White, H. J., Particle charging in electrostatic precipitation. *AIEE Trans.*, 70 (1951) 1186-1191.

White, H. J., *Industrial Electrostatic Precipitation*, Addison-Wesley, Reading, MA, 1963, 33-47.

Yernault, J. C., Inhalation therapy: a historical perspective. *Eur. Respir. Rev.*, 4 (1994) 65-67.

Yeo, S., Lim, G., Debenedetti, P. G. and Bernstein, H., Formation of microparticulate protein powders using a supercritical fluid antisolvent. *Biotech. Bioeng.*, 41 (1993) 341-346.

Zografi, G., States of water associated with solids. *Drug Dev. Ind. Pharm.*, 14 (1988) 1905-1926.

APPENDIX I. CALCULATION OF THEORETICAL PARTICLE COLLECTION EFFICIENCIES INSIDE THE ELECTROSTATIC PRECIPITATOR USING PARTICLE CHARGING THEORY

AI.a INTRODUCTION

Aerosol velocities in an electric field can be much higher than gravitational or inertial velocities (Hinds, 1982). This fact is exploited in the design and use of electrostatic precipitators. The electrostatic precipitation process consists of three fundamental steps; particle charging, particle collection and removal of the collected dust (Oglesby and Nichols, 1978). Particles charging in electrostatic precipitation is usually achieved by two mechanisms: field charging and diffusion charging (Hinds, 1982). "Diffusion charging" is believed to be the dominant mechanism for aerosols smaller than 0.1 μm, where collisions result from the Brownian motion of ions and aerosols (Hinds, 1982). However, "Field charging" is thought to be the dominant mechanism for aerosols larger than or equal to 1 μm. For aerosols between these two sizes, charging is achieved by a combination of the two mechanisms. Both mechanisms require the production of unipolar ions (Hinds, 1982). To achieve useful aerosol charging for electrostatic precipitation, high concentrations of such unipolar ions are often produced by a corona discharge. Providing a sufficient nonuniform electric field

between a concentric wire (active electrode) and tube (grounded or passive electrode) can provide such a discharge, which is characterized by a thin layer of highly charged ions surrounding the wire. The ions then migrate towards the passive electrode (the tube in the precipitator) causing further ionization of the gas. If the gas contains fine particles, these are bombarded by the ions causing the aerosol particles to acquire high number of charges. The charged particles then migrate towards the passive electrode, where they are deposited. Particle deposition in electrostatic precipitators depend on a variety of factors, like particle size of the dust, volumetric air flow through the system, applied electric field strength, conductivity/resistivity of the collected dust and particle re-entrainment of particles in the air stream.

AI.b THEORETICAL CALCULATION OF AEROSOL COLLECTION EFFICIENCY IN A WIRE-IN-TUBE ELECTROSTATIC PRECIPITATOR

Theoretical particle collection efficiencies inside an electrostatic precipitator can be calculated using the Deustch-Anderson equation (Hinds, 1982):

$E' = 1 - e^{(V_{TE} * A/Q)}$ ..... Equation AI.1

where E' is the collection efficiency, V_{TE} is the terminal electrostatic velocity, A is the collection surface area and Q is the volumetric air flow rate. The terminal electrostatic velocity (V_{TE}) is given by:

$V_{TE} = neE / (3\pi\mu d)$ .....Equation AI.2

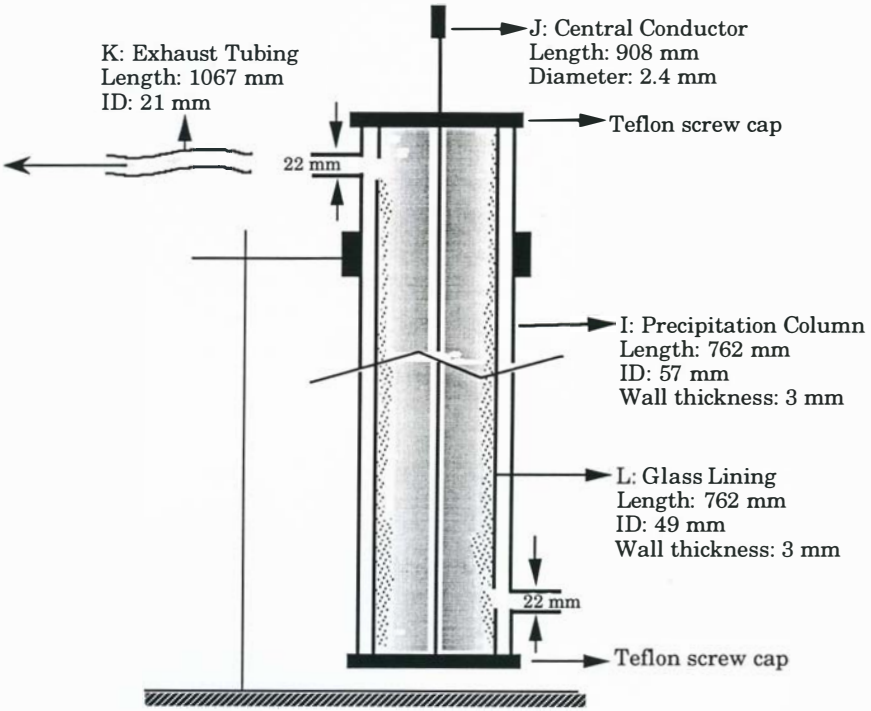

Figure AI.1 Exploded view of the electrostatic precipitation column shown with the central wire conductor, glass lining and exhaust tube with dimensions.

where E is the electric field strength, μ is the viscosity of air (1.81×10^{-4} dyn.s/cm^2), e is the charge on an electron (4.8×10^{-10} statcoulombs), d is the particle diameter and n is the number of charges on the particle.

The electric field strength (E) for a wire-in-tube geometry is given by:

$$E = \Delta W / [r_t \ln(r_t/r_w)] \quad \text{..... Equation AI.3}$$

where ΔW is the difference in voltage between wire and tube, r_t is the radius of the tube (in these studies it is the radius of the glass tubing-I = 2.4 cm, Figure AI.1) and r_w is the radius of the wire (r_w = 0.12 cm, Figure AI.1)

The number of charges on the particle (n, Equation AI.2) was calculated by making the following simplifying but not invalidating assumptions: 1) Turbulent air flow in the system (particle Reynolds number 1), 2) aerosol particles are charged by a field charging mechanism (uniform particle diameter of ≥ 1 μm at a drying temperature of 41 °C and 3) aerosols are uniformly distributed across every cross section of the precipitator. The number of charges (n) acquired by a particle during time t, in an electric field E if diffusion charging is neglected (assumed to be insignificant) is given by:

$$n = [3\varepsilon / (\varepsilon + 2)] \times [E\, d^2 / 4e] \times [(\pi e Z_i N_i t) / (1 + \pi e Z_i N_i t)] \quad \text{..... Equation AI.4}$$

where ε is the dielectric constant of the particle (assumed to be 5 for lactose, since most materials have $1 < \varepsilon < 10$, Hinds, 1982), E is the electric field strength, d is the diameter of the particle, e is the charge on an electron, Z_i is the mobility of the ions (approximately 450 cm^2/statvolts; Hinds, 1982), N_i

is the ion number concentration (when particles are intentionally charged by field charging, ion concentration N_i, is usually 10^7 /cm^3 or greater; Hinds, 1982) and t is the residence time of the aerosol in the column.

The effective collection surface area A (Equation IV.1) was calculated to be 1158.74 cm^2. This was internal surface area of the glass collection surface (L, Figure AI.1) minus the area of the exit and entry ports (Figure AI.1). Volumetric air flows through the column were measured as described in Appendix AII.

AI.c CALCULATION OF A TYPICAL THEORETICAL COLLECTION EFFICIENCY

A sample efficiency calculation is shown below. It was calculated using an applied precipitator voltage of 20 kV and a drying air flow of 29.1 liters/min and a temperature of 41 °C.

Particle diameter, d = 1 μm (10^{-4} cm)

Dielectric constant, $\varepsilon = 5$ (for lactose, since for most materials $1 < \varepsilon < 10$)

Charge on an electron, e = 4.8 x 10^{-10} statcoulomb

Ion number concentration, $N_i = 10^7$ /cm^3 (See Section AI.2)

Mobility of ions, Z_i = 450 cm^2/(statvolt.s) (See Section AI.2)

Volumetric air flow, Q = 29.1 liters/min (485 cm^3/s)

Length of the glass collection surface-L = 76.20 cm

Internal diameter of the glass collection surface-L = 4.9 cm (r_t = 2.45 cm)

Diameter of the wire conductor-J = 0.24 cm (r_w = 0.12 cm)

Collection surface area, A = 1158.7 cm^2

Difference in voltage between wire and tube, ΔW = 20 kV

From Equation AI.3

$E = 20 / [2.45 \ln(2.45 / 0.12)]$

= 2.71 kV/cm

= 9.03 statvolts/cm [1 statvolt = 300 V; cgs units are used for the advantage of simplified equations]

STEP 1: Calculate the residence time,t of the aerosol in the column:

$t = (\pi r_t^2 \times$ length of glass tube$) / Q$

= 2.9 s

STEP 2: Calculate $[3\varepsilon / (\varepsilon + 2)] = 2.14$

STEP 3: Calculate $[E d^2 / 4e]$ = [9.03 (statvolt/cm) x $(10^{-4})^2$ (cm^2)] / [4 x (4.8 x 10^{-10}) (statcoulomb)]

= 47.03 [no units since statvolt.cm = statcoulomb; Hinds,1982]

STEP 4: Calculate $\pi e Z_i N_i t = \pi$ [(4.8 x 10^{-10}) (statcoulomb) x 450 {cm^2 / (statvolt.s)} x (107 /cm^3) x 2.9 s]

= 19.68 [no units since statvolt.cm = statcoulomb]

STEP 5: Using Equation AI.4 calculate n

$n = (2.14 \times 47) \times [19.68 / (1+19.68)]$

$= 96$

Terminal electrostatic velocity V_{TE} can now be calculated from Equation AI.3

STEP 6: Calculate $V_{TE} = [96 \times (4.8 \times 10^{-10})$ (statcoulomb) x 9.07 (statvolt/cm)] / $[3 \pi \times (1.81 \times 10^{-4})$ (dyn.s / cm^2) x $(10^{-4})^2$ (cm^2)]

= 2.45 cm/s

STEP 7: Knowing the volumetric air flow (Q), collection surface area (A) and V_{TE} Equation AI.1 can now be applied to calculate the efficiency E'

$E' = 1 - e^{[-2.45 \text{ (cm/s)} \times 1158.74 \text{ (cm2)} / 485 \text{ (cm3/s)}]}$

$= 0.9971.$

Expressed as a percentage this is = 99.71%

Collection efficiencies calculated using the above method for two flow regimes of 29.1 liters/min and 50.6 liters/min and different electrostatic precipitator voltages are shown in Table AI.1. These values were used for generating the theoretical collection efficiency curves shown in Figure IV.15.

Table AI.1 Theoretical collection efficiencies inside the electrostatic precipitator column, at two air flow rates of 29.1 liters/min and 50.6 liters/min calculated using the method oulined in Appendix AI.

EP Voltage (kV)	% Collection Efficiency (E')[a]
Drying air flow = 29.1 liters/min	
5	30.73
10	76.83
15	96.29
20	99.71
Drying air flow = 50.6 liters/min	
5	18.44
10	55.60
15	83.95
20	96.11

[a] Calculated from Equation AI.1

APPENDIX II. DETERMINATION OF TOTAL VOLUMETRIC AIR FLOW THROUGH THE PARTICLE COLLECTION APPARATUS

AII.a INTRODUCTION

This Appendix describes the determination of volumetric air flows through the particle collection apparatus used in Chapter IV, at different voltage settings of the autotransformer controlling air flow rate from the hot air gun (D, Figure IV.1). Flows were determined using a calibrated pneumotachograph attached to a micromanometer.

AII.b CALIBRATION OF THE PNEUMOTACHOGRAPH HEAD

A pneumotachograph (Catalog #F10L, Mercury Electronics, Glasgow, Scotland, UK) was cleaned and calibrated using a calibrated flow meter (rotameter size #5, catalog #F1500, Gilmont Instruments Inc., Barrington, IL). The experimental set up for calibration of the pneumotachograph is shown in Figure AII.1. The flow control valve (Figure AII.1) was adjusted to give different scale readings on the flowmeter (center of the ball). At each setting of the flow valve, the apparent cumulative volume of air (1 atm and 70 °F) flowing through the pneumotachograph head in 5 seconds was measured using the VP-5 Micromanometer (VP5, Mercury Electronics, Glasgow, Scotland, UK), in

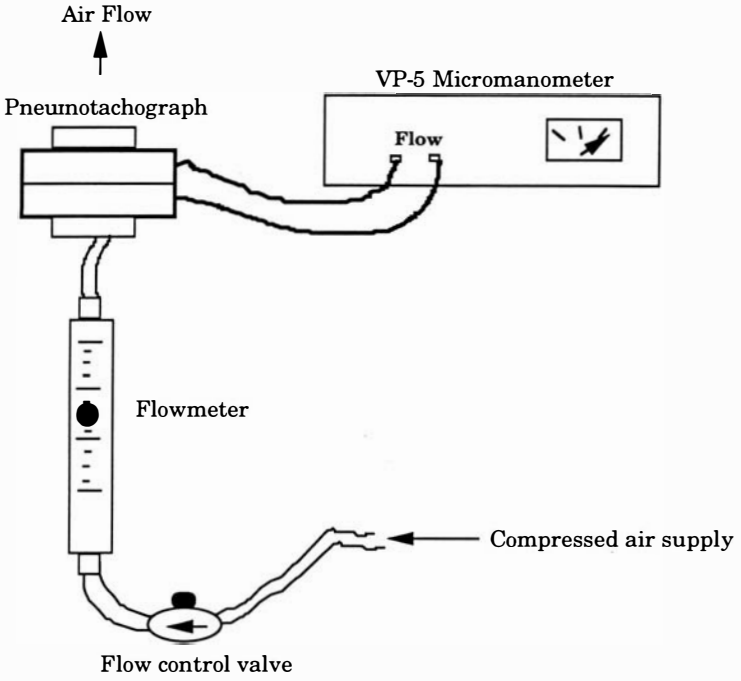

Figure AII.1 Calibration of the pneumotachograph using a calibrated flowmeter and a micromanometer.

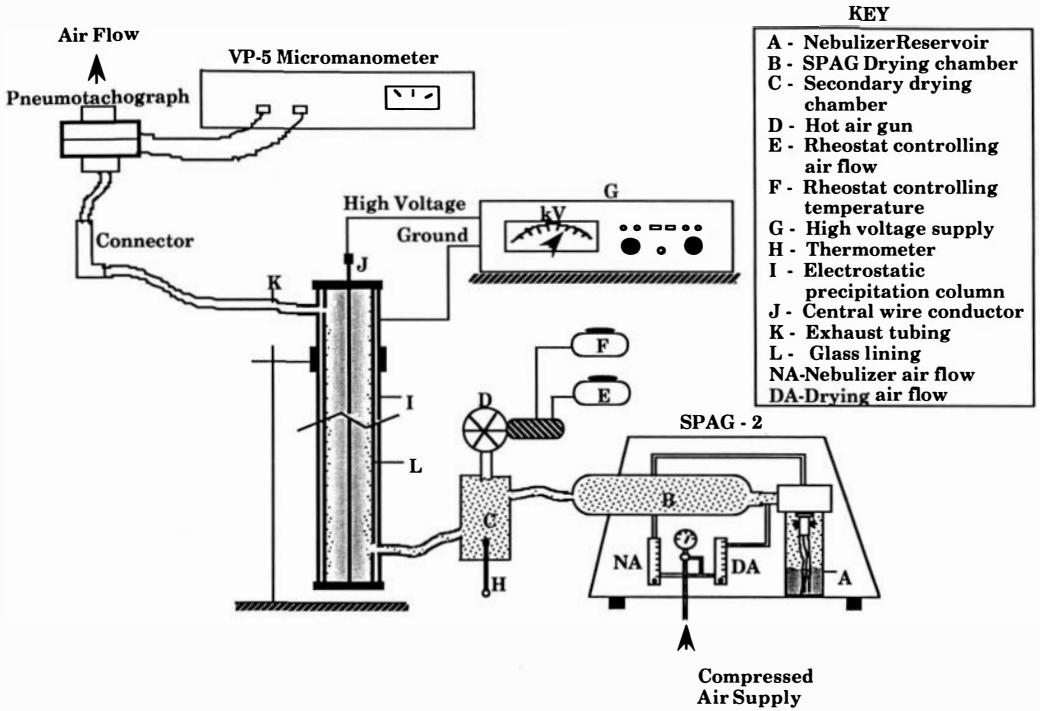

Figure AII.2 Experimental set up for the measurement of volumetric air flow through the apparatus using a calibrated pneumotachograph at different voltage setting on rheostat E.

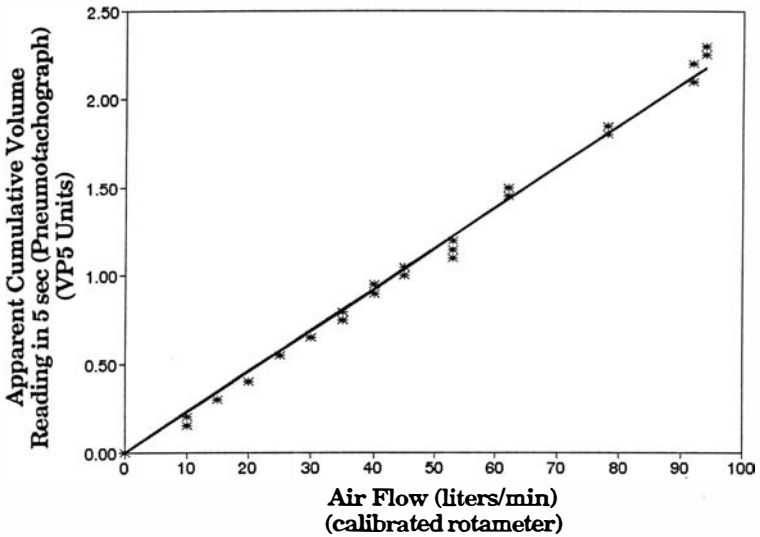

Figure AII.3 Calibration plot of apparent cumulative air volume entering the pneumotachograph head in 5 seconds (VP5 Units) vs air flow in liters/min. Plotted values are experimental determinations. The straight line is the best fit by linear regression [$y = 0.02317x$, $r^2 = 0.99$, standard error of slope = 0.00014, $n = 56$]

replicates of four. Average apparent cumulative volume readings read from the VP-5 were used to construct a calibration curve of cumulative volume (in 5 s) vs flow in liters/min (calculated by interpolation of scale readings from calibration plot for the Gilmont flowmeter). This plot is shown in Figure AII.3.

AII.c MEASUREMENT OF VOLUMETRIC AIR FLOWS IN THE PARTICLE COLLECTION APPARATUS USING THE CALIBRATED PNEUMOTACHOGRAPH AND THE MICROMANOMETER

The exhaust tube of the apparatus was connected to the pneumotachograph head as shown in Figure AII.2. The nebulizer was operated without any aqueous solutions in the reservoir. The nebulizer air flow (NA, Figure AII.2) was set at 7 liters/min using the flowmeter on the SPAG-2 corresponding to nebulizer air flow. Drying air (DA, Figure AII.2) was set at 10 liters/min using the flowmeter on the SPAG-2 corresponding to drying air flow. Rheostat controlling air flow (E, Figure AII.2) of the hot *air* gun (D, Figure AII.2) was set at different voltages. For each voltage setting cumulative volume of air flowing through the pneumotachograph in 5 seconds (VP5 meter readings) was determined in replicates of four. Each apparent cumulative volume reading was converted to true volumetric flow rate (liters/min) by interpolation from the calibration curve (Figure AII.3). The average of four such flow determinations for each voltage setting is shown Table AII.1. Two flow rates of 29.1 liters/min

(corresponding to a voltage of 8 V) and 50.6 liters/min (corresponding to a voltage of 12 V) were used in experiments in Chapter IV.

Table AII.1 Volumetric flow rate at differerent voltage settings on the rheostat controlling air flow (E, Figure AII.1) of the hot air gun.

Voltage Setting (V)	Air Flow (liters/min)[a]
4	5.8 (0.8)
6	19.3 (0.8)
8	29.1 (0.8)
10	41.2 (1.3)
12	50.6 (1.5)
14	57.8 (0.8)
16	64.1 (0.8)
18	69.9 (1.3)
20	73.9 (1.5)

[a] Values are mean (sample SD), n=4

APPENDIX III. SUMMARY OF RAW DATA FOR ALKALINE PHOSPHATASE ENZYME ACTIVITES AND PROTEIN CONCENTRATIONS (IN BSAE) USED IN CALCULATION OF ENZYME SPECIFIC ACTIVITIES

This Appendix summarizes the raw data for enzyme activities of bacterial (Table AIII.1) and bovine intestinal (Table AIII.2) alkaline phosphatase and protein concentrations in the solutions assayed. These data were used for the determination of mean specific acivities as reported in Chapter V (Tables V.4 and V.6).

Table AIII.1 Summary of raw data for bacterial alkaline phosphatase enzyme (BAP) activity and protein concentrations (in BSAE). This data was used to calculate mean specific activities as given in Table V.4 (Chapter V). BAP - Sugar free BAP; BAPL - BAP with lactose; BAPT - BAP with trehalose; BAPS - BAP with sucrose and BAPM - BAP with mannitol.

INITIAL SOLUTION													
	Enzyme Activity (Units/ml)							Protein Concentration (μg BSAE/ml)					
BAP	63.0	54.0	54.7	58.7	60.7	59.9		4.1	3.8	3.9	3.6	3.5	3.5
BAPL	63.6	56.7	60.0	59.9	62.6	59.1		4.2	3.2	3.6	4.0	4.1	4.1
BAPT	60.8	57.6	59.4	60.3	56.3	59.3		4.2	4.1	3.5	3.9	4.0	4.2
BAPS	55.3	59.0	61.8	57.4	60.4	60.1		3.6	3.6	3.8	3.8	4.2	4.3
BAPM	49.1	45.2	59.8	55.2	60.7	60.7		3.2	2.5	3.3	3.7	4.2	4.2
NEBULIZER RESERVOIR													
	Enzyme Activity (Units/ml)							Protein Concentration (μg BSAE/ml)					
BAP	89.2	65.1	77.1	60.1	93.1	101.6		6.1	4.8	5.7	3.6	5.4	5.9
BAPL	108.7	36.6	61.1	92.9	114.6	75.5		6.6	2.1	3.7	6.6	7.6	5.3
BAPT	93.8	88.9	52.4	72.7	95.4	85.8		6.7	6.8	2.8	5.0	6.8	6.3
BAPS	90.2	81.4	59.4	80.0	95.4	85.1		6.3	4.7	4.2	5.6	6.7	5.9
BAPM	62.1	41.9	60.6	90.8	103.8	85.1		4.0	2.4	3.6	6.2	7.3	6.1
SPRAY DRIED													
	Enzyme Activity (Units/ml)							Protein Concentration (μg BSAE/ml)					
BAP	20.3	25.1	72.9					1.6	2.1	6.3			
BAPL	25.2	22.4	19.3					2.0	1.7	1.8			
BAPT	62.1	38.0	56.3					5.1	3.2	3.8			
BAPS	40.4	42.9	66.2					3.4	3.4	5.0			
BAPM	13.9	18.4	63.4					1.8	1.8	6.3			
SPRAY DRIED AND STORED													
	Enzyme Activity (Units/ml)							Protein Concentration (μg BSAE/ml)					
BAP	70.8	66.2	41.4					6.9	6.6	3.7			
BAPL	43.0	24.9	54.1					3.8	2.6	4.2			
BAPT	54.5	21.0	50.9					4.7	2.2	4.4			
BAPS	35.4	54.8	35.3					2.9	5.3	3.4			
BAPM	16.8	14.7	19.4					2.4	1.7	1.7			

Table AIII.2 Summary of raw data for bovine intestinal alkaline phosphatase enzyme (BIAP) activity and protein concentrations (in BSAE). This data was used to calculate mean specific activities as given in Table V.6 (Chapter V). BIAP - Sugar free BIAP; BIAPL - BIAP with lactose; BIAPT - BIAP with trehalose; BIAPS - BIAP with sucrose and BIAPM - BIAP with mannitol.

INITIAL SOLUTION													
	Enzyme Activity (Units/ml)							Protein Concentration (μg BSAE/ml)					
BIAP	30.0	29.9	31.0	29.1	33.0	33.6		3.3	3.2	3.3	3.6	4.1	3.9
BIAPL	31.4	30.9	38.8	29.4	34.3	32.0		3.2	3.3	3.3	3.7	4.1	3.3
BIAPT	32.8	34.4	29.2	32.4	31.9	31.4		3.5	3.5	3.4	4.0	4.1	3.9
BIAPS	31.3	33.5	31.3	33.5	30.7	30.1		3.6	3.3	3.3	4.2	4.1	3.8
BIAPM	32.0	30.1	31.3	33.4	30.9	34.6		3.6	3.4	3.3	4.0	3.9	3.5
NEBULIZER RESERVOIR													
	Enzyme Activity (Units/ml)							Protein Concentration (μg BSAE/ml)					
BIAP	41.6	35.9	37.8	57.0	47.1	43.5		4.5	3.8	4.0	6.8	5.5	4.8
BIAPL	42.5	42.8	52.9	36.5	42.8	42.5		4.4	4.4	4.3	5.0	4.9	4.1
BIAPT	30.5	32.8	46.3	42.3	41.2	44.0		3.2	3.3	4.6	5.7	5.3	4.9
BIAPS	37.7	50.6	45.1	44.5	42.4	38.7		4.2	5.2	4.6	5.5	5.3	4.7
BIAPM	38.4	41.0	38.6	44.5	42.2	45.5		4.2	4.5	4.0	5.3	4.9	4.5
SPRAY DRIED													
	Enzyme Activity (Units/ml)							Protein Concentration (μg BSAE/ml)					
BIAP	27.1	23.9	24.0					4.2	4.0	4.1			
BIAPL	33.1	33.8	41.4					3.5	3.5	3.4			
BIAPT	42.3	42.1	28.9					4.4	4.2	3.1			
BIAPS	31.1	31.8	27.9					3.4	3.3	2.8			
BIAPM	16.5	19.6	16.7					3.3	3.7	3.1			
SPRAY DRIED AND STORED													
	Enzyme Activity (Units/ml)							Protein Concentration (μg BSAE/ml)					
BIAP	26.3	22.7	17.1					5.3	4.3	4.0			
BIAPL	34.3	29.0	29.5					4.3	3.0	3.4			
BIAPT	27.6	26.3	30.8					3.3	3.0	3.3			
BIAPS	29.9	25.1	35.1					3.6	2.5	3.5			
BIAPM	6.5	14.3	16.1					1.9	3.1	3.1			

APPENDIX IV. THERMAL ANALYSIS OF CRYSTALLINE SUGARS AND THEIR SPRAY DRIED FORMS

This Appendix presents the thermogravimetric analysis (TGA) and differential scanning calorimetry (DSC) profiles of different sugar forms. DSC and TGA were performed as described in Sections III.b.2.4 and III.b.2.5 respectively (Chapter III).

In each of the Figures subscript 0 and 30 refer to before and after storage for 30 days at different humidities. Key: A=Coarse fraction, B=Fine fraction, C=Spray dried. Subscripts: a=Stored in sealed bottles over P_2O_5; b=23% RH, c=52% RH, d=75% RH and e=93% RH. Only TGA was performed on A and B before and after exposure at different RH.

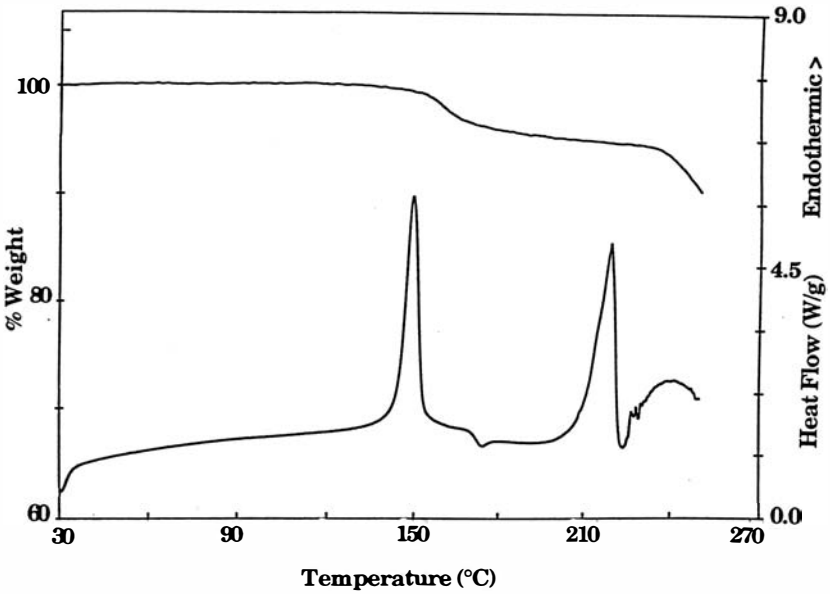

Figure AIV.1 TGA (top) and DSC (bottom) profiles for forms A_0, B_0, $A_{30a,b,c,d,e}$ and $B_{30a,b,c,d,e}$ of lactose.

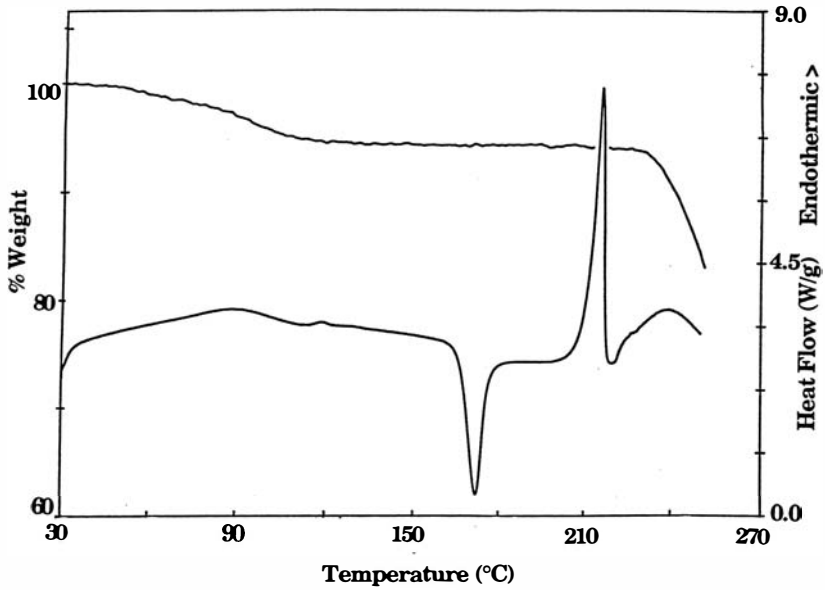

Figure AIV.2 TGA (top) and DSC (bottom) profiles for forms C_0 and C_{30a} of lactose.

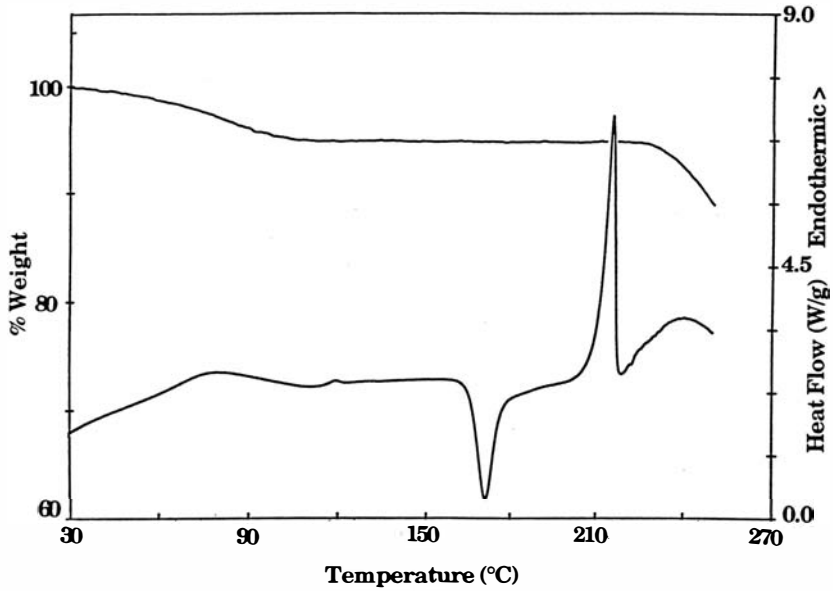

Figure AIV.3 TGA (top) and DSC (bottom) profiles for form C_{30b} of lactose.

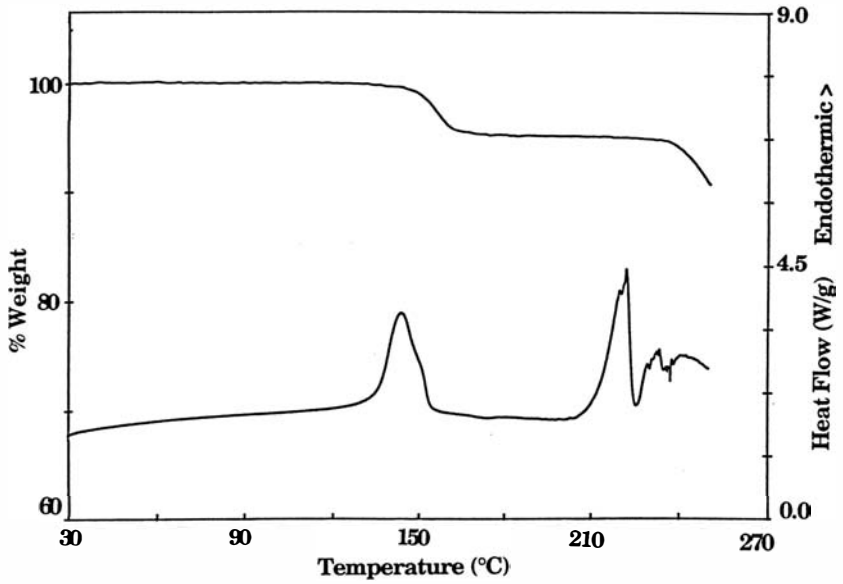

Figure AIV.4 TGA (top) and DSC (bottom) profiles for forms $C_{30c,d,e}$ of lactose.

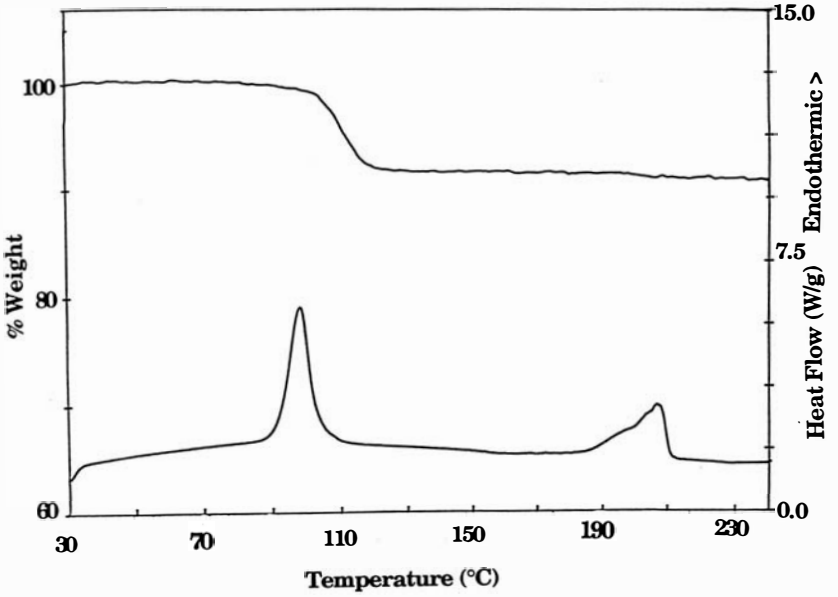

Figure AIV.5 TGA (top) and DSC (bottom) profiles for forms A_0, B_0, $A_{30a,b,c,d,e}$ and $B_{30a,b,c,d,e}$ of trehalose.

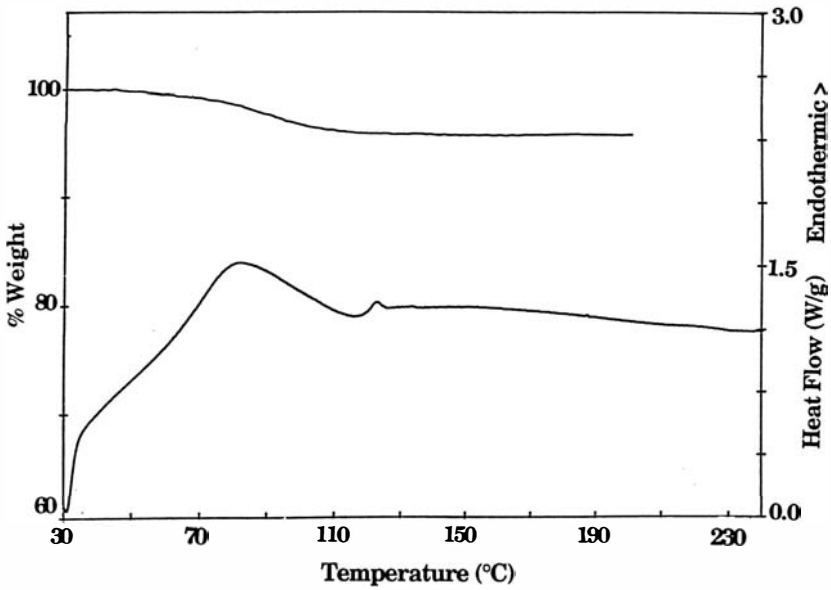

Figure AIV.6 TGA (top) and DSC (bottom) profiles for forms C_0 and C_{30a} of trehalose.

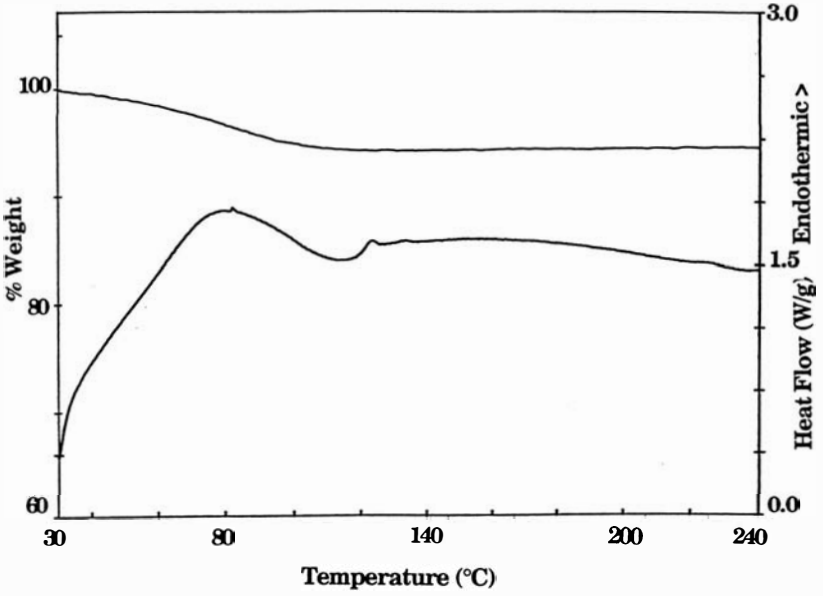

Figure AIV.7 TGA (top) and DSC (bottom) profiles for form C_{30b} of trehalose.

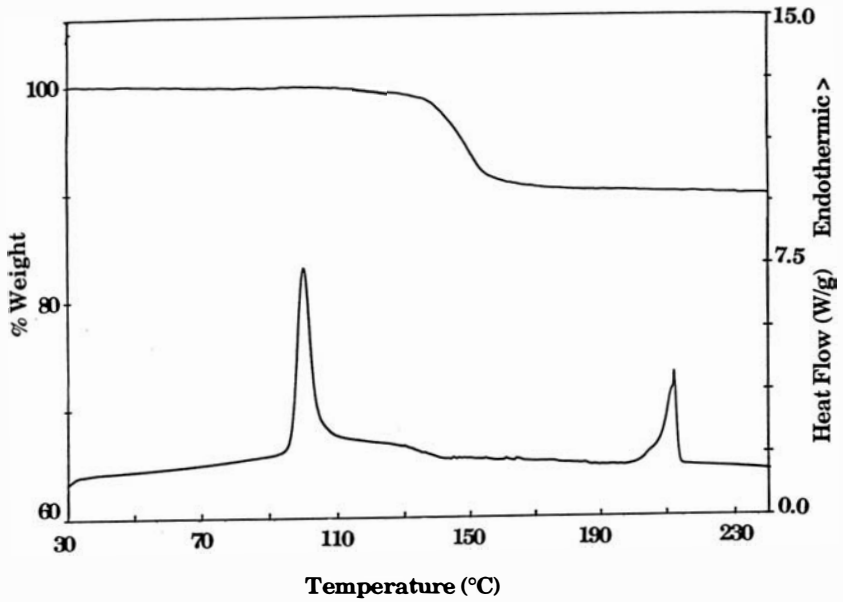

Figure AIV.8 TGA (top) and DSC (bottom) profiles for forms $C_{30c,d,e}$ of trehalose.

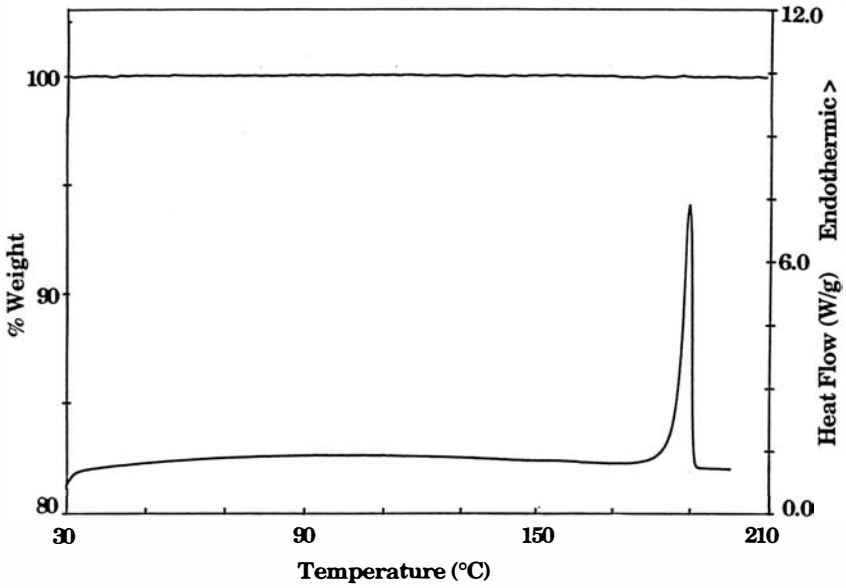

Figure AIV.9 TGA (top) and DSC (bottom) profiles for forms A_0, B_0, $A_{30a,b,c,d}$ and $B_{30a,b,c,d}$ of sucrose.

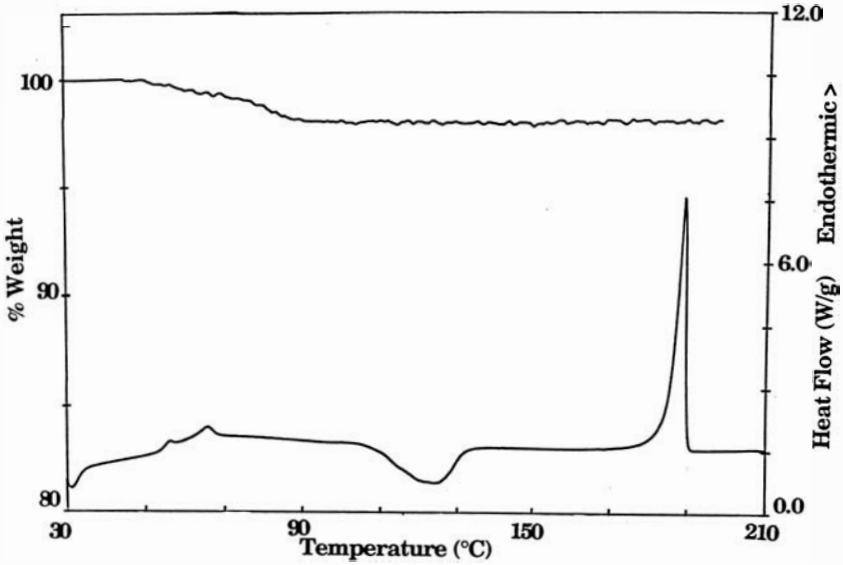

Figure AIV.10 TGA (top) and DSC (bottom) profiles for forms C_0 and C_{30a} of sucrose.

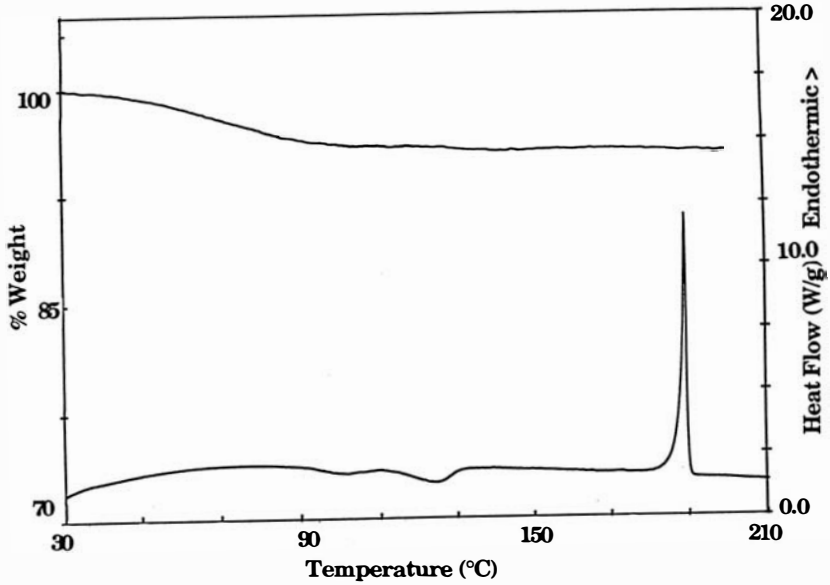

Figure AIV.11 TGA (top) and DSC (bottom) profiles for form C_{30b} of sucrose.

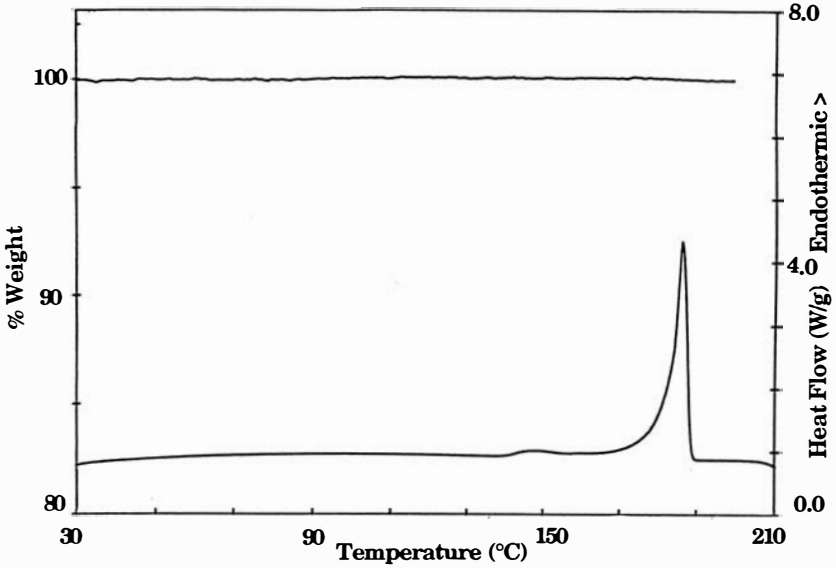

Figure AIV.12 TGA (top) and DSC (bottom) profiles for forms $C_{30c,d}$ of sucrose.

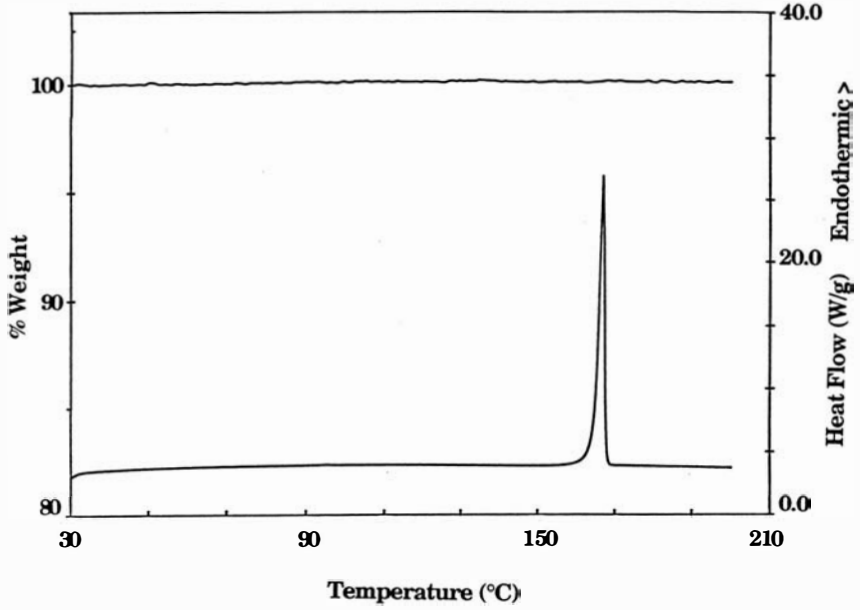

Figure AIV.13 TGA (top) and DSC (bottom) profiles for forms A_0, B_0, $A_{30a,b,c,d,e}$ and $B_{30a,b,c,d,e}$ of mannitol.

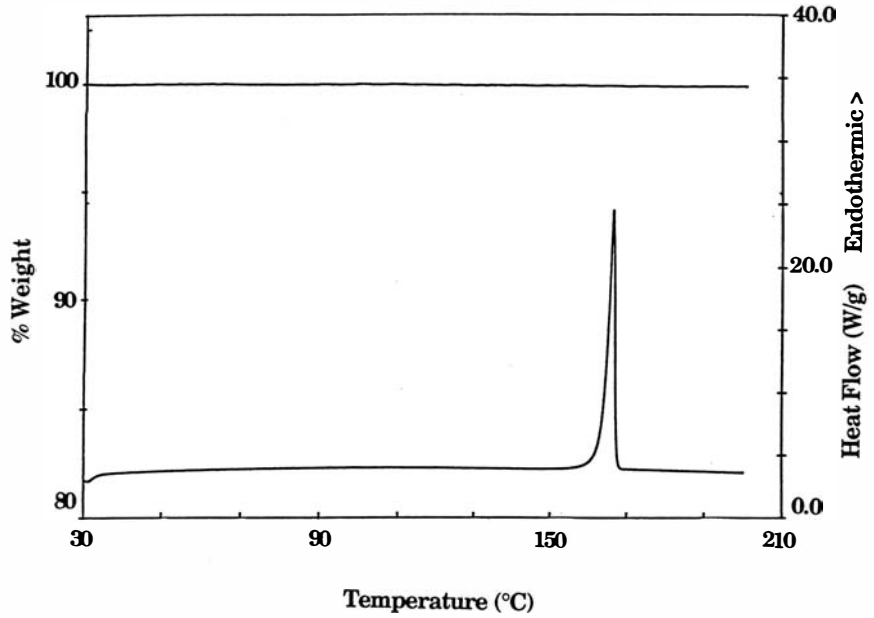

Figure AIV.14 TGA (top) and DSC (bottom) profiles for forms C_0 and C_{30a} of mannitol.

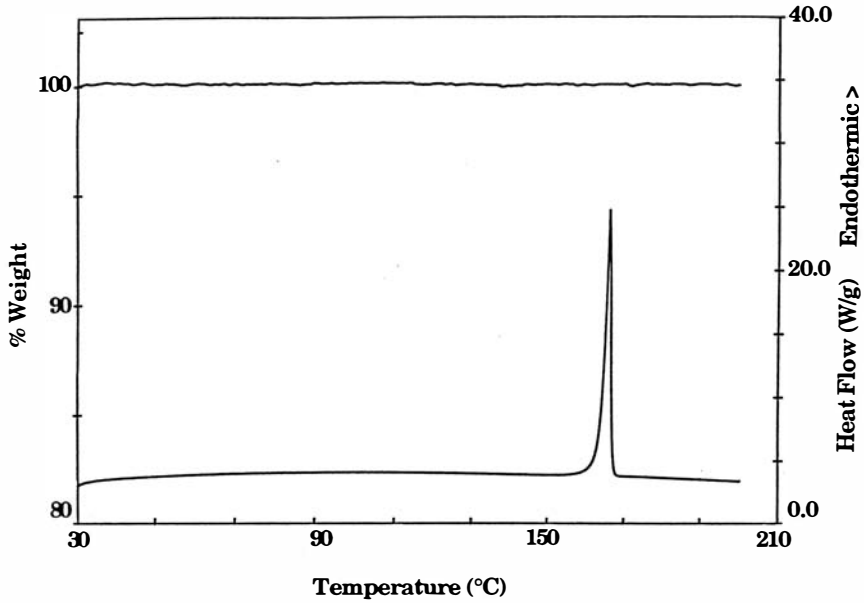

Figure AIV.15 TGA (top) and DSC (bottom) profiles for form C_{30b} of mannitol.

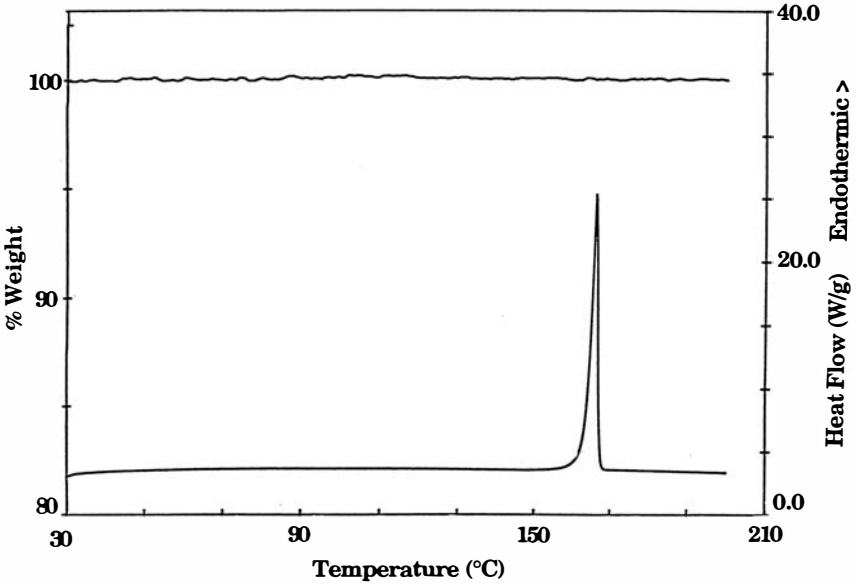

Figure AIV.16 TGA (top) and DSC (bottom) profiles for forms $C_{30c,d,e}$ of mannitol.

APPENDIX V. PARTICLE SIZE DETERMINATION OF SPRAY DRIED SUGARS USING THE AEROSIZER® WITH THE AERODISPERSER®

This Appendix presents the particle size distributions as measured by the Aerosizer® with the Aerodisperser®. The instrument was operated under the conditions described in Section III.b.2.6 (Chapter III).

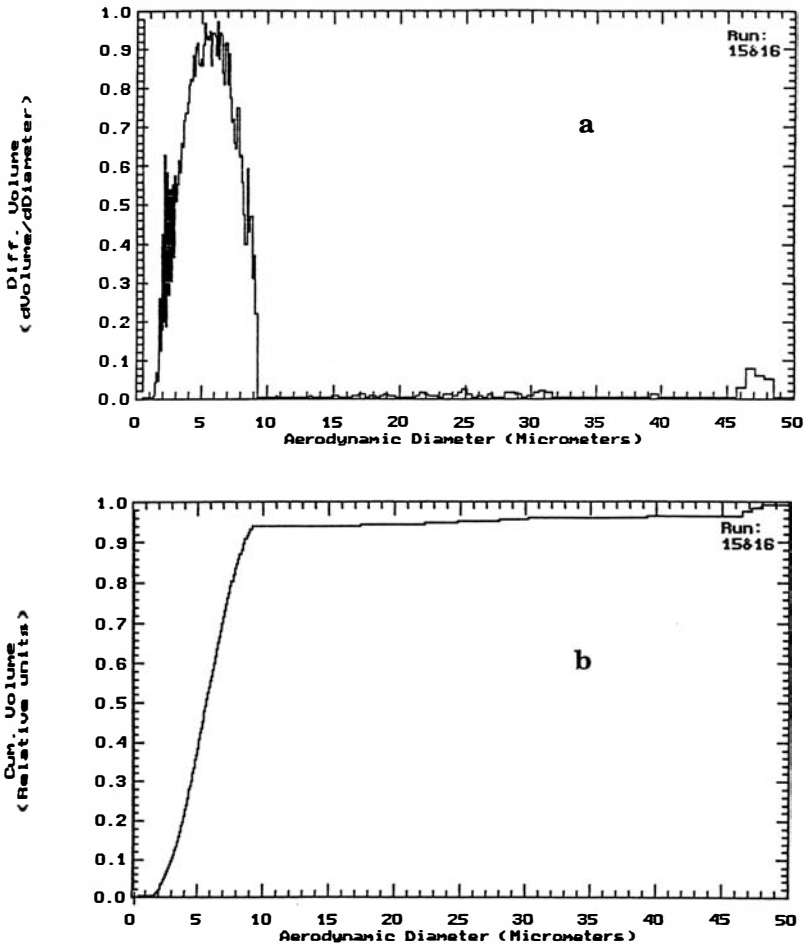

Figure AV.1 Particle size distributions of spray dried lactose presented as (a) volume distributions normalized to the highest peak in the distribution and (b) cumulative percent mass undersize.

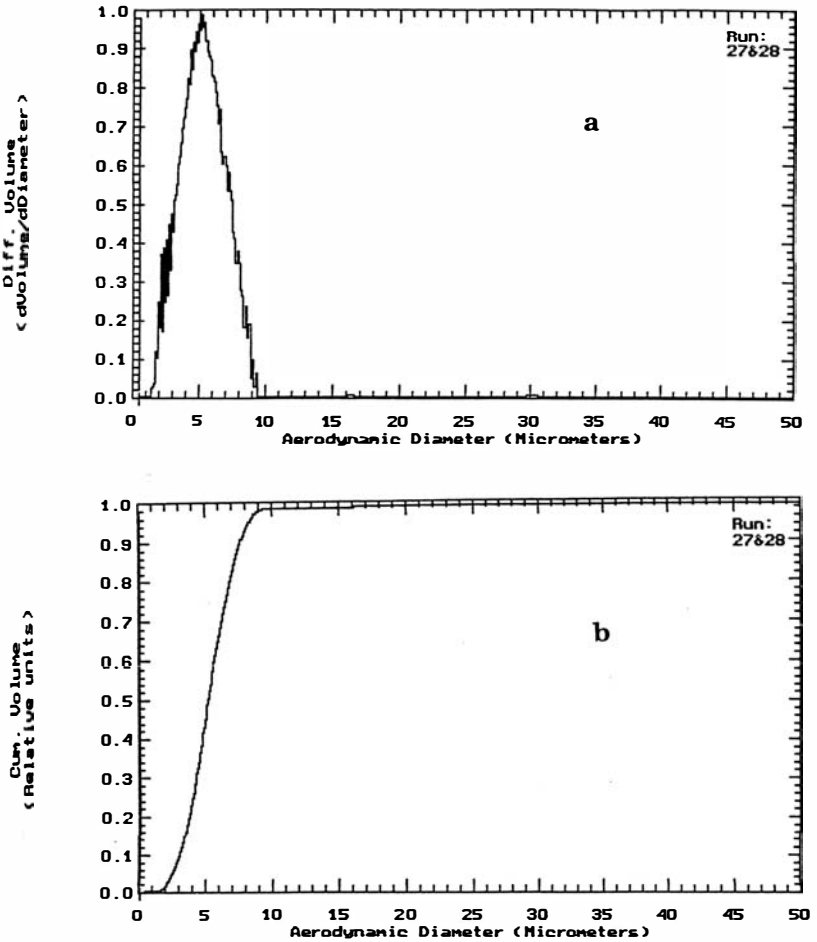

Figure AV.2 Particle size distributions of spray dried trehalose presented as (a) volume distributions normalized to the highest peak in the distribution and (b) cumulative percent mass undersize.

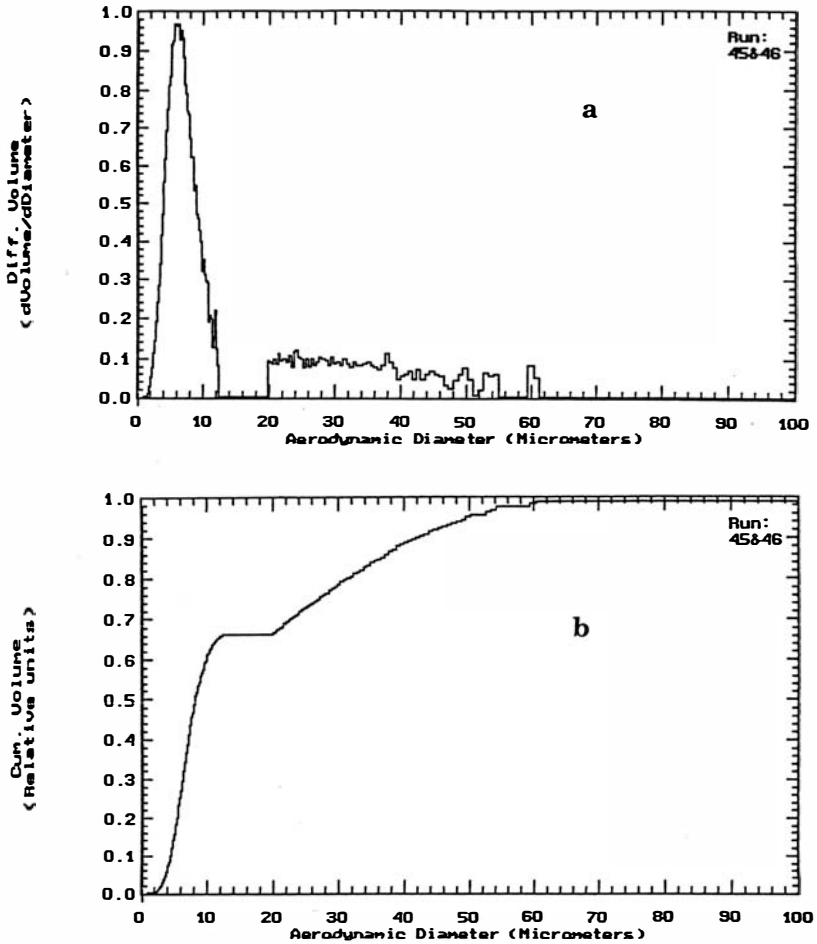

Figure AV.3 Particle size distributions of spray dried sucrose presented as (a) volume distributions normalized to the highest peak in the distribution and (b) cumulative percent mass undersize.

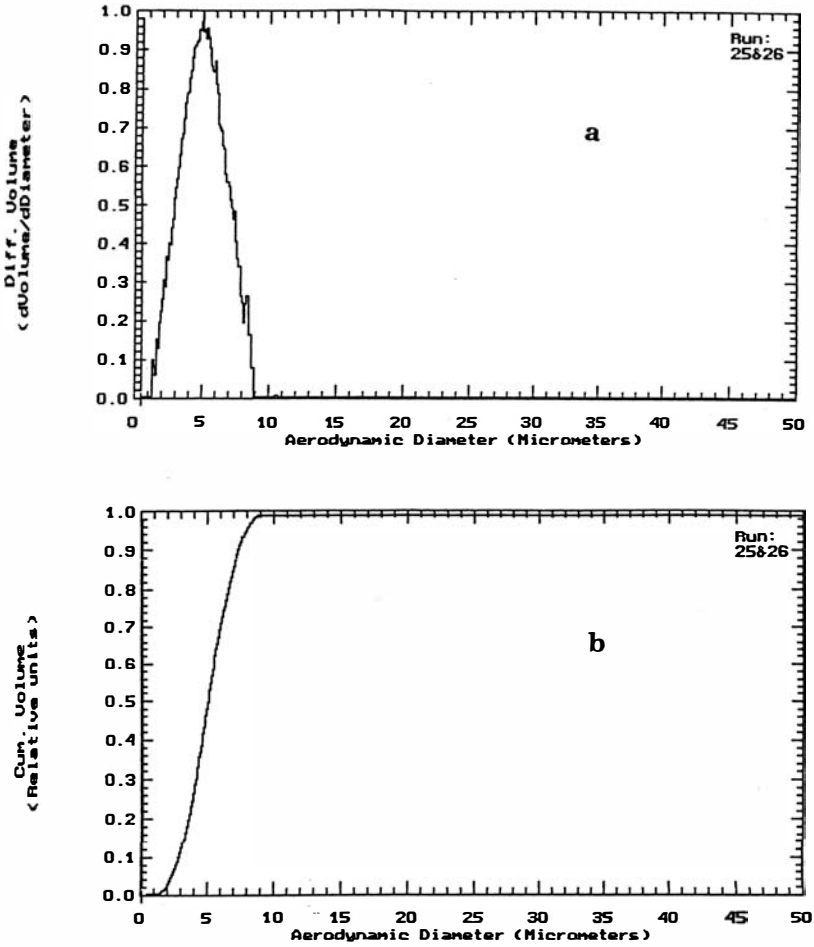

Figure AV.4 Particle size distributions of spray dried mannitol presented as (a) volume distributions normalized to the highest peak in the distribution and (b) cumulative percent mass undersize.

APPENDIX VI. PARTICLE SIZE MEASUREMENT OF CRYSTALLINE SIEVE FRACTIONS OF SUGARS USING SCANNING ELECTRON MICROSCOPY (SEM) AND OPTICAL MICROSCOPY

This appendix presents SEMs of crystalline sieve fractions. Powder was mounted onto metal stubs and coated with gold-palladium using an Eiko IB-2 Ion Coater (Eiko Engineering, Ibaraki, Japan), followed by SEM (Joel JSM-820, Peabody, MA).

Particle size distributions were determined using optical microscopy (Optiphot, Nikon, Tokyo, Japan). More than 300 particles were counted for each sugar sample. SEMs of lactose, trehalose and sucrose sieve fractions showed the particles shaped like cubes and mannitol fractions appeared plate like. For lactose, trehalose and sucrose samples, both length and breadth of each particle was measured. Average of length and breadth was taken as the side of the cube (assumed geometry for these sugars) for volume calculations. For mannitol the length and breadth was measured. Volumes were calculated using a cuboid shape (length x breadth x depth). Depth of the mannitol particles was assumed to be 10 μm for easier calculations. Particle size distributions for each fraction are presented as the cumulative percent volume undersize and number distribution.

a

b

Figure AVI.1 SEMs of (a) "coarse fraction" and (b) "fine fraction" of lactose.

a

b

Figure AVI.2 SEMs of (a) "coarse fraction" and (b) "fine fraction" of trehalose.

a

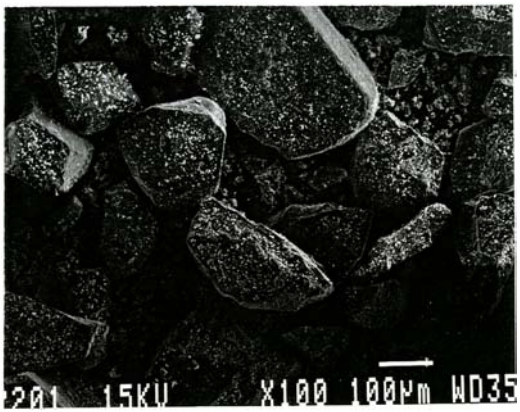

b

Figure AVI.3 SEMs of (a) "coarse fraction" and (b) "fine fraction" of sucrose.

a

b

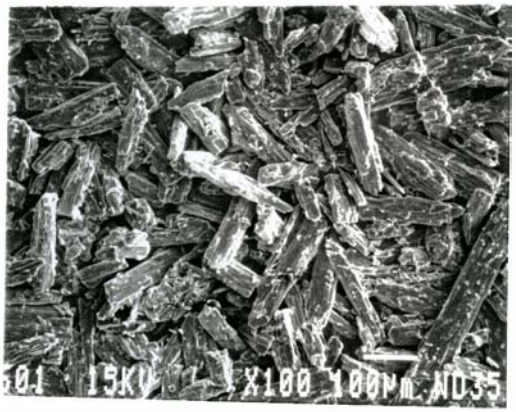

Figure AVI.4 SEMs of (a) "coarse fraction" and (b) "fine fraction" of mannitol.

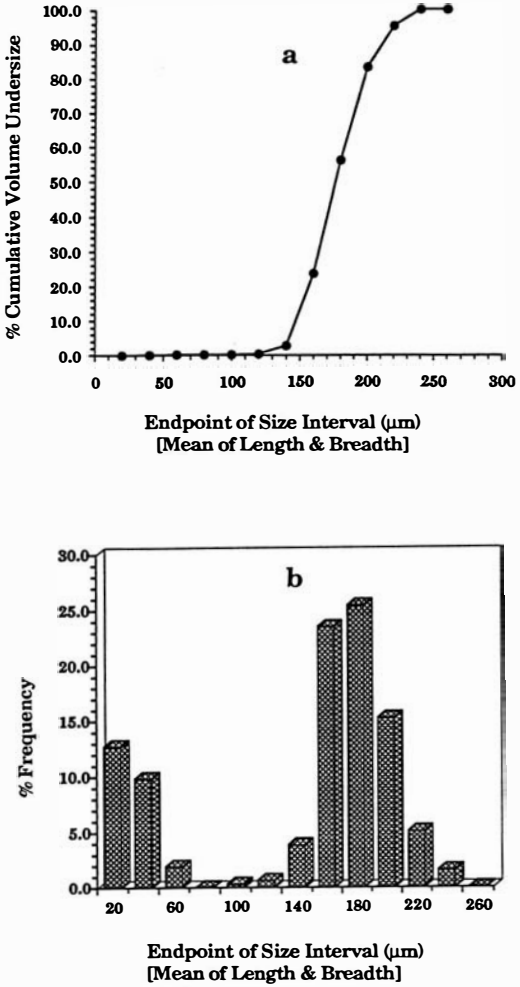

Figure AVI.5 Particle size distributions of "coarse fraction" of lactose presented as (a) percent cumulative volume undersize and (b) number distributions.

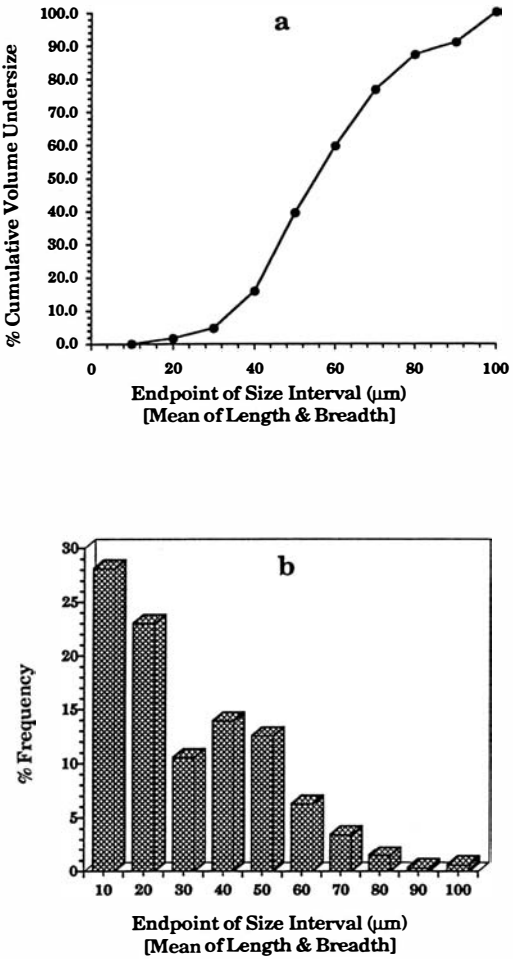

Figure AVI.6 Particle size distributions of "fine fraction" of lactose presented as (a) percent cumulative volume undersize and (b) number distributions.

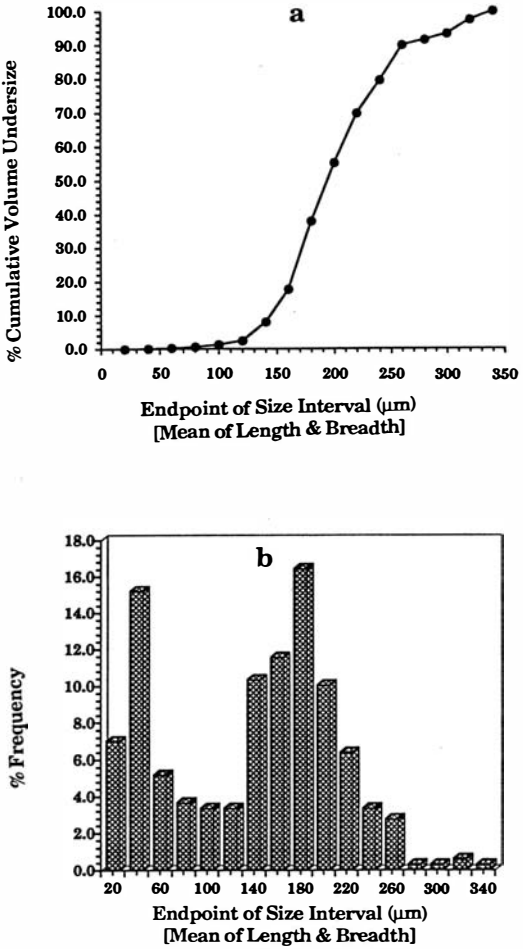

Figure AVI.7 Particle size distributions of "coarse fraction" of trehalose presented as (a) percent cumulative volume undersize and (b) number distributions.

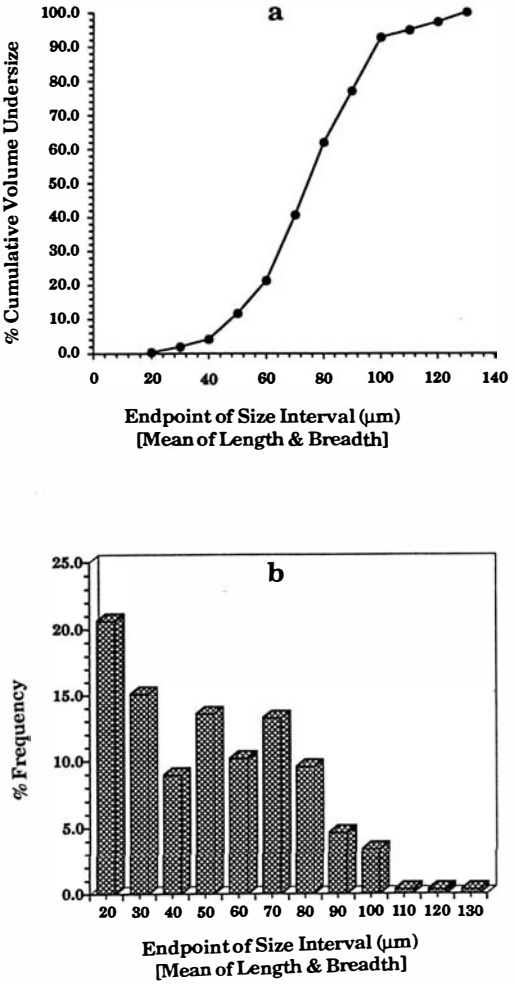

Figure AVI.8 Particle size distributions of "fine fraction" of trehalose presented as (a) percent cumulative volume undersize and (b) number distributions.

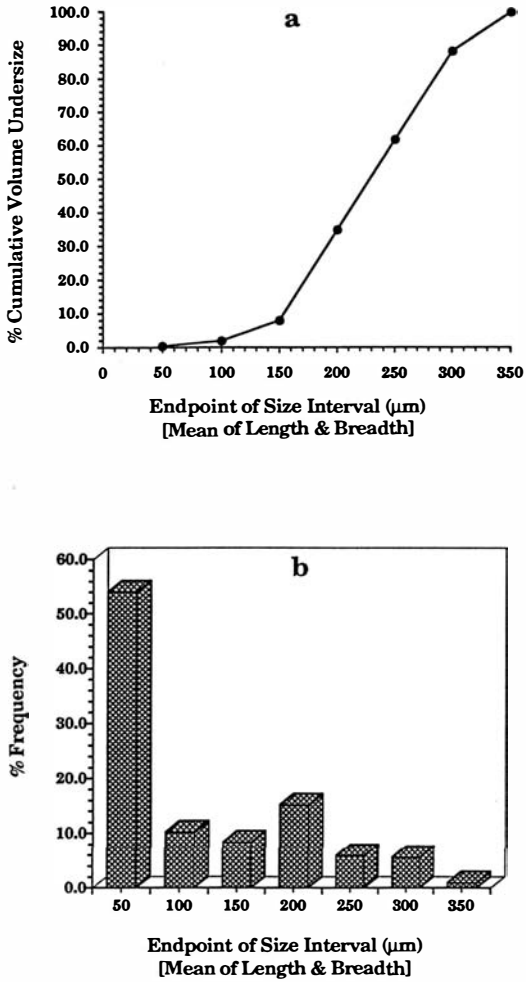

Figure AVI.9 Particle size distributions of "coarse fraction" of sucrose presented as (a) percent cumulative volume undersize and (b) number distributions.

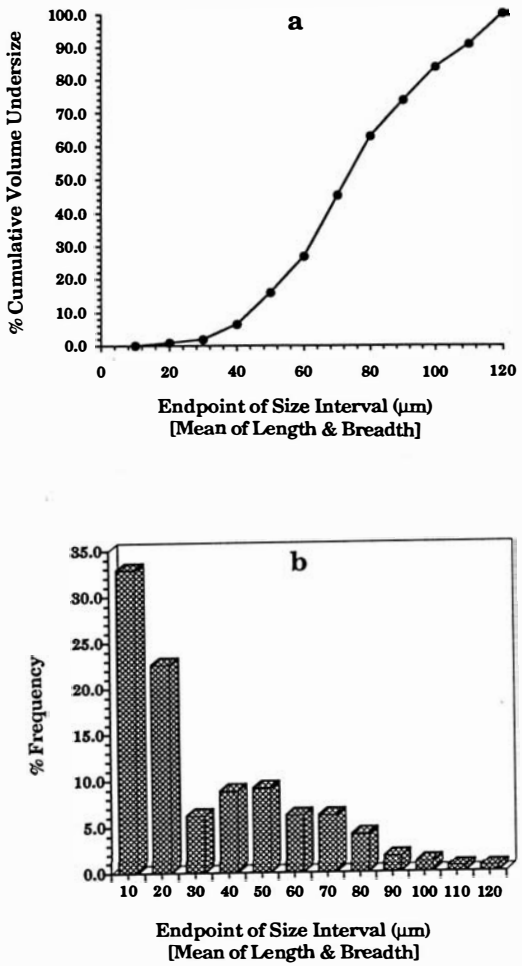

Figure AVI.10 Particle size distributions of "fine fraction" of sucrose presented as (a) percent cumulative volume undersize and (b) number distributions.

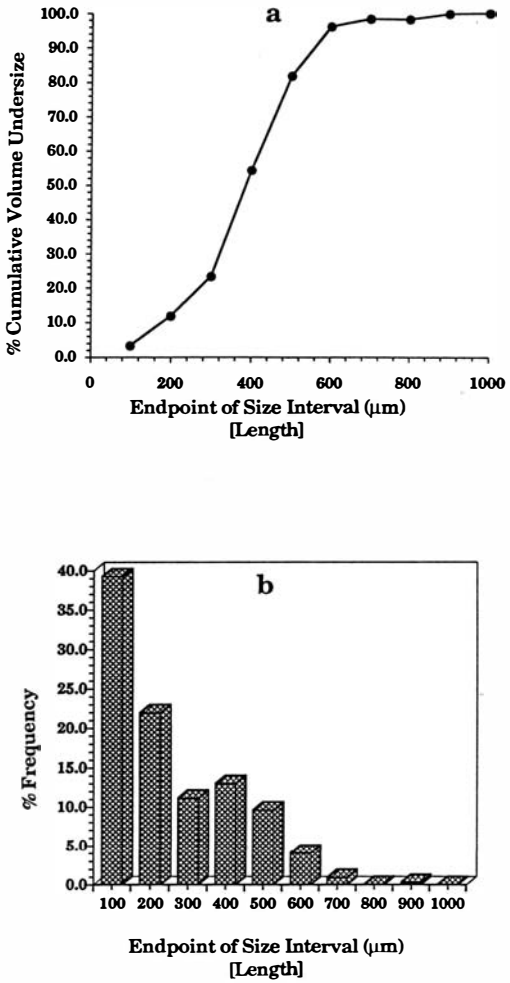

Figure AVI.11 Particle size distributions of "coarse fraction" of mannitol presented as (a) percent cumulative volume undersize and (b) number distributions.

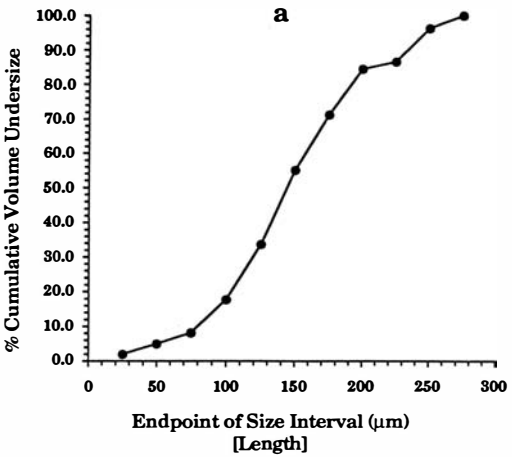

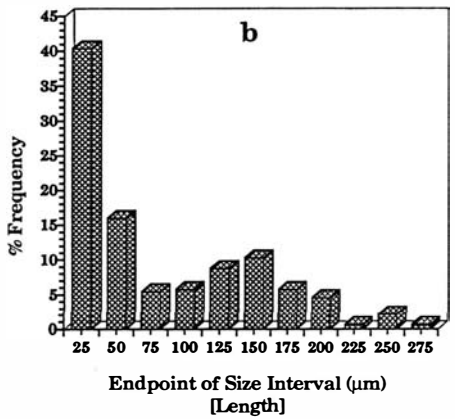

Figure AVI.12 Particle size distributions of "fine fraction" of mannitol presented as (a) percent cumulative volume undersize and (b) number distributions.

APPENDIX VII. X-RAY POWDER DIFFRACTION (XRPD) OF CRYSTALLINE SUGARS AND THEIR SPRAY DRIED FORMS

This Appendix presents the X-ray diffraction patterns for different forms of each sugar at different storage conditions. X-ray diffraction was performed as described in Section III.b.2.8 (Chapter III).

In each Figure subscripts 0 and 30 refer to before and after storage for 30 days at different relative humidities. Key: A=Coarse fraction, B=Fine fraction, C=Spray dried. Subscripts: a=Stored in sealed bottles over P2O5, b=23% RH, c=52% RH, d=75% RH and e=93% RH. XRPD was not performed on coarse and fine fractions after storage at different relative humidities.

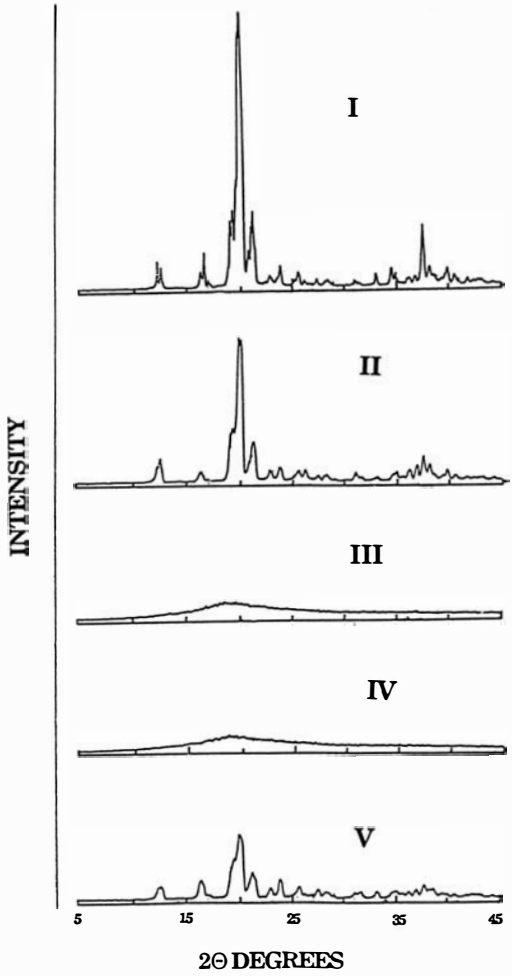

Figure AVII.1 XRPD patterns for lactose. (I) A_0 (II) B_0 (III) C_0 and C_{30a} (IV) C_{30b} (V) $C_{30c,d,e}$

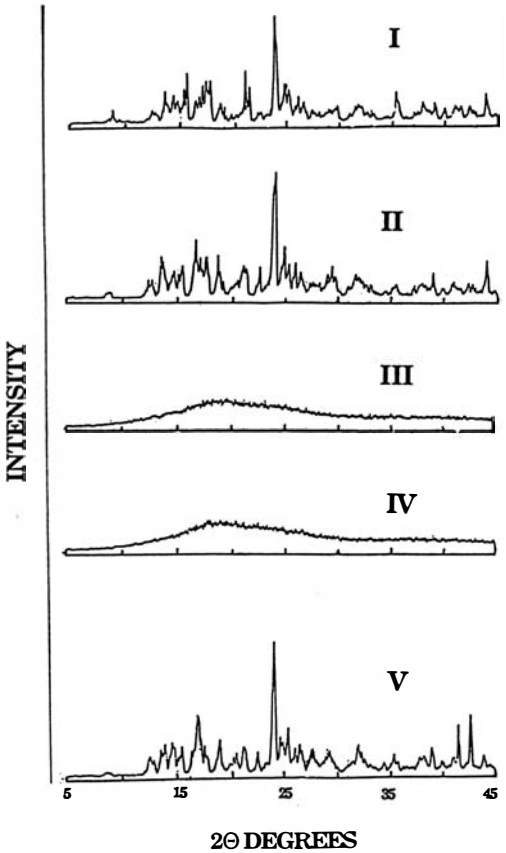

Figure AVII.2 XRPD patterns for trehalose. (I) A_0 (II) B_0 (III) C_0 and C_{30a} (IV) C_{30b} (V) $C_{30c,d,e}$

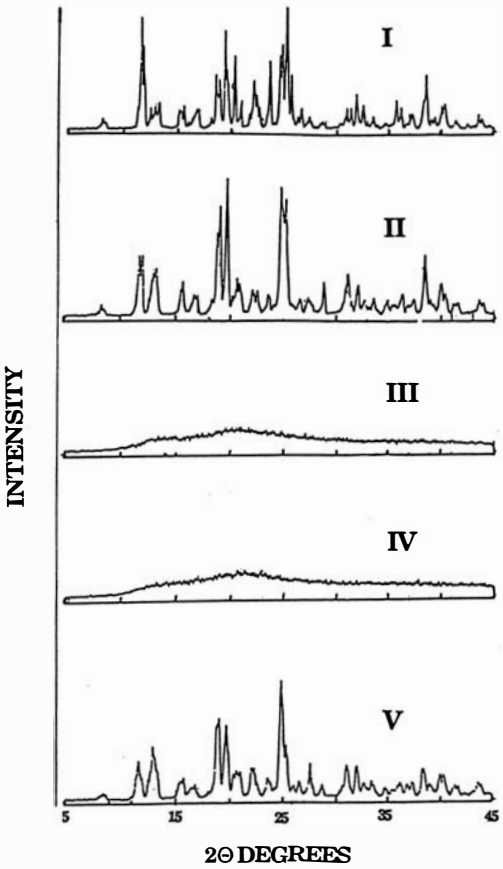

Figure AVII.3 XRPD patterns for sucrose. (I) A_0 (II) B_0 (III) C_0 and C_{30a} (IV) C_{30b} (V) $C_{30c,d}$

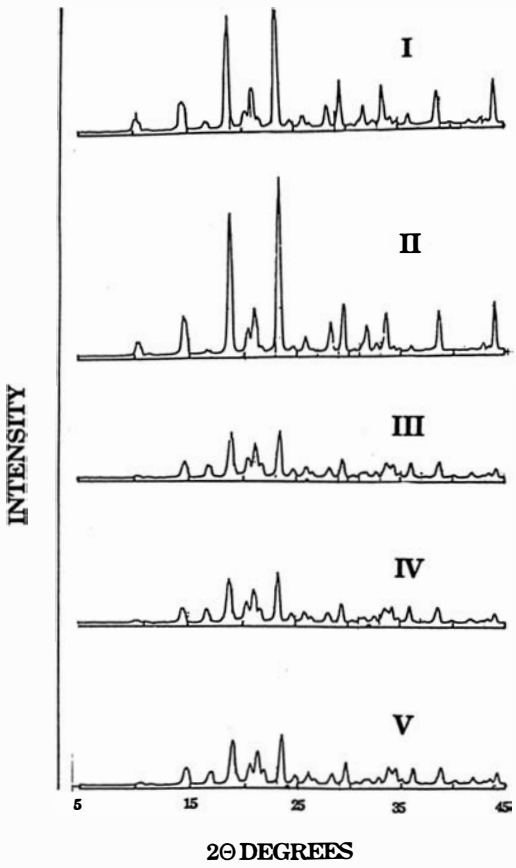

Figure AVII.4 XRPD patterns for mannitol. (I) A_0 (II) B_0 (III) C_0 and C_{30a} (IV) C_{30b} (V) $C_{30c,d,e}$

APPENDIX VIII. HOT STAGE MICROSCOPY OF SPRAY DRIED SUGARS OBSERVED UNDER CROSSED POLARS

This Appendix presents photomicrographs of spray dried lactose and sucrose. Hot stage microscopy was performed as described in Section III.b.2.7 (Chapter III). Phase transformations in amorphous sugars (spray dried lactose, trehalose and sucrose), such as glass-to-rubber, recrystallization and melting were observed and photomicrographed under crossed polars (Nikon N2000, Nikon, Tokyo, Japan). Spray dried trehalose did not show any recrystallization event and is not shown in this Appendix.

a

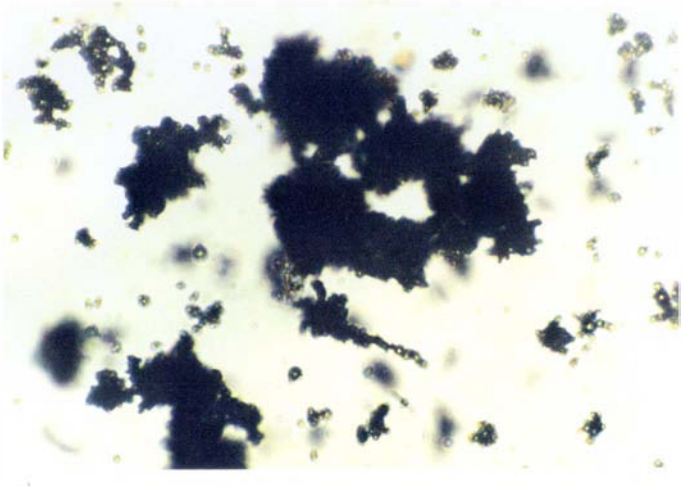

b

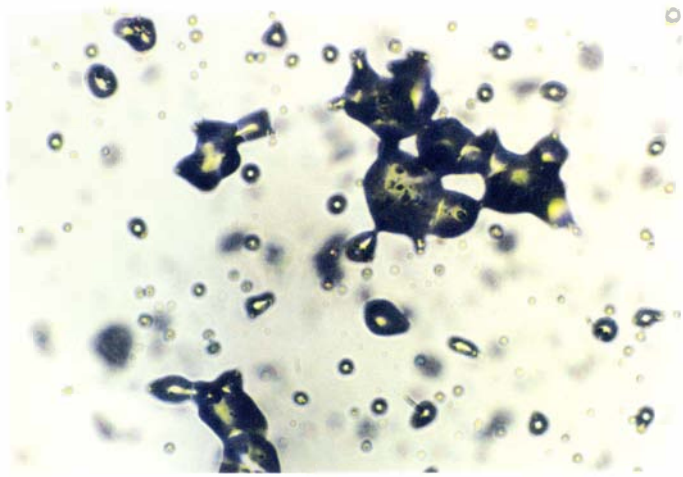

Figure AVIII.1 Photomicrograph of spray dried lactose under crossed polars at (a) 30 °C and (b) 140 °C.

a

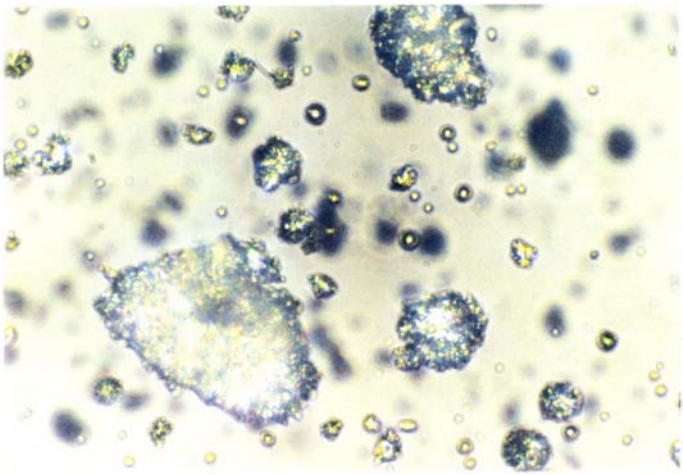

b

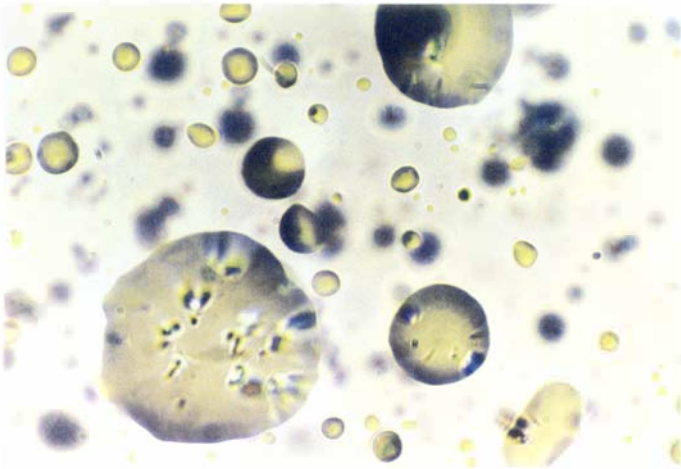

Figure AVIII.2 Photomicrograph of spray dried lactose under crossed polars at (a) 170 °C and (b) 190 °C.

a

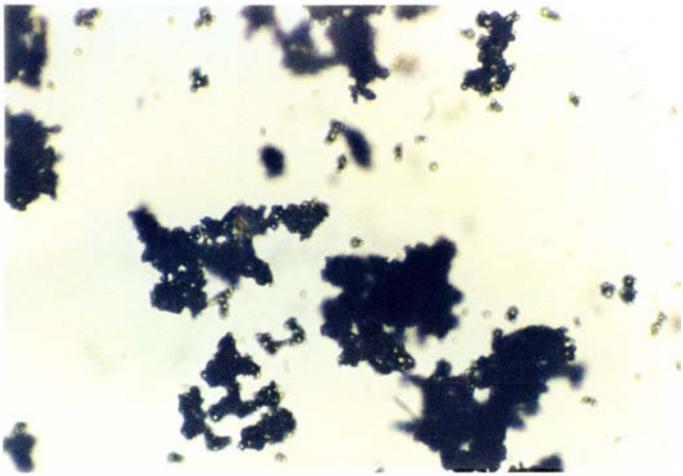

b

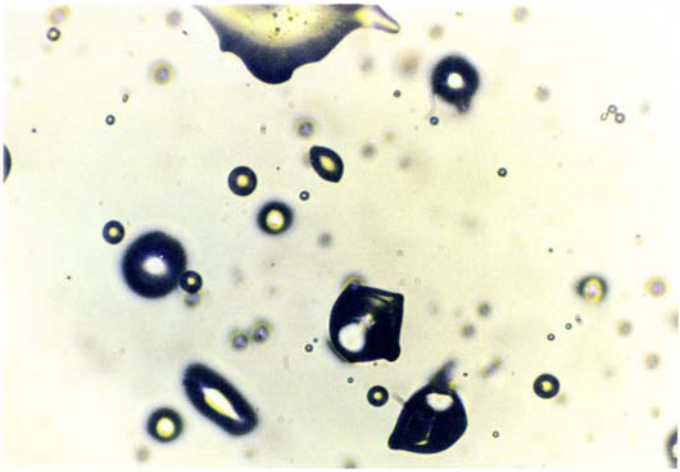

Figure AVIII.3 Photomicrograph of spray dried sucrose under crossed polars at (a) 30 °C and (b) 106 °C.

a

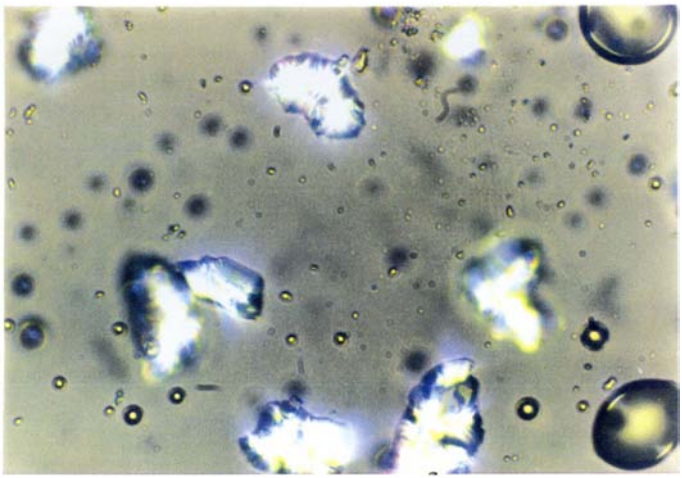

b

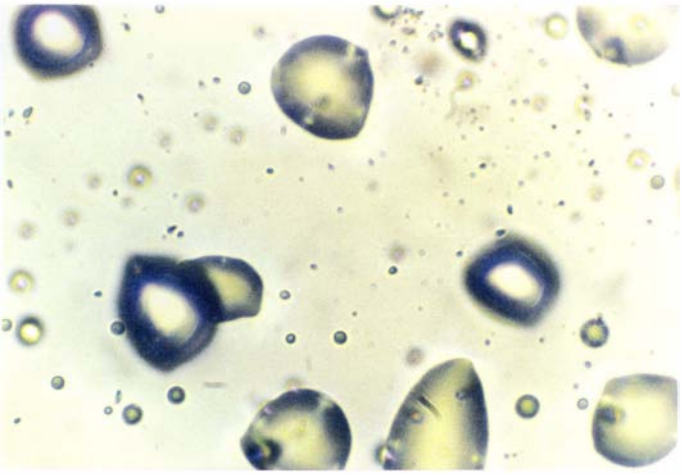

Figure AVIII.4 Photomicrograph of spray dried sucrose under crossed polars at (a) 151 °C and (b) 192 °C.

APPENDIX IX. INSTRUCTIONS MANUAL FOR THE SMALL PARTICLE AEROSOL GENERATOR (SPAG)

This Appendix presents the instruction manual for the use of the Small Particle Aerosol Generator (SPAG 2; ICN Pharmaceuticals, Costa Mesa, CA).

SMALL PARTICLE AEROSOL GENERATOR MODEL SPAG-2*

6000 SERIES MODEL

INSTRUCTIONS FOR USE

WARNING:

RIBAVIRIN AEROSOL SHOULD NOT BE USED FOR INFANTS REQUIRING ASSISTED VENTILATION BECAUSE PRECIPITATION OF THE DRUG IN THE RESPIRATORY EQUIPMENT MAY INTERFERE WITH SAFE AND EFFECTIVE VENTILATION OF THE PATIENT. Conditions for safe use with a ventilator are still in development.

Federal law restricts this device to sale by or on the order of a physician.

*For use in the administration of Virazole® (Ribavirin) only. This device may not be used for the administration of any other drug.

ICN Pharmaceuticals, Inc.
ICN Plaza
3300 Hyland Ave
Costa Mesa, CA 92626
(714) 545-0100
Medical Emergency (800) 572-7400

WARNING:

RIBAVIRIN AEROSOL SHOULD NOT BE USED FOR INFANTS REQUIRING ASSISTED VENTILATION BECAUSE PRECIPITATION OF THE DRUG IN THE RESPIRATORY EQUIPMENT MAY INTERFERE WITH SAFE AND EFFECTIVE VENTILATION OF THE PATIENT. Conditions for safe use with a ventilator are still in development.

A. INTRODUCTION

The Small Particle Aerosol Generator Model-2 (SPAG-2) is indicated for administration of Virazole® (ribavirin) aerosol only. Ribavirin aerosol is indicated in the treatment of carefully selected hospitalized infants and young children with severe lower respiratory tract infections due to respiratory syncytial virus (RSV).

B. GENERAL OPERATION OF THE SPAG-2 AEROSOL GENERATOR

The pneumatic flow system of the SPAG-2 is depicted in Figure 1. The SPAG-2 is driven by a pressurized gas (air or blended oxygen) source, which passes through an external pressure compensated flowmeter before entering the SPAG-2. The incoming gas is regulated to 26 psig (179 KPa), and then is directed, via a manifold and pressure compensated flowmeters, to both the nebulizer and the drying chamber.

The nebulizer generates a fine aerosol of hydrated Virazole®, and the drying chamber further dehumidifies the aerosol. The mass median diameter of the aerosol particles is approximately 1.3 micron.

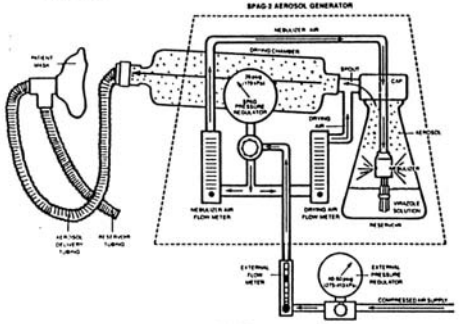

FIGURE 1.

SCHEMATIC OF GAS FLOW THROUGH THE SPAG-2
SMALL PARTICLE AEROSOL GENERATOR

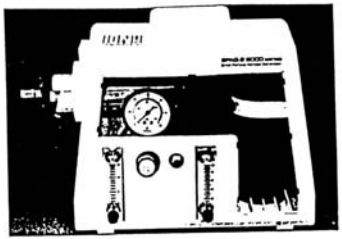

SPAG-2 Front

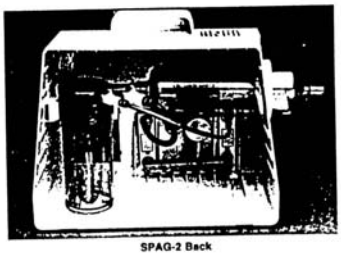

SPAG-2 Back

FIGURE 2

C. ASSEMBLY OF THE SPAG-2 AEROSOL GENERATOR

1. Each shipping carton contains the following items:

   1 - SPAG-2.

   2 - 500 ml. reservoirs (polysulfone plastic).

   2 - Reservoir caps (polysulfone plastic), with gasket and O-rings.

   2 - Nebulizers.

   2 - Drying chambers (polysulfone plastic).

   2 - Cleaning wires for nebulizer (0.011" dia., stainless steel).

   12 - Lengths nebulizer tubing (silicone).

   2 - Extra nebulizer cleanout screws (stainless steel).

   2 - Extra nebulizer washers (Teflon®).

   2 - Operator's manuals.

   The spare parts included with the SPAG-2 will allow operation with little or no downtime.

2. Operation of the SPAG-2 requires that the following equipment and items be provided by the hospital or clinic:

   - Compressed gas source, regulated to 40–60 psig (pounds per square inch gauge) (275–413 kPa). Use air which meets specifications for medical breathing use, unless the physician prescribes oxygen which must be blended.

   - If greater than 21% oxygen is to be delivered to the patient, an oxygen blender should be used. Fraction of inspired oxygen (F_iO_2) should be monitored at the point of patient delivery.

     CAUTION: Oxygen therapy requires careful monitoring.

   - Flowmeter, pressure compensated, capable of measuring 15 liters per minute at 50 psig (344 kPa).

   - Hose to supply gas to the SPAG-2 (equipped with a standard 9/16–18 hemispherical connector).

   - Aerosol conduction tubing, 22 mm diameter.

   Further equipment required will depend on the particular mode of aerosol administration. Virazole® aerosol may be delivered to a face mask, hood, or tent.

Cap Assembly (includes gasket and O-rings, Part no. 4014)

Nebulizer Assembly (Part no. 4015)

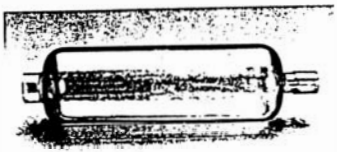

Drying Chamber (Part No. 1084)

Reservoir
(Part no. 1093)

Accessory Package
(Part no. 4012)
2 - Teflon® nebulizer washe
2 - s.s. nebulizer screws
2 - cleanout wires

Nebulizer Tubing
(Part no. 4016)
12 - lengths nebulizer tubi

3. Check all 3 nebulizer orifices with the cleaning wire to ensure they are not occluded. Insert the nebulizer stem into the swage fitting in the center of the reservoir cap. Tighten the swage firmly with the hand tight nut.

4. Inspect the reservoir cap gasket for cleanliness. Place the cap onto the reservoir containing the Virazole® solution (see page 13 for instructions describing preparation of Virazole®). Twist the cap clockwise to seal the cap onto the reservoir. Make sure that the nebulizer pick-up tubes are not flush against the bottom of the reservoir.

5. Place the cap/reservoir assembly into the housing and snap it into place in the bracket.

6. Connect the drying air flow (black hose) quick coupling to the larger fitting on the cap spout. Connect the nebulizer air flow (blue hose) quick coupling to the smaller fitting on the body of the cap. Press each quick coupling in with a twisting motion until it snaps into place.

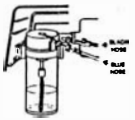

7. Insert the drying chamber through the side hole in the SPAG housing, and push onto the cap spout O-ring. The flow direction arrow on the chamber must point away from the cap.

8. Connect the aerosol tubing (supplied by the user) to the outlet port of the drying chamber.

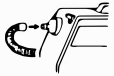

NOTE: The length of the aerosol conduction tubing between the SPAG-2 and the mask, hood or tent should be kept as short as conveniently possible to minimize collection of aerosol during operation. The tubing should be changed at least daily.

9. For use with a hood, the aerosol delivery tubing from the SPAG-2 should be placed into the inlet port of the hood.

10. For use with a face mask, a standard "T" piece should be connected to the mask. The aerosol delivery tubing from the SPAG-2 should be connected to one of the open ends of the "T". Additional aerosol tubing is attached to the branch of the "T" for a reservoir. This reservoir tubing is for optimal Virazole delivery. The length of the reservoir tubing will depend on the patient's tidal volume. The practitioner should follow the hospital's procedure for determining the patient's tidal volume.

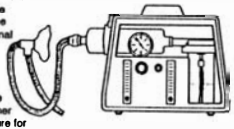

11. For use with a tent, the tent must be set-up with the customary air flow and cooling systems. The aerosol delivery tubing from the SPAG-2 should be connected to the inlet port of the tent.

D. SPAG-2 OPERATING PROCEDURE

NOTE: If greater than 21% oxygen is to be delivered to the patient, an oxygen blender should be used. Fraction of inspired oxygen (F_iO_2) should be monitored at the point of patient delivery.

WARNING:

Whenever two or more oxygen blending systems are used, all blending systems must be adjusted when any changes are made in F_iO_2.

CAUTION: **The gas source must be connected to the SPAG-2 and turned on whenever the SPAG-2 is in use. The source must be regulated in the range 40–60 psig (275–413 kPa). Use air which meets specifications for medical breathing use, unless the physician prescribes oxygen which must be blended. Oxygen therapy requires careful monitoring.**

1. Connect the SPAG-2 to the external flowmeter (provided by user). Open the external flowmeter control valve completely. It is important that the external flowmeter does not restrict gas flow to the SPAG-2.
2. Open the nebulizer flowmeter valve completely (approximately six turns counter-clockwise from the closed position).
3. Disengage the lock sleeve on the SPAG-2 pressure regulator by pulling the adjustment knob outward. Adjust the pressure regulator knob (clockwise to increase) until 26 psig (179 kPa) is indicated on the SPAG-2 pressure gauge.
4. Open the drying air flowmeter valve from the closed position until the external flowmeter indicates the desired total flow through the unit. It is suggested that the external flowmeter should read approximately 15 liters per minute (LPM) when using a hood or a tent, and approximately 12 LPM when using a face mask.
5. Readjust the SPAG-2 pressure regulator to 26 psig (179 kPa).
6. Verify that the external flowmeter reading is correct and, if necessary, adjust it again by turning the drying air flowmeter valve.

7. The SPAG-2 is correctly adjusted when the operating parameters stabilize into the following ranges:

   a. Regulator pressure = 26 ± 2 psig (165–193 kPa).

   b. Nebulizer flowmeter = range from 6–10 LPM.

   c. Drying air flowmeter = range from 2–9 LPM.

   Read all rates of flow at the center of the indicator ball.

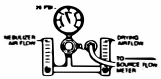

8. TROUBLESHOOTING

   8.1 INCORRECT AIR FLOW READING: Ensure that the SPAG-2 flows have stabilized before deciding that they are out of tolerance.

   a. Nebulizer air flow: If the indicated nebulizer air flow is greater than the specification in 7(b) above, check for leaks in the connections delivering air to the nebulizer. Ensure that the cleanout screw in the nebulizer is not leaking. If the flow is less than the specification in 7(b), clean the nebulizer and check for occlusions in the orifices. If these measures do not bring the flow into the correct range, change the nebulizer.

   b. Drying chamber air flow: Ensure that the flow to the nebulizer is within the specified range before troubleshooting the drying chamber air flow. If the flow to the drying chamber cannot be adjusted within the specified range, check for leaks or occlusions in the plumbing connections.

   8.2 NEBULIZER FUNCTION

   a. Check that all three (3) orifices of the nebulizer are spraying correctly by looking for about a one inch diameter "spray spot" on the wall of the flask. If any problem is detected, clean or change the nebulizer.

   b. The SPAG-2 should nebulize the drug solution from the reservoir at a rate of 12.5–15.0 ml/hour. If the nebulization rate is slow, ensure that the external flowmeter (provided by the user) is completely opened, and that the nebulizer orifices are not clogged. Change the silicone tubing or the nebulizer/tubing assembly after ensuring that other operating parameters are correct. If the nebulization rate appears to be fast, check for excessive leaks at the cap gasket.

9. **Monitor the operation of the SPAG-2 for approximately ten minutes and adjust any settings accordingly.**

   CAUTION: During operation, water/drug collection may form in the reservoir cap spout, inside the drying chamber, at the outlet port of the drying chamber and in the 22 mm aerosol conduction tubing. Monitor these components hourly. Collection may increase after 10 hours of operation. If excessive collection is seen, these components should be cleaned or replaced.

10. **Before inactivating the aerosol generator, assure that the patient has been removed from the aerosol and has an alternative source of oxygen or air. To inactivate the aerosol generator, turn off the gas source.**

E. STERILIZATION OF SPAG-2 WETTED COMPONENTS.

All parts of the SPAG-2 are clean as delivered. It is the responsibility of the user to sterilize all wetted parts before beginning each course of therapy. At a minimum, sterilization of all wetted parts should be done daily.

Sterilize, by autoclaving, the following parts:

1. Drying chamber (polysulfone plastic).
2. Reservoir (polysulfone plastic).
3. Reservoir cap (polysulfone plastic) with gasket and O-rings.
4. Nebulizer assembly with tubing.

Autoclave these items by standard procedures.

Hospital personnel should follow the same procedures used for monitoring bacterial contamination of respiratory equipment when caring for the SPAG-2.

F. CLEANING OF COMPONENTS

1. Any Virazole® solution remaining in the reservoir after treatment should be discarded.

2. Virazole® is a very water soluble material. The components (reservoir, cap, nebulizer and drying chamber) can be effectively cleaned with warm tap water and mild detergent. After cleaning, rinse with warm tap water and then with distilled or deionized water.

3. Extra attention should be given to cleaning the nebulizer. Do not disassemble unless an occlusion is suspected. Probe the orifices of the nebulizer with the 0.011" cleaning wire to dislodge any material. Ensure that the wire is inserted completely into each of the three small inner holes on the side of the nebulizer tip. After cleaning and rinsing the nebulizer, shake to remove water from the small passageways.

4. If disassembly of the nebulizer becomes necessary, remove the small cleanout screw (withwasher) and the silicone tubing. Probe all orifices with the cleaning wire. Soak all nebulizer parts in warm to hot water containing detergent, rinse thoroughly, then blow dry with compressed air. Reassemble the nebulizer.

5. The reservoir, cap, nebulizer, and drying chamber should be sterilized by autoclaving (See Section E).

6. The housing can be cleaned with any disinfectant currently used by the hospital for cleaning the exterior of similar respiratory therapy equipment (e.g. ventilators, IPPB devices). For example, Sanamaster III (quaternary compound), 1 oz/gallon.

G. PREPARATION OF VIRAZOLE® FOR USE IN THE SPAG-2

Virazole® is supplied as 6 grams of lyophilized drug per 100 ml vial for aerosol administration only. By sterile technique, dissolve the drug in sterile USP water for injection or inhalation in the 100 ml vial. Transfer to the clean, sterilized 500 ml SPAG-2 reservoir, and further dilute to a final volume of 300 ml with sterile USP water for injection or inhalation. The final concentration should be 20 mg/ml. Important: This water should not have had any antimicrobial agent or other substance added. The solution should be inspected visually for particulate matter and discoloration prior to administration. Solutions that have been placed in the SPAG-2 unit should be discarded at least every 24 hours and when the liquid level is low before adding newly reconstituted solution.

Using the recommended drug concentration of 20 mg/ml Virazole® as the starting solution in the drug reservoirof the SPAG-2unit, the average aerosol concentration for a 12 hour period would be 190 micrograms/liter (0.19 mg/l) of air.

Vials containing the lyophilized drug powder should be stored in a dry place at 15–25°C (59–78°F). Reconstituted solutions may be stored, under sterile conditions, at room temperature (20–30°C, 68–86° F) for 24 hours. Solutions which have been placed in the SPAG-2 unit should be discarded at least every 24 hours.

NOTE: Levels of ribavirin in the environment are expected to be low during proper administration of the drug. To help minimize incidental exposure, ribavirin should be administered in a well-ventilated hospital setting. Hospital staff responsible for aerosol delivery should consider using a protective face cover (nose and mouth) to reduce incidental exposure. Common surgical masks do not provide a significant amount of protection. The 3M® Model 9970 personal mask has been identified as one which supplies significant protection when properly fitted.

H. **SELECTED REPLACEMENT PARTS FOR THE SPAG-2**

Replacement parts and technical assistance for the SPAG-2 may be obtained by contacting your local representative or the ICN office listed below. When ordering, please specify the model SPAG-2 and device serial number, as well as the part number and description of the item desired.

Device Serial No.	Part Description	Part No.
All serial nos.	O-ring for cap nebulizer air port	1106
	O-ring for cap drying air port	1107
	O-ring for cap spout	1115
	Drying chamber (polysulfone plastic)	1084
	Accessory package (2 cleaning wires, nebulizer screws and washers)	4012
6000-15999	Reservoir	1093
	Reservoir cap gasket	1122
	Cap assembly (includes gasket, O-rings)	4014
	Nebulizer assembly	4015
	Silicone tubing for nebulizer (12 lengths)	4016
3100-5999	Cap assembly (includes gasket, fittings)	4010
	Reservoir	1047
	Reservoir cap gasket	1068
	Nebulizer assembly	4004
	Silicone tubing for nebulizer (12 lengths)	4007

ICN Pharmaceuticals, Inc.
3300 Hyland Avenue
Costa Mesa, CA 92626
Telephone: (714) 545-0100
(800) 572-7400 (24 hour answering service)

Virazole®
(Ribavirin)

PRESCRIBING INFORMATION

WARNING:

RIBAVIRIN AEROSOL SHOULD NOT BE USED FOR INFANTS REQUIRING ASSISTED VENTILATION BECAUSE PRECIPITATION OF THE DRUG IN THE RESPIRATORY EQUIPMENT MAY INTERFERE WITH SAFE AND EFFECTIVE VENTILATION OF THE PATIENT. [illegible]

[illegible] CONTRAINDICATIONS.

DESCRIPTION:

Virazole® (ribavirin) Aerosol, an antiviral drug, is a sterile, lyophilized powder to be reconstituted for aerosol administration. Each 100 ml glass vial contains 6 grams of ribavirin, and when reconstituted to the recommended volume of 300 ml with sterile water for injection or sterile water for inhalation (no preservatives added), will contain 20 mg/ml ribavirin, pH approximately 5.5. Aerosolization is to be carried out in a SPAG-2 nebulizer only.

Ribavirin is 1-beta-D-ribofuranosyl-1,2,4-triazole-3-carboxamide, with the following structural formula:

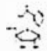

Ribavirin, a synthetic nucleoside, is a stable, white, crystalline compound [illegible]

CLINICAL PHARMACOLOGY:

Antiviral effects

[illegible]

Immunologic effects

[illegible]

Microbiology:

[illegible]

Pharmacokinetics:

[illegible]

INDICATIONS AND USAGE:

[illegible]

Diagnosis:

[illegible]

CONTRAINDICATIONS:

[illegible]

WARNINGS:

[illegible]

PRECAUTIONS:

General:

[illegible]

Drug Interactions:

[illegible]

Carcinogenesis, mutagenesis, impairment of fertility:

[illegible]

ICN Pharmaceuticals, Inc.

1957-02
Rev. 1-86

16

300

VITA